

NASA
Reference
Publication
1272

January 1992

The Atmospheric Effects
of Stratospheric Aircraft:
A First Program Report

M. J. Prather, H. L. Wesoky,
R. C. Miake-Lye, A. R. Douglass,
R. P. Turco, D. J. Wuebbles,
M. K. W. Ko, and A. L. Schmeltekopf

(NASA-RP-1272) THE ATMOSPHERIC EFFECTS OF
STRATOSPHERIC AIRCRAFT: A FIRST PROGRAM
REPORT (NASA) 227 p CACL 13B

N92-19121
--THRU--
N92-19127
Unclas
0064286

H1/45

NASA

1N-45
64286
P-227

**NASA
Reference
Publication
1272**

1992

**The Atmospheric Effects
of Stratospheric Aircraft:
A First Program Report**

M. J. Prather, H. L. Wesoky,
R. C. Miake-Lye, A. R. Douglass,
R. P. Turco, D. J. Wuebbles,
M. K. W. Ko, and A. L. Schmeltekopf
*NASA Office of Space Science and Applications
Washington, D.C.*



National Aeronautics and
Space Administration
Office of Management
Scientific and Technical
Information Program

Contents

1	The Atmospheric Effects of Stratospheric Aircraft: A First Program Report <i>Michael J. Prather and Howard L. Wesoky, Eds.</i>	10
2	High-Speed Civil Transport Aircraft Emissions <i>Richard C. Miake-Lye, et al.</i>	13 ⁵¹
3A	Natural Cycles, Gases <i>Anne R. Douglass, et al.</i>	33 ⁵²
3B	Upper Atmosphere Aerosols: Properties and Natural Cycles <i>Richard P. Turco</i>	63 ⁵³
4	Designing a Methodology for Future Air Travel Scenarios <i>Donald J. Wuebbles, et al.</i>	93 ⁵⁴
5	Ozone Response to Aircraft Emissions: Sensitivity Studies with 2-D Models <i>Malcolm K. W. Ko, et al.</i>	115 ⁵⁵
6	Lower Stratospheric Measurement Issues Workshop Report <i>Arthur L. Schmeltekopf</i>	159 ⁵⁶
7	High-Speed Research Program/Atmospheric Effects of Stratospheric Aircraft Research Summaries	187 ^{omit}
A	Appendix: List of Reviewers	A-1 ^{omit}

CMIT
PRIMARY

Chapter 1

The Atmospheric Effects of Stratospheric Aircraft: A First Program Report

Introduction

Michael J. Prather
National Aeronautics and Space Administration
Goddard Institute for Space Studies
New York, NY

Howard L. Wesoky
National Aeronautics and Space Administration
Office of Aeronautics and Space Technology
Washington, DC

Editors

ABSTRACT

This document presents a first report from the Atmospheric Effects of Stratospheric Aircraft (AESA) component of NASA's High-Speed Research Program (HSRP). Studies have indicated that, with sufficient technology development, future high-speed civil transport aircraft could be economically competitive with long-haul subsonic aircraft. However, uncertainty about atmospheric pollution, along with community noise and sonic boom, continues to be a major concern; and this is addressed in the planned 6-year HSRP begun in 1990. Building on NASA's research in atmospheric science and emissions reduction, the AESA studies are guided by a panel of international scientists, with particular emphasis on stratospheric ozone effects. Because it will not be possible to directly measure the impact of an HSCT aircraft fleet on the atmosphere, the only means of assessment will be prediction. The process of establishing credibility for the predicted effects will likely be complex and involve continued model development and testing against climatological patterns. In particular, laboratory simulation of heterogeneous chemistry and other effects, and direct measurements of well-understood tracers in the troposphere and stratosphere, will continue to be used to improve the current models.

INTRODUCTION

The desire for faster civil aircraft has long been recognized. A supersonic fleet and the impact of its exhaust products in the upper atmosphere were the subject of intense study during the early 1970s (e.g., *Climatic Impact Assessment Program* in the U.S.) (1-6). Emissions from aircraft perturb the chemical and physical environment in which they are emitted: exhaust products such as odd-nitrogen compounds (e.g., $\text{NO}_x = \text{NO} + \text{NO}_2$) and water vapor accumulate in the atmosphere and can lead to photochemical depletion of the stratospheric ozone layer. Scientific assessment of the environmental effects of the proposed fleet ended rapidly with the recognition that a large fleet of supersonic transports (SSTs) was not economically practical. The Anglo-French Concorde was placed in commercial service about 15 years ago, but it serves only first-class passengers with a very small fleet of 13 SSTs, and is not considered economically competitive with existing subsonic aircraft.

Recent NASA-sponsored studies (7-9) show that, with sufficient technology development, future high-speed civil transport (HSCT) aircraft could be economically competitive with long-haul subsonic aircraft. Table 1 compares Concorde and projected HSCT characteristics. Given the expected range of HSCTs, they could serve an important role in the rapidly growing international travel market for flights of 9000 km or more.

Table 1. Current Outlook: Concorde versus HSCT

Concorde (SST)		Projected HSCT
6,600	Range (km)	9,300-12,000
100	Payload (passengers)	250-300
180,000	Takeoff weight (kg)	340,000
Exempt	Community noise standard	Far 36, Stage 3
Premium	Fare levels	Standard

Global atmospheric pollution, community noise, and sonic boom still persist as major environmental roadblocks to HSCTs; and these three concerns are the focus of NASA's HSRP (10). The HSRP began funding research in 1990 and plans to continue funding through 1995. The general course of the 6-year program is first to understand basic phenomena (e.g., stratospheric ozone, combustor emissions, sonic boom propagation, etc.), to prepare computer models or other engineering design tools, and finally to verify these tools with experiments. The atmosphere presents a special case, since the possible global effects cannot be empirically tested without building and flying a large HSCT fleet. Furthermore, the atmosphere is inherently neither controllable nor deterministic on a long-term meteorological scale, and thus our predictive models, the keystone of an assessment, cannot be easily validated as in "laboratory controlled" experiments.

AESA is the component of HSRP responsible for assessing the effects of HSCTs on stratospheric ozone, atmospheric chemistry, and climate. It builds on the strong research community developed and currently supported by NASA's Upper Atmosphere Programs. AESA studies are directed at improving our basic understanding of the circulation and chemistry of the stratosphere and upper troposphere. The structure and history of HSRP/AESA are outlined in this chapter. The Program has asked several scientists to put together papers that either summarize our current knowledge of key elements in atmospheric science or lay the foundation for succeeding assessments. These monographs have been reviewed by the atmospheric science and engineering community and form the basis of this first HSRP/AESA Program Report.

AESA OVERVIEW

The HSRP/AESA Program was founded in 1988 by an agreement between the NASA Office of Aeronautics and Space Technology and the Office of Space Science and Applications. The primary goal of the AESA studies is to prepare the scientific basis for a critically reviewed assessment of the impact of a fleet of HSCTs on the atmosphere, particularly on perturbations to stratospheric ozone. It was recognized that such an assessment must be built on open scientific research, including communications with the international science community.

The HSRP/AESA studies were initiated with the guidance of an advisory panel consisting of prominent members from the international atmospheric sciences community; it also includes members from a public interest group, regulatory agencies, and the aircraft industry. The current membership is given in Table 2. The AESA Advisory Panel helps review research proposals, analyzes the current status of atmospheric science (with respect to AESA Program needs), and develops the overall strategy for AESA studies. It does not advocate specific recommendations for research; this task is the responsibility of the NASA Program managers. The first panel meeting was convened in December 1988 and defined the scientific issues critical to the assessment of an HSCT fleet. This workshop led to the draft of a call for research in support of HSRP/AESA studies. The advisory panel continues to review the Program and overall strategy for the HSCT assessment.

CONNECTION WITH OZONE ASSESSMENTS

In 1975 Congress directed NASA to "develop and carry out a comprehensive program of research, technology, and monitoring of the phenomena of the upper atmosphere so as to provide for an understanding of and to maintain the chemical and physical integrity of the Earth's upper atmosphere." Since then, the Upper Atmosphere Research Program (UARP) has directed this research, focusing on the effects of increasing stratospheric chlorine caused by the manufacture of chlorofluorocarbons (CFCs). The UARP has reported biennially to Congress (11) and has led

Table 2. Atmospheric Effects of Stratospheric Aircraft: Advisory Panel

(a) Scientific Panel Members

Dr. R. A. Cox	Natural Environment Research Council, United Kingdom
Prof. Frederick L. Dryer	Princeton University
Prof. Dieter H. Ehhalt	Institute for Atmospheric Chemistry, Germany
Prof. James R. Holton	University of Washington
Prof. Harold S. Johnston	University of California, Berkeley
Dr. Nicole Louisnard	ONERA, France
Dr. Jerry D. Mahlman	NOAA / Geophysical Fluid Dynamics Lab
Prof. Taroh Matsuno	University of Tokyo / Geophysical Institute, Japan
Prof. Mario J. Molina	Massachusetts Institute of Technology
Dr. Michael Oppenheimer	Environmental Defense Fund
Prof. R. Alan Plumb	Massachusetts Institute of Technology
Dr. A. R. Ravishankara	NOAA / Environmental Research Lab
Dr. Arthur L. Schmeltekopf	NOAA / Aeronomy Lab, Retired
Dr. Adrian F. Tuck	NOAA / Aeronomy Lab
Dr. Steven C. Wofsy	Harvard University
Dr. Donald J. Wuebbles	Lawrence Livermore National Lab
Dr. Michael J. Prather	NASA Goddard Institute for Space Studies, co-chair
Dr. Robert T. Watson	NASA Headquarters, co-chair
Mr. Howard L. Wesoky	NASA Headquarters, executive secretary

(b) Ex Officio Members

Mr. Robert E. Anderson	NASA Headquarters
Ms. Estelle P. Condon	NASA Ames Research Center
Dr. William L. Grose	NASA Langley Research Center
Mr. John S. Hoffman	Environmental Protection Agency
Mr. Nicholas P. Krull	Federal Aviation Administration
Dr. Michael J. Kurylo	NASA Headquarters
Dr. Jarvis Moyers	National Science Foundation
Mr. Richard Niedzwiecki	NASA Lewis Research Center

(c) Official Observers

Mr. Willard J. Dodds	General Electric
Mr. Edwin J. Graber	NASA Lewis Research Center
Mr. Michael Henderson	Boeing
Mr. Richard Hines	Pratt and Whitney
Mr. Richard L. Kurkowski	NASA Ames Research Center
Mr. Alan K. Mortlock	McDonnell Douglas
Mr. Allen H. Whitehead	NASA Langley Research Center

several international scientific assessments of the potential effects of human activities on the atmosphere, particularly on stratospheric ozone, documenting the appearance of the Antarctic ozone hole and its subsequent attribution to the use of synthetic chemicals, particularly CFCs.

Many governments around the world, including that of the United States, have recognized that the ozone layer must be protected to safeguard human health, as well as aquatic and terrestrial ecosystems, from damage caused by enhanced levels of ultraviolet radiation. In particular, it was recognized that the use of chemicals containing chlorine (in the form of CFCs) and bromine (in the form of halons) constitutes a potential threat to the stability of the ozone layer. More than 20 nations, including the United States, signed the Vienna Convention for the Protection of the Ozone Layer in Vienna, Austria, in March 1985 and the Montreal Protocol on Substances that Deplete the Ozone Layer, in Montreal, Canada, in September 1987. The United States and more than 45 other nations have subsequently ratified both the Vienna Convention and the Montreal Protocol.

The Vienna Convention and the Montreal Protocol recommend that all regulatory decisions be based on a scientific understanding of the issues. The international scientific assessment in 1989 (12) provided a basis for decisions at the 1990 London review of the protocol. A new United Nations Environmental Program/World Meteorological Organization (UNEP/WMO)-directed scientific assessment is in preparation for the 1992 meeting of the Montreal Protocol parties; in addition to a discussion of CFCs, it includes a brief review of the impact of rockets and stratospheric aircraft on the ozone layer.

PRELIMINARY REVIEW OF HSCTs

More than 15 years have elapsed since the last formal assessments of the environmental impact of stratospheric, supersonic aircraft. The UARP asked Prof. Harold Johnston (University of California, Berkeley) to review the current understanding of aircraft emissions and their impact on the stratosphere. Prof. Johnston was one of the first scientists to point out the environmental danger that SSTs pose to the ozone layer (13), was a key figure in the Climatic Impact Assessment Program (CIAP), and continues to play an active role in assessing the effects of aircraft on the stratosphere (14). The UARP also requested a group of experts (including Prof. Johnston) under the chair of Dr. Anne Douglass (Goddard Space Flight Center) to expand the Johnston review into the group's consensus. The Johnston review (15) and the Douglass report (16) were published in January 1991.

AESA RESEARCH

NASA Research Announcement NRA-89-OSSA-16 "The Atmospheric Effects of Stratospheric Aircraft: Modeling and Measurement in Support of the High-Speed Research Program" was released in July 1989, and solicited proposals directed toward understanding and predicting the atmospheric effects of a projected fleet of stratospheric aircraft. Specific topics included:

1. Global stratosphere/ozone models (two-dimensional)
2. Aircraft emission scenarios
3. Three-dimensional chemical transport models
4. Plume chemistry and dispersion
5. Chemistry: fundamentals of gas-phase and aerosol reactions
6. Tropospheric chemistry models
7. Climate impact
8. Atmospheric observations and field campaigns

The second NASA Research Announcement (NRA-90-OSSA-20, August 1990) was similar to the first and extended the call for proposals: deadlines were November 1990 and May 1991. These NASA Research Announcements have solicited the participation of the international scientific community.

More than 45 proposals were received in response to the first NRA, and 23 scientific proposals were initially accepted as part of the AESA Program. Funding of atmospheric research began in early 1990. In response to the second NRA, over 35 proposals were received by the first deadline and a similar number by the final deadline. The principal investigators supported by HSRP/AESA are listed in Table 3, grouped by topic of research. Note that the HSRP atmospheric assessment consists of a hierarchy of theoretical models, laboratory experiments, and field measurements. Foreign investigators are welcome in the program and undergo the same peer review process that is applied to U.S. investigators. They cannot be directly supported by NASA funds; they are supported by their governments on a cooperative basis. It is the work of these principal investigators, currently participating in AESA studies, that serves as the primary basis for the present report.

A primary objective of the AESA studies is significant progress in improving and verifying the theoretical models of the atmosphere and, hence, a reduction in the uncertainties of current assessments. The models will be used on a regular basis to compare the relative impact of a set of projected emission scenarios, which will be defined through interaction of the AESA studies with other elements (e.g., market studies, combustor technology, etc.) of the HSRP. Based on the model predictions resulting from this program, it may be possible to optimize the emissions and operations of future aircraft fleets in order to minimize, and possibly avoid, detrimental impacts on the atmosphere. However, it should be noted that the goal of the HSRP is not to determine what levels of aircraft emissions and ozone loss are environmentally acceptable, but rather, more simply, to determine what atmospheric effects can be expected for given levels of engine technology and aircraft fleet operations.

FIRST PROGRAM REPORT

The chapter titles for this document indicate the scope of AESA studies. Much of this work has been reported previously at the Lower Stratospheric Measurement Issues Workshop conducted at the NASA Ames Research Center, Moffett Field, CA, in October 1990 or at the First HSRP/AESA Annual Meeting, Virginia Beach, VA, January 1991. A sound basis for the assessment activity was prepared in these early studies, and this document should serve as a foundation for future assessments. Future reports of AESA studies will be made regularly, and they will be coordinated with open scientific meetings sponsored by the HSRP.

Chapters 2, 3A and 3B provide parallel discussions of the range of chemical species emitted by aircraft and of what we know about the natural cycles of those species in the stratosphere today. Chapter 4 lays the basis for future scenarios for air travel and how that travel demand might be met by a mix of subsonic and supersonic fleets. The development of realistic, three-dimensional, time-varying scenarios for HSCT flights is critical to the overall assessment, which must also consider increases in the subsonic fleet and global changes in atmospheric composition and climate. Chapter 5 presents a preliminary assessment of the impact of an HSCT fleet on stratospheric ozone. These results must be considered principally as a sensitivity study, since they did not include a complete set of emissions (see chapter 2) and, further, the participating two-dimensional global ozone models have some known deficiencies. The results of a workshop on stratospheric measurements in support of HSRP/AESA (NASA Ames, October 1990) are presented in chapter 6. Chapter 7 contains brief, individual reports from the principal investigators supported by HSRP/AESA.

ACKNOWLEDGMENTS

We gratefully acknowledge the work of the scientists who authored and reviewed these chapters. The principal authors and contributors are listed on each chapter, and the reviewers are given in the appendix. The tireless efforts of Cindy Alami, Nancy Brown, Rose Kendall, Kathy Wolfe, and the staff of ARC Professional Services Group were essential in the editing and preparation of this document.

Table 3. AESA Principal Investigators

2-D Global Chemical Models and Stratospheric Ozone Assessment

G. P. Brasseur	NCAR
A. R. Douglass	NASA Goddard
R. S. Harwood	University of Edinburgh, United Kingdom
I. S. A. Isaksen	University of Oslo, Norway
M. K. W. Ko	AER, Inc.
J. A. Pyle	University of Cambridge, United Kingdom
R. K. Seals	NASA/Langley
R. L. Shia	AER, Inc.
D. J. Wuebbles	LLNL

3-D Chemical Transport Models and Longitudinal Asymmetry

G. P. Brasseur	NCAR
A. R. Douglass	NASA Goddard
R. A. Plumb	Massachusetts Institute of Technology
R. B. Rood	NASA Goddard
H. R. Schneider	AER, Inc.

Emissions, Plume Chemistry and Other Modeling

V. U. Khattatov	Central Aerological Obs., U.S.S.R.
C. E. Kolb	Aerodyne Research, Inc.
R. C. Miake-Lye	Aerodyne Research, Inc.
R. P. Turco	University of California, Los Angeles
G. K. Yue	NASA Langley

Laboratory and Theoretical Studies of Chemical Mechanisms

D. R. Crosley	SRI International
R. R. Friedl	JPL
M.-T. Leu	JPL
M. J. Molina	Massachusetts Institute of Technology
K. R. Ryan	CSIRO, Australia
M. A. Tolbert	SRI International
D. R. Worsnop	Aerodyne Research, Inc.

Atmospheric Observations and Field Experiments

J. G. Anderson	Harvard University
D. Baumgardner	NCAR
D. F. Blake	NASA Ames
D. W. Fahey	NOAA Aeronomy Lab
R. S. Hipskind	NASA Ames
J. S. Langford	Aurora Flight Sciences Corp.
D. M. Murphy	NOAA Aeronomy Lab
R. F. Pueschel	NASA Ames
P. Whitefield	University of Missouri, Rolla
J. C. Wilson	University of Denver
S. C. Wofsy	Harvard University

REFERENCES

1. CIAP, Climatic Impact Assessment Program, Report of Findings: The Effects of Stratospheric Pollution by Aircraft, DOT-TST-75-50, edited by A.J. Grobecker, S.C. Coroniti, and R.H. Cannon, Jr., U.S. Department of Transportation, Washington, D.C., 1974.
2. CIAP Monograph 3, The Stratosphere Perturbed by Propulsion Effluent, DOT-TST-75-53, U.S. Department of Transportation, Washington, D.C., 1975.
3. COMESA, The Report of the Committee on Meteorological Effects of Stratospheric Aircraft, 1972-75.
4. NAS, Environmental Impact of Stratospheric Flight: Biological and Climatic Effects of Aircraft Emissions in the Stratosphere, National Academy of Sciences, Washington, D.C., 1975.
5. COVOS, Final Report, Comite d'etudes sur les Consequences des Vols Stratospheriques, Activities, 1972 - 1976, Societe Meteorologique de France, Boulogne, France, 1976.
6. Oliver, R.C., Aircraft Emissions: Potential Effects on Ozone and Climate, Federal Aviation Administration, U.S. Department of Transportation, Final Report, FAA-EQ-77-3, March 1977.
7. McLean, F.E., Supersonic Cruise Technology, NASA SP-472, 1985.
8. Boeing Commercial Airplanes, High-Speed Civil Transport Study: Summary, NASA CR 4234, September 1989.
9. Douglas Aircraft Company, Study of High-Speed Civil Transports: Summary, NASA CR 4236, August 1990.
10. Wesoky, H.L., M.J. Prather, and G.G. Kayten, NASA's High-Speed Research Program: An Introduction and Status Report, SAE 901923, October 1990.
11. Watson, R.T., M.J. Kurylo, M.J. Prather, and F.M. Ormond, Present State of Knowledge of the Upper Atmosphere 1990: An Assessment Report, NASA Reference Publication 1242, September 1990.
12. Scientific Assessment of Stratospheric Ozone: 1989, World Meteorological Organization, Global Ozone Research and Monitoring Project, Report No. 20.
13. Johnston, H.S., Reduction of stratospheric ozone by nitrogen oxide catalysts from supersonic transport exhaust, *Science*, 173, 517-522, 1971.
14. Johnston, H.S., D. Kinnison, and D.J. Wuebbles, Nitrogen oxides from high altitude aircraft: An update of the potential effect on ozone, *J. Geophys. Res.*, 94, 16351-16363, 1989.
15. Johnston, H.S., M.J. Prather, and R.T. Watson, The Atmospheric Effects of Stratospheric Aircraft: A Topical Review, NASA Reference Publication 1250, January 1991.

16. Douglass, A.R., M.A. Carroll, W.B. Demore, J.R. Holton, I.S.A. Isaksen, H.S., Johnston, and M.K.W. Ko, The Atmospheric Effects of Stratospheric Aircraft: A Current Consensus, NASA Reference Publication 1251, January 1991.

51-45
64287

p.18
N92-19122

Chapter 2

High-Speed Civil Transport Aircraft Emissions

R. C. Miake-Lye
Aerodyne Research, Inc.
Billerica, MA

AE 171047

Contributors

J. A. Matulaitis, F. H. Krause, W. J. Dodds
GE Aircraft Engines
Cincinnati, OH

GG 100602

M. Albers and J. Hourmouziadis
MTU Motoren-und Turbinen Union
Munchen, Federal Republic of Germany

M 7279919

K. L. Hasel and R. P. Lohmann
Pratt & Whitney
East Hartford, CT

PO 869404

C. Stander and J. H. Gerstle
Boeing Commercial Aircraft Company
Seattle, WA

BR 798021

G. L. Hamilton
McDonnell Douglas Aircraft Company
Long Beach, CA

D1957175

ABSTRACT

Estimates are given for the emissions from a proposed high-speed civil transport (HSCT). This advanced-technology supersonic aircraft would fly in the lower stratosphere at a speed of roughly Mach 1.6 to Mach 3.2 (470 to 950 m/sec or 920 to 1,850 knots). Because it would fly in the stratosphere at an altitude in the range of 15 to 23 km commensurate with its design speed, its exhaust effluents could perturb the chemical balance in the upper atmosphere. The first step in determining the nature and magnitude of any chemical changes in the atmosphere resulting from these proposed aircraft is to identify and quantify the chemically important species they emit.

This chapter summarizes relevant earlier work, dating back to the Climatic Impact Assessment Program (CIAP) studies of the early 1970s and current propulsion research efforts at NASA and at its High-Speed Research Program (HSRP) contractors' laboratories. Recent work funded by HSRP is providing estimates of the chemical composition of an HSCT's exhaust, and these emission indices (EIs) are presented. Other aircraft emissions that are not due to combustion processes are also summarized; these emissions are found to be much smaller than the exhaust emissions. Future advances in propulsion technology, in experimental measurement techniques, and in understanding of upper-atmospheric chemistry may affect these estimates of the amounts of trace exhaust species or their relative importance, and revisions will probably be necessary in the future.

INTRODUCTION AND BACKGROUND

The upper atmosphere has been perturbed by anthropogenic chemicals. Most notable of these are the chlorofluorocarbons (CFCs), which are implicated in the depletion of stratospheric ozone and the creation of the Antarctic ozone hole. Because of the variety of technical advantages they offered, these chemically inert species were developed for industrial processes and consumer products before it was realized that they were photo-chemically reactive in the upper atmosphere. A full understanding of the detailed chemical balance and how it is affected by perturbations caused by pollutants is still being developed. Because of this awareness of the anthropogenic effects on the stratosphere, the exhaust emissions from the proposed HSCTs are being analyzed.

The exhaust species under most extensive scrutiny at present are the oxides of nitrogen, NO and NO₂, collectively denoted as NO_x. The potential for catalytic destruction of ozone by exhaust NO_x in the stratosphere was recognized (1) in the early 1970s, when the U.S. supersonic transport (SST) was being studied. The Climatic Impact Assessment Program (CIAP) was undertaken to consolidate and extend existing knowledge of the chemistry, physics, and technology of supersonic flight in the stratosphere and the effects of the consequential exhaust emissions. The results and conclusions of that program are summarized in its proceedings (2-5) and monographs (6-11). The state of knowledge and technology on aircraft emissions, as of 1975, is presented in the CIAP Monograph 2 (7), "Propulsion Effluents in the Stratosphere."

Aircraft propulsion technology has advanced in the intervening years such that the reasons the U.S. SST was not considered viable can now be addressed with technical improvements (12-14). The evolution of such technically improved engines has actually made NO_x reduction more difficult, as the combustor pressure and temperatures have risen to improve propulsion efficiency. Yet, reduction of NO_x levels below that achieved with SST-era technology appears to be necessary to avoid major stratospheric ozone depletion. To achieve this, combustors must be improved, requiring the results from current research aimed at controlling local temperatures and equivalence ratios throughout the combustion process. A pivotal ques-

14

tion concerns the quantitative effects on the atmosphere of the reduced levels of exhaust trace species emitted from the advanced-technology propulsion systems that would power the proposed HSCT.

The understanding of stratospheric chemistry and transport has also made enormous strides. The role of heterogeneous chemistry, in particular, was not apparent when commercial stratospheric flight was last considered. An awareness of chemistry on the surface of condensed water and/or condensed aqueous solutions has grown out of the need to understand the Antarctic ozone hole. Now, this heterogeneous chemistry must be accounted for in the global stratospheric chemical balance; it also must be assessed for a possible role in the wake of stratospheric aircraft. In the aircraft wake, the locally high (relative to ambient concentrations) trace-species concentrations may encounter condensed water in the condensation (contrails) in the exhaust behind the aircraft.

Additional data concerning condensation nuclei (CN) emitted by the aircraft are required for understanding the possible role of heterogeneous chemistry, both globally and in the wake. These CN are essential for the formation of contrails, and their number density affects the contrail particle sizes and number densities. The chemical nature of the CN surfaces controls their ability to condense water: typically, newly formed soot has a small fraction of its number density as active CN. The CN, in the form of ambient condensed sulfate particles, exhaust carbonaceous soot particles, and possibly other exhaust particulates are critical for initiating the condensation process that can occur, under some conditions, in the proposed stratospheric flight paths. Measurements of CN number densities and knowledge of their condensation properties are necessary to predict droplet lifetimes and settling distances and, thus, their role in wake chemistry and transport and in global stratospheric aerosol loading.

Once a condensed surface is present, additional chemical species must be accounted for, and additional chemical reactions occurring on the condensed phase/vapor interface must be introduced in the overall chemical balance. HNO_3 and N_2O_5 , formed by further reactions of NO_x , have been shown to figure prominently in the heterogeneous chemistry occurring in the polar stratospheric clouds that drive the Antarctic ozone hole. These species could also react with aerosols in the contrail, if and when concentrations of species and particles are high enough for sufficiently long durations.

The list of chemically relevant exhaust species now goes beyond the major combustion products of CO_2 and H_2O and the trace species NO_x . A fuller set of "odd-nitrogen" compounds, termed NO_y , including NO_x , NO_3 , N_2O_5 , HNO_3 , and (although not an exhaust species) ClONO_2 , must be considered as aerosol-active species, in addition to SO_2 and soot particles. The total unburned hydrocarbons (THC) and CO in the exhaust represent combustion inefficiencies and play a role in important stratospheric HO_x (OH , HO_2) chemistry.

The techniques used to measure these species will be discussed in the next section, followed by a brief summary of how engine emissions are being projected for the next generation of low NO_x , sustained supersonic propulsion systems. The projected estimates will be discussed in a following section and compared with past measurements on related, predecessor engines. Finally, a set of estimates for emissions from the aircraft that are not a result of the propulsion system will be reviewed.

MEASUREMENT APPROACHES

Quantitative measurements of exhaust emissions are carried out only in ground-based facilities. In fact, emissions have rarely been measured during aircraft flight, and then, only qualitative results were obtained (15-17). Ground-based measurements of entire engines must

be performed in a test facility that can reproduce ambient conditions, including pressure and temperature, if quantities appropriate to high-altitude flight are to be measured. Such tests are exceedingly expensive (18) and require considerable preparation and support, so there is strong motivation to perform simpler measurements on components of the engine separately in smaller laboratory-based facilities.

Primarily, these simpler measurements consist of reproducing the flow conditions in a trial combustor, or a simplified version of one, and making measurements at its exit. The flow into and out of the combustor can be calculated reliably for a chosen engine cycle. The more benign conditions encountered during laboratory component testing increase the accuracy of individual measurements.

Most gaseous species are measured using continuous-sampling probes that take a small volume of the exhaust-gas flow from the component to the measurement instrument, controlling the temperature and flow velocity, and thus the delay until time of measurement. The species currently being measured routinely include CO_2 , H_2O , CO , NO , NO_2 , SO_2 , and the THC (19-20), both as an undifferentiated sum of total C and as individual hydrocarbon species in more detailed batch sampling studies (21-23). Batch samples are analyzed using gas chromatography and/or mass spectroscopy to quantify the various hydrocarbon species present, as well as H_2 , O_2 , N_2 , CO , and CO_2 . Particulates, in the form of carbonaceous soot, have been a concern for decades; originally, attempts were directed toward reducing the visible smoke emitted with the exhaust. These particulate emissions have typically been reported as an SAE "smoke number" (SN) (20) that can be related to total particulate mass fairly reliably (24) but, when particle size distributions, number densities, and CN activity are needed, this approach to measurement is not adequate. More detailed sizing measurements have been performed (25), but are not routine.

Chemiluminescence detectors have been used to measure NO as well as NO_x . For NO_x measurements, the NO_2 fraction of the NO_x is first converted to NO , and the chemiluminescence generated when the net NO reacts with ozone is quantified (19). NO_2 is determined as the difference between an NO measurement and the corresponding NO_x measurement. NO_x measurements have conventionally been reported as the total mass of NO_2 , plus the mass equivalent of NO oxidized to NO_2 . Thus, NO_x is conventionally reported as the NO_2 gram equivalent of the total measured species (19,26), independent of the oxidation state (even though it is, typically, mostly NO near the exit of gas turbine engines). This convention, unfortunately, has not always been stated explicitly, generating some confusion in interpreting these numbers in the broader community. In this chapter, NO , NO_2 , and NO_x emissions will all be reported as gram equivalents of NO_2 . Generally, other NO_y species (e.g., HNO_3) have not been measured to determine whether significant levels are present.

While chemiluminescent NO_x measurements have been, and continue to be, the standard NO_x measurement technique, ultraviolet absorption measurements of NO were made as part of the CIAP program (27). A big discrepancy was observed between NO measured using absorption and NO_x quantified by collecting exhaust with a relatively crude probe and analyzing it with a chemiluminescent instrument; the UV absorption was as much as 4 to 5 times greater than the chemiluminescent NO_x measurement (28). This discrepancy was biggest in high-temperature and high-velocity flows such as those that would be encountered in the supersonic exhaust from any HSCT engine. Improvements in probe design and line-of-sight measurement methods may allow these differences to be resolved, but apparently there is no quotable reference study that addresses the discrepancies between optical and sampling measurements. Given the need for accurate and reliable emissions estimates for modeling the stratospheric impact of these vehicles, these differences must be understood and an optimal measurement strategy adopted.

Flame ionization has been used to quantify the THC, while nondispersive infrared techniques are used to measure CO, CO₂, and water vapor (19). The amount of SO₂ emitted is directly related to the sulfur content of the fuel and, thus, is not controlled by combustor design. When SO₂ is measured, a nondispersive ultraviolet technique is employed. The SAE SN is measured for particulates emissions by collecting particles as a known volume exhaust sample is drawn through a filter and quantifying the change in the filter's reflectance (20).

Radical species, particularly OH, may be chemically active in the exhaust leaving the engine nozzle. Although it is not one of the standard exhaust species usually reported, superequilibrium OH concentrations were measured in the exhaust of a turbojet for supersonic flight conditions during CIAP (27). The observed superequilibrium ratio was large (>10) in non-afterburning operation, but approached unity for afterburning cases. Thus, OH concentrations and chemical effects are expected to depend on engine configuration and cycles (duct-burning versus turbofan/turbojet). If an important role in exhaust chemical processing of NO_y and CN is established, some reliable measurement of OH would be necessary.

The measurement of a species in the exhaust flow determines its local concentration or mass fraction, but with the variety of combustor designs, engine cycles, and bypass ratios currently under consideration for these engines, different amounts of air end up in the exhaust for a given fuel flow rate. It has been convenient to normalize the emission rate, on a mass basis, of a given species by the mass flow rate of fuel. Thus, an emission index (EI X) is defined as

$$EI_{(Y)X} = \frac{(\text{g/s species X})}{(\text{kg/s fuel})} \quad (1)$$

Emissions expressed as volume fractions require conversion using species molecular masses (19) to arrive at an EI. For nearly complete combustion, calculation of an EI effectively normalizes by the rate of enthalpy addition to the air, as it passes through the engine.

The preceding subscript (Y) is not a standard notation, but it will be used in this chapter to indicate that the EI of species X is being reported as the mass equivalent of species Y. This notation resolves any possible ambiguities associated with reporting NO_x EIs and allows the reporting convention, in terms of NO₂, to be explicit. THC is also a mixture of compounds, and its EIs are reported in terms of CH₂, CH_α (where α is the fuel atomic hydrogen/carbon ratio) (19), or CH₄; the latter will be used here. A missing preceding subscript for a pure species will be taken to mean that its emission index is expressed in terms of its own mass, i.e., Y is identical to X. Clearly, EIs can only be meaningfully summed if the subscripts match.

It is worth emphasizing that the normalization used in defining the EI does not account for propulsion efficiency and so does not represent the best overall reduction of net emissions from an engine. For instance, if a particular scheme reduced EI_{(NO₂)NO_x} by 10% but required a 15% greater overall fuel flow rate to achieve the same thrust, there would be a penalty resulting from poorer fuel consumption as well as the increase in emissions. The Environmental Protection Agency parameter for landing-takeoff cycle conditions (29) represents a means of including the propulsion performance in the emissions estimation method. A similar approach could be used to compare engines in supersonic cruise operation for assessment of an HSCT's impact on the stratosphere.

Further, the total performance of the aircraft is not being considered; the most likely relationship is that a heavier aircraft results from emission reduction procedures (12-14). An increase in aircraft weight translates into more fuel burned and, thus, an increase in net emis-

sions for a given EI. Therefore, the net emissions from an HSCT will depend on the total aircraft design, not simply on an EI. On the other hand, combustor emissions performance will be optimized by lowering the important EIs and, since improved combustor design will lower NO_x emissions for any given propulsion system or airframe configuration, lowering EIs is a key factor in improving the overall emissions performance of an aircraft.

NO_x ESTIMATION METHODS

Extensive NO_x emissions measurements have been performed over the years on many engines and engine components. Development work is proceeding toward a "low NO_x" HSCT combustor, but a complete prototype engine is still a long way from the test cells. Estimates for the expected emission performance of a given design are calculated by using semi-empirical correlations that have been developed and refined in the past emission measurement programs. These correlations account for the experimentally observed pressure and temperature dependences of the net NO_x emission for a given combustor. Insofar as changes in combustor design do not alter the overall chemical kinetics, the correlations can be used to guide the combustor development efforts.

The essentially square-root dependence of EI(NO₂)NO_x on combustor pressure and the exponential dependence on combustor inlet temperature were used in correlations for CIAP work, and current correlations have evolved from them. Over the range of combustor designs measured to date, these dependencies have been demonstrated to fit the observed data well, with a single multiplicative coefficient reflecting a given combustor's overall emission performance. For example, GE Aircraft Engines (GEAE) uses a correlation:

$$EI_{(NO_2)}NO_x = 0.0986 \left[\frac{p_3}{1 \text{ atm}} \right]^{0.4} \exp \left(\frac{T_3}{194.4 \text{ K}} - \frac{H_0}{53.2 \text{ g H}_2\text{O/kg dry air}} \right) \quad (2)$$

for their "dual annular" low NO_x combustor for the NASA Experimental Clean Combustor Program (ECCP) (30). In the correlation, p_3 is the combustor inlet pressure, and T_3 is the combustor inlet temperature. The effect of ambient humidity H_0 is to reduce NO_x production, but at the low humidity levels encountered in the stratosphere, this correction will be negligible. GEAE's previous combustors used in the CF6 series engines are also approximated by this correlation, with the multiplicative constant (0.0986) increased by 25% and a constant value of 2.2 added to the entire expression for the CF6-80C, and a 35% increase and 1.7 added for the CF6-50C.

The coefficient of GEAE's correlation is affected by the specific combustor design, including the residence time that a parcel of reacting fluid remains within the combustor. This particular effect is included parametrically in the correlations of Pratt and Whitney and NASA by referencing a representative combustor velocity. These two correlations are the same, except that NASA's does not correct for water vapor effects; both include a reciprocal reference velocity, V_{ref} , dependence appropriate to the combustor flow and a dependence on T_4 , the combustor exit temperature, reflecting the temperature rise resulting from combustion heat release.

$$EI_{(NO_2)}NO_x \sim \frac{p_3^{0.5} T_4}{V_{\text{ref}}} \exp \left(\frac{T_3}{288 \text{ K}} - \frac{H_0}{53.2 \text{ g H}_2\text{O/kg dry air}} \right) \quad (\text{P\&W}) \quad (3)$$

$$EI_{(NO_2)}NO_x \sim \frac{p_3^{0.5} T_4}{V_{\text{ref}}} \exp \left(\frac{T_3}{288 \text{ K}} \right) \quad (\text{NASA LeRC}) \quad (4)$$

The general functional dependence of these correlations is shown in the figure below, where $EI_{(NO_2)NO_x}$ is plotted using the GEAE correlation for pressures from 10 to 14 atmospheres and temperatures between 770 K and 1000 K. Pratt and Whitney's and NASA's correlations have a similar functional form for reasonable values of T_4 , allowing for the combustion heat release and overall equivalence ratio. For $T_4 \sim T_3 + 1100$ K, a multiplicative constant can be chosen for the Pratt and Whitney NASA correlation so that the temperature and pressure dependences agree with the GE correlation within 5% to 10%.

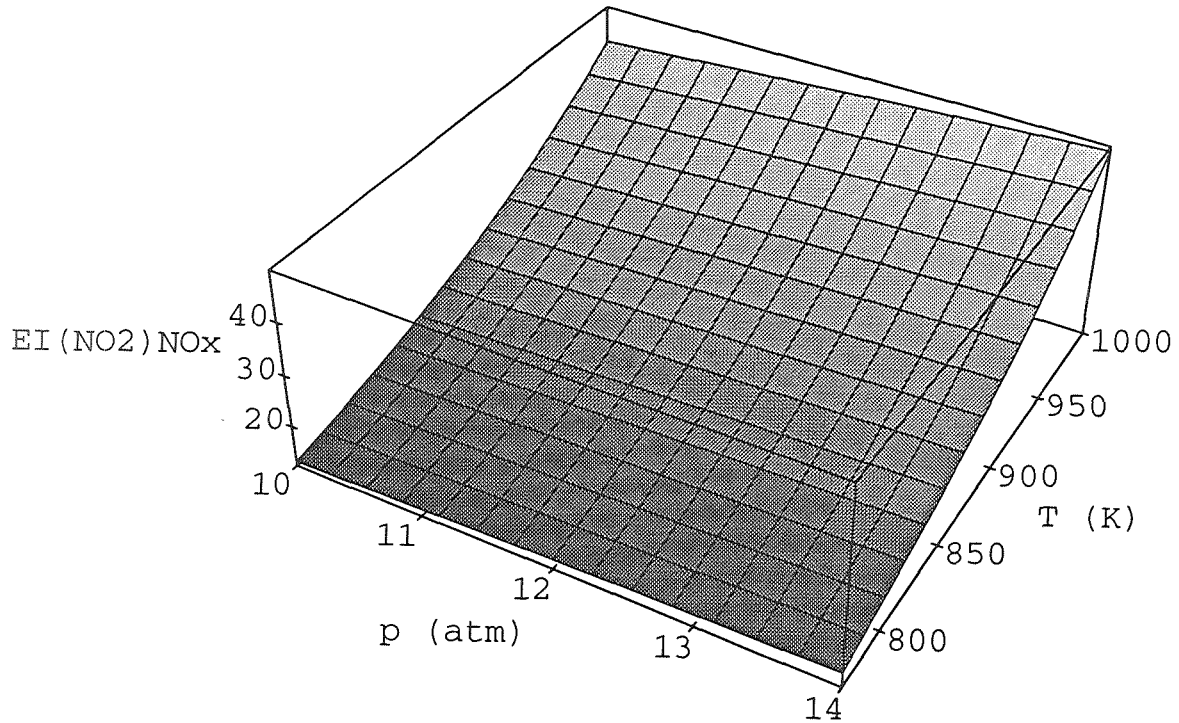


Figure 1. GEAE's correlation of $EI_{(NO_2)NO_x}$ as a function of $10 \text{ atm} \leq p_3 \leq 14 \text{ atm}$ and $770 \text{ K} \leq T_3 \leq 1000 \text{ K}$ for the ECCP technology combustor.

For estimating $EI_{(NO_2)NO_x}$ for the Lean, Premixed, Prevaporized (LPP) combustor, GEAE uses the correlation: (31)

$$EI_{(NO_2)NO_x} = t_{res} \exp\left(-72.28 + 2.8 T_{adia}^{0.5} - \frac{T_{adia}}{38.02}\right), \quad (5)$$

where t_{res} is the combustor residence time in milliseconds and T_{adia} is the adiabatic flame temperature expressed in kelvins.

These correlations are used to estimate the emissions performance of a combustor for conditions that have yet to be tested. Indeed, the most promising candidate NO_x reduction schemes have not yet been tested at the conditions expected in HSCT combustors. Promising experiments (32) indicate that advanced combustor concepts may achieve significant reductions at p_3, T_3 appropriate to HSCT engine cycles. However, this indication is based on experiments at less severe operating conditions extrapolated to the desired p_3, T_3 . Future experiments will clarify the performance of this combustor approach at the anticipated HSCT conditions and further test the correlations for an as-yet-uncalibrated technology.

EMISSION INDICES

Emission indices were measured for several engines intended for supersonic flight during the 1970s (18,33,34). Some of the results of this time period are shown in Table 1. Included are measurements of the engine of the one supersonic civilian transport that has operated commercially, the Olympus engine of the Concorde airplane. An important distinction must be made in comparing these EIs with those calculated for the proposed HSCT engine. The increased propulsion efficiency inherent in the designs for the HSCT dictates higher combustor inlet temperatures (and pressures) than were used in the 1970s engines. The amount of NO_x produced under these more severe conditions would be much greater than that measured in these earlier engines if the same combustor technology was used. Substantial improvements in the combustor design, improving the mixing, controlling the local equivalence ratio, and minimizing the residence time, are required to decrease the NO_x emissions relative to these engines while simultaneously maintaining the higher operating pressure ratios, and thus combustor inlet temperatures, necessary for the required cycle efficiency.

Table 1 also shows emissions measurements for two afterburning military turbojet engines (18,33,34). The measurements for the J58 engines were in preparation for the YF-12 in-flight NO_x field measurements. The study of these engines demonstrated trends of EIs versus altitude, fuel-air ratio, Mach number, and the presence or absence of afterburning for a specific engine. The optimized design of an engine designed to fly within a narrow range of flight conditions may not necessarily reflect all of these trends, however.

While it is significant that $\text{EI}_{(\text{NO}_2)\text{NO}_x}$ was reduced by a factor of ~ 2 during afterburning operation, this cannot be employed as a reduction method for HSCT propulsion. The reduction occurs because the afterburning fuel is consumed at lower pressure and temperature after expansion through the turbine, but this is coupled to increased EI CO, EI THC, and, most notably, substantial increases in specific fuel consumption and, possibly, more total NO_x produced. Increases in specific fuel consumption, in particular, could not be tolerated for sustained supersonic cruise in an economically viable commercial aircraft.

Table 1. Measured 1970s Supersonic Engine Emission Indices

Measured 1970's Supersonic Engine Emission Indices			
Species	Olympus 593 ¹⁸	YJ93-GE-3 ¹⁸	J58 ^{33,34}
CO	1.4 - 4.6	3.4 - 38.7	1 - 120
$(\text{NO}_2)\text{NO}_x$	17 - 20	1.81 - 12.03	2 - 20
$(\text{NO}_2)\text{NO}$	16 - 19	1.83 - 10.69	
NO_2	0.2 - 1.3		
$(\text{CH}_4)\text{THC}$		0.03 - 0.8	0.03 - 12

Pratt and Whitney's calculated emissions performance for their proposed Turbine Bypass Engine (35) is included in Table 2. General emissions levels are given, but engine cycles have been optimized to different degrees for each case so, for example, the fact that $\text{EI}_{(\text{NO}_2)\text{NO}_x}$ is slightly greater for Mach 2.4 should not necessarily be construed as indicative of greater NO_x emissions for that case. The changes in CO_2 and H_2O emissions at Mach 3.2 relative to the lower speeds are due to a fuel change. The higher-velocity flight conditions require a different fuel (JP-7 instead of the more commonly used Jet A) with a higher thermal stability

and a concomitant increase in the H/C and H₂O/CO₂ ratios. The soot/particulate EI is calculated from the SAE SN. This is a quantitative measure of particulate emissions, but is not based on direct measurement of the emitted particulate mass (20). The calculated emissions performance of GEAE's Variable Cycle Engine (36) is quantified in Table 3. The NO_x emissions were based on the correlation of equation 5.

Table 2. Pratt and Whitney Estimates for Engine Emissions Indices (35)

Pratt and Whitney Estimates for Engine Emission Indices ³⁵			
Species	Mach 1.6 18.3 km	Mach 2.4 19.8 km	Mach 3.2 21.3 km
CO ₂	3165.5	3165.5	3117
H ₂ O	1233	1233	1350
CO	1.1	1.3	1.9
(NO ₂)NO _x	5.3	6.4	5.1
(NO ₂)NO	4.5	5.4	4.3
NO ₂	0.8	1.0	0.8
SO ₂	1.0	1.0	1.0
soot/particulates	0.02	0.02	0.02
(CH ₄)THC	0.1	0.1	0.2
SAE Smoke Number	18.4	19.7	14.0
Fuel	Jet A	Jet A	JP-7

Table 3. GE Aircraft Engines Estimates for Engine Emission Indices (36)

GE Aircraft Engines Estimates for Engine Emission Indices ³⁶		
Species	Mach 2.4 16.8 km	Mach 3.2 21.3 km
CO ₂	3156	3135
H ₂ O	1240	1290
CO	< 5	< 6
(NO ₂)NO _x	5.7	7.0
(NO ₂)NO	5.1	6.3
NO ₂	0.6	0.7
SO ₂	1.2	1.2
soot/particulates	-	-
(CH ₄)THC	< 0.1	< 0.1
SAE Smoke Number	≪1	≪1
Fuel	Jet A	JP-7

MTU Motoren- und Turbinen-Union in Munich Germany estimates emissions performance of HSCT engines (37) for both existing and expected future technology as indicated in Table 4.

Table 4. MTU Estimates for Engine Emission Indices (37)

MTU Estimates for Engine Emission Indices ³⁷		
Species	Mach 2 14.8 - 18.2 km	Mach 3 19.9 - 23.6 km
Advanced Proven Technology		
CO	4.0	4.0
(NO ₂)NO _x	26 - 21	19 - 15
(CH ₄)THC	0.4	0.4
Future Technology (15 to 20 years)		
CO	2.6	2.6
(NO ₂)NO _x	11 - 9	8 - 7
(CH ₄)THC	0.3	0.3

In CIAP, consensus predictions were formulated (38) for exhaust emissions for anticipated emission reduction technologies to be used in the SST program. Those predictions were for technological development that was never pursued to the point of demonstration of its potential. However, they serve as a point of reference for current predictions and are included in Table 5. The last column in Table 5 gives the range of EIs under consideration for preliminary assessments.

The range of CO₂ and H₂O emissions is purely a function of fuel composition, changes in these emissions are related to changes in fuel composition that increase its thermal stability, as becomes necessary around Mach 3. SO₂ is also a function of the fuel itself, all the fuel sulfur is believed to be emitted as SO₂. Carbon monoxide and total unburned hydrocarbons (THC) emission estimates will have a broad range, as long as both duct burning and unaugmented turbojet or low-bypass turbofan options are being considered, but are nonetheless bounded by fuel consumption constraints for an economically viable vehicle.

NO_x emissions have the most extensive range, as well as the greatest possibilities for control within the operational envelope that an HSCT will function. The upper limit is conservative, in the sense that it uses an estimate made with the GE correlation for the GEAE/NASA ECCP combustor for which measurements have been made. The low value of 5 is not a firm prediction of future technology but, rather, an HSRP goal. These low values make use of extrapolations employing the correlations and basic laboratory data, sometimes using gaseous fuel experiments (31), to estimate the best performance foreseeable at this time. It is hoped that, in the course of the current HSRP effort, these ranges in particular can be narrowed.

AIRFRAME EMISSIONS

The exhaust from the engines represents the largest amount of material that is left in the flight path by an airplane. However, the exhaust species that are directly involved in ozone

Table 5. Estimates for HSCT EIs in the Stratosphere

Estimates for HSCT EIs in the Stratosphere			
Species	CIAP Turbojet ³⁸	CIAP Duct-burning ³⁸	HSRP/AESA Current Range
CO ₂			3120 - 3170
H ₂ O			1230 - 1350
CO	3	15 - 30	1.1 - 6
(NO ₂)NO _x	3 - 14	3 - 12	5 - 50†
(NO ₂)NO			4 - 45†
SO ₂			0 - 1
soot/particulates	0.02	0.02	—
(CH ₄)THC	0.1 - 0.5	3 - 10	<0.1 - 0.2

†The upper value represents existing proven technology that is not likely to be used in its current form in a future HSCT aircraft.

chemistry are trace species. Because they comprise a small fraction of the total exhaust mass, the relative amounts of other minor emissions from the proposed HSCT need to be quantified to evaluate their potential contribution to the total aircraft emissions. These additional airframe emissions, as distinguished from the engine emissions contained in the exhaust, originate from (1) aircraft systems involved in controlling or supporting flight operations and (2) passenger systems providing services on board. Estimates for these two classes of emissions for an HSCT will be made in the following subsections.

The various fluids carried on the aircraft could potentially leak from the vehicle and find their way into the atmosphere. In making the following estimates, some worst-case assumptions will be made by assuming that an estimate for a fluid loss corresponds to an emission into the stratosphere. In fact, lost fluid could remain primarily within the aircraft, and any portion that escapes may do so when the plane is on the ground or during takeoff, landing, or while passing through the troposphere. The emissions escaping the vehicle at high-altitude cruise could settle out of the stratosphere without vaporizing at the low temperatures (200-250 K) encountered. The estimates given are intended to provide a crude upper bound for the quantities of these species that might be released in the stratosphere. If any of these estimates suggests that an airframe emission species is important to stratospheric chemistry, more refined quantitation would be required to model its effects.

Since the exhaust emissions are reported as EIs in grams of emitted species per kilogram fuel burned, a comparison of those exhaust EIs and the aircraft emissions requires a correspondence relating these two quantities. Aircraft emissions are not caused by the consumption of fuel in any direct sense but, rather, are associated with (1) routine operation, and thus flight time or number of flights, or (2) random, unusual events that have some low frequency of occurrence. Conversion of these aircraft emissions to an equivalent emission index (EEI) will be made by using an estimate of the fuel burn rate appropriate for the generalized design of a Mach 2.4 HSCT aircraft and making the conversion from time to fuel mass.

Aircraft Systems

All the mechanical and electrical systems needed to control an HSCT in flight have not yet been designed in detail, so the amounts of materials carried on board or used during operation cannot be specified. Corresponding quantities from existing aircraft cannot be substituted without qualification, since particular systems can be highly configuration-dependent; beyond that, the HSCT is a substantially different vehicle from a subsonic aircraft; thus, its systems may differ significantly from those aircraft for which quantities are available. On the other hand, the types of systems needed are basically the same as those currently in use, and available information on existing aircraft can be used to provide crude estimates of emissions resulting from these sources.

The most ample fluid carried is, of course, the engine fuel. The economical use of fuel is a driving criterion in designing the aircraft, so little unburned fuel is allowed to escape from the aircraft. Fuel is dumped, very occasionally, if too much is carried for a safe landing, but this is an emergency measure performed when approaching a landing and the aircraft is below about 2 km. Thus, fuel is not dumped in the stratosphere. Fuel tanks may be vented during flight, releasing some vaporized fuel, and this may be a bigger factor for a supersonic aircraft with significant skin heating than it is for subsonic aircraft, but no estimate for such vapor loss has yet been obtained.

Hydraulic fluid is used to control mechanical devices in the aircraft, and regular maintenance requires replenishing the hydraulic system reservoirs. Boeing (39) estimates that regular seepage or leakage amounts to 20 gallons (70 kg) of hydraulic fluid (composed of phosphate esters) lost from the hydraulic systems per year per airplane. In addition, aircraft are designed with redundant hydraulic systems to ensure control in the event that one system fails. Failures are rare events; even so, an estimate of an average loss rate by Boeing (39) is 1 gallon (3 kg) per year per airplane as a result of system failure. (This is based on a loss of 6 gallons of fluid on average in an event that occurs 50 times in 10^6 flight hours, as extracted from reliability reports for existing subsonic commercial aircraft, and 3311 flight hours per year per airplane for these subsonic transports.) While it will be assumed that these 70 kg per year per airplane (or 2×10^4 kg/ 10^6 flight hours) of phosphate esters are deposited in the stratosphere, for the low-vapor-pressure hydraulic fluids especially, it is not likely that this emission could appear in the stratosphere as a chemically reactive species.

Oil is used as a lubricant for the engines as well as some auxiliary devices; infrequently, some oil is discharged after an accidental leak. Some oil/air mist may be vented from the oil reservoir tanks (40). Some oil is consumed within the engine as well: some is burned in the combustor, some exits with the exhaust. The emissions that result from oil consumed within the engine would be quantified in a measurement of the total exhaust emissions and, thus, in fact represent an engine emission that is indiscernible from the emissions caused by fuel consumption. It is worth noting, however, that as an engine ages, changes in oil consumption may result in changes in exhaust emissions as well.

Accidental leakage of oil, like that of hydraulic fluid, will not necessarily leave the aircraft, nor will any oil that leaves necessarily remain in the stratosphere. However, as an upper bound, Boeing (39) cites a value of five incidences in 10^6 flight hours, each releasing an average 20 kg of oil. This amounts to a loss of 0.3 kg per year per aircraft of a fluid composed primarily of long-chain aliphatic hydrocarbons, with trace additives of phosphate esters and metal compounds.

Other less quantifiable emissions (41) could arise from the venting of the lead-acid and/or nickel-cadmium batteries used for reserve power; this would result in negligible amounts

of H₂ and O₂ being released. (The amount of emissions resulting from mists of KOH and H₂SO₄ electrolytes would be even smaller and not likely to leave the aircraft.) Auxiliary power units (APUs) are small gas-turbine engines that would not be used in cruise typically and would emit much smaller amounts of an exhaust that is not unlike that from the main engines. Windshield washer fluid is more likely to be used at lower altitudes, and the glycol solution used is unlikely to result in even a small fraction of the "blue ice" emissions (see below). Finally, novel anti-icing techniques may make use of glycol solutions that would be carried on board, although not used in the stratosphere above hazardous clouds, but emissions from this fluid, too, are not expected to amount to any more than the "blue ice" fluids at stratospheric altitudes.

Passenger Systems

A variety of systems within the airplane's cabin are devoted to serving the passengers on board. Several refrigeration systems are typically available for air conditioning, refrigeration of food and drink in the galley, and sometimes cooling of avionics (more correctly categorized as an aircraft system requirement). Until replacement refrigerants are found, these systems will contain CFCs, and any leakage that exits the aircraft in the stratosphere will be depositing CFCs where they are photochemically active. Douglas (41) estimates that 0.2 kg per year per airplane is typically used to maintain a representative aircraft's refrigerant systems.

Galley cooling and avionics cooling do not necessarily require CFC-based refrigeration (recirculating liquids are currently employed in some situations), so the amount of refrigerant aboard a yet-to-be-developed airplane could be minimized, if direct deposition in the stratosphere must be minimized. In a similar vein, fire extinguishers on current aircraft contain halons (41), a source of bromine and chlorine when photochemically activated in the stratosphere. Whether there is any greater risk from stratospheric flight with CFCs and halons (or their replacements) than flight in the upper troposphere with existing aircraft would determine the need for replacement or tighter control of leaks and accidental release on board an HSCT. For long-lived halocarbons, the consequences of release in the lower stratosphere are not substantially different from release at the surface. Furthermore, the current Montreal Protocol will lead to the phase out of CFCs and halons by the year 2000, and thus, refrigeration and fire extinguishers on the HSCT fleet will use available alternatives.

Lavatory holding tanks have received some media attention over the past several years as a result of mishaps attributed to "blue ice," lavatory fluid that has leaked from the holding tank as a result of faulty maintenance, frozen in the cold atmosphere, and then broken free. This has caused damage to aircraft when it was ingested in the engine or to property on the ground after impact. From the point of view of safety, this is a major problem, and efforts have been made to eradicate totally any possibility of leakage. As far as emissions are concerned, the low (and probably decreasing) frequency of occurrence and the likely substantial descent before complete vaporization suggest that lavatory fluids will not contribute to total aircraft emissions in the stratosphere. Based on one incident involving 30 kg per 10⁶ flight hours, Boeing (39) estimates that less than 1 cup of fluid is lost per year per aircraft, using current reliability data.

For subsonic aircraft, oxygen service is available for passengers "in the event of sudden loss of cabin pressure." While this service is seldom used, some system leakage might occur from gaseous systems (42) (used for crew and perhaps passengers for high-altitude flight). Chemical O₂ generation packs (43), as used in many subsonic airplanes would only emit during use. Purity requirements for passenger respiration units limit Cl, CO, and CO₂ levels to 0.1, 20, 1000 ppmv respectively, so even if these units are used, only oxygen with trace impurities is released. However, oxygen is a major atmospheric constituent, and even a major release of gas from the emergency oxygen system could not affect stratospheric chemistry. The substantially lower static pressures in the stratosphere necessitate more sophisticated depressurization

safety measures for HSCTs. Potential emissions from such safety systems must be evaluated, particularly if they use fluids not already employed in other systems.

Calculation of Equivalent Emission Indices (EEIs) for Airframe Emissions

To compare the amounts of these airframe emissions with those from the engine, an EEI will be defined. Simply, the average emission amount in grams released in a given flight time will be divided by the total amount of fuel used during cruise in the same time period, i.e.:

$$EEI X = \frac{\text{average emission rate of X g/s}}{\text{fuel burn rate kg/s}} \quad (6)$$

Using the total of 3311 flight hours per year per aircraft for existing subsonic aircraft (as used above) to arrive at a mean emission rate from the subsonic reliability data, and taking a fuel burn rate of 9 kg/s as representative for Mach 2.4 flight, the emission estimates noted above can be converted to EEIs for HSCT cruise; these are listed in Table 6. Note that a similar value of 3100 stratospheric flight hours is considered representative for HSCT flight (39) as well. Again, it is assumed that all the lost fluids are emitted and vaporized in the stratosphere which, in many of these cases, is not likely to happen; so these quantities should be interpreted as upper-bound estimates.

Table 6. Upper Bound Estimates for Airframe Emissions in the Stratosphere

Upper Bound Estimates for Airframe Emissions in the Stratosphere		
Emission	kg / 10 ⁶ flight hours	Equivalent Emission Index
Aircraft Systems		
lubrication oil burst	1 × 10 ²	3 × 10 ⁻⁶
hydraulic fluid burst	1 × 10 ³	3 × 10 ⁻⁵
hydraulic fluid leaks	2 × 10 ⁴	5 × 10 ⁻⁴
fuel dump	n/a†	n/a†
fuel vent	no estimate	no estimate
Passenger Systems		
refrigerants	1 × 10 ²	4 × 10 ⁻⁶
'blue ice'	30	1 × 10 ⁻⁶

†Not applicable. Fuel is not dumped at stratospheric altitudes. Corresponding tropospheric quantities would be 3 × 10⁶ kg / 10⁶ flight hours, EEI = 0.1 (39).

Tables 2-4 show that the largest stratospheric emission from the airframe is substantially less than the smallest emission from the engine and several orders of magnitude less than NO_y emissions. Since the airframe emissions are upper-bound estimates, it appears that these airframe emissions can be neglected, relative to those from the engine. Two notable exceptions might be refrigerants and gaseous fire extinguishers; if these species are highly photochemically active, the effects of direct deposition in the stratosphere would need to be assessed. If there are no highly reactive catalytic effects from any of the other airframe emissions, it appears that their contribution to the net aircraft emissions can be neglected.

CONCLUDING REMARKS

Estimates have been provided for the emissions from a proposed HSCT in stratospheric flight. The emissions from the aircraft are expected to be dominated by the effluents from the engine; emissions from the airframe are probably negligible. Current estimates for the NO_x emissions have been calculated by engine companies for the proposed engine cycles using correlations that have been developed over the past several decades of NO_x reduction programs. These estimates will have to be validated with future tests of components and full engines as development proceeds.

More complete measurements of particulate size distributions and number densities, and of aerosol-active species, will be required if heterogenous chemistry is to be accurately modeled, both in the wake of individual airplanes and globally. New measurements of NO_y speciation will be necessary to catalog the "odd-nitrogen" emissions completely and to resolve uncertainties in measuring high-temperature, high-velocity exhaust gases with a sampling probe.

ACKNOWLEDGMENTS

The author would like to thank the contributors for their materials and discussions concerning their contributions and R. W. Niedzwiecki and J. D. Holdeman of NASA Lewis Research Center for references and useful discussions. Many useful comments and suggestions were received from the several reviewers of an earlier draft of this chapter.

REFERENCES

1. Johnston, H., Reduction of stratospheric ozone by nitrogen oxide catalysts from supersonic transport exhaust, *Science*, 173, 517-522, 1971.
2. Barrington, A.E., ed., Climatic Impact Assessment Program, Proceedings of the Survey Conference, February 15-16, 1972, DOT-TSC-OST-72-13, 1972.
3. Broderick, A.J., ed., Proceedings of the Second Conference on the Climatic Impact Assessment Program, DOT-TSC-OST-73-4, 1973.
4. Broderick, A.J., and T.M. Hard, eds., Proceedings of the Third Conference on the Climatic Impact Assessment Program, DOT-TSC-OST-74-15, 1974.
5. Hard, T.M., and A.J. Broderick, eds., Proceedings of the Fourth Conference on the Climatic Impact Assessment Program, DOT-TSC-OST-75-38, 1976.
6. CIAP Monograph 1, The Natural Stratosphere of 1974, DOT-TST-75-51, U.S. Department of Transportation, Washington, D.C., 1975.
7. CIAP Monograph 2, Propulsion Effluents in the Stratosphere, DOT-TST-75-52, U.S. Department of Transportation, Washington, D.C., 1975.
8. CIAP Monograph 3, The Stratosphere Perturbed by Propulsion Effluents, DOT-TST-75-53, U.S. Department of Transportation, Washington, D.C., 1975.
9. CIAP Monograph 4, The Natural and Radiatively Perturbed Troposphere, DOT-TST-75-54, U.S. Department of Transportation, Washington, D.C., 1975.
10. CIAP Monograph 5, The Impacts of Climatic Change on the Biosphere, DOT-TST-75-55, U.S. Department of Transportation, Washington, D.C., 1975.
11. CIAP Monograph 6, Economic and Social Measures of Biologic and Climatic Change, DOT-TST-75-56, U.S. Department of Transportation, Washington, D.C., 1975.
12. Boeing Commercial Airplane Co., High-Speed Civil Transport Study, NASA CR-4234, 1989.
13. Boeing Commercial Airplane Co., High-Speed Civil Transport Study - Summary, NASA CR-4234, 1989.
14. Douglas Aircraft Co., Study of High-Speed Civil Transports, NASA CR-4235, 1989.
15. Holdeman, J.D., Dispersion of Turbojet Engine Exhaust in Flight, NASA TN D-7382, 1973.
16. Farlow, N.H., V.R. Watson, M. Loewenstein, K.L. Chan, H. Hoshizaki, R.J. Conti, and J.W. Meyer, Measurements of Supersonic Jet Aircraft Wakes in the Stratosphere, Second International Conference on the Environmental Impact of Aerospace Operations in the High Atmosphere, American Meteorology Society, Boston, pp. 53-58, 1974.
17. Hoshizaki, H., et al., in CIAP Monograph 3, Chapter 2, 1975.
18. Broderick, A.J., et al., in CIAP Monograph 2, Chapter 4, 1975.

19. Aerospace Recommended Practice ARP 1256A, Procedure for the Continuous Sampling and Measurement of Gaseous Emissions from Aircraft Turbine Engines, SAE, 1980.
20. Aerospace Recommended Practice ARP 1179A, Aircraft gas turbine engine exhaust smoke measurement, SAE, 1980.
21. Spicer, C.W., M.W. Holdren, F.F. Lyon, and R.M. Riggin, Composition and Photochemical Reactivity of Turbine Engine Exhaust, ESL-TR-84-61, 1985.
22. Spicer, C.W., M.W. Holdren, S.E. Miller, D.L. Smith, R.N. Smith and D.P. Hughes, Aircraft Emissions Characterization, ESL-TR-87-63, 1988.
23. Stumpf, S.A., and W.S. Blazowski, Detailed Investigations of Organic Compound Emissions from Aircraft Gas Turbine Engines, *I.E.E.E. Annals*, No. 75CH1004-I-27-1, 1976.
24. Blazowski, W.S., and R.F. Sawyer, in CIAP Monograph 2, Chapter 3, 1975.
25. Low, H.C., C.J. Scott, and A. Veninger, Correlated Fuel Property Effects on an F402-RR-406A (Pegasus) Engine Combustor, ASME Paper 90-GT-276, 1990.
26. *Federal Register*, (July 17, 1973) Emission Standards and Test Procedures for Aircraft, Vol. 38, No. 136, 19088-19102; (July 22, 1974) Supersonic Aircraft Pollution, Vol. 39, No. 141, 26653-26655; (March 24, 1978) Control of Air Pollution from Aircraft and Aircraft Engines, Vol. 43, No. 58, 12614-12634; (December 30, 1982) Control of Air Pollution from Aircraft and Aircraft Engines; Emission Standards and Test Procedures, Vol. 47, No. 251, 58462-58474.
27. McGregor, W.K., B.L. Seiber, and J.D. Few, in the Second Conference on CIAP, 214-229, 1973.
28. Few, J.D., and H.S. Lowry III, Reevaluation of Nitric Oxide Concentration in Exhaust of Jet Engines and Combustors, AEDC-TR-80-65, 1981.
29. Jones, R.E., Gas turbine engine emissions, Problems, progress and future, *Prog. Energy Combust. Sci.* 4, 73-113, 1978.
30. Gleason, C.C., and D.W. Bahr, Experimental Clean Combustor Program (ECCP), NASA CR-135384, 1979.
31. Roffe, G., and K.S. Venkataramani, Emission Measurements for a Lean Premixed Propane/Air System at Pressures up to 30 Atmospheres, NASA CR159421, 1978.
32. Tacina, R.R., Low NO_x Potential of Gas Turbine Engines, AIAA paper 90-0550, 1990.
33. Holdeman, J.D., Exhaust emission calibration of two J-58 afterburning turbojet engines at simulated high-altitude, supersonic flight conditions, NASA TN D-8173, 1976.
34. Holdeman, J.D., Measurements of Exhaust Emissions from Two J-58 Engines at Simulated Supersonic Cruise Flight conditions, ASME paper 76-GT-8, 1976.
35. Hasel, K.L.; Pratt & Whitney, East Hartford, CT; personal communication.

36. Matulaitis, J.A.; GE Aircraft Engines, Cincinnati, OH; personal communication.
37. Albers, M., and J. Hourmouziadis, MTU, Munich, FRG; personal communication.
38. Grobman, J., and R.D. Ingebo, in CIAP Monograph 2, Chapter 5, 1975.
39. Gerstle, J.H., and C. Stander, Boeing, Seattle, WA; personal communication.
40. Dagget, D.; Rolls-Royce, Inc., Atlanta, GA; personal communication.
41. Hamilton, G.L.; Douglas Aircraft Co., Long Beach, CA; personal communication.
42. Aerospace Standard AS 8010A, Aviator's Breathing Oxygen Purity Standard, SAE, 1986.
43. Aerospace Standard AS 1304, Continuous Flow Chemical Oxygen Generators, SAE, 1973.

5245 (T)
64288

N92-19123²⁷

Chapter 3A

Natural Cycles, Gases

A. R. Douglass, C. H. Jackman
R. B. Rood, A. C. Aikin, and R. S. Stolarski
National Aeronautics and Space Administration
Goddard Space Flight Center
Greenbelt, MD

M. P. McCormick
National Aeronautics and Space Administration
Langley Research Center
Hampton, VA

D. W. Fahey
National Oceanic and Atmospheric Administration
Aeronomy Laboratory
Boulder, CO

NC999967

ND 210491

NJ920944

ABSTRACT

The major gaseous components of the exhaust of stratospheric aircraft are expected to be the products of combustion (CO_2 and H_2O), odd nitrogen (NO , NO_2 , HNO_3), and products indicating combustion inefficiencies (CO and total unburned hydrocarbons, THC). The species distributions are produced by a balance of photochemical and transport processes. A necessary element in evaluating the impact of aircraft exhaust on the lower stratospheric composition is to place the aircraft emissions in perspective within the natural cycles of stratospheric species. Following are a description of mass transport in the lower stratosphere and a discussion of the natural behavior of the major gaseous components of the stratospheric aircraft exhaust. The roles of soot and SO_2 are discussed in the next chapter.

MASS TRANSPORT IN THE LOWER STRATOSPHERE

The natural cycle of long-lived species is dominated by transport. A qualitative picture of the zonal and time averaged stratospheric transport was proposed by Brewer (1) to explain the observed sharp decrease in water vapor at the middle latitude tropopause. In this description, air rises in the tropics and is transported poleward and downward at middle and high latitudes. Transport from the troposphere to the stratosphere is limited to the tropics, where the tropopause temperatures are coldest. The temperatures are cold enough to produce saturation with respect to ice, and the ice particles fall. This freeze-dry mechanism thus provides a limit to the amount of water vapor that is allowed to enter the stratosphere. Although the water vapor measurements are even lower than would be allowed by the average temperatures of the tropical tropopause, indicating that the actual mechanism by which air enters the stratosphere is more complicated, this qualitative picture of mass transport is consistent with measurements of other species. Dobson (2) pointed out that this concept of a circulation (the Brewer-Dobson circulation) is consistent with ozone observations, which show the highest ozone concentrations in the polar stratosphere, away from the tropical source region. Observations of species such as N_2O , which have tropospheric sources and significant loss processes only in the mid to upper stratosphere, are also compatible with the Brewer-Dobson circulation.

Even though transport processes in the atmosphere are three-dimensional (3-D), two-dimensional (2-D) formulations provide a convenient conceptual framework to discuss global processes. Furthermore, 2-D models remain at the center of assessment calculations because they are computationally manageable. On the most basic level, stratospheric transport can be viewed as advection by a large-scale mass transport circulation such as the Brewer-Dobson circulation discussed in the previous paragraph. Coupled with this advective circulation is large-scale quasi-horizontal mixing caused by Rossby waves. The general characteristics of these two transport mechanisms are lucidly discussed by Mahlman (3).

Even though the 2-D framework does offer a useful format in which to discuss global transport processes, the mechanics of casting the 3-D circulation into two dimensions are not straightforward. Because of this, the best determination of the 2-D advective transport is not clear. The simplest idea is to use geometric zonal means about latitude circles to calculate a meridional and vertical velocity. This sort of averaging, termed the Eulerian mean, yields a meridional flow that is not like the Brewer-Dobson circulation. This difference between the expected mass flow and the Eulerian mean arises because of a compensating circulation that is driven by the planetary (Rossby) waves. This compensating circulation is a practical manifestation of the non-interaction theorem which states that planetary waves have no effect on the mean flow in the absence of transience, dissipation, or nonlinearity. While these constraints are never strictly met, there is a large compensation between the waves and the Eulerian mean flow, and hence, the advective mass circulation is a small residual that must be derived from two larger, competing terms.

34
~~PRECEDING PAGE BLANK NOT FILMED~~

Alternatives to the Eulerian mean have proven very effective in recasting the 2-D problem. These are discussed in some detail in chapter 6 of *Atmospheric Ozone 1985* (4). Theoretically, the most useful framework has proven to be the Lagrangian mean circulation. Averages in the Lagrangian mean follow wavy material tubes, and the Lagrangian mean velocity tracks this material tube. In the instance of the Eulerian circulation mentioned above, it is found that the Lagrangian mean circulation associated with planetary waves is an advective circulation directed opposite to the Eulerian zonal mean and with slightly greater magnitude. Dunkerton (5) showed that the Brewer-Dobson view of mass transport should be interpreted as a Lagrangian mean. Though the concept of the Lagrangian mean is useful theoretically, the necessity of averaging over wavy material tubes makes a Lagrangian mean model impractical.

Other estimates of the mean meridional circulation include the transport circulation, the diabatic circulation, and the residual circulation. Of these estimates, the residual circulation is the most frequently used because it is relatively simple to calculate from transformed Eulerian mean equations. These equations are derived by consideration of the large-scale equations of motion and combining the heat flux term with the Eulerian advective velocity, to yield a residual advective velocity. This procedure effectively captures some, but not all, of the characteristics of the noninteraction theorem. Comparisons of the Lagrangian mean and residual circulations for simple systems were discussed by Rood and Schoeberl (6), who showed differences between the two circulations on the order of 30%.

Residual circulation models have had considerable success in their representations of stratospheric constituent distributions. Calculations for species such as N_2O and column O_3 , using both Eulerian mean and residual circulation 2-D models, are in qualitative agreement with available global measurements (7). The fact that the residual circulation does offer an approximation to the mass flow of the atmosphere is useful in the discussions below. The transport effects of the planetary waves, "diffusive transport," constitute a complicated issue that will not be considered further here. Both chapter 6 of *Atmospheric Ozone 1985* (4) and Andrews et al. (8) offer more detailed discussions of transport processes.

A crucial issue for the High-Speed Research Program (HSRP) is the transport from the stratosphere to the troposphere. Exchange processes are discussed in detail in chapter 5 of *Atmospheric Ozone 1985* (4) and they are considerably more complicated than can be represented by 2-D transport descriptions. Accurate representations of convective processes and subplanetary scale eddies are essential ingredients of stratosphere/troposphere exchange. Three-dimensional models have not effectively dealt with these problems. The data record has only begun to identify and address the mechanisms of exchange. Aside from tropical convection, it is very likely that significant mass exchange is driven by quasi-horizontal eddies in latitudinally and longitudinally confined regions.

In a time-averaged global domain, the residual circulation can be used to provide at least a crude estimate of the mass exchange between the stratosphere and the troposphere. This can then be used to estimate stratospheric residence time and, hence, the relative perturbation to the background field caused by a pollutant. Consider a stratospheric volume bounded below by the tropopause, above by the 50 mb surface, and extending in latitude (ϕ) from 30°N to 90°N. The vertical mass flux, F , is calculated according to

$$F = 2\pi r_e^2 \int_{\phi = 30^\circ N}^{\phi = 90^\circ N} \rho_0 w^* d(\sin\phi) \quad (1)$$

where r_e is the radius of the earth (cm), ρ_0 is the density (g cm^{-3}), and w^* is the residual vertical velocity (cm s^{-1}) across the tropopause or the 50-mb surface. As noted previously, the estimate of mass exchange calculated using the residual circulation is incomplete because eddy transports are not included. There is additional uncertainty because the residual circulation is determined from the heating rate calculations in the lower stratosphere. The heating and cooling terms are nearly balanced, and the net heating from which the residual circulation is derived is small. Sensitivity of calculations to small changes in the heating rates is considered by Jackman et al. (9).

The value of F_{trop} is estimated to be $1.4 - 2.4 \times 10^{17} \text{ kg yr}^{-1}$. This estimate is based on an evaluation of two residual circulations, RC1 from the NASA/Goddard 2-D model (10) and RC2 from the model discussed by Shia et al. (11). These may be compared with the estimate of Holton (12) for the mass flux through the 100-mb surface of $1.3 \times 10^{17} \text{ kg yr}^{-1}$, and the minimum estimate of $1 \times 10^{17} \text{ kg yr}^{-1}$ given by Robinson (13). An extreme upper limit of $5.8 \times 10^{17} \text{ kg yr}^{-1}$ is obtained using a circulation RC3, which has larger values of the diabatic heating in the lower stratosphere. This is considered an extreme limit because of poor agreement between the annual variation of total ozone calculated using the RC3 circulation and Total Ozone Mapping Spectrometer (TOMS) measurements (9).

The downward vertical mass flux across the 50-mb surface is about $9 \times 10^{16} \text{ kg yr}^{-1}$ for RC1, RC2, and RC3. Because the vertical flux out of the layer exceeds the vertical flux into the layer, there must be poleward horizontal transport into the region across 30°N . The total mass in this region is about $21 \times 10^{16} \text{ kg}$; the outflow values cited previously imply a turnover time of 0.9 to 1.5 years for this northern-hemisphere segment of the lower stratosphere.

This simple model may be used for first-order estimates of the buildup of pollutants in the lower stratosphere resulting from aircraft exhaust. For any species with a continuity equation may be written for the stratospheric volume described in the previous section

$$\partial\chi/\partial t = [F_{\text{in}} \chi_i - F_{\text{out}} \chi] / M + P/M - L\chi \quad (2)$$

where F_{in} and F_{out} are the annual mass fluxes of air into and out of the region, χ_i is the mass mixing ratio of the incoming air-mass flux (F_{in}), M is the air mass of the stratospheric volume (kg), P is the total photochemical production rate (kg s^{-1}), and L is the averaged loss frequency (s^{-1}). In the presence of aircraft, there is an additional source (P_{aircraft}). At steady-state, $\partial\chi/\partial t = 0$, and the additional χ associated with the aircraft source is

$$\chi_{\text{aircraft}} = P_{\text{aircraft}} / (F_{\text{out}} + LM) \quad (3)$$

An upper limit estimate to χ_{aircraft} can be made by dropping the chemical term (LM). For fuel use of $7.7 \times 10^{10} \text{ kg yr}^{-1}$ and the outflow estimated above,

$$\chi_{\text{aircraft}} = (7.7 \times 10^7 \text{ EI}) / (1.4-2.4 \times 10^{17}), \quad (4)$$

where EI is the emission index (g/kg fuel). The conversion to volume mixing ratios, summarized in Table 1, is performed by scaling with the ratio of 29 over the mean molecular weight of the emitted species.

Table 1. Approximate Perturbations χ' to Stratospheric Trace Gases
(7.7×10^{10} kg of fuel/year)

Species	EI (gm/kg fuel)	Molecular weight	Background	Perturbation
CO ₂	3100	44	350 ppmv	0.7 - 1.2 ppmv
CO	5	28	10 - 50 ppbv	1.7 - 1.8 ppbv
H ₂ O	1200	18	2 - 6 ppmv	0.6 - 1.1 ppmv
NO _y	15	46	2 - 16 ppbv	3.0 - 5.2 ppbv

CARBON DIOXIDE (CO₂)

Carbon dioxide is a product of combustion and one of the major components of aircraft exhaust. The EI for CO₂ (chapter 1) is roughly 3100 g of CO₂ per kg of fuel. Carbon dioxide is chemically inert in the lower stratosphere, i.e., there are no significant photochemical production or loss processes. Measurements of the mixing ratio profile indicate little height dependence (14,15), which is expected in view of the steadily increasing tropospheric values. Current tropospheric measurements indicate a volume mixing ratio of about 350 ppmv (16). Assuming that this value is representative of the lower stratosphere, there are approximately 1×10^{14} kg in the bounded area described in the previous section. For an estimated fleet fuel usage of 7.7×10^{10} kg/yr, this corresponds to the source of CO₂ of 2×10^{11} kg yr⁻¹. The average increase in CO₂ over this volume is 0.7 to 1.2 ppmv (Table 1), less than 1% of the background level.

CARBON MONOXIDE (CO)

Carbon monoxide reacts in the lower stratosphere with the hydroxyl radical. The photochemical lifetime, taken from the NASA/Goddard 2-D model (10), is given in Figure 1. Although short lived in the upper stratosphere, the lifetime of CO in the lower stratosphere (1 to 4 years) is comparable to its turnover time (1 to 3 years). Carbon monoxide provides a measure of combustion inefficiency, and the estimated EI values are all less than 5 g of CO per kg of fuel. Although this source of CO ($< 3.8 \times 10^8$ kg/yr for 7.7×10^{10} kg of fuel) may be comparable to the natural source of CO (about 6.5×10^8 kg/yr for the bounded region, largely a result of methane oxidation), the long lifetime indicates that the perturbation will be controlled by mass flow through the region. If chemical effects are neglected, the expected perturbation to the volume mixing ratio is less than 2 ppbv, compared with the natural level in the lower stratosphere of 10 to 50 ppbv (Table 1).

WATER VAPOR (H₂O)

Water vapor is a product of combustion and an important component of aircraft exhaust. The normal H₂O mixing ratios in the lower stratosphere are low (3-5 ppmv), as will be discussed further in this section. The perturbation is estimated to be 0.6 - 1.1 ppmv, which is significant compared with the background values (Table 1). Because of its importance to the lower stratosphere, a more thorough examination of available data is warranted. Water vapor is the major source for odd hydrogen radicals in the stratosphere, generated through reactions with excited atomic oxygen O(1D). Odd hydrogen reactions contribute to the ozone loss throughout

the stratosphere and are most frequent in the lower stratosphere and mesosphere (17). They also modify the ozone destruction efficiency of odd nitrogen and odd chlorine compounds, making chlorine more effective and nitrogen less effective. The amount of water vapor incorporated in aerosols is potentially critically important for the efficiency of heterogeneous reactions (18,19,20), which may directly affect the balance of odd nitrogen and odd chlorine species in the lower stratosphere. The formation of polar stratospheric clouds, either nitric acid trihydrate or ice clouds, depends on the stratospheric temperature and on the amount of water vapor available. The most important photochemical process that affects stratospheric water is oxidation of methane (CH_4), which produces about half of the water vapor in the upper stratosphere. A detailed discussion of the photochemistry of CH_4 , the production of stratospheric H_2O , and the role of molecular hydrogen (H_2) is provided by LeTexier et al. (21).

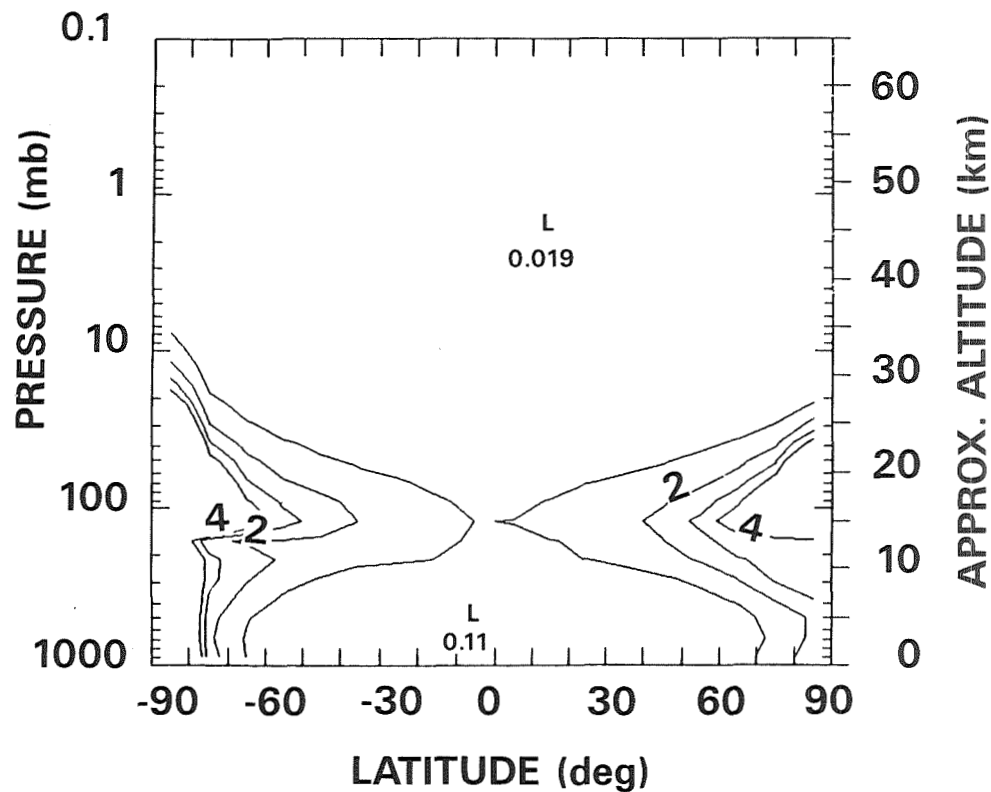


Figure 1. The photochemical lifetime of CO (years) (March) taken from the NASA/GSFC 2-D model.

Water vapor measurements have long been considered a useful indicator of stratospheric transport. Early sonde measurements of the water vapor profile showed a rapid decrease in the mixing ratio profile above the midlatitude tropopause. The measured values were substantially lower than the tropopause saturation mixing ratio at middle latitudes. The Brewer-Dobson circulation was proposed as an explanation for these observations (1,2). Rising air enters the stratosphere only in the tropics, where there is rising motion, and is transported poleward and downward at middle and high latitudes. The stratospheric water vapor mixing ratio is limited by the cold temperatures of the tropical tropopause. More recent measurements (22) have demonstrated the existence of a hygropause, a minimum in water vapor mixing ratio above the tropopause at 19-22 km between 30°N and 30°S.

Various techniques have been applied to the measurement of stratospheric water. These were reviewed by the WMO in 1986 (4). Although there are measurements of individual profiles that use assorted techniques, until recently balloon-borne frost point hygrometer measurements provided the most complete picture of annual behavior. In Figure 2, taken from Mastenbrook and Oltmans (23), the annual variation of water vapor (mass mixing ratio) is given for 1964-76 at Washington, DC (39°N, 77°W). The annual cycle near 50-100 mb is much weaker compared with the annual cycle near 150 mb. Similar behavior is seen for a data set taken at Boulder, CO (40°N, 105°W) for 1981-89 (Figure 3). In the lower stratosphere, near 70 mb, there is still a seasonal cycle, with a maximum value in the second half of the year. The seasonal motion of the tropopause is clearly visible, reaching a maximum altitude (i.e., highest H₂O) in August to September. The increase in mixing ratio with altitude indicates the production of H₂O from CH₄.

The first global measurements of water vapor were provided by the Limb Infrared Monitor of the Stratosphere (LIMS) experiment for the period November 1978 through May 1979 (24). The vertical resolution of the measurements is 4 km. At 50 mb, there is a pronounced latitudinal gradient, as shown in Figure 4, consistent with upward motion in the tropics. The gradient is much weaker at 10 mb. The magnitude of the annual variation is consistent with that derived from the frost point hygrometer measurements shown in Figures 2 and 3. Zonal mean profiles for each month during the LIMS period are given in Figure 5(a-g). These measurements are in general agreement with rising motion in the tropics, downward motion at the high latitudes, and a high-altitude source.

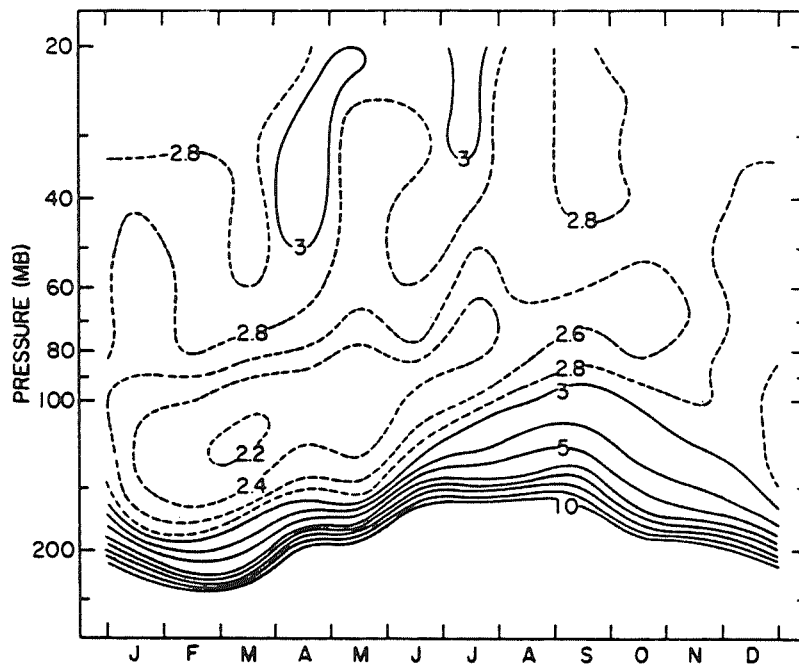


Figure 2. Annual variation of stratospheric water vapor (mass mixing ratio) based on balloon-borne frost point hygrometer measurements at Washington, DC, for the period 1974-76 (Mastenbrook and Oltmans [23]).

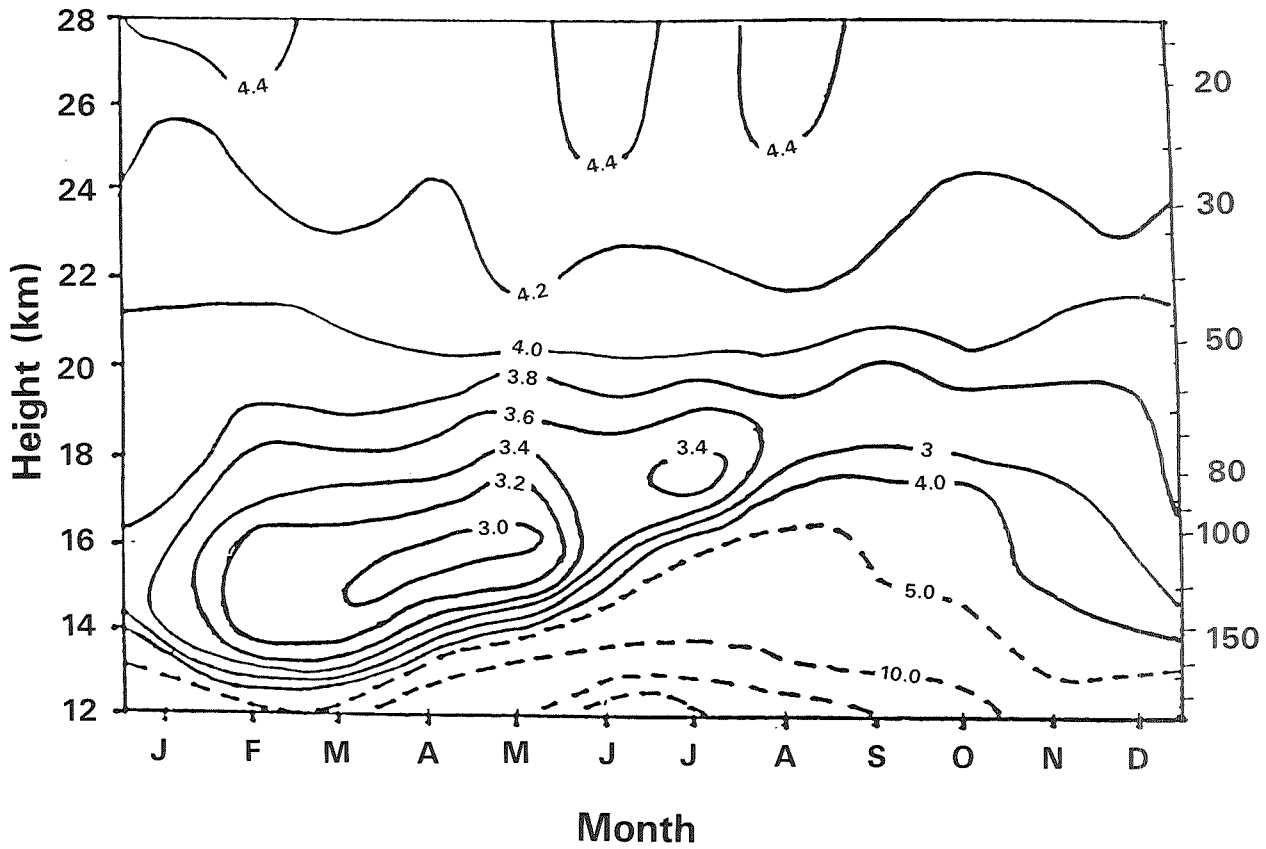


Figure 3. Annual variation of stratospheric water vapor (volume mixing ratio) based on balloon-borne frost point hygrometer measurements at Boulder, CO for the period 1981-89.

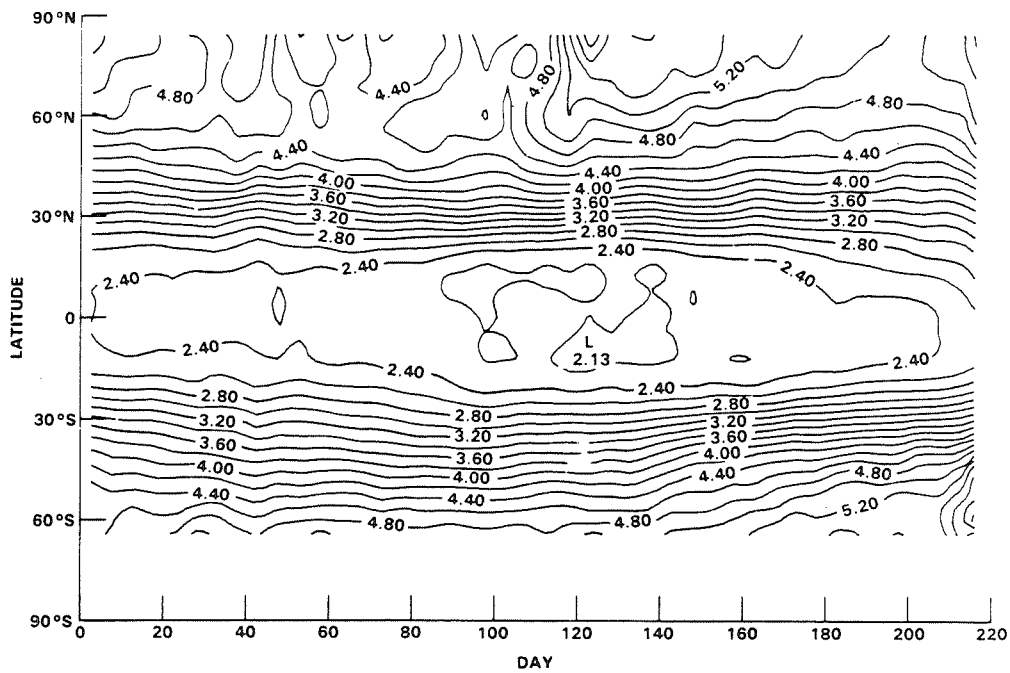


Figure 4. LIMS water vapor latitude versus time cross section at 50 mb (0.25-ppmv intervals, 5-day means).

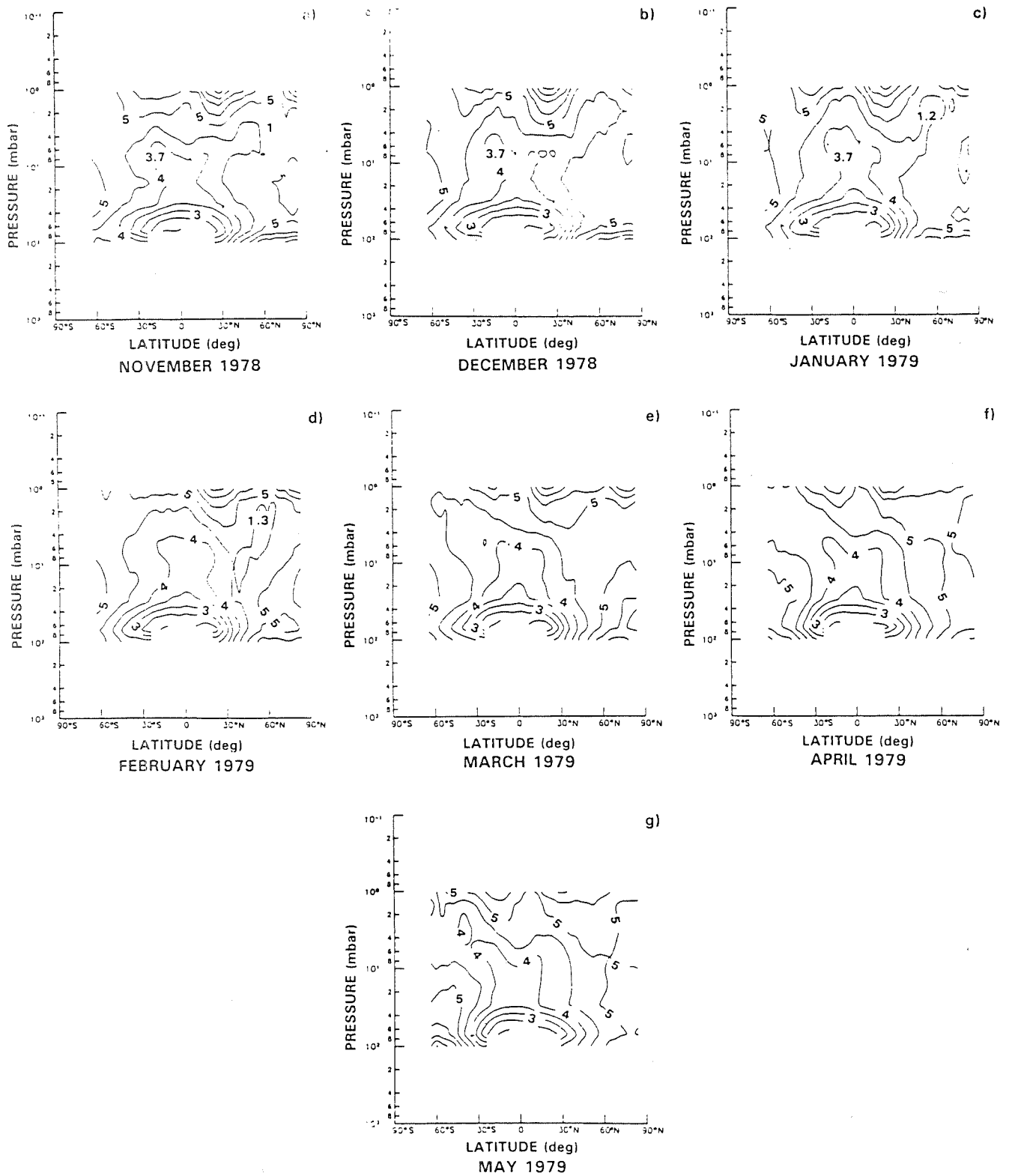


Figure 5. LIMS monthly zonal mean water vapor pressure versus latitude cross sections for (a) November and (b) December 1978 and (c) January, (d) February, (e) March, (f) April, and (g) May 1979 (0.5-ppmv contour intervals).

The Stratospheric Aerosol and Gas Experiment (SAGE II) aboard the Earth Radiation Budget Satellite was launched in 1984. The vertical resolution of this solar occultation instrument is 1 km. The SAGE II measurements provide a much longer data record than previously available, and furnish a picture of seasonal and year-to-year variability in the upper troposphere and stratosphere over much of the globe. The water vapor data, validation studies, and initial results are discussed by Rind et al. (25,26), Chiou et al. (27), Chu et al. (28), Larsen et al. (29), McCormick et al. (30), and Oltmans et al. (31). Validation studies conducted after the Sage II launch have included comparisons with correlative balloon-borne frost point hygrometer and a limited number of aircraft Lyman-alpha flights. Figures 6(a) and 6(b) are examples of comparisons with frost point measurements over Boulder and Lyman-alpha measurements over southern high latitudes, respectively.

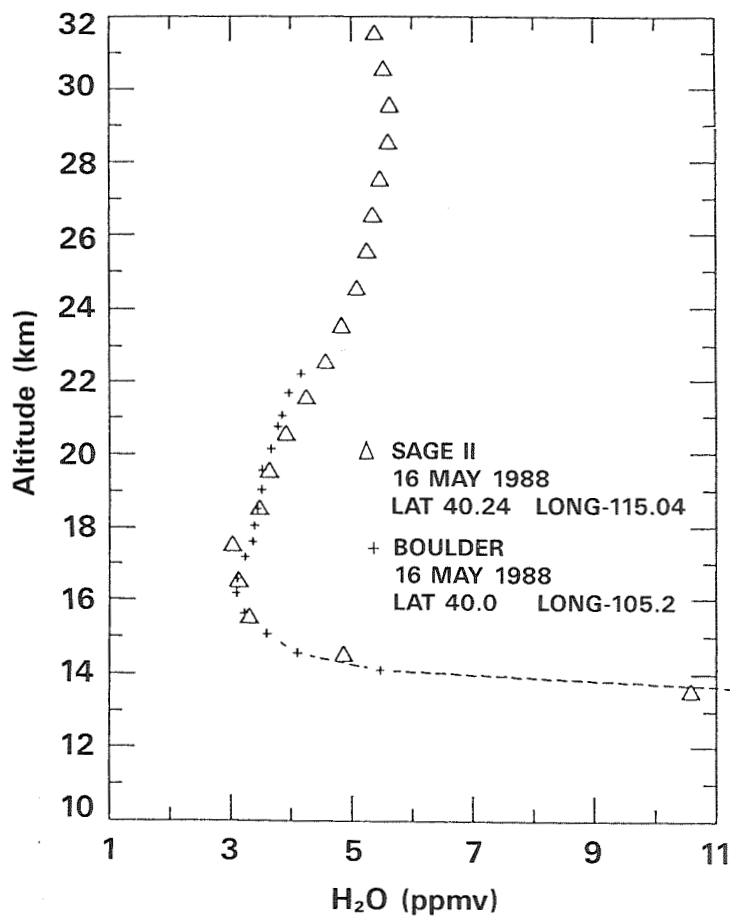


Figure 6(a). Comparison of SAGE II measurements with frost point hygrometer measurements near Boulder CO.

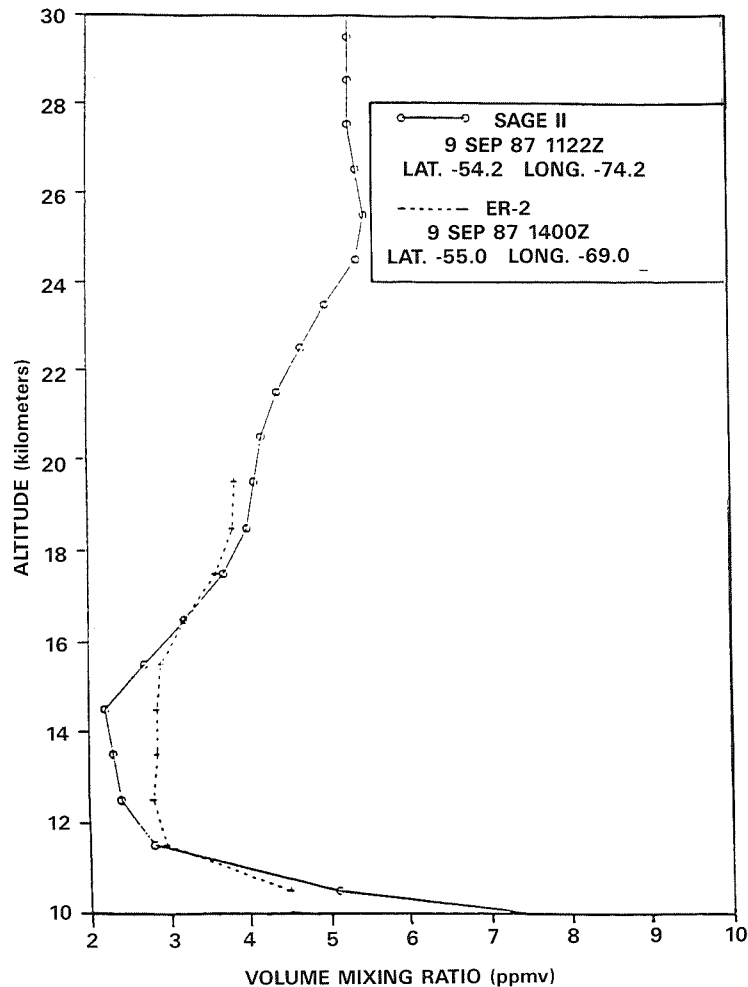


Figure 6(b). Comparison of SAGE II measurements with aircraft Lyman-alpha measurements at southern middle latitudes.

A time series of the average water-vapor-mixing ratio between 30° N and 40° N is given in Figure 7. There is excellent agreement between the seasonal pattern in the SAGE II data and the 7 years of balloon measurements made over Boulder (Figure 3). Both show a minimum in early winter near the altitude range 14-15 km. The minimum has its lowest value in March, and thereafter weakens and shifts to higher altitudes. The balloon data show that the magnitude of the seasonal variation near 100 mb at mid to high latitudes is smaller than might be expected based on the LIMS data, but the phases of the variations are similar.

The altitude-latitude cross section of SAGE II water vapor mixing ratios are given for May 1987 in Figure 8. The SAGE measurements are also consistent with the Brewer-Dobson view of mass transport and a high altitude source. These measurements compare well with the measurements in Figure 5(g) from the LIMS instrument.

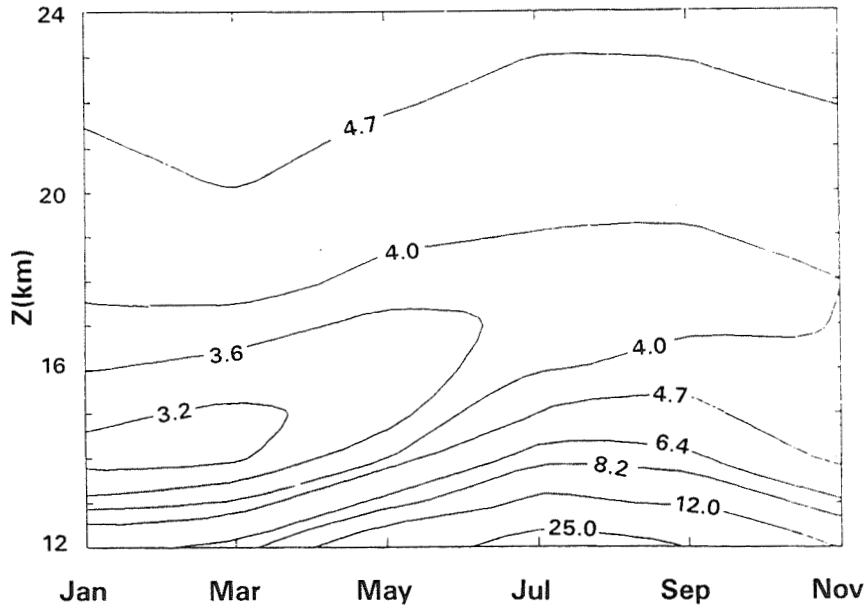


Figure 7. Annual variation of stratospheric water vapor (volume mixing ratio, ppmv) from SAGE II measurements, 1987, 30°N-40°N.

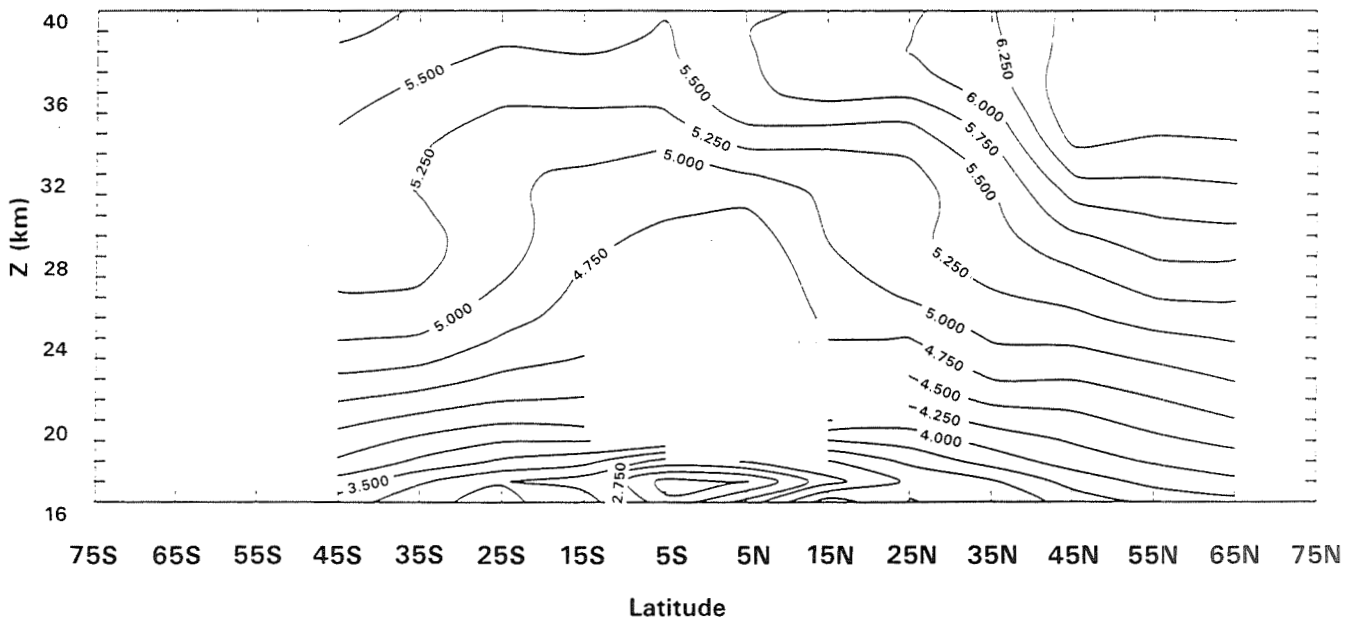


Figure 8. The latitude-altitude distribution of SAGE II measurements of water vapor (volume mixing ratio, ppmv) for May 1987.

ODD NITROGEN

Odd nitrogen species (primarily NO and NO₂) constitute an important trace component of aircraft exhaust. The anticipated perturbation to total odd nitrogen is significant compared with the normal background values, to be discussed later. Odd nitrogen species (total odd nitrogen = NO_y = N+NO+NO₂+NO₃+2*N₂O₅+HNO₃+ HNO₄+ClONO₂; NO_x = NO+NO₂+NO₃) are extremely important to the stratospheric ozone balance. Odd nitrogen is computed to account for about 50% of the total ozone loss below 40 km and between 60 and 90% of the ozone loss in the lower stratosphere (17). Although there are many measurements of individual odd nitrogen species, there are few measurements that can be interpreted as presenting a global picture of total odd nitrogen. The natural cycles must be derived from a combination of models and data. Following is a discussion of sources of stratospheric odd nitrogen, including nitrous oxide oxidation, galactic cosmic rays (GCRs), lightning (with upflux from the troposphere to the stratosphere), solar proton events (SPEs), relativistic electron precipitations (REPs), and dissociation of N₂ in the thermosphere (with downflux through the mesosphere to the stratosphere). Nuclear explosions, specifically above-ground detonations with energies above 1 megaton, also can produce large amounts of odd nitrogen in the stratosphere. The only loss processes for total odd nitrogen are recombination of N and NO in the upper stratosphere and mesosphere, and transport to the troposphere.

Natural Sources of Odd Nitrogen

The major source of stratospheric odd nitrogen results from nitrous oxide oxidation (N₂O + O[¹D] → NO + NO); several groups have computed globally averaged annual production rates (32-36). An example of the model computation of the odd nitrogen production rate from the oxidation of N₂O for March (dashed line) is given in Figure 9. This production rate was taken from a 2-D model computation wherein the N₂O levels were constrained by stratospheric and mesospheric sounder (SAMS) measurement, and the O₃ levels were constrained by measurement from the solar backscatter ultraviolet (SBUV) data [see Figure 9a, Jackman et al. (36)]. The global annually averaged production of odd nitrogen from this source is about 2.6 × 10³⁴ molecules yr⁻¹ and is compared with other odd nitrogen sources in Table 2.

Table 2. Comparison of Odd Nitrogen Sources and Sinks in the Stratosphere

Source	Magnitude (10 ³³ molecules yr-1)
Nitrous oxide oxidation N ₂ O + O(¹ D) → NO + NO	26.
Galactic cosmic rays	3.7 (solar minimum) 2.7 (solar maximum)
Lightning	11.
Solar proton events	1.5 (maximum in 1972)
Thermospheric downflux	?
Relativistic electron precipitations	?
Nuclear explosions	24. (1961 & 1962 nuclear tests)
High speed civil transport planes	14. (emission index = 15)
SINK	
Reforming of molecular nitrogen N + NO → N ₂ + O	8.4
Transport to the troposphere	32.

Galactic cosmic rays produce odd nitrogen in the lower stratosphere and upper troposphere. The earth's magnetic field influences the GCRs to a certain extent, such that more GCRs affect the atmosphere at higher geomagnetic latitudes. Galactic cosmic rays produce odd nitrogen through dissociation or dissociative ionization processes in which N_2 is converted to $N(4S)$, $N(2D)$, or N^+ (33,37,38). Rapid chemistry is initiated after N_2 dissociation, and most of the atomic nitrogen is rapidly converted to NO and NO_2 . The GCR mean production rate of odd nitrogen [solid line, taken from Figure 13 of Jackman et al. (36)] is compared with the oxidation of N_2O source in Figure 9. A solar cycle variation is apparent in the GCR flux. The stratospheric component of the odd nitrogen production is estimated to be a maximum of 3.7×10^{33} molecules yr^{-1} during solar minimum and a minimum of 2.7×10^{33} molecules yr^{-1} during solar maximum (33).

Natural production of odd nitrogen is dominated in the middle and upper stratosphere by N_2O oxidation and in the lower stratosphere at the higher latitudes by the GCRs. Since the odd nitrogen family has a lifetime of months in the middle and lower stratosphere, transport of odd nitrogen created at higher altitudes and lower latitudes is significant, and thus the GCR source of odd nitrogen has been computed to increase odd nitrogen in the lower stratosphere at high latitudes by only about 10% (37).

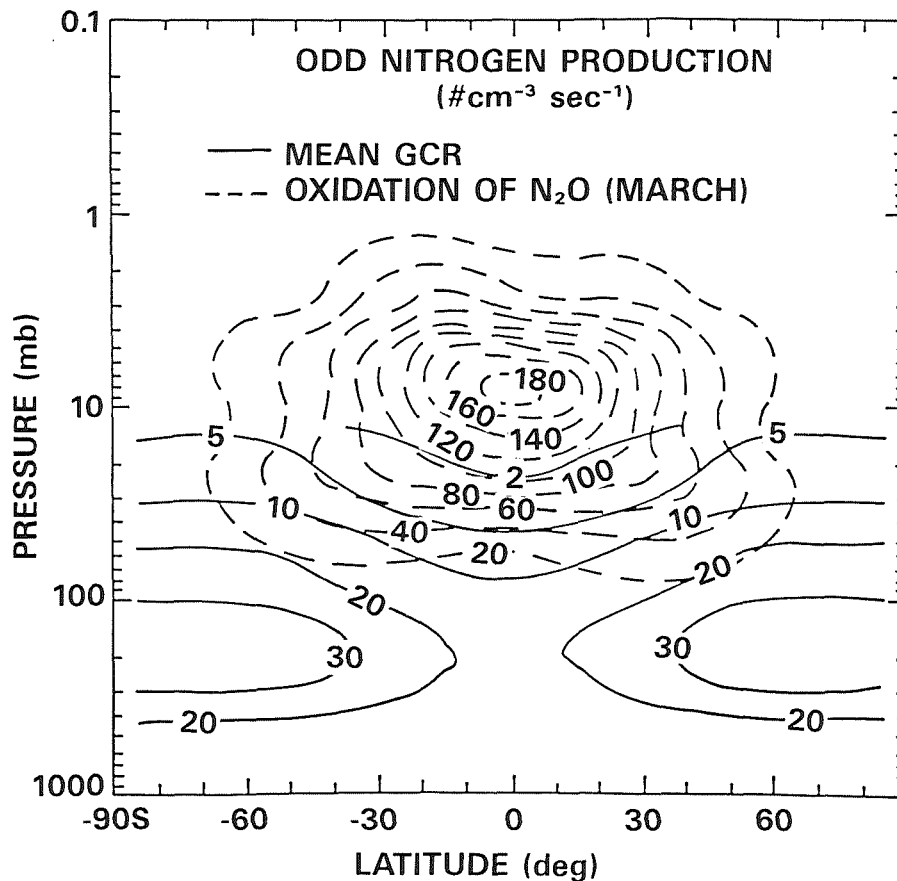


Figure 9. Odd nitrogen production (number $cm^{-3} sec^{-1}$) caused by GCRs (solid line, from Figure 13 of Jackman et al. (36) and oxidation of nitrous oxide (dashed line, from Figure 9 of Jackman et al. (36).

Lightning is responsible for the production of significant amounts of odd nitrogen (of order 3×10^{35} molecules yr^{-1}) from N_2 in the free troposphere (35, 39-43). This source, along with others of tropospheric NO_y , can reach the stratosphere through the transport of tropospheric air across the tropopause. For example, the model source of lightning designated "H2" by Ko et al. (35) transports 1.1×10^{34} molecules of NO_y yr^{-1} to the stratosphere when included in the NASA/Goddard 2-D model. Lower stratospheric background mixing ratios are increased substantially by including this lightning source. However, preliminary analysis of the STEP (Stratosphere Troposphere Exchange Project) data near the tropical tropopause show exceedingly low values of odd nitrogen (<0.5 ppbv). The correlation of odd nitrogen with N_2O found on the aircraft missions to both the Antarctic (AAOE, Airborne Antarctic Ozone Experiment) and the Arctic (AASE, Airborne Arctic Stratospheric Expedition) is also consistent with the view that air entering the stratosphere contains low concentrations of odd nitrogen (44a,44b).

The production of odd nitrogen species by SPEs was predicted and shown to affect upper-stratospheric ozone (45). Since solar protons generally are at lower energies than GCRs, they produce NO at higher altitudes; they are constrained more significantly by the earth's magnetic field and affect the atmosphere only in the polar cap region (geomagnetic latitudes greater than about 60°). SPEs are sporadic, with durations up to several days; more SPEs occur close to the solar maximum.

The increase in polar NO after the July 1982 SPE was inferred to be about 6×10^{14} NO molecules cm^{-2} (4.1×10^{32} molecules NO_y) at polar latitudes from the SBUV instrument (46), in good agreement with the calculated NO increase of 7×10^{14} NO molecules cm^{-2} (4.8×10^{32} molecules NO_y) in the polar cap (47). The August 1972 SPE was one of the biggest events in the past 30 years, and computations revealed that a substantial production of odd nitrogen (1.5×10^{33} molecules NO_y) was associated with this event at polar latitudes in the middle to upper stratosphere (47).

The influence of extreme ultraviolet, auroral electrons, and photoelectrons on the odd nitrogen budget of the stratosphere, through transport of odd nitrogen from the thermosphere downwards through the polar mesosphere to the upper stratosphere, has been studied by several groups (33,38,48-56). EUV, auroral electrons, and photoelectrons are capable of dissociating N_2 to form atomic nitrogen in the thermosphere. Transport of this odd nitrogen to the mesosphere and upper stratosphere is possible, but certain conditions must be present. The lifetime of odd nitrogen in the sunlit mesosphere is short, and it is only during the long period of polar night at high latitudes, when a period of several weeks of darkness is typical, that significant downward transport is possible. Solomon et al. (51) undertook a detailed 2-D model study of thermosphere-middle atmosphere coupling. Enhancements in the odd nitrogen distribution in the mesosphere and upper stratosphere were found to occur when the thermospheric production of odd nitrogen was included [compare Figures 8 and 17 of Solomon et al. (51)]. These enhancements of NO_x in the middle atmosphere, caused by thermospheric downflux of odd nitrogen, are especially significant in the hemisphere that was most recently polar night. Measurements by the LIMS of NO_2 have also indicated that odd nitrogen may be enhanced in the mesosphere and, to a lesser degree, in the upper stratosphere during polar night (55). The magnitude of the thermospheric downflux of NO_x into the stratosphere is highly uncertain and variable, but probably small.

In the past 15 years, it has been proposed that REPs make important contributions to the polar odd nitrogen budget of the mesosphere and upper stratosphere (57-62). The frequency and flux spectra of these REPs is still under discussion. Baker et al. (59) show evidence of large fluxes of relativistic electrons at geostationary orbit measured by the Spectrometer for Energetic Electrons (SEE) instrument on board spacecraft 1979-053 and 1982-019. REPs, which are actually depositing energy into the middle atmosphere, have been measured by

instruments aboard sounding rockets (63). These rocket measurements have typically indicated much smaller fluxes of relativistic electrons than measured by the SEE instrument. REPs that display the large fluxes measured by Baker et al. (59) are computed to show an important influence on the NO_y budget in the lower mesospheric-upper stratospheric region by Callis et al. (62). However, REPs with the smaller fluxes measured by Goldberg et al. (63) would cause a relatively insignificant change in odd nitrogen amounts in the middle atmosphere at this production rate. More work is necessary to determine which REP events are more typical. The global magnitude of the REP source of stratospheric odd nitrogen is also highly uncertain but probably small.

Sources of Odd Nitrogen Related to Human Activity

The natural source of odd nitrogen is increasing because the source gas, N_2O , is increasing. The global rate of increase of N_2O is about 0.7 ppbv yr^{-1} ; the global average concentration is currently above 308 ppbv (16). At this rate of increase, assuming a linear increase in N_2O at all altitudes, the natural source of odd nitrogen will increase by 10% in 40 years. For comparison, the source of NO_y from stratospheric aircraft for with EI of 15 and $7.7 \times 10^{10} \text{ kg of fuel yr}^{-1}$ is 1.4×10^{34} molecules yr^{-1} , nearly 40% of the natural source.

Atmospheric nuclear explosions, affecting the 7-to 30-km regime, cause sufficiently high temperatures in the fireball that thermal decomposition of N_2 and O_2 occurs, followed by the formation of NO (64-66). The nuclear tests in 1961 and 1962 by the Soviet Union and the United States were thought to be responsible for the production of 2.4×10^{34} molecules of odd nitrogen (16).

Sinks of Odd Nitrogen

There are two major sinks for odd nitrogen in the stratosphere: the recombination of N and NO in the middle to upper stratosphere, to form N_2 and O, and transport to the troposphere. Nitric oxide (NO) is photodissociated easily in the upper stratosphere, forming atomic nitrogen (N) and atomic oxygen (O). Some of this N then reacts with NO, to form molecular nitrogen (N_2); the rest reacts with O_2 to reform NO. The lower stratospheric odd nitrogen abundance is principally regulated by transport of odd nitrogen to the troposphere, with subsequent rainout of the HNO_3 and HO_2NO_2 constituents [see Jackman et al. (36)].

The global annually averaged loss for the first process is about 8.4×10^{33} molecules yr^{-1} (Jackman and Douglass, 2-D model computation, 1990). The remainder of the globally averaged production is balanced by the transport of stratospheric odd nitrogen to the troposphere ($4.0 \times 10^{34} - 0.8 \times 10^{34} = 3.2 \times 10^{34}$), the dominant loss mechanism for stratospheric odd nitrogen. Thus the amount of odd nitrogen in the lower stratosphere depends critically on the circulation in the lower stratosphere and stratosphere/troposphere exchange.

Odd Nitrogen Distribution

The global distribution of total odd nitrogen may be calculated using a 2-D model, keeping in mind that the model transport in the upper troposphere/lower stratosphere is important to determining distribution and residence time of total odd nitrogen. Although there are no global measurements of total odd nitrogen, Callis et al. (67) estimate total odd nitrogen from nighttime LIMS measurements of NO_2 and HNO_3 . Using a model, they show that this sum represents 68, 78, 85, and 90% of total odd nitrogen at, respectively, 28, 34, 37, and 40 km. The estimate from LIMS for March (Figure 10) can be compared to the calculations of the Jackman and Douglass model (Figure 11), or to several model distributions given by Jackman et al. (7). Although the data represent a lower limit because all species are not included, notably

N_2O_5 , the model values are somewhat lower than the measurements in the lower stratosphere. It should be noted that the lower stratospheric LIMS values of NO_2 depend on the NO_2 climatology used in the retrievals resulting from a loss of NO_2 signal from altitudes below 40 mb (68). Thus the LIMS data can provide constraints on the odd nitrogen species but do not provide a direct measure of NO_y .

In situ measurements of total odd nitrogen taken aboard the NASA ER-2 aircraft provide several points for direct comparison between models and data. The ambient total odd nitrogen is measured by catalytic conversion of the higher-oxide species to NO and subsequent detection of NO in the chemiluminescent reaction with reagent O_3 . All odd nitrogen species of importance in the stratosphere are included in this technique (69). Although measured odd nitrogen in the lower stratosphere and upper troposphere has substantial natural variability on a wide range of scales, the data are sufficient to derive representative averages at some locations and seasons. Extensive measurements in the winter hemispheres near $55^\circ S$ and $60^\circ N$ show odd nitrogen values less than 0.5 ppbv in the troposphere, up to about 10 km altitude, increasing to about 3 ppbv near 16 km and to about 8 ppbv near 20 km (70,71). Values of 3 to 8 ppbv between 19 and 21 km were measured near $40^\circ N$ in October (72). Measurements near $10^\circ S$ in January and February gave tropospheric odd nitrogen values similar to those measured at high latitudes but significantly lower values in the lower stratosphere. Odd nitrogen values near $10^\circ S$ increase from about 0.5 ppbv near the tropopause to about 2.5 ppbv near 21 km (73). The model values in Figure 11 underestimate the measured total odd nitrogen. Previous ER-2 NO measurements have suggested this discrepancy (4,74). The ATMOS (Atmospheric Trace Molecule Spectroscopy) measurements of total odd nitrogen are as much as 40% larger than the results from some model calculations for the lower stratosphere (75).

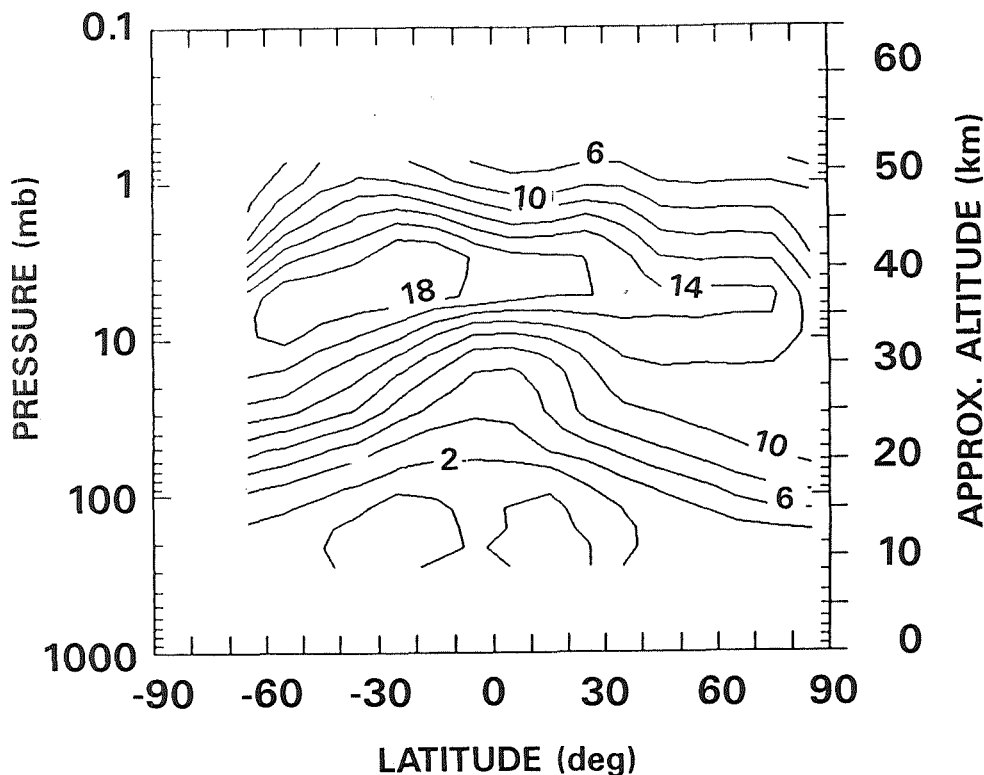


Figure 10. LIMS nighttime $HNO_3 + NO_2$ for March 1979, a lower limit for total NO_y .

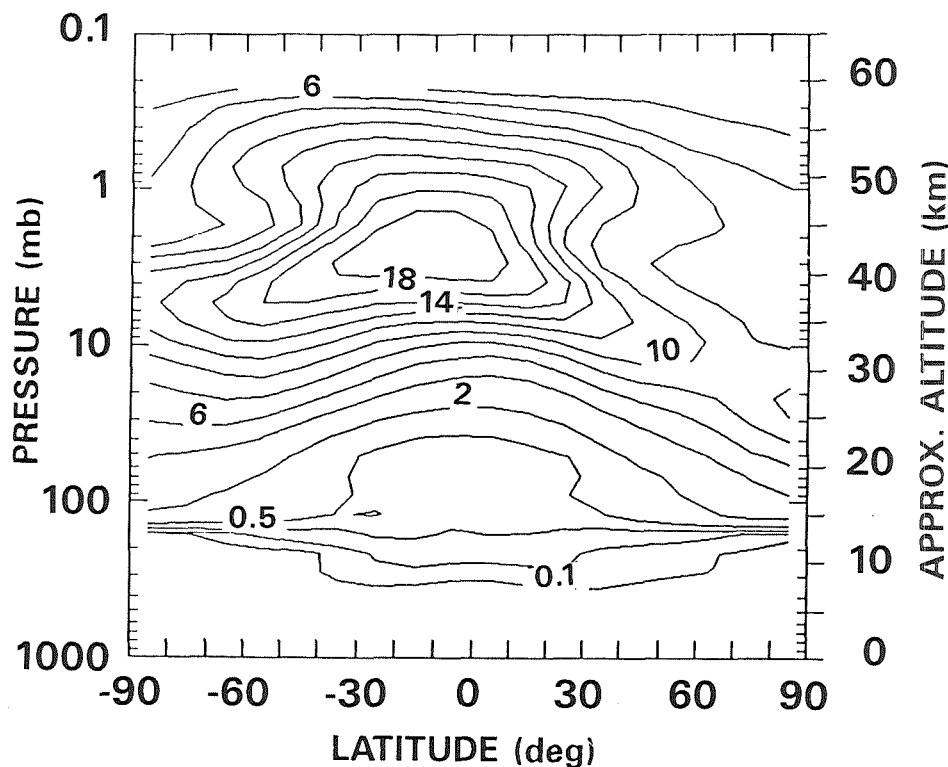


Figure 11. A 2-D model calculation of total odd nitrogen (March).

Partitioning of Odd Nitrogen Species

The lifetimes for interchange reactions among key odd nitrogen species, calculated from the NASA/Goddard 2-D model, are given for March equinox in Figure 12. Once HNO_3 is formed in the lower stratosphere, it is relatively long lived (> 50 days for middle and high latitudes). The lifetime of N_2O_5 is short, except in high latitudes in winter. The equilibrium between NO and NO_2 is established quickly; thus, the fractions of NO and NO_2 in the aircraft exhaust are not important for assessment calculations. Some studies have likewise shown an insensitivity to the relative partitioning between NO_x and HNO_3 in stratospheric injections, but this is not likely to be the case for tropospheric emissions.

However, the current understanding of odd nitrogen chemistry in the lower stratosphere does not explain all of the observations. For example, measured values of wintertime HNO_3 exceed model calculated values (35). Some investigators have suggested that the heterogeneous reaction of N_2O_5 on polar stratospheric clouds (PSCs) in the polar vortex may produce the observed values (76). Rood et al. (77) have found, with 3-D model calculations, that there is insufficient mixing between the polar vortex and middle latitudes to account for the HNO_3 deficit. Measurements of reaction rates show that $\text{N}_2\text{O}_5 + \text{H}_2\text{O}$ reactions occur on sulfuric acid, even though some of the other processes that occur on PSC surfaces (e.g., $\text{HCl} + \text{ClONO}_2$) do not (18). Hofmann and Solomon (78) suggested that such heterogeneous reactions on background aerosols could account for the observations. These processes are important for understanding the natural balance of HNO_3 and NO_x . The potential impact of aircraft exhaust on stratospheric ozone is sensitive to this balance.

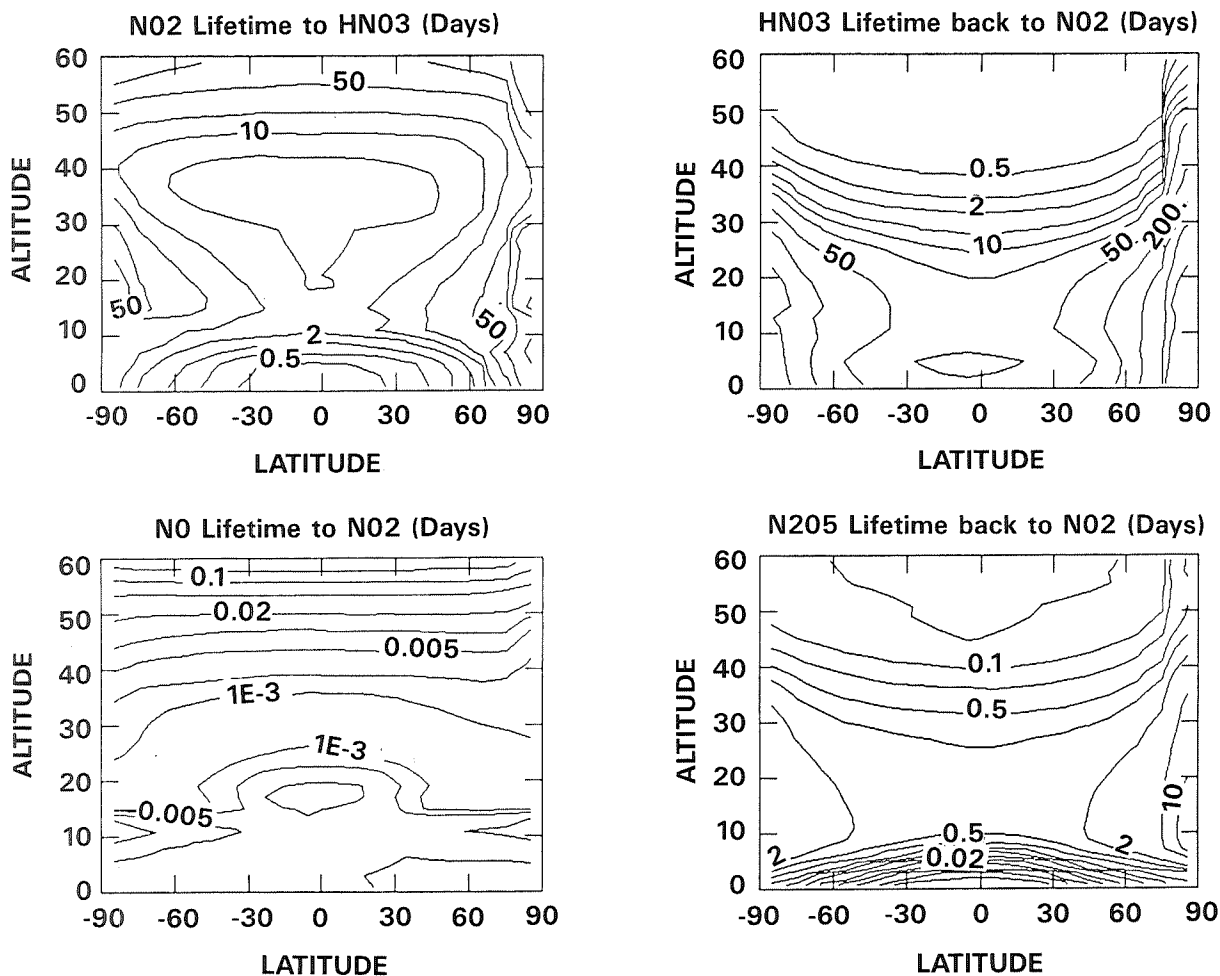


Figure 12. Lifetimes for interconversions among odd nitrogen species (March).

HYDROCARBONS

The lower troposphere contains a wide variety of hydrocarbons. Most of these are destroyed by reactions with the hydroxyl radical. Only those species with photochemical lifetimes longer than a few months reach the tropical tropopause in sufficient concentration to affect stratospheric chemistry. This restricts the population to methane (CH₄) and the nonmethane hydrocarbons (NMHC) acetylene (C₂H₂), ethane (C₂H₆), and propane (C₃H₈).

The methane distribution is fairly well established on several spatial scales. Data from the period 1983-87, from the surface and mid-troposphere, indicate that CH₄ is increasing by about 1% per year (16). During the 1980s, the average free tropospheric mixing ratio in the northern hemisphere was about 1.7 ppm, while in the southern hemisphere it was somewhat less, 1.6 ppm. The stratospheric distribution has been determined by several groups measuring primarily at midlatitudes and using balloon-borne instruments. The SAMS measurements pro-

vide a global picture of the behavior of CH_4 above 20 mb. The maximum stratospheric mixing ratio is seen in the tropical lower stratosphere; the mixing ratio decreases poleward and with altitude. A detailed description of the data and comparison with model calculations are given by Jones and Pyle (79).

Nonmethane hydrocarbons have considerable seasonal and spatial variation in the troposphere and we may expect similarly large variations in the lower stratosphere as well. Average lifetimes for C_3H_8 , C_2H_2 , and C_2H_6 are 0.06 yr, 0.1 yr, and 0.25 yr, respectively, but vary according to locale and may be much shorter in the tropics. Based on limited observations, we may describe the distribution of NMHCs as follows. The NMHCs increase from the South Pole towards the equator, (80-84), peaking at northern midlatitudes. Typical tropospheric northern midlatitude values for the NMHCs are 0.2 ppb acetylene, 2 ppb ethane, and 0.6 ppb propane. The seasonal cycle is dominated by variations in OH. In the Arctic, ethane has a maximum mixing ratio in the winter; and is 2 times less in summer. The annual variation of propane is greater (85). In Antarctica (86), ethane has a winter value of 0.45 ppb, with a summer mixing ratio of 0.3 ppb. The corresponding figures for acetylene are 20 and 10 ppt, respectively, and the propane content varies from 0.05 to 0.1. ppb.

Vertical distributions of the NMHCs in the stratosphere have only been measured at northern midlatitudes. With the exception of a limited number of satellite measurements, information has been by balloon-borne samplers (83,87-90) or by analysis of solar absorption spectra taken from the ground or aircraft (91-93). The vertical profile of ethane is nearly constant to 10-km altitude, with a mixing ratio between 1.5 and 2 ppb. The mixing ratio drops by an order of magnitude at 15 km and by 2 orders of magnitude at 25 km. This vertical distribution is confirmed by analysis of spectra profiles of solar infrared radiation (94). The measured vertical profiles of propane are confined to altitudes below 20 km. At 10 km, mixing ratios are between 0.2 and 0.8 ppb; at 17 km, the mixing ratio is 0.1 ppb. Acetylene, as measured at 10 km by direct sampling, has a value between 0.1 and 0.23 ppb. By 16 km, the mixing ratio is 0.02 ppb. The vertical distribution of molecules like ethane could be important in the chemistry of the stratosphere by serving as a tracer for the OH and Cl radical profiles (95). The breakdown of the NMHCs can modify the photochemistry of the lower stratosphere and upper troposphere (96-99).

The lifetimes of NMHCs can be significantly shorter in the stratosphere than in the troposphere as a result of reactions with Cl and are often less than 1 month. If this estimate of the lifetime is correct, the magnitude of the increase in the concentrations of the hydrocarbons in aircraft exhaust is controlled by photochemical loss rather than transport. Pollutant molecules are destroyed by reactions with OH and Cl, the perturbation is limited directly by the amount of pollutant in the aircraft exhaust. An important role of CH_4 and NMHCs in the lower stratosphere is to convert Cl to HCl and to produce ozone by reactions of NO with oxidation products, e.g., HO_2 and CH_3O_2 . The rate of oxidation of background CH_4 in the lower stratosphere ($1-5 \times 10^{10}$ molecules $\text{cm}^{-3} \text{s}^{-1}$) is much larger than the source of hydrocarbons in the aircraft exhaust (about 1×10^8 molecules $\text{cm}^{-3} \text{s}^{-1}$ if mixed in the northern hemisphere over an altitude thickness of 5 km). The picture could be somewhat more complicated by addition of reactions to form nitrates such as peroxy acetyl nitrate (PAN) in the high NO_x environment of the aircraft plume. However, although PAN is somewhat longer lived than the hydrocarbons, the summer lifetime is less than 3 months, and the maximum perturbation is still controlled by photochemistry.

CONCLUSION

The species considered here, most obviously the odd nitrogen species, influence the photochemical balance of the lower stratosphere. Perturbations to these species may have a direct impact on the ozone concentration in the lower stratosphere, even though time scales for photochemical processes such as ozone destruction are in the range of several years. For the species that are long lived in the lower stratosphere, the magnitudes of the possible perturbations to the background values of the components of stratospheric aircraft exhaust are controlled by the mass flow through the region in which the aircraft exhaust is mixed. This underscores the importance of understanding stratosphere/troposphere exchange and the circulation in the lower stratosphere where, it has been proposed, the high-speed civil transport will fly.

REFERENCES

1. Brewer, A.W., Evidence for a world circulation provided by the measurements of helium and water vapor distribution in the stratosphere, *Quart. J. Roy. Met. Soc.*, 75, 351-363, 1949.
2. Dobson, G.M.B., Origin and distribution of the polyatomic molecules in the atmosphere, *Proc. Roy. Soc. London Ser. A*, 236, 187-193, 1956.
3. Mahlman, J.D., Mechanistic Interpretation of Stratospheric Tracer Transport, in *Advances in Geophysics, Vol. 28, Issues in Atmospheric and Oceanic Modeling*, edited by Syukuro Manabe, Academic Press, Inc., 301-326, 1985.
4. World Meteorological Organization, Atmospheric ozone 1985: Assessment of our understanding of the processes controlling its present distribution and change, *Global Ozone Res. and Monitoring Proj. Rep. 16*, Geneva, 1986.
5. Dunkerton, T.J., On the mean meridional mass motions of the stratosphere and mesosphere, *J. Atmos. Sci.*, 35, 2325-2333, 1978.
6. Rood, R.B., and M.R. Schoeberl, A mechanistic model of Eulerian, Lagrangian mean, and Lagrangian ozone transport by steady planetary waves, *J. Geophys. Res.*, 88, 5208, 5218, 1983.
7. Jackman, C.H., R.K. Seals, Jr., and M.J. Prather, Two-Dimensional Intercomparison of Stratospheric Models, NASA Conference Publication 3042, 1989.
8. Andrews, D.G., J.R. Holton, and C.B. Leovy, *Middle Atmosphere Dynamics*, Academic Press, Inc., 1987.
9. Jackman, C.H., A.R. Douglass, P.D. Guthrie, and R.S. Stolarski, The sensitivity of total ozone and ozone perturbation scenarios in a two-dimensional model due to dynamical inputs, *J. Geophys. Res.*, 97, 9873-9887, 1989.
10. Douglass, A.R., C.H. Jackman, and R.S. Stolarski, Comparison of model results transporting the odd nitrogen family with results transporting separate odd nitrogen species, *J. Geophys. Res.*, 94, 9862-9872, 1989.
11. Shia, R.L., Y.L. Unig, M. Allen, R.W. Zurek, and D. Crisp, Sensitivity study of advection and diffusion coefficients in a two-dimensional stratospheric model using excess carbon 14 data, *J. Geophys. Res.*, 94, 18,467-18,484, 1989.
12. Holton, J.R., On the global exchange of mass between the stratosphere and troposphere, *J. Atmos. Sci.*, 47, 392-395, 1990.
13. Robinson, G.D., The transport of minor atmospheric constituents between troposphere and stratosphere, *Quart. J. Roy. Meteor. Soc.*, 106, 227-253, 1980.
14. Volz, A., U. Schmidt, J. Rudolph, D.H. Ehhalt, F.J. Johnson, and A. Khedim, "Vertical Profiles of Trace Gases as Mid-Latitudes," Jul-Report No. 1742, Kernforschungsanlage, Julich, Federal Republic of Germany, 1981.

15. Gamo, T., M. Tsutsumi, H. Sakai, T. Nakazawa, M. Tanaka, H. Honda, H. Kubo, and T. Itoh, Carbon and oxygen isotopic ratios of carbon dioxide of a stratospheric profile over Japan, *Tellus*, 41b, 127-133, 1989.
16. World Meteorological Organization, Report of the International Ozone Trends Panel 1988, *Global Ozone Research and Monitoring Project - Report No. 18*, Geneva, 1990.
17. Jackman, C.H., R.S. Stolarski, and J.A. Kaye, Two-dimensional monthly average ozone balance from limb infrared monitor of the stratosphere and stratospheric and mesospheric sounder data, *J. Geophys. Res.*, 91, 1103-1116, 1986.
18. Tolbert, M.A., M.J. Rossi, and D.M. Golden, Heterogeneous interactions of ClONO₂, HCl and HNO₃ with sulfuric acid surfaces at stratospheric temperatures, *Geophys. Res. Lett.*, 15, 851-854, 1988.
19. Worsnop, D., M. Zahniser, C. Kolb, L. Watson, J. Van Doren, J. Jayne, and P. Davidovits, Mass accommodation coefficient measurements for HNO₃, HCl, and N₂O₅ on water, ice, and aqueous sulfuric acid droplet surfaces, paper presented at the Polar Ozone Workshop, NASA/NOAA/NSF/CMA, Snowmass, CO May 9-13, 1988.
20. Mozurkewich, M., and J.G. Calvert, Reaction probability of N₂O₅ on aqueous aerosols, *J. Geophys. Res.*, 93, 15,889-15,896, 1988.
21. LeTexier, H., S. Solomon, and R.R. Garcia, The role of molecular hydrogen and methane oxidation in the water vapor budget of the stratosphere, *Quart. J. Roy. Meteor. Soc.*, 114, 281-295, 1988.
22. Kley, D., A.L. Schmeltekopf, K. Kelley, R.H. Winkler, T.L. Thompson, and M. McFarland, Transport of water vapor through the tropical tropopause, *Geophys. Res. Lett.*, 9, 617-620, 1982.
23. Mastenbrook, H.J., and S.J. Oltmans, Stratospheric water variability for Washington, DC/Boulder, CO: 1964-82, *J. Atmos. Sci.*, 40, 2157-2165, 1983.
24. Russell, J.M., III, J.C. Gille, E.M. Remsberg, L.L. Gordley, P.L. Bailey, H. Fischer, A. Girard, S.R. Drayson, W.F.J. Evans, and J.E. Harries, Validation of water vapor results measured by the Limb Infrared Monitor of the Stratosphere experiment on NIMBUS 7, *J. Geophys. Res.*, 89, 5115-5124, 1984.
25. Rind, D., E-W. Chiou, W.P. Chu, S. Oltmans, J. Lerner, J.C. Larsen, M.P. McCormick, and L.R. McMaster, Positive water vapor feedback in climate models confirmed by satellite data, *Nature*, 349, 500-503, 1991.
26. Rind, D., E-W. Chiou, W. Chu, S. Oltmans, J. Lerner, J. Larsen, M.P. McCormick, and L. McMaster, Overview of the SAGE II water vapor observations: method, validation and data characteristics, submitted to *J. Geophys. Res.*, 1991.
27. Chiou, E-W., M.P. McCormick, L. McMaster, W.P. Chu, J.C. Larsen, D. Rind, and S. Oltmans, Intercomparison of stratospheric water vapor observed by satellite experiments, submitted to *J. Geophys. Res.*, 1991.

28. Chu, W., E-W. Chiou, J.C. Larsen, L. Thomason, D. Rind, J.J. Buglia, M.P. McCormick, and L.R. McMaster, Algorithms and error estimates for SAGE II water vapor retrievals. submitted to *J. Geophys. Res.*, 1991.
29. Larsen, J.C., D. Rind, S. Oltmans, E-W. Chiou, W.P. Chu, M.P. McCormick, and L.R. McMaster, Comparison of the SAGE II Tropospheric water vapor to radiosonde measurements, submitted to *J. Geophys. Res.*, 1991.
30. McCormick, M.P., E-W. Chiou, L.R. McMaster, W.P. Chu, J.C. Larsen, D. Rind, and S. Oltmans, Seasonal variations of water vapor, submitted to *J. Geophys. Res.*, 1991.
31. Oltmans, S., W. Chu, E. Chiou, L.R. McMaster, M.P. McCormick, D. Rind, and J. Larsen, submitted to *J. Geophys. Res.*, 1991.
32. Johnston, H.S., O. Serang, and J. Podolski, Instantaneous global nitrous oxide photochemical rates, *J. Geophys. Res.*, *84*, 5077-5082, 1979.
33. Jackman, C.H., J.E. Frederick, and R.S. Stolarski, Production of odd nitrogen in the stratosphere and mesosphere: An intercomparison of source strengths, *J. Geophys. Res.*, *85*, 7495-7505, 1980.
34. Crutzen, P.J., and U. Schmailzl, Chemical budgets of the stratosphere, *Planet. Space Sci.*, *31*, 1009-1032, 1983.
35. Ko, M.K.W., M.B. McElroy, D.K. Weisenstein, and N.D. Sze, Lightning: A possible source of stratospheric odd nitrogen, *J. Geophys. Res.*, *91*, 5395-5404, 1986.
36. Jackman, C.H., P.D. Guthrie, and J.A. Kaye, An intercomparison of nitrogen-containing species in Nimbus 7 LIMS and SAMS data, *J. Geophys. Res.*, *92*, 995-1008, 1987.
37. Nicolet, M., On the production of nitric oxide by cosmic rays in the mesosphere and stratosphere, *Planet. Space Sci.*, *23*, 637-649, 1975.
38. Legrand, M.R., F. Stordal, I.S.A. Isaksen, and B. Rognerud, A model study of the stratospheric budget of odd nitrogen, including effects of solar cycle variations, *Tellus*, *41B*, 413-426, 1989.
39. Noxon, J.F., Atmospheric nitrogen fixation by lightning, *Geophys. Res. Lett.*, *3*, 463-465, 1976.
40. Tuck, A.F., Production of nitrogen oxides by lightning discharges, *Quart. J. Roy. Met. Soc.*, *102*, 749-755, 1976.
41. Chameides, W.L., D.H. Stedman, R.R. Dickerson, D.W. Rusch, and R.J. Cicerone, NO_x production in lightning, *J. Atmos. Sci.*, *34*, 143-149, 1977.
42. Logan, J.A., Nitrogen oxides in the troposphere: Global and regional budgets, *J. Geophys. Res.*, *88*, 10,785-10,807, 1983.
43. Borucki, W.J., and W.L. Chameides, Lightning: Estimates of the rates of energy dissipation and nitrogen fixation, *Rev. Geophys.*, *22*, 363-372, 1984.

- 44a. Fahey, D.W., K.K. Kelly, S.R. Kawa, A.F. Tuck, M. Loewenstein, K.R. Chan, and L.E. Heidt, Observations of denitrification and dehydration in the winter polar stratospheres, *Nature*, 344, 321-324, 1990.
- 44b. Fahey, D.W., S. Solomon, S.R. Kawa, M. Loewenstein, J.R. Podolske, S.E. Strahan, and K.R. Chan, A diagnostic for denitrification in the winter polar stratospheres, *Nature*, 345, 698-702, 1990.
45. Crutzen, P.J., I.S.A. Isaksen, and G.C. Reid, Solar proton events: Stratospheric sources of nitric oxide, *Science*, 189, 457-458, 1975.
46. McPeters, R.D., A nitric oxide increase observed following the July 1982 solar proton event, *Geophys. Res. Lett.*, 13, 667-670, 1986.
47. Jackman, C.H., A.R. Douglass, R.B. Rood, R.D. McPeters, and P.E. Meade, Effect of solar proton events on the middle atmosphere during the past two solar cycles as computed using a two-dimensional model, *J. Geophys. Res.*, 95, 7417-7428, 1990.
48. Strobel, D.F., Odd nitrogen in the mesosphere, *J. Geophys. Res.*, 76, 8384-8393, 1971.
49. McConnell, J.C., and M.B. McElroy, Odd nitrogen in the atmosphere, *J. Atmos. Sci.*, 30, 1465-1480, 1973.
50. Brasseur, G., and M. Nicolet, Chemospheric processes of nitric oxide in the mesosphere and stratosphere, *Planet. Space Sci.*, 21, 939-961, 1973.
51. Solomon, S., P.J. Crutzen, and R.G. Roble, Photochemical coupling between the thermosphere and the lower atmosphere, 1, Odd nitrogen from 50 to 120 km, *J. Geophys. Res.*, 87, 7206-7220, 1982.
52. Frederick, J.E., and N. Orsini, The distribution and variability of mesospheric odd nitrogen: A theoretical investigation, *J. Atmos. Terr. Phys.*, 44, 479-488, 1982.
53. Garcia, R.R., S. Solomon, R.G. Roble, and D.W. Rusch, A numerical response of the middle atmosphere to the 11-year solar cycle, *Planet Space Sci.*, 32, 411-423, 1984.
54. Solomon, S., and R.R. Garcia, Transport of thermospheric NO to the upper stratosphere?, *Planet. Space Sci.*, 32, 399-409, 1984.
55. Russell, J.M., III, S. Solomon, L.L. Gordley, E.E. Remsberg, and L.B. Callis, The variability of stratospheric and mesospheric NO₂ in the polar winter night observed by LIMS, *J. Geophys. Res.*, 89, 7267-7275, 1984.
56. Brasseur, G., Coupling between the thermosphere and the stratosphere: The role of nitric oxide, *MAP Handbook*, Volume 10, 1984.
57. Thorne, R.M., Energetic radiation belt electron precipitation: A natural depletion mechanism for stratospheric ozone, *Science*, 195, 287-289, 1977.
58. Thorne, R.M., The importance of energetic particle precipitation on the chemical composition of the middle atmosphere, *Pure Appl. Geophys.*, 118, 128-151, 1980.

59. Baker, D.N., J.B. Blake, D.J. Gorney, P.R. Higbie, R.W. Klebesadel, and J.H. King, Highly relativistic magnetospheric electrons: A role in coupling to the middle atmosphere?, *Geophys. Res. Lett.*, 14, 1027-1030, 1987.
60. Sheldon, W.R., J.R. Benbrook, and E.A. Bering III, Comment on "Highly relativistic magnetospheric electrons: A role in coupling to the middle atmosphere?," *Geophys. Res. Lett.*, 15, 1449-1450, 1988.
61. Baker, D.N., J.B. Blake, D.J. Gorney, P.R. Higbie, R.W. Klebesadel, and J.H. King, Reply, *Geophys. Res. Lett.*, 15, 1451-1452, 1988.
62. Callis, L.B., D.N. Baker, J.B. Blake, J.D. Lambeth, R.E. Boughner, M. Natarajan, R.W. Klebesadel, and D.J. Gorney, Precipitating relativistic electrons: their long-term effect on stratospheric odd nitrogen levels, *J. Geophys. Res.*, 96, 2939-2976, 1991.
63. Goldberg, R.A., C.H. Jackman, J.R. Barcus, and F. Soraas, *J. Geophys. Res.*, 89, 5581-5596, 1984.
64. Johnston, H., G. Whitten, and J. Birks, Effect of nuclear explosions on stratospheric nitric oxide and ozone, *J. Geophys. Res.*, 78, 6107-6135, 1973.
65. Foley, H.M., and Ruderman, M.A., Stratospheric NO production from past nuclear explosions, *J. Geophys. Res.*, 78, 4441-4450, 1973.
66. Gilmore, F.R., The production of nitrogen oxides by low-altitude nuclear explosions, *J. Geophys. Res.*, 80, 4553-4554, 1975.
67. Callis, L.B., M. Natarajan, and J.M. Russell III, Estimates of the stratospheric distribution of odd nitrogen from the LIMS data, *Geophys. Res. Lett.*, 12, 259-262, 1985.
68. Remsberg, E.E., and J.M. Russell III, The Near Global Distributions of Middle Atmospheric H₂O and NO₂ Measured by the Nimbus 7 LIMS Experiment, in *Transport Processes in the Middle Atmosphere*, edited by G. Visconti and R. Garcia, D. Reiden Publishing Company, 87-102, 1987.
69. Fahey, D.W., C.S. Eubank, G. Hubler, and F.C. Fehsenfeld, Evaluation of a catalytic reduction technique for the measurement of total reactive odd nitrogen NO_y in the atmosphere, *J. Atmos. Chem.*, 3, 435-468, 1985.
70. Fahey, D.W., D.M. Murphy, K.K. Kelly, M.K.W. Ko, M.H. Proffitt, C.S. Eubank, G.V. Ferry, M. Loewenstein, and K.R. Chan, Measurements of nitric oxide and total reactive nitrogen in the Antarctic stratosphere: observations and chemical implications, *J. Geophys. Res.*, 94, 16,665-16,681, 1989.
71. Kawa, S.R., D.W. Fahey, L.C. Anderson, M. Loewenstein, and K.R. Chan, Measurements of total reactive nitrogen during the Airborne Arctic Stratospheric Expedition, *Geophys. Res. Lett.*, 17, 485-488, 1990.
72. Kawa, S.R., D.W. Fahey, S. Solomon, W.H. Brune, M.H. Proffitt, D.W. Tooney, D.E. Anderson, Jr., L.C. Anderson, and K.R. Chan, Interpretation of aircraft measurements of NO, ClO, and O₃ in the lower stratosphere, *J. Geophys. Res.*, 95, 18,597-18,609, 1990.

73. Fahey, D.W., Unpublished data, 1991.
74. Loewenstein, M., W.J. Borucki, H.F. Savage, J.G. Borucki, and R.C. Whitten, Geographical variations of NO and O₃ in the lower stratosphere, *J. Geophys. Res.*, **83**, 1875-1882, 1978.
75. Russell, J.M., III, C.B. Farmer, C.T. Rinsland, R. Zander, L. Froidevaux, G.C. Toon, B. Gao, J. Shaw, and M. Gurnson, Measurements of Odd Nitrogen Compounds in the Stratosphere by the ATMOS Experiment on Space Lab 3, *J. Geophys. Res.*, **93**, 1718-1736, 1988.
76. Austin, J., R.R. Garcia, J.M. Russell III, S. Solomon, and A.F. Tuck, On the atmospheric photochemistry of nitric acid, *J. Geophys. Res.*, **91**, 5477-5485, 1986.
77. Rood, R.B., J.A. Kaye, A.R. Douglass, D.J. Allen, S. Steenrod, and E.M. Larson, Wintertime nitric acid chemistry: implications from three-dimensional model calculations, *J. Atmos. Sci.*, **47**, 2696-2709, 1990.
78. Hofmann, D.J., and S. Solomon, Ozone destruction through heterogeneous chemistry following the eruption of El Chichon, *J. Geophys. Res.*, **94**, 5029-5042, 1989.
79. Jones, R.L., and J.A. Pyle, Observations of CH₄ and N₂O by the NIMBUS 7 SAMS: A comparison with in situ data and two-dimensional numerical model calculations, *J. Geophys. Res.*, **89**, 5263-5279, 1984.
80. Rudolph, J., and D.H. Ehhalt, Measurements of C₂-C₅ hydrocarbons over the North Atlantic, *J. Geophys. Res.*, **86**, 11959-11964, 1981.
81. Singh, H.B., and L.J. Salas, Measurement of selected light hydrocarbons over the Pacific Ocean: latitudinal and seasonal variations, *Geophys. Res. Lett.*, **9**, 842-845, 1982.
82. Blake, D.R., and F.S. Rowland, Global atmospheric concentrations and source strength of ethane, *Nature*, **321**, 231-233, 1986.
83. Ehhalt, D.H., J. Rudolph, F. Meixner, and U. Schmidt, Measurements of selected C₂-C₅ hydrocarbons in the background troposphere: vertical and latitudinal variations, *J. Atm. Chem.*, **3**, 29-52, 1985.
84. Singh, H.B., W. Viezee, and Louis J. Salas, Measurements of selected C₂-C₅ hydrocarbons in the troposphere: latitudinal, vertical and temporal variations, *J. Geophys. Res.*, **93**, 15861-15878, 1988.
85. Tille, K.J.W., M. Savelsberg, and K. Bachmann, Airborne measurements of nonmethane hydrocarbons over western europe: vertical distributions, seasonal cycles of mixing ratios and source strengths, *Atmos. Environ.*, **19**, 1751-1760, 1985.
86. Rudolph, J., A. Khedim, and D. Wagenbach, The seasonal variation of light nonmethane hydrocarbons in the Antarctic troposphere, *J. Geophys. Res.*, **94**, 13,039-13,044, 1989.
87. Robinson, E., Hydrocarbons in the atmosphere, *Pure Appl. Geophys.*, **116**, 372-384, 1978.

88. Cronn, D., and E. Robinson, Tropospheric and lower stratospheric vertical profiles of ethane and acetylene, *Geophys. Res. Lett.*, 6, 641-644, 1979.
89. Rudolph, J., D.H. Ehhalt, and A. Tonnissen, Vertical profiles of ethane and propane in the stratosphere, *J. Geophys. Res.*, 86, 7267-7272, 1981.
90. Aikin, A.C., C.C. Gallagher, W.C. Spicer, and M.W. Holdren, Measurement of methane and other light hydrocarbons in the troposphere and lower stratosphere, *J. Geophys. Res.*, 92, 3135-3138, 1987.
91. Goldman, A., F.J. Murcray, R.D. Blatherwick, J.R. Gillis, F.S. Bonomo, F.H. Murcray, and D.G. Murcray, Identification of acetylene (C_2H_2) in infrared atmospheric absorption spectra, *J. Geophys. Res.*, 86, 12143-12146, 1981.
92. Goldman, A., C.P. Rinsland, F.J. Murcray, D.G. Murcray, M.T. Coffey, and W.G. Mankin, Balloon-borne and aircraft infrared measurements of ethane (C_2H_6) in the upper troposphere and lower stratosphere, *J. Atmos. Chem.*, 2, 211-221., 1984.
93. Coffey, M.T., W.G. Mankin, A. Goldman, C.P. Rinsland, G.A. Harvey, V. Malathy Devi, and G.M. Stokes, Infrared measurements of atmospheric ethane (C_2H_6) from aircraft and ground based solar absorption spectra in the 3000 cm^{-1} region, *Geophys. Res. Lett.*, 12, 199-202, 1985.
94. Rinsland, C.P., R. Zander, C.B. Farmer, R.H. Norton, and J.M. Russell III, Concentrations of ethane (C_2H_6) in the lower stratosphere and upper troposphere and acetylene (C_2H_2) in the upper troposphere deduced from atmospheric trace molecule spectroscopy/spacelab 3 spectra, *J. Geophys. Res.*, 92, 11951-11964, 1987.
95. Chameides, W.L., and R.J. Cicerone, Effects of nonmethane hydrocarbons in the atmosphere, *J. Geophys. Res.*, 83, 947-952, 1978.
96. Aikin, A.C., J.R. Herman, E.J. Maier, and C.J. McQuillan, Atmospheric chemistry of ethane and ethylene, *J. Geophys. Res.*, 87, 1982.
97. Aikin, A.C., J.R. Herman, E.J. Maier, and C.J. McQuillan, Influence of peroxyacetyl nitrate (PAN) on odd nitrogen in the troposphere and lower stratosphere, *Planet. Space Sci.*, 31, 1075-1082, 1983.
98. Kasting, J.F., and H.B. Singh, Nonmethane hydrocarbons in the troposphere: impact upon the odd hydrogen and odd nitrogen chemistry, *J. Geophys. Res.*, 91, 13,229-13,256, 1986.
99. Singh, H.B., and J.F. Kasting, Chlorine-hydrocarbon photochemistry in the marine troposphere and lower stratosphere, *J. Atm. Chem.*, 7, 261-285, 1988.

53-45-①
64289

N92-19124
p.2

Chapter 3B

Upper-Atmosphere Aerosols: Properties and Natural Cycles

Richard Turco
University of California
Los Angeles, CA

CD 146 017

ABSTRACT

The middle atmosphere is rich in its variety of particulate matter, which ranges from meteoritic debris, to sulfate aerosols, to polar stratospheric ice clouds. Volcanic eruptions strongly perturb the stratospheric sulfate (Junge) layer. High-altitude "noctilucent" ice clouds condense at the summer mesopause. The properties of these particles, including their composition, sizes, and geographical distribution, are discussed, and their global effects, including chemical, radiative, and climatic roles, are reviewed. Polar stratospheric clouds (PSCs) are composed of water and nitric acid in the form of micron-sized ice crystals. These particles catalyze reactions of chlorine compounds that "activate" otherwise inert chlorine reservoirs, leading to severe ozone depletions in the southern polar stratosphere during austral spring. PSCs also modify the composition of the polar stratosphere through complex physicochemical processes, including dehydration and denitrification, and the conversion of reactive nitrogen oxides into nitric acid. If water vapor and nitric acid concentrations are enhanced by high-altitude aircraft activity, the frequency, geographical range, and duration of PSCs might increase accordingly, thus enhancing the destruction of the ozone layer (which would be naturally limited in geographical extent by the same factors that confine the ozone hole to high latitudes in winter). The stratospheric sulfate aerosol layer reflects solar radiation and increases the planetary albedo, thereby cooling the surface and possibly altering the climate. Major volcanic eruptions, which increase the sulfate aerosol burden by a factor of 100 or more, may cause significant global climatic anomalies. Sulfate aerosols might also be capable of activating stratospheric chlorine reservoirs on a global scale (unlike PSCs, which represent a localized polar winter phenomenon), although existing evidence suggests relatively minor perturbations in chlorine chemistry. Nevertheless, if atmospheric concentrations of chlorine (associated with anthropogenic use of chlorofluorocarbons) continue to increase by a factor of two or more in future decades, aircraft emissions of sulfur dioxide and water vapor may take on greater significance.

INTRODUCTION

Particles and clouds in the stratosphere and mesosphere have been under study for more than 100 years. High-altitude aerosols were the subject of scientific speculation during the 1880s, when the powerful eruption of Krakatoa caused spectacular optical displays worldwide, attracting attention to the upper atmosphere. The presence of a permanent tenuous particle layer in the lower stratosphere was postulated in the 1920s through studies of the twilight glow (1). The first in situ samples of these particles showed they are composed of sulfates, most likely concentrated sulfuric acid (2-5). Subsequent research was spurred by the realization that stratospheric particles can influence the surface climate of Earth by modifying atmospheric radiation (6). Such aerosols can also affect the trace composition of the atmosphere, ozone concentrations, and the electrical properties of air (7).

Stratospheric particulates have been sampled by balloon ascents and high-altitude aircraft to determine their properties directly (8). The aerosols have also been observed remotely from the ground and from satellites using both active (lidar) and passive (solar occultation) techniques (remote sensing instruments have been carried on aircraft platforms as well) (9,10). In connection with the experimental work, models have been developed to test theories of particle formation and evolution, to guide measurement strategies, to provide a means of integrating laboratory and field data, and to apply the diverse scientific knowledge gained to answer practical questions related to issues of global changes in climate, depletion of the ozone layer, and related environmental problems (11).

In the following sections, primarily stratospheric, but also mesospheric, particles are described, and their global effects are discussed. Figure 1 illustrates many of the species of

64

aerosols that have been identified in the upper atmosphere. The diagram provides information on the size dispersion and concentration of these diverse particulates (12). Table 1 provides a summary of the key characteristics of stratospheric aerosols.

Table 1. Characteristics of Stratospheric Aerosols

Particle type	Sulfate aerosol	Type-I PSC	Type-II PSC	Meteoric dust	Rocket exhaust
Physical state	Liquid or slurry with crystals	Solid nitric acid trihydrate, solid solutions	Solid crystal, hexagonal or cubic basis	Solid granular irregular or spherical	Solid spheres or irregular surface ablated debris
Particle radius (μm , 10^{-6}m)	0.01 - 0.5, Amb. 0.01 - 10, Volc.	0.3 - 3	1 - 100	1 - 100, Micro-meteorites 0.01 - 0.1, smoke	0.1 - 10
Number (# cm^{-3})	~1- 10	~0.1-10	<<1	10^{-6} , 100 μm 10^{-3} , 1 μm	10^{-4} , 10 μm 10^{-2} , 1 μm
Principal composition	$\text{H}_2\text{SO}_4/\text{H}_2\text{O}$ ~70%/30%	$\text{HNO}_3/\text{H}_2\text{O}$ ~50%/50%	H_2O	SiO_2 , Fe, Ni, Mg; C	Al_2O_3
Trace composition	NH_4^+ , NO_3^-	HCl SO_4^{2-}	HNO_3 , HCl	SO_4^{2-} - (surface)	Cl^- , SO_4^{2-} - (surface)
Physical characteristics	Dust inclusions, in solution	Equidimensional crystalline or droplets	Elongated crystals with polycrystalline structure	Irregular mineral grains, grain defects	Homogeneous composition; smooth spheres

STRATOSPHERIC SULFATE AEROSOLS

The presence of trace amounts of sulfur-bearing gases in the stratosphere favors the formation of sulfuric acid aerosols (13-18). In particular, carbonyl sulfide in the background atmosphere is largely responsible (19) for the tenuous, ubiquitous ambient sulfate haze observed in the stratosphere (20-21). The general properties of these aerosols are summarized in Table 2. The processes that control this haze also influence the formation and evolution of volcanically induced aerosols. Accordingly, investigations of the ambient stratospheric aerosol layer provide insights into the behavior of volcanic eruption clouds above the tropopause.

Background Aerosols

It is fairly well established now that the ambient stratospheric sulfate layer is formed as a result of the chemical transformation of sulfur-bearing gases (carbonyl sulfide, OCS, and sulfur dioxide, SO_2) transported into the stratosphere from the troposphere or injected there by major volcanic eruptions (19). Chemical reactions of these precursor sulfur gases lead to the produc-

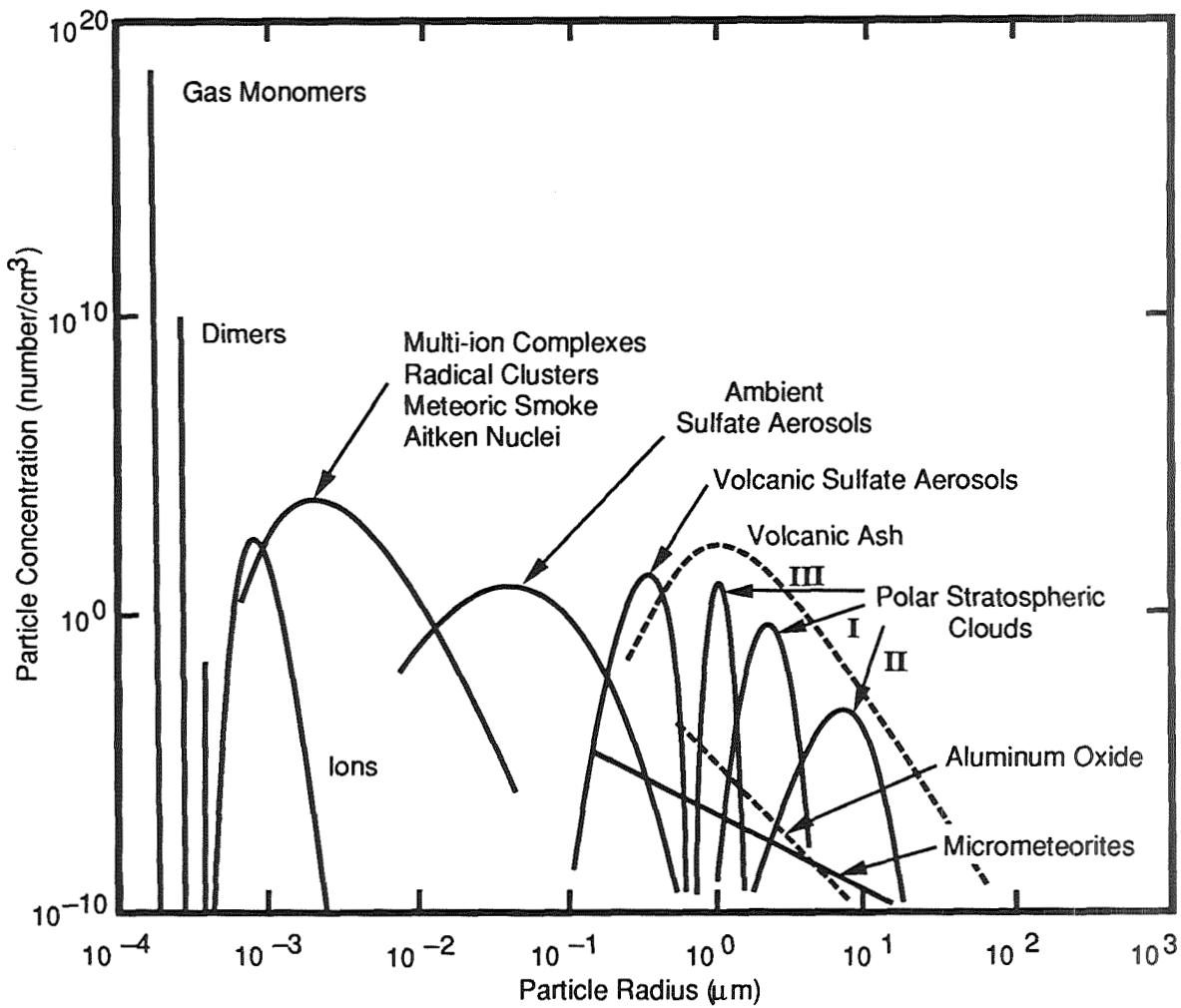


Figure 1. Spectrum of particles in the Earth's middle atmosphere. Shown are the approximate size distributions for particles with different origins. The total (number) concentration of each type of particle is roughly indicated by the peak value on the vertical scale. Some aerosols are highly variable in concentration and properties, particularly the "ash" component of volcanic eruption clouds; typically, these particles will fall out of the stratosphere within a few months following an eruption.

tion of condensible sulfur compounds — primarily H_2SO_4 [detected in situ by Arnold et al., (22)]. The sulfur conversion process is dominated by the reaction sequence: (23)



Table 2. Properties of Stratospheric Sulfate Aerosols

Composition	H ₂ SO ₄ /H ₂ O (~70%/30%); traces of sulfates, nitrates, nitryls, chlorides
Origin	OCS, CS ₂ (also volcanic sulfur emissions); tropospheric sulfides; SO ₂ photochemical oxidation to H ₂ SO ₄ via OH; high-altitude aircraft SO ₂ emissions (contribution unknown)
Properties	Liquid spheres, perhaps slurry and some solids; < 1 ppbm; ~1-10 cm ⁻³ ~ 0.05 μm radius
Distribution	Global; 12 to 30 km altitude; latitudinal and seasonal variations
Mass Budget	~ 0.1 Tg-S/yr (background); ~ 1-100 Tg-S (volcanic event)
Residence Time	~ 1-2 yr (average, based on radioactive tracer studies)
Effects	Shortwave radiation scattering (τ < 0.01); longwave absorption/emission (τ << 0.01); heterogeneous chemical conversion of NO _x to HNO ₃
Influences	Natural and anthropogenic OCS sources; volcanic activity; stratospheric dynamics
Trends	Variable over 2 orders of magnitude following major volcanic eruptions (e.g., El Chichon). Possible long-term increase of ~ 6%/yr by mass

Reactions (2) and (3) are so rapid that sulfur radicals (e.g., HSO₃) never achieve a significant concentration, and thus do not play a role in the chemical evolution of the aerosol cloud (except as an intermediary sulfur species). Although reaction (3) may require the presence of surfaces to occur rapidly, it does not limit the overall oxidation rate of sulfur dioxide. Importantly, reaction sequence (1) and (2) does not consume odd-hydrogen, HO_x, as would the competing process consisting of reactions (1) and (4),



Hence, HO_x oxidizes SO₂ catalytically, and the rate of SO₂ conversion can remain high throughout the evolution of a volcanic cloud provided there is sufficient recycling of HO₂ to OH.

The properties of the sulfate particle layer are strongly influenced by microphysical processes, including heterogeneous nucleation, growth by condensation, evaporation of volatiles, coagulation, and gravitational sedimentation (24). Some of the complex physicochemical interactions responsible for the formation of the stratospheric aerosol layer are illustrated schematically in Figure 2; the potential contributions of naturally occurring meteoritic particles and ion clusters to sulfate aerosol formation are also indicated. Exhaust particles from Space Shuttle or high-altitude aircraft operations would enhance the condensation nuclei abundances. Detailed discussions of microphysical processes can be found in several papers, reviews, and books (25,26).

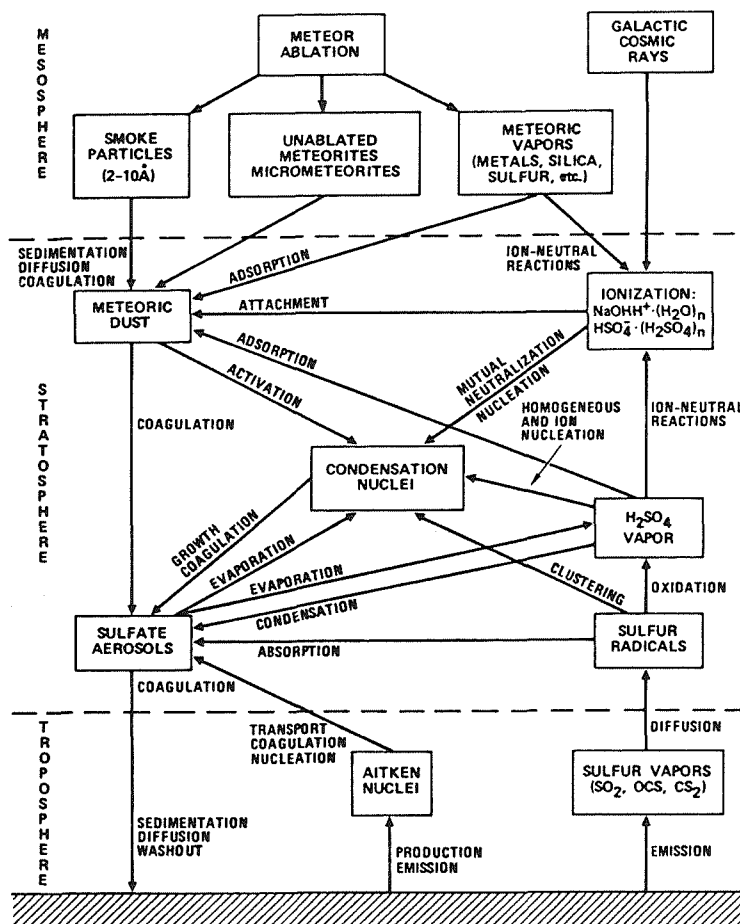


Figure 2. Diagram depicting the physical and chemical processes that affect stratospheric aerosols. Meteoritic debris, positive and negative ions, and tropospheric Aitken nuclei can serve as nucleation sources for sulfate aerosols and ice clouds. These particles can grow, evaporate, coagulate, and fall vertically. The particles are also carried in stratospheric winds and diffuse under the influence of small scale turbulent eddies.

Volcanic Aerosols

Table 3 summarizes the general properties of the aerosols generated by a modest-to-large volcanic eruptions (that is, one in which the eruption column penetrates the tropopause and deposits substantial quantities of gases and particles in the stratosphere) (27-32).

The general microphysical development and properties of volcanic eruption plumes are exemplified by the behavior of the El Chichon eruption cloud (33,34). The primary eruption of El Chichon occurred on April 4, 1982; solid debris and gases were injected to altitudes of about 30 km over the Yucatan Peninsula (35). Many observations of the clouds were made, and these data have been compared to model simulations that include the relevant physical and chemical processes (36,37). It should be noted that high-altitude sampling of the El Chichon volcanic clouds was very limited. Data collected by the Solar Mesosphere Explorer satellite suggest that the post-eruption aerosols reached altitudes of 40 km (38,39). Lidar measurements, on the other hand, indicated that the El Chichon particles remained below about 30 km for several months after the eruption.

Table 3. Properties of Volcanic Aerosols

Composition	Silicates; H ₂ SO ₄ /H ₂ O (~70%/30%); traces of sulfates, nitrates, chlorides, etc.
Origin	Terrestrial material, gaseous SO ₂ with chemical oxidation to H ₂ SO ₄ via OH
Properties	Liquid spheres; solid mineral particles dominant the first month; ~ 100-1000 ppbm; (highly variable); ~1-10 cm ⁻³ ; ~ 0.3 μm radius
Distribution	Regional (days); zonal (weeks); hemispheric (months); global (year); 12-35 km altitude
Mass Budget	Per event: SO ₂ (~ 1-100 Tg-S); H ₂ O (~ 10-1000 Tg); HCl (~ 0.01-10 Tg); mineral ash (> 100-10,000 Tg)
Residence Time	~ 1-3 yr (average, based on radioactive tracer and aerosol decay studies)
Effects	Shortwave scattering of sunlight leads to surface cooling; Longwave absorption warms the stratosphere; Injection of H ₂ O, HCl, etc., possibly alters composition; Enhanced heterogeneous reactions on sulfate aerosol surfaces; Possible ozone perturbations; Stratospheric stability / tropospheric dynamics affected; Nuclei for upper tropospheric cirrus
Influences	Geophysical; no anthropogenic influences; geological setting determines effects; impact on ozone may be affected by chlorine levels
Trends	Random significant eruptions are ~20 years on average; major eruptions are ~100 years apart

The size distributions of volcanic aerosols (shown in Figure 3 for an El Chichon simulation) exhibit a tri-modal structure that evolves with time. The principal size modes are: a nucleation mode, which is most prominent at early times and at sizes near 0.01 μm; a sulfate accumulation mode, which evolves initially from the nucleation mode (by coagulation and condensation) and increases in size to about 0.3 μm after 1 year; and a large-particle "ash" mode (of solid mineral and salt particles) that settles out of the layer in 1 or 2 months. A primary feature of the volcanic aerosol size distribution after several months is a greatly enhanced sulfate accumulation mode. The increased aerosol size is caused by accelerated growth in the presence of enhanced sulfuric acid vapor concentrations that are maintained by continuing SO₂ chemical conversion.

Figure 4 illustrates the evolution of volcanic aerosol optical depths at mid-visible wavelengths, associated with the scattering of light by the sulfuric acid droplets. The calculations correspond to the sulfur injection scenarios used by Pinto et al. (40); i.e., SO₂ mass injections of 10 Tg (1 Tg = 1 × 10¹² g = 10⁶ metric tons) (i.e., like El Chichon), and 100 and 200 Tg (possibly similar to Tambora, 1815). At early times, and over limited geographical regions, the

optical depths can exceed a value of 2. However, after 1 year of evolution by growth, coagulation, and fallout, the average optical depth for even the largest SO₂ injection has fallen to about 0.5. These results suggest that nonlinear physical/chemical interactions occurring in volcanic eruption clouds severely limit the aerosol optical depth that can be maintained over a period of several years (40) (i.e., the time span required to induce substantial long-term climatic impacts, see also section on Radiation and Climate Effects). Conversely, the efficiency for producing radiative effects *per unit mass of sulfur* injected is greatest for smaller injections. Accordingly, high-altitude aircraft emissions of SO₂ hold the potential for creating significant global-scale radiative effects.

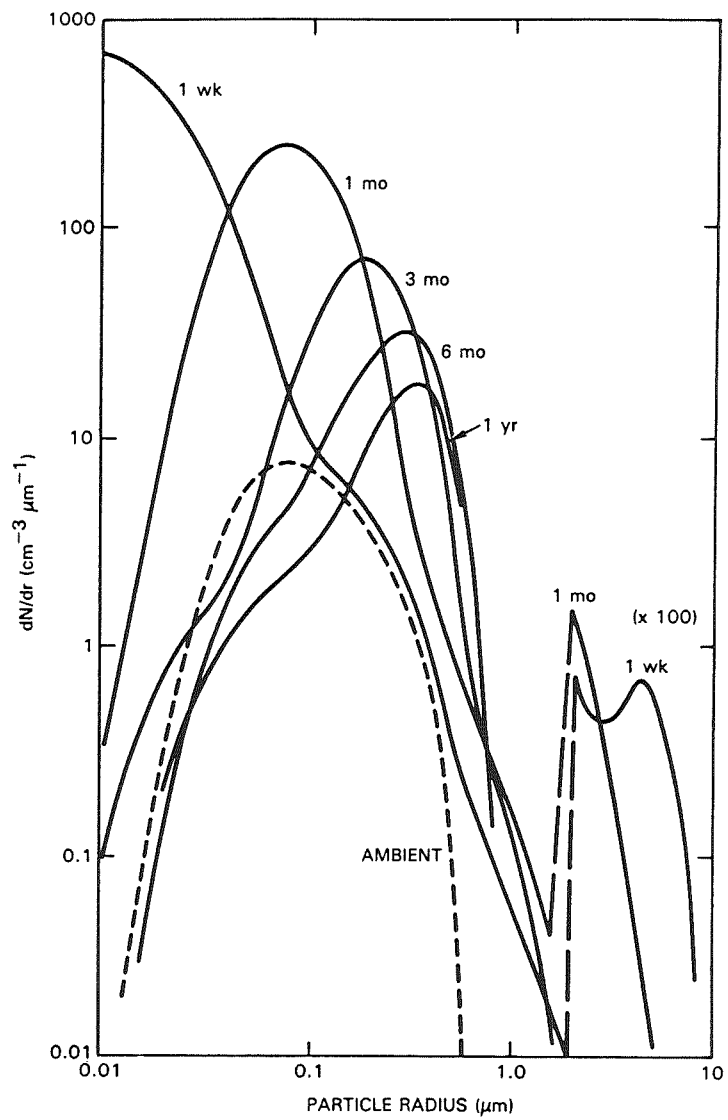


Figure 3. Evolution of the aerosol size distribution at 20 km in the simulated El Chichon eruption cloud. Size distributions are shown at various times, and are compared to the ambient size distribution (36).

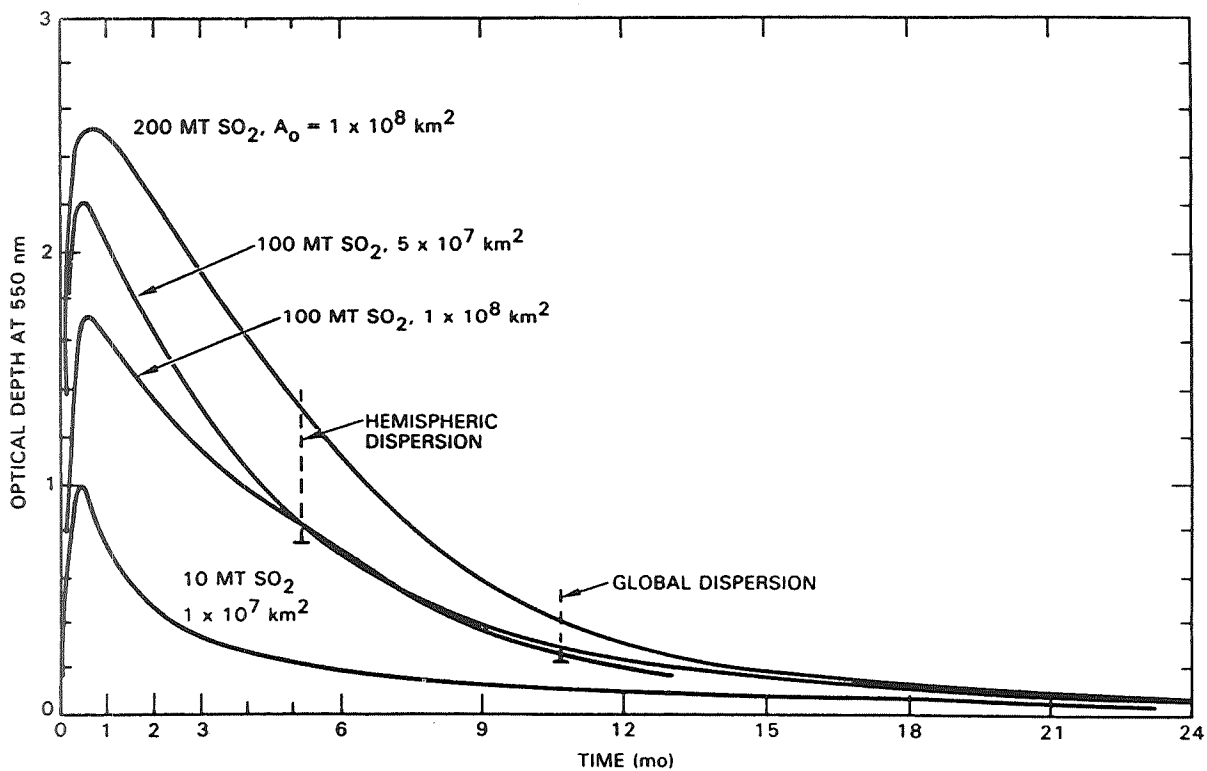


Figure 4. Volcanic aerosol optical depths (zenithal) versus time for the volcanic cloud simulations discussed by Pinto et al. (40). Indicated on the figure are the times required for the cloud to disperse over a hemisphere, or over the globe (40).

The sulfate aerosol mode radius peaks earlier with larger SO_2 injections and remains elevated throughout the history of the eruption cloud. In the simulations shown, the mode radius grows as large as $0.7 \mu\text{m}$, which greatly exceeds the ambient sulfate mode radius, $r \sim 0.05 \mu\text{m}$. In the instance of very large eruptions, the mode radius returns to its ambient value only after a period of several years. The mode radius is important in determining the rate at which sulfate is removed from the stratosphere. The sulfate mass flux from the stratosphere is proportional to the fallspeed, v , of the aerosols multiplied by their mass, m . Since $m \propto r^3$ and $v \propto r^{1 \rightarrow 2}$ in the regime of interest, the mass loss rate is, $m \propto r^{4 \rightarrow 5}$. The optical depth per unit mass of aerosol varies roughly as $1/r$ in the size range of interest. Hence, the decrease in optical depth in Figure 4 can be seen to have two causes: (1) the growth in particle size that reduces the optical efficiency; and (2) a rapid decrease in the total sulfate mass caused by sedimentation (after a month or so). These nonlinear interactions greatly limit the potential climatic effects of explosive volcanism.

POLAR STRATOSPHERIC CLOUDS (PSCs)

The properties of stratospheric clouds in polar regions (PSCs), (41) have been defined by a decade of satellite observations (see Table 4) (42-45). Based on optical and physical evidence, PSCs fall into two broad categories, which are referred to here as Type I and Type II PSCs. Type I PSCs consist of an aerosol haze of micron-sized nitric acid ice particles composed of HNO_3 and H_2O [in roughly a 50/50 mixture by weight, similar to the trihydrate $\text{HNO}_3 \cdot 3\text{H}_2\text{O}$] (46,47). Type II PSCs are apparently composed of water-ice crystals (48). Some statistical properties of PSCs derived from satellite observations are summarized in Figure 5 (45).

Table 4. Properties of Polar Stratospheric Clouds

Composition	Type I: HNO ₃ /H ₂ O (~50%/50%); Type-II: water ice; possibly traces of HCl, HNO ₃ , etc.
Origin	Type I: nucleation on sulfate, T<195 K; Type II: ice nucleation on Type I, T<189 K
Properties	Type I: ~1-10 ppbm; <1 cm ⁻³ ; 0.3 μm; Type II: ~1 ppmm; <<1 cm ⁻³ ; 3 μm radius; solid crystalline structures
Distribution	Polar winter stratospheres (>60° latitude); 14-24 km altitude; winter and early spring; S. H., June-October, widespread Type I and II; N. H., December-March, sporadic I, occasional II
Mass Budget	Type I: ~ 1-10 ppbm HNO ₃ per winter season; Type II: ~ 1-5 ppmm H ₂ O per winter
Residence Time	Type I: ~ 1 day, to weeks (temperature control, to sedimentation control); Type II: ~ hours (condensation/sedimentation/evaporation control)
Effects	Activation of chlorine reservoirs (Type I and II); conversion of NO _x into HNO ₃ (Type I); dehydration of the polar stratosphere (Type II); denitrification of the polar vortex (Type I and II)
Influences	Stratospheric polar meteorology; tropospherically driven wave events; vortex stability and temperature; springtime warming events; possible role of changes in CH ₄ , H ₂ O and NO _y
Trends	Tied to trends in polar meteorology, especially temperature

The Type I PSCs are considered the most common form, accounting for perhaps 80 to 90% of all cloud sightings. These PSCs exhibit an onset at temperatures near 195 K, whereas the more massive Type II PSCs appear to condense at colder temperatures (<187 K) consistent with the measured frost point of water vapor in the polar stratosphere (48,49). It should be expected, therefore, that Type I haze would predominate the totality of cloud observations in the earliest part of the Antarctic winter season, and that the frequency of Type II clouds would increase with the progression of winter and cooling of upper air layers. On the other hand, the observed dehydration and denitrification of the Antarctic winter stratosphere would, over the course of time, reduce the frequency of cloud formation at specific temperature thresholds (50). In the late winter and early spring, predictions and observations indicate that PSCs will dissipate abruptly when the upper strato-sphere warms (51).

Most likely, the nuclei for nitric acid ice deposition are the background sulfuric acid aerosols (46). Observational evidence on the extent to which sulfate particles are nucleated in PSCs is mixed. Aircraft measurements taken in the Antarctic ozone hole in September 1987 suggest that many, if not most, of the sulfate particles may be activated into nitric acid haze particles (52,53). On the other hand, balloon-borne aerosol measurements taken at McMurdo Station during the same period, and more recent data from the Arctic winter stratosphere, indicate that, although layers of ~1 micron-size haze particles are frequently present, on occasion the

fraction of the sulfate particles activated into haze is quite small, roughly 1 in 10^3 (54,55). If sulfate particle nucleation is limited to a small fraction of the total number of particles, the resulting large sizes of haze particles will have important implications for stratospheric denitrification (56-58).

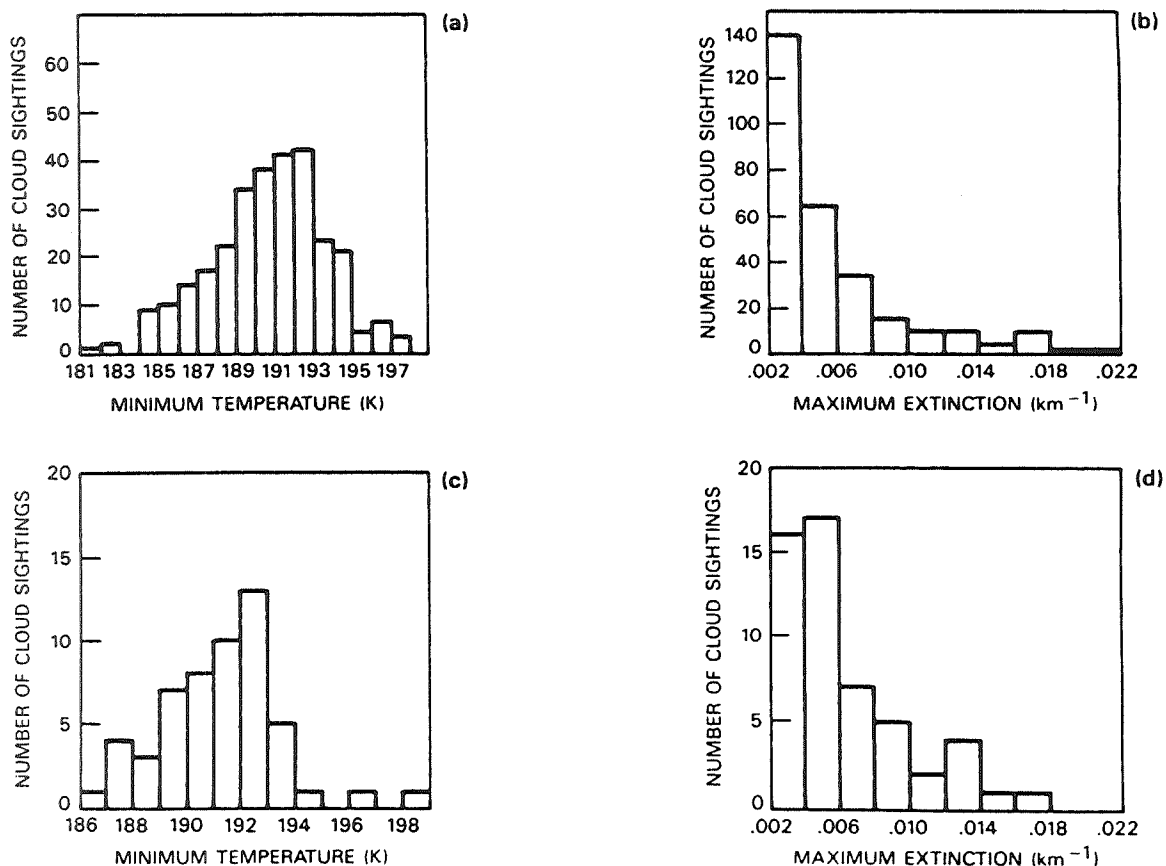


Figure 5. Statistics of polar stratospheric clouds. Panels (a) and (b) refer to the Southern Hemisphere, panels (c) and (d) to the Northern Hemisphere. The histograms represent the total ensemble of cloud sightings by the SAM-II satellite in 1986. Panels (a) and (c) show the number of cloud observations as a function of the minimum temperature in the vertical temperature profile estimated for each satellite observation. A PSC "sighting" is defined by an extinction greater than $1 \times 10^{-3} \text{ km}^{-1}$ at 3 km or more above the local tropopause. Panels (b) and (d) show the number of clouds with maximum extinctions within specific intervals. The data indicate an onset of PSC formation at approximately 195 K, with a predominance of clouds at the low extinction end of the spectrum (i.e., Type-I PSCs) (45).

In situ measurements of odd-nitrogen species provide direct evidence for the existence of nitric acid particles in the antarctic winter stratosphere (52,53,59). That evidence is supported by infrared spectroscopic measurements of condensed HNO_3 (60) and column measurements of depletion of the HNO_3 vapor column amount (61,62). In addition, Hanson and Mauersberger (63,64), in a series of detailed laboratory studies, have quantified the compositions and vapor pressures of the nitric acid ices under the conditions of interest, and they concluded that the nitric acid trihydrate is probably the stable form in the stratosphere.

OTHER STRATOSPHERIC AEROSOLS

Only brief mention has been made of the other types of particulates shown in Figure 1. The properties of two important varieties of these particles — spacecraft alumina debris and meteoritic dust — are summarized in Table 5 (65-67). Data collected by Zolensky et al. (68) reveal a 10-fold increase in the stratospheric burden of alumina particles and other debris associated with space activities during the decade, 1976-1986.

SOOT

Because aircraft engines also generate soot (graphitic carbon, elemental carbon, or black carbon), the presence of soot in the ambient stratosphere is of interest. To date, there have been no definitive measurements of soot aerosol in the stratosphere. Observations of light absorption (single-scatter albedo) by stratospheric aerosols show a very small residual absorption that has not been assigned to any particular species (69). Several impactor samples taken in the stratosphere have revealed soot or soot-like particles (70,71). One suggested source for these particles is fragments of carbonaceous chondrites of extraterrestrial origin (70). Large forest fires have also been observed to deposit smoke near the tropopause, and some of this aerosol would consist of soot. Deep convective storms may lift polluted air containing soot into the lower stratosphere. Substantial concentrations of soot aerosol, comprising Arctic haze, are found in the Arctic polar winter troposphere up to the height of the tropopause (72,73).

Because of a lack of data, the morphology and global budget of soot particles in the upper atmosphere remain uncertain. Nonetheless, only a very small input of soot to the stratosphere — less than 0.001 Tg-C/yr — might be expected.

NOCTILUCENT CLOUDS

Noctilucent (night-luminous) clouds (NLCs) have been under continuous investigation since the late 1800s (74-76). NLCs are the extreme manifestation of terrestrial water clouds, residing more than 80 km above the ground and lending a spectacular appearance to the nighttime sky. Yet, despite decades of remote observation, and occasional in situ probing, the physics of noctilucent clouds has not been entirely quantified. Reasons include the remoteness of the clouds, which makes observation difficult, and the complexity of the cloud processes, which involve particle microphysics, atmospheric dynamics, photochemistry and ionization processes (77-80). Table 6 summarizes our current understanding of noctilucent cloud properties, based on a number of studies and reviews (81-86); see also *Journal of Geophysical Research*, volume 94, number D12, 1989.

Table 5. Properties of Alumina Particles and Meteoritic Dust

Alumina Particles	
Composition	Al ₂ O ₃ ; surface traces of Cl, S, etc.
Origin	Ablated space debris; solid-fueled rocket exhaust
Properties	Solid spheres; << 0.1 ppbm; >1 μm radius; ~1x10 ⁻⁶ cm ⁻³
Distribution	Globally distributed above 12 km; observations lacking, concentrated in flight corridors?
Mass Budget	~ 0.001 Tg-Al ₂ O ₃ per year
Residence Time	< 1 yr (average, based on particle size distribution)
Effects	Provide ready nuclei for aerosols/clouds; surfaces for chemical processing
Influences	Space activity; re-entry and burn-up of old spacecraft and launch vehicles; vehicle launch rates
Trends	Apparent tenfold increase from 1976-1986
Meteoritic Dust	
Composition	SiO ₂ , Fe, Ni, C, etc.; trace of Cl, S
Origin	Interplanetary dust; ablation debris
Properties	Solid particles, some spheres; micrometeorites; << 0.1 ppbm; >1 μm radius; <1x10 ⁻⁷ cm ⁻³ ; smoke particles: ~ 0.01 μm; <100 cm ⁻³
Distribution	Distributed more-or-less globally above 12 km (observations lacking)
Mass Budget	~ 0.02 Tg/yr (global influx, meteoroid events, distribution undetermined)
Residence Time	< 1 mo (micrometeorites); 1-10 yr (meteoritic "smoke")
Effects	Provide ready nuclei for aerosols and clouds; surfaces for chemical processing
Influences	Meteor showers, cometary encounters
Trends	None are obvious

Table 6. Properties of Noctilucent Clouds

Composition	Principally water ice; some meteoritic debris
Origin	Water vapor nucleation onto ions or meteoritic dust particles
Properties	Ice crystals, likely cubic; < 1 ppm; < 0.05- μ m radius; ~ 10 cm ⁻³ ; optical depths, typically 10^{-4} to 10^{-5} , maximum $\sim 10^{-3}$
Distribution	Mesopause region (~ 82 km) at high latitudes ($>45^\circ$) in the summer hemisphere; temperature of formation, ~ 130 K
Mass Budget	~ 1 ppm H ₂ O at 80 km
Residence Time	Minutes to hours (sedimentation/evaporation control)
Effects	Ionization depletion; minor effects on solar or terrestrial radiation
Influences	Water vapor accumulation in the upper atmosphere; possibly release of water by rocket engines
Trends	Significant increase over last century concurrent with buildup of atmospheric methane

Sunlight scattered from noctilucent clouds has a very minor effect on the radiation balance at high latitudes. NLC particles can scavenge electrons and ions and thus alter the local charge balance. Noctilucent clouds may also control the water vapor abundance in the thermosphere by providing a "cold trap" near the mesopause. As space missions and rocket launches become more frequent, more water vapor will be deposited in the mesosphere, so noctilucent clouds may become more common (87). Besides the vehicles launched for space exploration, more rockets may be launched to exploit the solar system for energy and mineral resources. High-altitude aircraft flights may lead to further increases in the amount of water vapor in the upper atmosphere. Thomas et al. (88) have proposed that the apparent increase in NLC frequency over the last century is associated with the observed increase in the concentration of methane (and, hence, water vapor) in the upper atmosphere.

A semi-stationary summertime layer of noctilucent clouds — referred to as polar mesospheric clouds, or PMCs — has been detected and characterized by the Solar Mesosphere Explorer satellite (89). The PMCs and NLCs have similar microphysical and chemical origins: NLCs represent the weak, equator-ward manifestation of PMCs. The clouds, at their densest, have vertical optical depths of $\sim 10^{-3}$, with typical optical depths one to two orders of magnitude smaller.

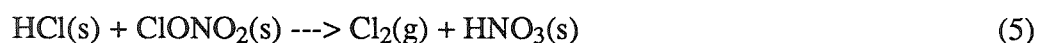
HETEROGENEOUS CHEMICAL PROCESSES AND OZONE DEPLETION

The recent discovery of an ozone "hole" over Antarctica in late austral winter and early spring (90) has led to considerable research on the causative processes (e.g., seminal discussions are given by Solomon et al. (91); Crutzen and Arnold (47); McElroy et al. (92,93)). Much of the subsequent research is collected in special journal issues, including *Geophysical*

Research Letters, volume 13, number 12, 1986; and volume 15, number 8, 1988; *Journal of Geophysical Research*, volume 94, numbers D9 and D14, 1989; *Geophysical Research Letters*, volume 17, number 4, 1990; see also Solomon (94).

Laboratory studies show that a fast surface-catalyzed reaction of HCl with chlorine nitrate (ClONO₂) can occur on PSC particles to produce "active" chlorine (Cl₂, HOCl, and ClNO₂) (95-101). Through known homogeneous photochemical processes (102), this enhanced activated chlorine may explain most, if not all, of measured ozone deficits (103,104). The intense interest in PSCs has led to a new focus on the possible role of other stratospheric aerosols in heterogeneous chemical reactions that might affect stratospheric composition and ozone depletion (105).

The key heterogeneous chemical processes that occur on PSC particles are:



In these chemical equations, "s" indicates that the species is likely to be adsorbed on the particle surface prior to reaction, and "g" indicates that the species rapidly desorbs from ice surfaces and is likely to be found in the gas phase (106). Chlorine activation via reactions 5 through 7 is very likely to proceed to completion on PSCs, with or without occasional solar illumination, in the early part of polar winter. This conclusion was recently confirmed by laboratory studies (107). Chlorine activation — in combination with denitrification, which is caused by PSC particle sedimentation, and de-NO_x-ification, which is the conversion of NO_x to nitric acid as in reaction (8) — results in a perturbed stratospheric composition that is extremely destructive to ozone. If the stratospheric abundances of water vapor and/or nitric acid vapor were to increase substantially in the future, PSCs could appear more widely and cause chemical perturbations over much larger regions. Similarly, continued cooling of the stratosphere caused by increasing burdens of carbon dioxide might enhance PSC formation and chemical activity.

It has been suggested chlorine activation and other heterogeneous chemical processes may occur on background sulfate aerosols (105). The significance of such reactions is that the resulting perturbation could be global in scale, and not confined to the polar winter as they are in the ozone hole. Modeling studies support the possibility of large, widespread ozone depletions associated with heterogeneous chemistry, if the rates of one or more of reactions (5) through (7) — particularly reaction (5) — are rapid (108). In these scenarios, increasing stratospheric concentrations of background HCl and ClONO₂, derived from chlorofluorocarbons could be activated over global scales if sulfate levels were enhanced by anthropogenic activity (109) or by a future major volcanic eruption.

Laboratory measurements show that the reaction of N₂O₅ with H₂O (reaction 8) occurs efficiently on sulfuric acid surfaces (110,111) [this reaction also occurs on PSCs, but is quite sensitive to the fractional composition of water in the ice particles (97)]. There is, however, little evidence for the rapid reactions of chlorine gases (i.e., reactions 5 through 7) on sulfate particles, either in laboratory studies (101,112) or atmospheric analyses (113). On the other hand, accelerating ozone depletions measured in the Northern Hemisphere (114) suggest a possible increase in the activity of chlorine that may be associated with heterogeneous chemical pro-

cesses. Accordingly, global-scale chemical perturbations connected with sulfate aerosol enhancements remain uncertain.

RADIATION AND CLIMATE EFFECTS

Many scientists, beginning with Benjamin Franklin (115), have studied the relation between volcanic explosions and climate/weather change (116-121). Existing research indicates that, in the years after a major volcanic eruption, anomalous weather patterns and regional- to global-scale cooling is likely (122-127). The connection between volcanoes and climate is most directly made through the radiative effect of volcanically induced sulfate aerosols on the global radiation budget (122,128). The volcanic aerosols, when formed in the stratosphere where they can be rapidly dispersed around the Earth, increase the reflectivity of the atmosphere and reduce incoming solar energy (129). The aerosols also produce a modest infrared-trapping effect, which is not sufficient to reverse the cooling caused by the increased reflectivity (122). The net effect of a major volcanic eruption sending sulfur gases into the stratosphere is an average global cooling of perhaps $\sim 0.5^{\circ}\text{C}$ for 1 year or more; this effect is limited, to a great extent, by the thermal inertia of the oceans and the relatively short residence time of volcanic aerosols in the atmosphere (130). Many statistical correlations have linked volcanic eruptions in one year with global cooling in the following years. For example, records of tree rings (131) and other climate proxies (117) support the volcanic cooling hypothesis.

The explosive energy of a volcanic eruption may not be an accurate indicator of its climatic impact. More important is the quantity of sulfur gases (particularly SO_2) injected into the stratosphere. However, the average climate effect of an explosive eruption appears to be limited to a maximum temperature decrease of $\sim 1^{\circ}\text{C}$, even for the largest eruptions. This fundamental limitation may be the result of highly nonlinear physical processes that restrict the buildup and persistence of the aerosol optical depth (40).

After a major volcanic eruption, the stratospheric aerosols settle into the upper troposphere over a period of several years. These sulfate particles are highly soluble and thus enhance the cloud condensation nuclei (CCN) population of the upper troposphere (26). Similarly, high-altitude aircraft operations might increase the CCN abundance in the upper troposphere and alter cloud properties and the radiative balance of the troposphere.

Human activities can also affect stratospheric aerosol properties. Direct emissions of SO_2 and soot from high-flying aircraft contaminate the natural sulfate layer. Rocket exhaust particles released into the stratosphere, and an increasing rate of ablation of debris from orbiting platforms (68), further enhance the concentration of stratospheric aerosols. Comprehensive studies have been carried out to estimate the potential climatic impacts of proposed fleets of high-altitude aircraft (the "supersonic transport", or SST, proposed in the early 1970s) (132), while other studies have focused specifically on the possible climatic effects of aerosols generated by SST operations and Space Shuttle launches (133). In each case, only minor global-scale effects have been predicted.

Figure 6 presents calculations of the sulfate aerosol size distribution and optical depth that result from an order-of-magnitude increase in either the OCS or SO_2 concentration in the upper troposphere. The modified size distribution contains significantly larger particles, which increase in the optical depth of the aerosol layer. For an OCS enhancement by a factor of 10, the optical depth is increased by a factor of almost 5 (134). Such increases, while smaller than those observed after major volcanic explosions (i.e., factors of 10-100), approach the threshold for climatic significance.

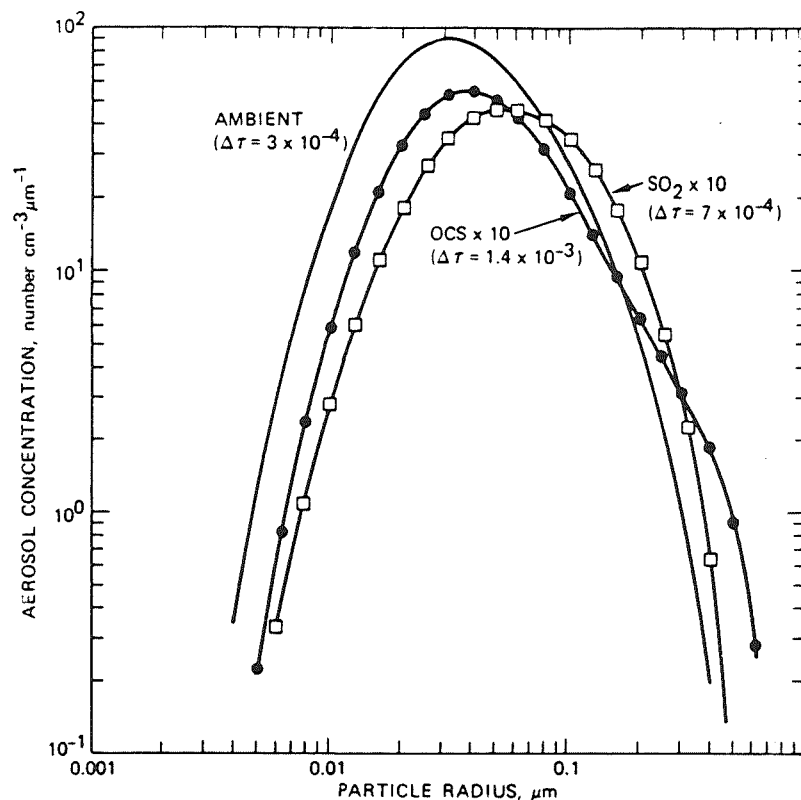


Figure 6. Calculated aerosol size distributions at 20 km for background stratospheric sulfur gas abundances, and for an increase by a factor of 10 in either the OCS or SO₂ abundance in the upper troposphere. Also indicated in each case is the aerosol optical depth corresponding to a layer 1-km thick centered at a height of 20 km (134).

OUTSTANDING SCIENTIFIC ISSUES

Some of the questions about the role of aerosols in upper-atmosphere chemistry and in climate change are summarized in Table 7. Because aerosols in the upper atmosphere can affect the state of the troposphere and biosphere, it will be important to establish baseline properties for these particles and monitor any changes in these properties. Among other signals of aerosol activity are variations in solar radiation reaching the lower atmosphere and surface and alterations in the chemistry of the ozone layer (38). Upper-atmospheric particles are subject to modification by many human activities, including high-altitude commercial and military flight. It remains to be determined whether such activities — at projected levels — can lead to climatic and other environmental changes. Specific scientific studies include:

- 1) Heterogeneous chemistry studies: Accurate laboratory studies on the reactivity of sulfate (sulfuric acid) aerosols should be carried out under realistic stratospheric conditions; as opportunities arise, in situ chemical perturbations associated with enhanced sulfate aerosols might be studied directly (e.g., after a volcanic eruption, or in a planned sulfur release).
- 2) Predictive model development: Forecasting the effects of natural events, such as volcanic eruptions and of various human activities on middle-atmosphere aerosols, upper-tropospheric aerosols, the global radiation budget, and climate, requires sophisticated models, which should be global in scale — optimally three-dimensional — and include accurate treatments of the appropriate dynamical, photochemical, microphysical and radiative processes.

Table 7. Questions and Uncertainties

Sulfate Aerosols

- Is the background sulfate mass increasing, and if so, why?
- Will proposed high-altitude aircraft traffic increase the mass and/or chemical activity of the global background sulfate aerosol layer?
- Is increased sulfate aerosol reactivity possible with increasing water vapor, among other factors?
- Are stratospheric particles a significant component of the global radiative energy balance under normal conditions, and thus of global climate change?

Volcanic Particulates

- Is there a measurable effect of volcanic eruptions on climate, or is the effect illusory?
- Are volcanic aerosols important for heterogeneous chemistry?
- What are the types and frequencies of volcanic eruptions that produce global effects?
- What are the injection efficiencies of SO₂, HCl, H₂O, and other gases?
- Are there strong nonlinear limits to the global effects of very large volcanic injections?

Polar Stratospheric Clouds

- Will high-altitude flight enhance water vapor concentrations, leading to a greater frequency, range and duration of PSCs?
- Will high-flying aircraft create long-lived contrails in the polar stratosphere and modify stratospheric chemistry and ozone?
- Are there other species/reactions (e.g., of NO_x), which might be important, on stratospheric ice particles?
- What is the precise composition and morphology of Type I and Type II ice particles?
- How does denitrification occur on Type I and Type II particles?
- Can we directly observe chlorine activation on Type I PSCs?

Soot

- What are the ambient sources and concentrations of soot particles in the stratosphere?
- Can the morphology or trace chemistry of soot be used to identify and quantify uniquely its sources?
- Can soot particles catalyze heterogeneous chemical processes under stratospheric conditions?
- Is soot absorption of shortwave radiation in the stratosphere dynamically or climatically significant?

Alumina Particles

- What increase in stratospheric alumina debris can we expect from future aerospace fleets, including rockets and aircraft?
- What is the reactivity of alumina particles coated with sulfates?
- Can the total surface area of alumina particles in the stratosphere be determined? Is it significant?
- Are these particles an important sink for sulfate, chloride, or other stratospheric materials?

Meteoritic Dust

- Are claims of potential significant chemical impacts in the stratosphere reasonable?
- What are the effects of meteoritic material on stratospheric composition above ~30 km, due to neutralization reactions, etc.?

Noctilucent Clouds

- Will water vapor emissions by high-altitude aircraft increase the frequency and range of NLCs?
 - Are the frequency and density of NLCs increasing in pace with methane or other gases?
-

- 3) Global aerosol monitoring program: A global monitoring program for middle atmosphere aerosol trends — particularly trends that may be associated with anthropogenic emissions but also transients associated with volcanic eruptions — could be built on existing and planned satellite and lidar measurement projects; in situ measurements would be necessary for calibration and detailed microphysical/radiative/chemical definition of the aerosols over time. The mesosphere could also be monitored for changes in key parameters, such as water vapor content and the occurrence of clouds.

ACKNOWLEDGMENTS

This work was supported by the National Aeronautics and Space Administration's High Speed Research Program under grant NASA/L NAG-1-1126 and Upper Atmosphere Program under grant NASA/W NAGW-2183.

REFERENCES

1. Volz, F.E., and R.M. Goody, The intensity of the twilight and upper atmospheric dust, *J. Atmos. Sci.*, 19, 385-406, 1962.
2. Junge, C.E., and J.E. Manson, Stratospheric aerosol studies, *J. Geophys. Res.*, 66, 2163-2182, 1961
3. Junge, C.E., Sulfur in the stratosphere, *J. Geophys. Res.*, 68, 3975, 1963.
4. Mossop, S.C., Stratospheric particles at 20 km, *Nature*, 199, 325-326, 1963.
5. Rosen, J.M., The vertical distribution of dust to 30 kilometers, *J. Geophys. Res.*, 69, 4673-4676, 1964.
6. Lamb, H.H., Volcanic Dust in the atmosphere, with a chronology and assessment of its meteorological significance, *Philos. Trans. Roy. Soc. London*, 266, 425-533, 1970.
7. Hirono, M., M. Fujiwara, and T. Itabe, Behavior of the stratospheric aerosols inferred from laser radar and small ion radiosonde observations, *J. Geophys. Res.*, 81, 1593-1600, 1976.
8. Hofmann, D.J., and J.M. Rosen, On the background stratospheric aerosol layer, *J. Atmos. Sci.*, 38, 168-181, 1981.
9. Fiocco, G., and G. Grams, Observation of aerosol layer of 20 km by optical radar, *J. Atmos. Sci.*, 21, 323-324, 1964.
10. McCormick, M.P., P. Hamill, T.J. Pepin, W.P. Chu, T.J. Swissler, and L.R. McMaster, Satellite studies of the stratospheric aerosol, *Bull. Amer. Meteorol. Soc.*, 60, 1038-1046, 1979.
11. Turco, R.P., R.C. Whitten, and O.B. Toon, Stratospheric aerosols: Observation and theory, *Rev. Geophys.*, 20, 233-279, 1982.
12. Toon, O.B., and N.H. Farlow, Particles Above the Tropopause: Measurements and models of stratospheric aerosols, meteoric debris, nacreous clouds, and noctilucent clouds, *Annual Rev. Earth Planet. Sci.*, 9, 19-58, 1981.
13. Rosen, J.M., The boiling point of stratospheric aerosols, *J. Appl. Meteorol.*, 10, 1044-1046, 1971.
14. Friend, J.P., R. Leifer, and M. Trichon, On the formation of stratospheric aerosols, *J. Atmos. Sci.*, 30, 465-479, 1973.
15. Castleman, A.W., Jr., H.R. Munkelwitz, and B. Manowitz, Isotopic studies of the sulfur component of the stratospheric aerosol layer, *Tellus*, 26, 222-234, 1974.
16. Bigg, E.K., Stratospheric particles, *J. Atmos. Sci.*, 32, 910-917, 1975.
17. Farlow, N.H., D.M. Hayes, and H.Y. Lem, Stratospheric aerosols: Undissolved granules and physical state, *J. Geophys. Res.*, 82, 4921-4929, 1977.

18. Gras, J.L., Change in the nature of stratospheric aerosol collected at 34°S, *Nature*, 271, 231-232, 1978.
19. Crutzen, P.J., The possible importance of CSO for the sulfate layer of the stratosphere, *Geophys. Res. Lett.*, 3, 73-76, 1976.
20. Lazrus, A.L., and B.W. Gandrud, Stratospheric sulfate aerosol, *J. Geophys. Res.*, 79, 3424-3431, 1974.
21. Gandrud, B.W., and A.L. Lazrus, Measurements of stratospheric sulfate mixing ratio with a multi filter sampler, *Geophys. Res. Lett.*, 8, 21-22, 1981.
22. Arnold, F., R. Fabian, and W. Joos, Measurements of the height variation of sulfuric acid vapor concentrations in the stratosphere, *Geophys. Res. Lett.*, 8, 293-296, 1981.
23. McKeen, S.A., S.C. Liu, and C.S. Kiang, On the chemistry of stratospheric SO₂ following volcanic eruptions, *J. Geophys. Res.*, 89, 4873-4881, 1984.
24. Hamill, P., O.B. Toon, and C.S. Kiang, Microphysical processes affecting the stratospheric aerosol particles, *J. Atmos. Sci.*, 34, 1104-1119, 1977.
25. Twomey, S., *Atmospheric Aerosols*, Elsevier, 1977.
26. Pruppacher, H.R., and J.D. Klett, *Microphysics of Clouds and Precipitation*, D. Reidel, Dordrecht, Holland, 1978.
27. Cadle, R.D., Some effects of the emissions of explosive volcanoes on the stratosphere, *J. Geophys. Res.*, 85, 4495-4498, 1980.
28. Farlow, N.H., et al., Size distributions and mineralogy of ash particles in the stratosphere from eruptions of Mount St. Helens, *Science*, 211, 832-834, 1981.
29. Gandrud, B.W., and A.L. Lazrus, Filter measurements of stratospheric sulfate and chloride in the eruption plume of Mount St. Helens, *Science*, 211, 826-827, 1981.
30. Chuan, R.L., D.C. Woods, and M.P. McCormick, Characterization of aerosols from eruptions of Mount St. Helens, *Science*, 211, 830-832, 1981.
31. Rampino, M.R., and S. Self, Sulfur rich volcanic eruptions and stratospheric aerosols, *Nature*, 307, 344-345, 1984.
32. Devine, J.D., H. Sigurdsson, A.N. Davis, and S. Self, Estimate of sulfur and chlorine yield to the atmosphere from volcanic eruptions and potential climatic effects, *J. Geophys. Res.*, 89, 6309-6325, 1984.
33. Hofmann, D.J., and J.M. Rosen, Sulfuric acid droplet formation and growth in the stratosphere after the 1982 eruption of El Chichon, *Science*, 222, 325-327, 1983.
34. Oberbeck, V.R., E.F. Danielsen, K.G. Snetsinger, and G.V. Ferry, Effect of the eruption of El Chichon on stratospheric aerosol size and composition, *Geophys. Res. Lett.*, 10, 1021-1024, 1983.
35. Krueger, A.J., Sighting of El Chichon sulfur dioxide clouds with the Nimbus 7 Total Ozone Mapping Spectrometer, *Science*, 220, 1377-1379, 1983.

36. Turco, R.P., "Volcanic Aerosols: Chemistry, Microphysics, Evolution and Effects, Proc. Workshop on Volcanism-Climate Interactions," U. Maryland, College Park, June 18-19, 1990, NASA Publ. 10062, 1991.
37. Turco, R.P., O.B. Toon, R.C. Whitten, P. Hamill, and R.G. Keesee, The 1980 eruptions of Mount St. Helens: Physical and chemical processes in the stratospheric clouds, *J. Geophys. Res.*, *88*, 5299-5319, 1983.
38. Watson, R.T., et al., "Present State of Knowledge of the Upper Atmosphere 1988: An Assessment Report," NASA Ref. Publ. 1208, Washington, D.C., 1988.
39. Watson, R.T., et al., *Report of the International Ozone Trends Panel - 1988*, World Meteorological Report No. 18, 1989.
40. Pinto, J.P., R.P. Turco, and O.B. Toon, Self-limiting physical and chemical effects in volcanic eruption clouds, *J. Geophys. Res.*, *94*, 11,165-11,174, 1989.
41. Stanford, J.L., On the nature of persistent stratospheric clouds in the Antarctic, *Tellus*, *29*, 530-534, 1977.
42. McCormick, M.P., H.M. Steele, P. Hamill, W.P. Chu, and T.J. Swissler, Polar stratospheric cloud sightings by SAM II, *J. Atmos. Sci.*, *39*, 1387-1397, 1982.
43. McCormick, M.P., and C.R. Trepte, SAM II measurements of Antarctic PSC's and aerosols, *Geophys. Res. Lett.*, *13*, 1276-1279, 1986.
44. McCormick, M.P., and C.R. Trepte, Polar stratospheric optical depth observed between 1978 and 1985, *J. Geophys. Res.*, *92*, 4297-4306, 1987.
45. Hamill, P., and R.P. Turco, "The Ozone Hole: The Role of Polar Stratospheric Cloud Particles," Paper AIAA-88-0211, American Institute of Aeronautics and Astronautics, 7 pp., Washington, D.C., 1988.
46. Toon, O.B., P. Hamill, R.P. Turco, and J. Pinto, Condensation of HNO₃ and HCl in the winter polar stratospheres, *Geophys. Res. Lett.*, *13*, 1284-1287, 1986.
47. Crutzen, P.J., and F. Arnold, Nitric acid cloud formation in the cold Antarctic stratosphere: A major cause for the springtime 'Ozone Hole', *Nature*, *324*, 651-655, 1986.
48. Poole, L.R., and M.P. McCormick, Airborne lidar observations of Arctic polar stratospheric clouds: Indications of two distinct growth stages, *Geophys. Res. Lett.*, *15*, 21-23, 1988.
49. Hamill, P., R.P. Turco, and O.B. Toon, On the growth of nitric and sulfuric acid aerosol particles under stratospheric conditions, *J. Atmos. Chem.*, *7*, 287-315, 1988.
50. McCormick, M.P., C.R. Trepte, and M.C. Pitts, Persistence of polar stratospheric clouds in the southern polar region, *J. Geophys. Res.*, *94*, 11,241-11,251, 1989.
51. Toon, O.B., R.P. Turco, J. Jordan, J. Goodman, and G. Ferry, Physical processes in polar stratospheric ice clouds, *J. Geophys. Res.*, *94*, 11,359-11,380, 1989.

52. Fahey, D.W., K.K. Kelly, G.V. Ferry, L.R. Poole, J.C. Wilson, D.M. Murphy, M. Loewenstein, and R.K. Chan, In-Situ measurements of total reactive nitrogen, total water vapor, and aerosols in a polar stratospheric cloud in the Antarctic, *J. Geophys. Res.*, *94*, 11,299-11,315, 1989.
53. Pueschel, R.F., K.G. Snetsinger, J.K. Goodman, O.B. Toon, G.V. Ferry, V.R. Oberbeck, J.M. Livingston, S. Verma, W. Fong, W.L. Starr, and R.K. Chan, Condensed nitrate, sulfate and chloride in the Antarctic stratospheric aerosols, *J. Geophys. Res.*, *94*, 11,271-11,284, 1989.
54. Hofmann, D.J., Stratospheric cloud micro-layers and small-scale temperature variations in the Arctic in 1989, *Geophys. Res. Lett.*, *17*, 369-372, 1989.
55. Hofmann, D.J., J. M. Rosen, J.W. Harder, and J.V. Hereford, Balloonborne measurements of aerosol, condensation nuclei, and cloud particles in the stratosphere at McMurdo Station Antarctica during the spring of 1987, *J. Geophys. Res.*, *94*, 11,253-11,269, 1989.
56. Salawitch, R.J., S.C. Wofsy, and M.B. McElroy, Influence of polar stratospheric clouds on the depletion of ozone over Antarctica, *Geophys. Res. Lett.*, *15*, 871-874, 1988.
57. Toon, O.B., R.P. Turco, and P. Hamill, Denitrification mechanisms in the polar stratospheres, *Geophys. Res. Lett.*, *17*, 445-448, 1990.
58. Drdla, K., and R.P. Turco, Denitrification through PSC formation: A 1-D model incorporating temperature oscillations, *J. Atmos. Chem.*, *12*, 319-366, 1991.
59. Gandrud, B.W., P.D. Sperry, K.K. Kelly, G.V. Ferry, and K.R. Chan, Filter measurement results from the Airborne Antarctic Ozone Experiment, *J. Geophys. Res.*, *94*, 11,285-11,297, 1989.
60. Kinne, S., O.B. Toon, G.C. Toon, C.B. Farmer, E.V. Browell, and M.P. McCormick, Measurements of Size and Composition of Particles in Polar Stratospheric Clouds from Infrared Solar Absorption Spectra, *J. Geophys. Res.*, *94*, 16,481-16,491, 1989.
61. Toon, G.C., C.B. Farmer, L.L. Lowes, P.W. Schaper, J.-F. Blavier, and R.H. Norton, Infrared aircraft measurements of stratospheric composition over Antarctica during September 1987, *J. Geophys. Res.*, *94*, 16,571-16,596, 1989.
62. Coffey, M.T., W.G. Mankin, and A. Goldman, Airborne measurements of stratospheric constituents over Antarctica in the austral spring of 1987, 2, Halogen and nitrogen trace gases, *J. Geophys. Res.*, *94*, 16,597-16,613, 1989.
63. Hanson, D., and K. Mauersberger, Vapor pressures of HNO₃/H₂O solutions at low temperatures, *J. Phys. Chem.*, *92*, 6167-6170, 1988.
64. Hanson, D., and K. Mauersberger, Laboratory studies of the nitric acid trihydrate: Implications for the south polar stratosphere, *Geophys. Res. Lett.*, *15*, 855-858, 1988.
65. Brownlee, D.E., G.V. Ferry, and D. Tomandl, Stratospheric aluminum oxide, *Science*, *191*, 1270-1271, 1976.

66. Hunten, D.M., R.P. Turco, and O.B. Toon, Smoke and dust particles of meteoric origin in the mesosphere and stratosphere, *J. Atmos. Sci.*, *37*, 1342-1357, 1980.
67. Turco, R.P., O.B. Toon, R.C. Whitten, and R.J. Cicerone, Space shuttle ice nuclei, *Nature*, *298*, 830-832, 1982.
68. Zolensky, M.E., D.S. MacKay and L.A. Kaczor, A tenfold increase in the abundance of large particles in the stratosphere, as measured over the period 1976-1984, *J. Geophys. Res.*, *94*, 1047-1056, 1989.
69. Clarke, A.D., R.J. Charlson, and J.A. Ogren, Stratospheric aerosol light absorption before and after El Chichon, *Geophys. Res. Lett.*, *10*, 1017-1020, 1983.
70. Chuan, R.L., and D.C. Woods, The appearance of carbon aerosol particles in the lower stratosphere, *Geophys. Res. Lett.*, *11*, 553-556, 1984.
71. Pueschel, R.F., A.D.A. Hansen, and D. Blake, private communication, 1991.
72. Hansen, A.D.A., and H. Rosen, Vertical distribution of particulate carbon in the Arctic haze, *Geophys. Res. Lett.*, *11*, 381, 1984.
73. Hansen, A.D.A., and T. Novakov, Aerosol black carbon measurements in the Arctic haze during AGASP-2, *J. Atmos. Chem.*, *9*, 347, 1989.
74. Hesstvedt, E., Note on the nature of noctilucent clouds, *J. Geophys. Res.*, *66*, 1985, 1961.
75. Witt, G., Height, structure and displacements of noctilucent clouds, *Tellus*, *19*, 1-18, 1962.
76. Witt, G., The nature of noctilucent clouds, *Space Res.*, *9*, 157-169, 1969.
77. Charlson, R.J., Noctilucent clouds: A steady-state model, *Quart. J. Roy. Meteorol. Soc.*, *91*, 517, 1965.
78. Reid, G.C., Ice clouds at the summer polar mesopause, *J. Atmos. Sci.*, *32*, 523-535, 1975.
79. Turco, R.P., O.B. Toon, R.C. Whitten, R.G. Keesee, and D. Hollenbach, Noctilucent clouds: Simulation studies of their genesis, properties and global influences, *Planet. Space Sci.*, *30*, 1147-1181, 1982.
80. McIntyre, M.E., On dynamics and transport near the polar mesopause in summer, *J. Geophys. Res.*, *94*, 14,617-14,628, 1989.
81. Fogle, B., and B. Haurwitz, Noctilucent clouds, *Space Sci. Rev.*, *6*, 278-340, 1966.
82. Theon, J.S., W. Nordberg, and W.S. Smith, Temperature measurements in noctilucent clouds, *Science*, *157*, 419-421, 1967.
83. Donahue, T.M., B. Guenther, and J.E. Blamont, Noctilucent clouds in daytime: Circumpolar particulate layers near the summer mesopause, *J. Atmos. Sci.*, *29*, 1205, 1972.

84. Avaste, O.A., A.V. Fedynsky, G.M. Grechko, V.I. Sevastyanov, and C.I. Willmann, Advances in noctilucent cloud research in the space era, *Pure Appl. Geophys.*, 118, 528-580, 1980.
85. Gadsden, M., Noctilucent clouds, *Space Sci. Rev.*, 33, 279-334, 1982.
86. Gadsden, M., and W. Schroder, The Nature of noctilucent clouds, *Gerlands Beitr. Geophysik Leipzig*, 98, 431-442, 1989.
87. Turco, R.P., O.B. Toon, R.C. Whitten, R.G. Keesee, and D. Hollenbach, A study of mesospheric rocket contrails and clouds produced by liquid-fueled rockets, *Space Solar Power Rev.*, 3, 223-234, 1982.
88. Thomas, G.E., J.J. Olivero, E.J. Jensen, W. Schroeder, and O.B. Toon, Relation between increasing methane and the presence of ice clouds at the mesopause, *Nature*, 338, 490, 1989.
89. Thomas, G.E., Solar mesosphere explorer measurements of polar mesospheric clouds (noctilucent clouds), *J. Atmos. Terrestrial Phys.*, 46, 819-824, 1984.
90. Farman, J.C., B.G. Gardiner, and J.D. Shanklin, Large losses of total ozone in Antarctica reveal seasonal ClO_x/NO_x interaction, *Nature*, 315, 207-210, 1985.
91. Solomon, S., R.R. Garcia, F.S. Rowland, and D.J. Wuebbles, On the depletion of Antarctic ozone, *Nature*, 321, 755-758, 1986.
92. McElroy, M.B., R.J. Salawitch, S.C. Wofsy, and J.A. Logan, Reductions of Antarctic ozone due to synergistic interactions of chlorine and bromine, *Nature*, 321, 759-762, 1986.
93. McElroy, M.B., R.J. Salawitch, and S.C. Wofsy, Antarctic O_3 : Chemical mechanisms for the spring decrease, *Geophys. Res. Lett.*, 13, 1296-1299, 1986.
94. Solomon, S., The mystery of the Antarctic ozone "hole," *Rev. Geophys.*, 26, 131-148, 1988.
95. Molina, M.J., T.-L. Tso, L.T. Molina, and F.C.-Y. Wang, Antarctic stratospheric chemistry of chlorine nitrate, hydrogen chloride, and ice: Release of active chlorine, *Science*, 238, 1253-1257, 1987.
96. Tolbert, M.A., M.J. Rossi, R. Malhotra, and D.M. Golden, Reaction of chlorine nitrate with hydrogen chloride and water at Antarctic stratospheric temperatures, *Science*, 238, 1258-1260, 1987.
97. Tolbert, M.A., M.J. Rossi, and D.M. Golden, Antarctic ozone depletion chemistry: Reactions of N_2O_5 with H_2O and HCl on ice surfaces, *Science*, 240, 1018-1021, 1988.
98. Tolbert, M.A., M.J. Rossi, and D.M. Golden, Heterogeneous interactions of chlorine nitrate, hydrogen chloride, and nitric acid with sulfuric acid surfaces at stratospheric temperatures, *Geophys. Res. Lett.*, 15, 847-850, 1988.

99. Leu, M.-T., Laboratory studies of sticking coefficients and heterogeneous reactions important in the Antarctic stratosphere, *Geophys. Res. Lett.*, *15*, 17-20, 1988.
100. Leu, M.-T., Heterogeneous reactions of N_2O_5 with H_2O and HCl on ice surfaces, *Geophys. Res. Lett.*, *15*, 851-854, 1988.
101. Hanson, D.R., and A.R. Ravishankara, The reaction probabilities of ClONO_2 and N_2O_5 on 40 to 75% sulfuric acid solutions, *J. Geophys. Res.*, in press, 1991.
102. Molina, L.T., and M.J. Molina, Production of Cl_2O_2 by the self reaction of the ClO radical, *J. Phys. Chem.*, *91*, 433-436, 1987.
103. Austin, J., et al., Lagrangian photochemical modeling studies of the 1987 Antarctic spring vortex. 2. Seasonal trends in ozone, *J. Geophys. Res.*, *94*, 16,717-16,735, 1989.
104. Anderson, J.G., W.H. Brune, S.A. Lloyd, D.W. Tooney, S.P. Sander, W.L. Starr, M. Loewenstein, and J.R. Podolske, Kinetics of O_3 destruction by ClO and BrO within the Antarctic vortex: An analysis based on in situ ER-2 data, *J. Geophys. Res.*, *94*, 11,480-11,520, 1989.
105. Hofmann, D.J., and S. Solomon, Ozone destruction through heterogeneous chemistry following the eruption of El Chichon, *J. Geophys. Res.*, *94*, 5029-5041, 1989.
106. Turco, R.P., O.B. Toon and P. Hamill, Heterogeneous physicochemistry of the polar ozone hole, *J. Geophys. Res.*, *94*, 16,493-16,510, 1989.
107. Moore, S.B., L.F. Keyser, M.-T. Leu, R.P. Turco, and R.H. Smith, Heterogeneous reactions on nitric acid trihydrate, *Nature*, *345*, 333-335, 1990.
108. Brasseur, G.P., C. Granier, and S. Walters, Future changes in stratospheric ozone and the role of heterogeneous chemistry, *Nature*, *348*, 626-628, 1990.
109. Hofmann, D.J., Increase in the stratospheric background sulfuric acid aerosol in the past 10 years, submitted to *Science*, 1990.
110. Mozurkewich, M., and J.G. Calvert, Reaction probability of N_2O_5 on aqueous aerosols, *J. Geophys. Res.*, *93*, 15,889-15,896, 1988.
111. Riehs, C.M., D.M. Golden, and M.A. Tolbert, Heterogeneous reaction of N_2O_5 on sulfuric acid surfaces representative of global stratospheric particulate, submitted to *J. Geophys. Res.*, 1991.
112. Watson, L.R., J.M. Van Doren, P. Davidovits, D.R. Worsnop, M.S. Zahniser, and C.E. Kolb, Uptake of HCl molecules by aqueous sulfuric acid droplets as a function of acid concentration, *J. Geophys. Res.*, *95*, 5631-5638, 1990.
113. Mather, J.H., and W.H. Brune, Heterogeneous chemistry on liquid sulfate aerosols: A comparison of in situ measurements with zero-dimensional model calculations, *Geophys. Res. Lett.*, *17*, 1283-1286, 1990.
114. Stolarski, R.S., P. Bloomfield, R.D. McPeters, and J.R. Herman, Total ozone trends deduced from Nimbus 7 TOMS data, *Geophys. Res. Lett.*, *18*, 1015-1018, 1991.

115. Franklin, B., Meteorological imaginations and conjectures, *Manchester Lit. Phil. Soc. Mem. Proc.*, 2, 122, 375, 1784.
116. Mitchell, J.M., Jr., Recent secular changes of the global temperature, *Ann. N. Y. Acad. Sci.*, 95, 235-250, 1961.
117. Lamb, H.H., *Climate: Present, Past and Future, Vol. 2, Climatic History and the Future*, Methuen, London, 1977.
118. Landsberg, H.E., and J.M. Albert, The summer of 1816 and volcanism, *Weatherwise*, 27, 63-66, 1974.
119. Oliver, R.C., On the response of hemispheric mean temperature to stratospheric dust: An empirical approach, *J. Appl. Meteorol.*, 15, 933-950, 1976.
120. Robock, A., A latitudinally dependent volcanic dust veil index, and its effect on climate simulations, *J. Volcan. Geotherm. Res.*, 11, 67-80, 1981.
121. Robock, A., The volcanic contribution to climate change of the past 100 years, in *Greenhouse-Gas-Induced Climatic Change: A Critical Appraisal of Simulations and Observations*, M.E. Schlessinger (ed.), Elsevier, in press, 1990.
122. Pollack, J.B., O.B. Toon, C. Sagan, A. Summers, B. Baldwin, and W. Van Camp, Volcanic explosions and climatic change: A theoretical assessment, *J. Geophys. Res.*, 81, 1071-1083, 1976.
123. Mass, C., and S.H. Schneider, Statistical evidence on the influence of sunspots and volcanic dust on long-term temperature records, *J. Atmos. Sci.*, 34, 1995-2004, 1977.
124. Robock, A., and C. Mass, The Mount St. Helens volcanic eruption of 18 May 1980: Large short-term surface temperature effects, *Science*, 216, 628-630, 1982.
125. Kelly, P.M., and C.B. Sear, Climatic impact of explosive volcanic eruptions, *Nature*, 311, 740-743, 1984.
126. Angell, J.K., and J. Korshover, Surface temperature changes following the six major volcanic episodes between 1780-1980, *J. Climate Appl. Meteorol.*, 24, 937-951, 1985.
127. Rampino, M.R., S. Self, and R.B. Stothers, Volcanic winters, *Ann. Rev. Earth Planet. Sci.*, 16, 73-99, 1988.
128. Bryson, R.A., and B.M. Goodman, Volcanic activity and climatic changes, *Science*, 207, 1041-1044, 1980.
129. Coakley, J.A., Jr., Stratospheric aerosols and the tropospheric energy budget: Theory versus observations, *J. Geophys. Res.*, 86, 9761-9766, 1981.
130. Hansen, J.E., W. Wang, and A.A. Lacis, Mt. Agung eruption provides test of a global climatic perturbation, *Science*, 199, 1065-1068, 1978.
131. LaMarche, V.C., and K.K. Hirschboeck, Frost rings in trees as records of major volcanic eruptions, *Nature*, 307, 121-126, 1984.

132. Grobecker, A.J., S.C. Coroniti, and R.H. Cannon, Jr., The effects of stratospheric pollution by aircraft: Report of findings, Climatic Impact Assessment Program Report DOT-TST-75-50, U.S. Dept. of Transportation, Washington, D.C., 1974.
133. Turco, R.P., O.B. Toon, J.B. Pollack, R.C. Whitten, I.G. Poppoff, and P. Hamill, Stratospheric aerosol modification by supersonic transport and space shuttle operations -- climate implications, *J. Appl. Meteorol.*, 19, 78-89, 1980.
134. Turco, R.P., R.C. Whitten, O.B. Toon, J.B. Pollack, and P. Hamill, OCS, stratospheric aerosols and climate, *Nature*, 283, 283-286, 1980.

54-45
64290

^{p. 20}
N92-19125

Chapter 4

Designing a Methodology for Future Air Travel Scenarios

Donald J. Wuebbles
Lawrence Livermore National Laboratory
Livermore, CA

LH075075

Contributors

Steven L. Baughcum and John H. Gerstle
Boeing Commercial Airplane Group
Seattle, WA

BR798021
BE494991

Jae Edmonds
Battelle Pacific Northwest Laboratory

Douglas E. Kinnison
Lawrence Livermore National Laboratory
Livermore, CA

LH075075

Nick Krull
Federal Aviation Administration
Washington, DC

FI950230

Munir Metwally and Alan Mortlock
McDonnell Douglas Corporation
Long Beach, CA

MP546517

Michael Prather
National Aeronautics and Space Administration
Goddard Institute for Space Studies
New York, NY

NC789443

92

PRECEDING PAGE BLANK NOT FILMED

INTRODUCTION

The growing demand on air travel throughout the world has prompted several proposals for the development of commercial aircraft capable of transporting a large number of passengers at supersonic speeds. Emissions from a projected fleet of such aircraft, referred to as high-speed civil transports (HSCTs), are being studied because of their possible effects on the chemistry and physics of the global atmosphere, in particular, on stratospheric ozone. At the same time, there is growing concern about the effects on ozone from the emissions of current (primarily subsonic) aircraft emissions.

Evaluating the potential atmospheric impact of aircraft emissions from HSCTs requires a scientifically sound understanding of where the aircraft fly and under what conditions the aircraft effluents are injected into the atmosphere. Multi-dimensional 2-D and 3-D models of the global atmospheric chemical, radiative, and dynamical processes are the primary tools used to assess the impact of such emissions.

Assessments of the understanding of the potential effects on the atmosphere will be made periodically. This report presents a preliminary set of emissions scenarios. A more complete assessment of the environmental impact of emissions from a commercially viable, reasonably mature fleet of HSCTs will be conducted in about 2 years. At that time, more realistic scenarios of both existing and projected future aircraft emissions will be needed for evaluation with state-of-the-art 2-D and 3-D global atmospheric models. These scenarios will be used to understand the sensitivity of environmental effects to a range of fleet operations, flight conditions, and aircraft specifications.

This chapter provides the baseline specifications for the scenarios: the criteria to be used for developing the scenarios are defined, the required database for initiating the development of the scenarios is established, and the state-of-the-art for those scenarios that already have been developed is discussed. This project will be continued in preparing for the next major assessment, and will be described in the next High-Speed Research Program/Atmospheric Effects of Stratospheric Aircraft Program Report.

An important aspect of the assessment will be the evaluation of realistic projections of emissions as a function of both geographical distribution (i.e., latitude and longitude) and altitude from an economically viable commercial HSCT fleet. With an assumed introduction date of around year 2005, it is anticipated that there will be no HSCT aircraft in the global fleet at that time (assuming that the Concorde have all been retired). However, projections show that, by 2015, the HSCT fleet could reach significant size. We assume these projections of HSCT and subsonic fleets for about 2015 can then be used as input to global atmospheric chemistry models to evaluate the impact of the HSCT fleets, relative to an all-subsonic future fleet. This chapter discusses the methodology, procedures, and recommendations for the development of future HSCT and the subsonic fleet scenarios used for this evaluation.

Boeing and McDonnell Douglas have been instrumental in developing the scenarios examined thus far within the NASA HSRP program. Both companies have special modeling capabilities to determine the emissions from a commercial aircraft fleet. (Note: Within the United States, the Analytical Technology Applications Corporation has developed a similar capability for the Federal Aviation Administration (FAA), but this model has not yet been used in developing emission scenarios for assessment studies.) Boeing and McDonnell Douglas made different assumptions in developing their scenarios.

94

SPECIAL CONSIDERATIONS TO SCENARIO DEFINITION

The general methodology for calculating realistic emission scenarios for both subsonic and HSCT fleets consists of several components.

1. Marketing projections would be made of the demand for air travel between cities (i.e., city-pairs) in the form of available seats per city-pair. This analysis would also consider the likely (conceptual) aircraft and the frequency of such flights (note that the frequency will likely depend on aircraft seating capacity, flight speed, and turnaround time).
2. For a given aircraft concept, a performance analysis of the aerodynamics and propulsion system would be done to determine the fuel consumption as a function of aircraft weight, range, engine power setting, and flight segment (e.g., taxi-idle, takeoff, climb, cruise, approach).
3. Fuel consumption would be determined as a function of geophysical distribution and altitude calculated by "flying" the aircraft along the routes between the city-pairs. Special features, such as supersonic flight only over water, waypoint routing, weather, environmental optimization, etc., can be incorporated at this stage.
4. Emissions would be calculated. While these will always be proportional to fuel consumption, emission indices (EIs) of some species such as NO_x , CO , and hydrocarbons will vary with the flight segment.

There may also be small corrections resulting from flight altitude, humidity, and air temperature. More detailed discussions of each of these topics, as they relate to scenario definition, is given later.

MARKETING ASSUMPTIONS

International air transportation is expected to increase steadily from now through the year 2015. During this time, the available seat miles (ASM, mileage between city-pairs determined by great circle route) is expected to increase from 1.6×10^{12} ASMs/year in 1987 to about 5×10^{12} ASMs/year in 2015 as shown in Figure 1 (1). Approximately $2.1\text{-}2.5 \times 10^{12}$ ASMs/year will be in long-range flights by 2015. It is assumed that the total ASMs will be approximately conserved when the HSCT is introduced, and that the HSCT will displace some of the long-range subsonic ASMs. The extent of displacement and the particular routes chosen for HSCTs, however, will depend strongly on the economics of the HSCT.

A viable HSCT fleet must be technologically feasible as well as profitable for the airline that uses it. This means that the operating costs of the HSCT must compete with those of current or future subsonic aircraft. These costs will depend on the characteristics of the aircraft (e.g., technology required, specific fuel consumption, range, capacity, and speed). Marketing studies show that the economic demand for a specific fleet size of HSCTs depends strongly on the operating costs relative to those of subsonic aircraft. In the most optimistic case, in which supersonic fares are assumed to be nearly the same as subsonic fares, the demand for an HSCT consisting of as many as 900 aircraft would be a reasonable assumption, by the year 2015 (1). As HSCT operating costs (and ticket prices) rise, the projected fleet size decreases. However, projections indicated that a minimum fleet size - 300 to 500 HSCTs - would be necessary to induce the airframe industry to develop an HSCT. An optimistic, but realistic, baseline scenario for assessing the atmospheric effects of an HSCT fleet in 2015 would be about 500 aircraft.

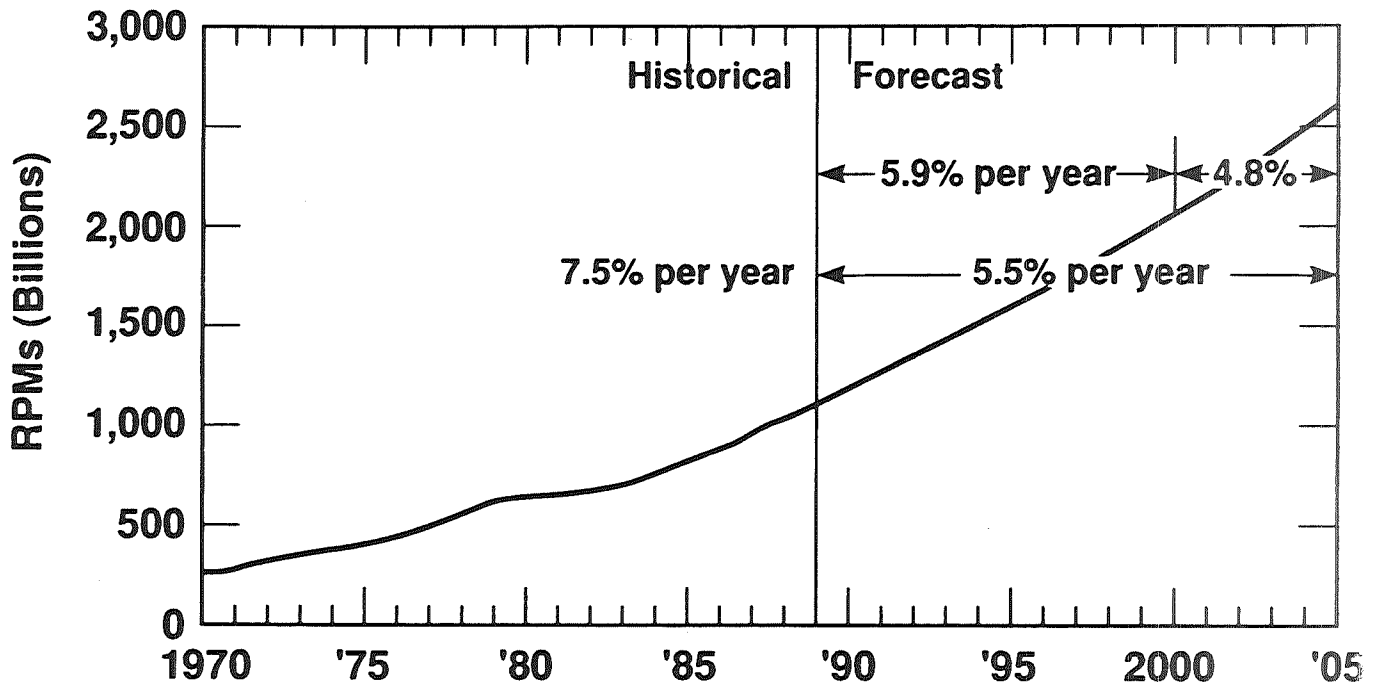
Performance Calculations

For a given aircraft or aircraft concept, aerodynamic and propulsion system analyses are done to calculate the fuel consumption as a function of aircraft weight, engine characteristics, payload factor, range, and flight segment (e.g., taxi-idle, takeoff, climb, cruise, and approach). In addition, the EIs of CO, hydrocarbons, NO_x and other emitted species must be evaluated for each flight segment for use in the scenario calculations.

Supersonic aircraft such as the Concorde generally fly a Breguet path; the cruise altitude increases continuously as the fuel is used. On the other hand, subsonic aircraft generally follow regulated paths of constant-pressure altitude. It is assumed, in the scenarios to be developed, that the HSCTs will also fly a Breguet path.

Fuel Consumption

The amount of fuel burned by the HSCT fleet in the assessment scenarios, it is assumed, is largely determined by aircraft performance parameters. In a complete economic scenario, these parameters are interrelated and must be accurately predicted. For example, a high estimate in aircraft drag would also lead to higher operating costs, higher ticket prices, and a decrease in



Note: Excludes U.S.S.R. However, due to changing conditions within the U.S.S.R., work is underway to include this market

Figure 1. World air travel forecasts in revenue passenger miles, based on Boeing (1).

passenger demand, thus moving toward a lower fleet fuel burn. These contrasting trends, for an apparently simple parameter like aerodynamic drag, illustrate the complexities involved in estimating the total annual fuel burn in marketing projections for a supersonic aircraft fleet.

We shall avoid having to consider the interplay between ticket costs and available seats being flown by HSCTs by specifying a minimum fleet of aircraft operating at maximum efficiency (i.e., number of hours in the air).

Engine Emissions

The primary engine exhaust products from commercial jet aircraft are carbon dioxide and water vapor. Secondary exhaust products include nitrogen oxides (NO_x), carbon monoxide (CO), hydrocarbons, and sulfur dioxide (SO_2). (See chapter 2 for a thorough review of emissions.) The relative amounts of NO_x , CO, and hydrocarbons depend on engine operations, particularly the thrust setting of the engine, and those at cruise conditions will differ significantly from those observed at takeoff and climb.

At this time, it appears that the use of alternative fuels would likely be too expensive because they would mean higher operating costs and because airports would have to be improved to handle such fuels. Therefore, the HSCTs considered here (Mach 1.6-2.4) use some form of Jet-A fuel. A report by Boeing (2) analyzed a set of 53 jet fuel samples obtained worldwide, and found that Jet-A consists of a range of hydrocarbons with a mean molecular weight of 164. The average hydrogen content was 13.8%, by weight.

The average sulfur content of the analyzed Jet-A samples was 0.042% by weight (EI(SO_2) = 0.8). Sulfur content of jet fuels depends on the refinery processes used to produce the jet fuel. Since sulfur poisons some of the catalysts used in refining, several of the advanced processes have led to significantly reduced sulfur levels. With increasing environmental regulation of aromatic content and sulfur impurities in fuels, it is likely that sulfur content in jet fuels will be reduced further.

The emission levels from aircraft engines are defined in terms of EIs, measured as grams of emission per kilogram of fuel burned. Emissions of water vapor, carbon dioxide, trace metals, and sulfur dioxide are essentially independent of combustor operation conditions and are solely a function of fuel composition. On the other hand, EIs for nitrogen oxides, carbon monoxide, and hydrocarbons depend on the combustor design and thrust settings for the engine (see chapter 2). There has been confusion in the past about the definition of an EI for NO_x ; this problem can be avoided if this EI is defined precisely (see chapter 2) as the weight of NO_2 (in grams per kilogram of fuel) plus the weight of NO as converted to NO_2 . This definition is consistent with the recommendations of the International Civil Aviation Organization and the FAA, and it is used throughout the HSRP.

BACKGROUND ATMOSPHERE

Atmospheric model calculations (3-6) have shown that the sensitivity of stratospheric ozone to HSCT emissions is dependent on the background atmosphere (particularly on the amount of total reactive chlorine, Cl_y , in the stratosphere). It is therefore important that model calculations for the year 2015 HSCT scenarios consider appropriate background concentrations of atmospheric constituents. The current rates of increase for many important atmospheric constituents are known reasonably well. It is also possible to project (with greater uncertainty) the effects of international controls on the production of chlorofluorocarbons (CFCs) over the next few decades. It should also be recognized, however, that it becomes increasingly uncertain, as trace gases predictions are extended into the future.

Table 1 shows (for the years 1990 and 2015) suggested tropospheric concentrations of long-lived trace constituents that influence the stratosphere. The projections for 2015 are based on scenario C of the 1991 assessment of stratospheric ozone now under way for the United Nations Environment Programme and the World Meteorological Organization. This background atmosphere assumes near-global compliance with the international agreements, including the CFC substitutes. This projection of the 2015 atmosphere will likely evolve as our knowledge of trace gas concentrations and budgets are improved; for example, the atmospheric composition listed in Table 1 has been updated since the calculations in chapter 5 were set. Sensitivity analyses using other trace gas concentrations may also need to be considered in future modeling studies.

Table 1. Suggested Background Atmosphere for Current (1990) and Projected (2015) Scenarios*

Species	1990	2015
CO ₂	354 ppmv	411 ppmv
CH ₄	1.8 ppmv	2.1 ppmv
N ₂ O	310 ppbv	330 ppbv
CH ₃ Cl	600 pptv	600 pptv
CFC-11	280 pptv	270 pptv
CFC-12	485 pptv	545 pptv (+110 pptv)†
CFC-113	57 pptv	81 pptv
CCl ₄	106 pptv	74 pptv
CH ₃ CCl ₃	159 pptv	17 pptv
HCFC-22	104 pptv	71 pptv
Halon-1211	2.5 pptv	0.9 pptv
Halon-1301	3.5 pptv	5.3 pptv
CH ₃ Br	15 pptv	15 pptv
Total Cl	3.6 ppbv	3.4 ppbv
Total Br	21 pptv	21 pptv

*This proposed composition differs from that used in the sensitivity studies in chapter 5, which were set at an earlier date. The background scenario for 2015 is based on Scenario C for the 1991 UNEP-WMO Ozone Assessment Report (in preparation), and assumes near-global compliance with the international agreements, along with inclusion of CFC substitutes (HCFCs, but treated as CFC-12 in the scenario).

† Additional 110 pptv of CFC-12 is included to account for the additional chlorine in the stratosphere resulting from HCFCs.

SUBSONIC EMISSION SCENARIOS

This section addresses the developments required for projecting emissions from the subsonic fleet for the 2015 period, as well as those necessary for analyses of the global atmospheric effects from past and current subsonic emissions. Limited model studies (3,5,6-8) have shown that the effects on tropospheric ozone from increases in subsonic emissions over the last several decades could be significant and need further examination (although this is not currently part of the HSRP Program). Improved analyses of current subsonic emissions, while inherently different from the projected HSCT emissions, still provide a useful test for evaluating model predictions.

Very limited information is available on past emissions. An analysis of aircraft emissions for the year 1975 was made by Athens et al. (9) and revised by Oliver (10). The overall accu-

racy of these analyses is unknown. Boeing has calculated emission scenarios for the year 1987, based on published subsonic commercial jetliner flights. They have also developed projections of emissions for commercial subsonic flights for the 2015 period. These scenarios have been documented in detail in a NASA report (1). All of the published analyses provide estimates of emissions as a function of altitude and latitude, but not longitude or season; only scheduled commercial passenger flights have been included. The methodology used by Boeing is described next.

Boeing 1987 Subsonic Emissions Scenario

Subsonic fleet emissions for 1987 were calculated using the airline fleets and schedules in the 1987 Official Airline Guide (OAG). The calculations considered only scheduled commercial passenger jet aircraft. Airplane types and flight frequency data were prepared and combined with the applicable fuel burn and emission data.

A total of slightly more than 29,000 city-pairs were considered; the total for weekly departures was 229,794. For simplification, subsonic aircraft flights were divided into two groups, depending on range. Approximately half the flights are flown with stage lengths of 400 statute miles or less. The mean altitude of these flights was defined to be 26,000 feet (about 7.9 km). Flights longer than 400 nautical miles were considered to have an average altitude of 37,000 ft (about 11.2 km). All aircraft were assumed to cruise at one of these two altitudes. Fuel consumption was calculated assuming a constant average fuel flow over the entire flight profile.

Fuel burn and emissions were calculated as follows. From the OAG data, 32 jet airplane types were considered, and their characteristics were tabulated. For each aircraft type, fuel burn and emissions were calculated for average fuel burn over a great circle route between all city-pairs served by that type and were grouped into 10° latitude bands. The EIs used were appropriate for cruise power settings, would be higher during the takeoff and climb segments, and would be lower during the descent and landing segments of the flight. The results of the calculations of total fuel consumption and the distribution of fuel consumption as a function of latitude are shown in Table 2.

Domestic flights in the Soviet Union, Eastern Europe, and China are not included in the OAG and thus were not included in the 1987 scenario. Scheduled commercial air cargo and turboprop commercial flights were also not included in the scenario. Further, the 1987 subsonic fleet scenario included only 58% of the scheduled commercial passenger departures. The other 42% were aircraft with turboprops and reciprocating engines; these are primarily low-altitude, short-range flights. In addition, the scenario did not include charter, general aviation (private), or military flights. Our scenario for the assessments clearly must include a more complete set of data on subsonic flights.

Boeing Subsonic Emissions Scenario for 2015

The composition of the subsonic fleets for the years 2000 and 2015 were assumed to have average stage lengths and service patterns comparable to the current (1987) aircraft types (i.e., new jet transport types would replace same capacity/range aircraft). Using the Boeing long-range forecasts of available seat miles (ASM) for these types and the average stage length and service patterns of these types, the number of departures was calculated for the years 2000 and 2015, using the 1987 ASM level as a base.

Future aerodynamic performance, fuel consumption, and emission characteristics of the generic subsonic fleet were estimated and described in detail in Boeing (1). The emissions data for the year 2000 was estimated by assuming that technology improvements would allow an average 100° F increase in combustor inlet temperature, with a resulting 20% increase in NO_x emissions.

Table 2. Total Fuel Consumption and Fractional Distribution of Fuel Use as a Function of Latitude Band for Commercial Jet Air Traffic, 1987 and 2015 (projected)*

	1987 (Subsonic)		2015 (Subsonic)		2015 (Subsonic + HSCT)		
Latitude Band	Subsonic at 26 kft	Subsonic at 37 kft	Subsonic at 26 kft	Subsonic at 37 kft	Subsonic at 26 kft	Subsonic at 37 kft	Supersonic at 60 kft
80-90°S	0.00%	0.00%	0.00%	0.00%	0.00%	0.00%	0.00%
70-80°S	0.00%	0.00%	0.00%	0.00%	0.00%	0.00%	0.00%
60-70°S	0.00%	0.00%	0.00%	0.00%	0.00%	0.00%	0.00%
50-60°S	0.03%	0.02%	0.00%	0.01%	0.00%	0.01%	0.00%
40-50°S	0.50%	0.10%	0.18%	0.15%	0.18%	0.13%	0.00%
30-40°S	1.60%	1.54%	1.30%	2.03%	1.29%	1.79%	2.81%
20-30°S	2.18%	1.51%	1.97%	1.61%	1.76%	1.54%	1.87%
10-20°S	1.05%	1.82%	0.38%	1.62%	0.38%	1.44%	2.24%
0-10°S	2.08%	1.74%	1.06%	1.68%	1.07%	1.66%	2.20%
0-10°N	2.62%	2.29%	1.60%	2.35%	1.63%	2.04%	8.99%
10-20°N	3.93%	4.07%	2.87%	3.69%	2.90%	3.30%	8.62%
20-30°N	7.85%	11.43%	5.86%	11.03%	5.95%	12.10%	8.48%
30-40°N	36.62%	30.64%	45.64%	31.66%	44.99%	32.40%	15.83%
40-50°N	29.48%	25.79%	27.43%	25.13%	27.98%	27.07%	30.91%
50-60°N	10.41%	15.69%	10.32%	15.67%	10.46%	13.54%	13.94%
60-70°N	1.63%	2.89%	1.38%	2.85%	1.40%	2.61%	1.36%
70-80°N	0.02%	0.38%	0.00%	0.41%	0.00%	0.30%	1.46%
80-90°N	0.00%	0.09%	0.00%	0.10%	0.00%	0.07%	1.27%
Total(10 ¹⁰ kg/yr)	1.14	7.24	1.71	1.52	1.63	1.48	6.59

*Data as analyzed by Boeing. Year 2015 air traffic distributions are shown for both a projected subsonic only fleet and for a fleet consisting of both subsonic and HSCT aircraft.

For the Year 2015, it was assumed that further increases in combustor inlet temperature would be offset by lower-NO_x technology combustors, so the only increase in emissions would derive from growth of the fleet. The results of the calculations of total fuel consumption, and the distribution of fuel consumption as a function of latitude, are shown in Table 2.

Development Needs

The available emissions scenarios have recognized limitations that need to be addressed over the next several years. It is critical to have accurate estimates of the changes in emissions from the subsonic fleet in the upper troposphere. Although secondary in importance, such analyses are needed to test current atmospheric models, as well as to improve the understanding of environmental effects from existing aircraft emissions.

Data Grids and Traffic Seasonality

Existing subsonic scenarios do not provide variations in emissions with longitude. While this is satisfactory for the 2-D models used for most analyses of aircraft effects, 3-D models will be used in HSRP assessments in the future. These calculations will require that emissions be expressed as a function of longitude and time of year, as well as altitude and latitude. The grid

structure needed for emissions will vary, depending on the models being used in the assessment.

The Boeing subsonic scenarios have assumed that all aircraft fly at one of two different altitudes. These scenarios need to be reevaluated using the actual flight patterns of the aircraft. Such scenarios can then be used to determine more accurately how much of the subsonic emissions are currently injected into the stratosphere.

There are no analyses of the effects resulting from seasonal variations in the subsonic emissions; however, seasonal variations in emissions are likely to have an impact on the predicted changes in ozone and should be included in the scenarios developed for subsonic emissions. At mid and high latitudes, the height of the tropopause varies dramatically with season. In addition to the effects in the troposphere, seasonal variations of current emissions in the lower stratosphere, particularly at high latitudes in the winter and spring, are of interest because of the possible interactions with the chemistry influencing ozone in the polar vortex.

Inclusion of Air Cargo, Military, and Other Aircraft

The Boeing scenario for subsonic emissions scenarios considered only published flights of commercial passenger jet aircraft. Based on jet fuel production estimates (11), the fuel consumption calculated by the Boeing 1987 subsonic emission scenario was only 53% of the total world jet fuel usage. Data on fuel production makes several estimates possible: aviation in the U.S.S.R. and Eastern Europe could account for 12% of the world total, while China could account for 2%. Estimates of U.S. military aviation fuel and U.S. private jet use account for 7% each. From these estimates, approximately 19% of the world jet fuel usage is still unaccounted for, but is probably allocated to charter, cargo, and turboprop aircraft. Cargo (freight) flights may account for a high fraction of the missing fuel use; this requires further analysis. Available forecasts suggest that air freight traffic will increase more rapidly than passenger traffic (12).

Estimates of the distribution of past, current, and future subsonic emissions will need to account for military aircraft, U.S.S.R. aviation, Chinese aviation, the worldwide cargo fleet, and perhaps commercial turboprop aircraft as well (although these probably fly too low for their emissions to be important globally). Unfortunately, such estimates are not currently available for inclusion in assessment studies.

PREVIOUS HSCT SCENARIOS

In spite of the renewed interest in building HSCT aircraft, only a limited number of scenarios have been developed for analyzing the potential effects from these aircraft. The most recent of these are the matrix of HSCT scenarios developed for this report (see chapter 5). Johnston et al. (4) performed a series of sensitivity analyses to examine the range of possible HSCT emissions, but no attempt was made to develop realistic scenarios. As part of NASA's initial study in 1989, Boeing (1) and McDonnell Douglas (13), developed a series of HSCT scenarios, which were used in atmospheric modeling studies by Ko et al. (5) and Isaksen et al. (6). More recently, Wuebbles and Kinnison (3) worked with McDonnell Douglas to develop and analyze the effects on ozone from a broad-based matrix of HSCT scenarios, assuming realistic flight paths with varying cruise altitudes and amounts of NO_x emissions; these scenarios are similar in concept, but not the same, to those that have been developed for this report.

The assumptions used by Boeing and McDonnell Douglas in their scenarios differ in several respects. To provide a historical perspective for further scenario development, this section describes the approaches used by Boeing and McDonnell Douglas in the development of their previous HSCT scenarios.

Boeing Projection

The introduction of the HSCT should lead to the replacement of some long-range subsonic aircraft. It was assumed in the total projected fleet that the long-range subsonic fleet would be reduced so as to keep the same total fleet ASM capacity as that of an all subsonic fleet. In a free economic market, the HSCT fleet size will depend on the extent to which the aircraft can (1) meet environmental requirements, (2) exceed capacity and range requirements of the airlines, and (3) compete economically with long-range subsonic aircraft. However, for these atmospheric effects studies, Boeing assumed a baseline scenario such that, by the year 2015, there would be a fleet of 625 HSCTs with a payload of 247 passengers, a cruise speed of Mach 2.4, an average stage length of 3400 nautical miles, and a utilization of about 9 hours per day. The baseline HSCT aircraft assumed 69,449 lb of fuel per hour (~18 km) at cruise conditions with a 65% payload. The average cruise altitude was estimated to be 60,000 ft.

Using Boeing's airline scheduling computer code, 235 market (city) pair routes were modeled. Fuel burn calculations were made for 10° latitude bands, with waypoint routing to avoid sonic booms over land. During over land flights, aircraft were assumed to cruise at Mach 0.9 and at a lower altitude. For those cases, the fuel use was consigned to 37,000 ft. The fuel use and latitudinal distribution for one of the year 2015 scenarios is given in Table 2.

McDonnell Douglas Projection

The overall procedure used by McDonnell Douglas in their HSCT scenario development for generating the annual fuel burn results is shown in Figure 2. In a general sense, the procedure shown in Figure 2 can be thought of as consisting of three basic steps: (1) estimate of location (altitude \times latitude) of fuel burn; (2) estimate of amount of fuel burn; and (3) calculation of NO_x molecules (and other constituents) from engine company EIs. These steps are explained in detail here.

Estimate of Location (Altitude \times Latitude of Fuel Burn)

The latitude and altitude of exhaust injection are a function of the worldwide route structure assumed for future HSCT operations and the mission flight profiles of the global flights. The HSCT will compete in the long-range passenger market. This consideration, combined with concerns about passenger traffic forecasts and over land operations, led to the selection of 10 International Air Transport Association (IATA) regions (out of 18 total worldwide) that appear to be appropriate for supersonic transport aircraft operation. For each of these 10 major flight routing regions, a representative city-pair was selected that best represents the average range and latitude distribution of flights in that region. The 10 regions, and the corresponding city-pairs, are shown in Figure 3.

A flight profile for the HSCT configuration under study is generated for each of the 10 city-pairs. The flight profile is 3-D with the flight path using great circle flight profiles. As seen in Figure 3, 7 of the 10 routes can be considered flights over water, while 3 are predominantly over land. The flight profiles (and fuel burns) for the overland routes do not account for operational constraints (i.e., subsonic), nor are the flight paths altered to avoid operation over land.

Estimate of Total Fuel Burn

The total fuel burn in a given region is a function of the passenger demand and load factor (i.e., percentage of seats occupied on a given flight) projected for that region. The number of flights per year were then calculated in the McDonnell Douglas scenarios by dividing the total fuel burn by the fuel burn of a single flight. The fleet size can then be determined based on the number of flights, aircraft speed, and turnaround time. The competitive position of an HSCT,

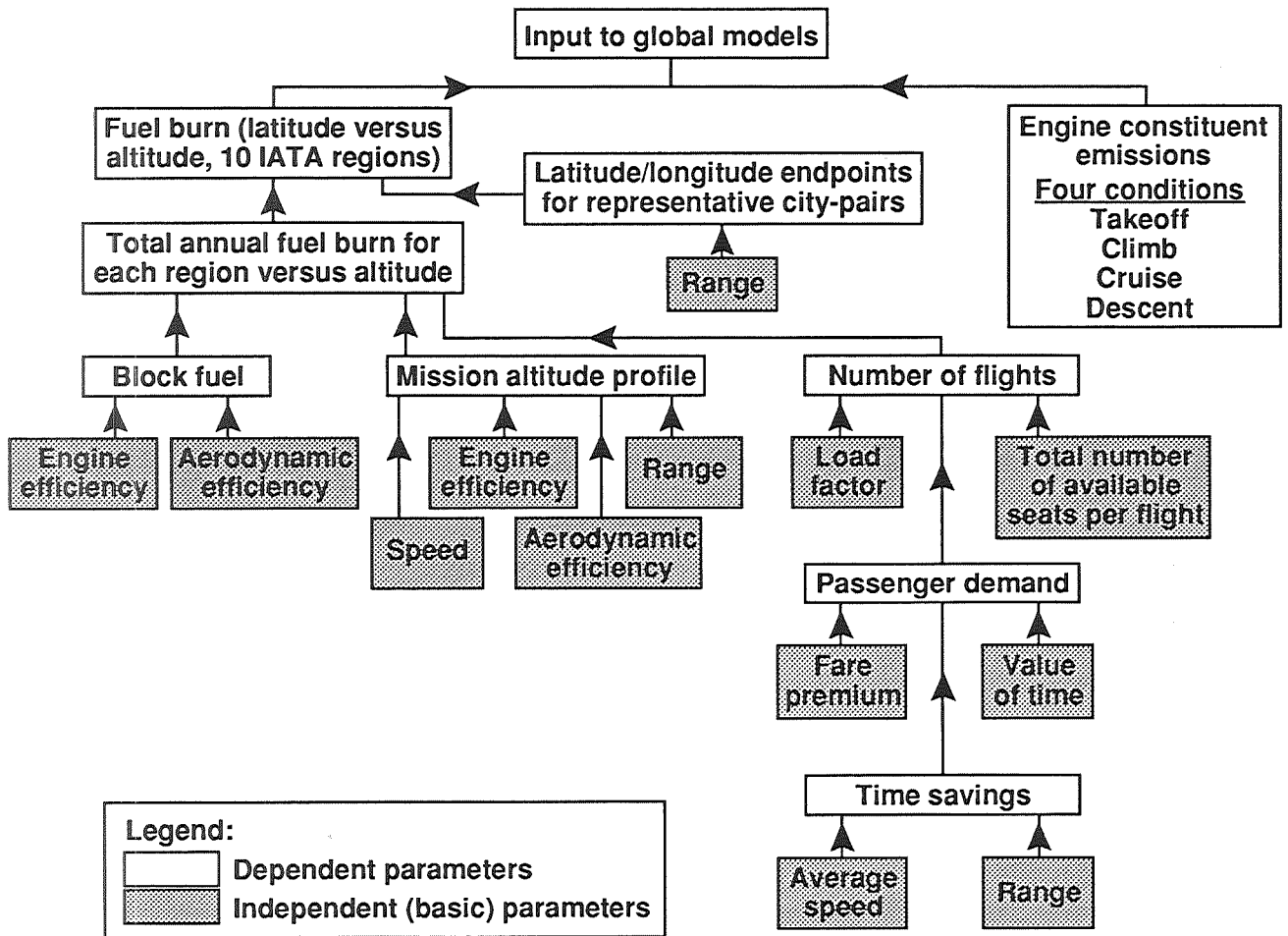
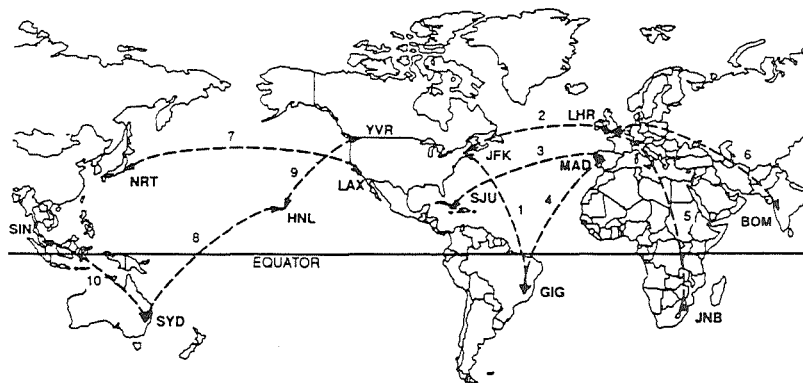


Figure 2. Data Flow for chart used by McDonnell Douglas for generating HSCT emission scenarios.



Region	City-pairs
1 North-South America	New York – Rio de Janeiro (JFK-GIG)
2 North Atlantic	New York – London (JFK-LHR)
3 Mid-Atlantic	San Juan – Madrid (SJU-MAD)
4 South Atlantic	Rio de Janeiro – Madrid (GIG-MAD)
5 Europe Africa	Johannesburg – London (JNB-LHR)
6 Europe Far East	Bombay – London (BOM-LHR)
7 North and Mid-Pacific	Los Angeles – Tokyo (LAX-NRT)
8 South Pacific	Honolulu – Sydney (HNL-SYD)
9 Intra-North America	Honolulu – Vancouver (HNL-YVR)
10 Intra-Far East and Pacific	Singapore – Sydney (SIN-SYD)

Figure 3. HSCT representative city-pairs used by McDonnell Douglas.

with respect to the subsonic fleet, was determined by contrasting the fare premium associated with supersonic flight with the time savings available through it. The time savings for a given flight is a function of the average speed and total distance of the flight. Thus, in the Mach 1-3 range, the passenger demand for an HSCT increases with increasing cruise speed and range. The total annual fuel burns and load factors by region for the three HSCT baseline configurations used by McDonnell Douglas are shown in Table 3.

To arrive at the most conservative scenario for emission (i.e., largest HSCT fuel use), the McDonnell Douglas group assumed a zero fare premium for HSCT flights and a 50% market capture for HSCT in the 10 regions under consideration.

Once the total fuel burn by region has been determined, it is superimposed on the 3-D route structure grid as determined previously. This results in 10 matrices, each showing the annual fuel burn data by altitude and latitude for one of the IATA regions. These matrices are summed together to produce one matrix that displays the total annual global fuel burn for an HSCT fleet by latitude and altitude.

Calculation of Aircraft Emissions

The calculation of NO_x emissions in a given altitude/latitude grid cell is a relatively simple calculation based on the NO_x EI (EI NO_x) of the engine under the appropriate operating conditions. The operating condition of the engine varies considerably over the flight profile, and hence it is not desirable to simply apply one EI NO_x (e.g., cruise) over the entire flight regime.

For a first-order approximation, it can be assumed that the engine cycle varies with downrange distance or altitude. There are, essentially, four stages to a Mach 3.2 HSCT mission profile: takeoff and subsonic climb (0-10 km), supersonic climb (10-18 km), cruise (18-24 km), and descent (24-0 km). These components are illustrated in Figure 4. The engine operating cycles approximately correspond to these four conditions.

Table 3. Total Annual Fuel Burned by Region for HSCT Baseline Configurations, as Used in HSCT Scenario by McDonnell Douglas

Region	Load factor (%)	Total annual fuel burn (1,000 kg)		
		Mach 1.6 Fleet size = 436	Mach 2.2 Fleet size = 440	Mach 3.2 Fleet size = 363
1. North-South America	63	786,220	789,075	847,345
2. North Atlantic	69	9,104,480	9,167,462	9,897,685
3. Mid-Atlantic	70	656,924	660,546	711,389
4. South Atlantic	70	1,028,543	1,025,231	1,087,798
5. Europe-Africa	61	1,972,390	1,996,343	2,177,999
6. Europe-Far East	79	3,093,521	3,097,565	3,310,548
7. North and Mid-Pacific	73	10,905,871	10,879,303	11,550,727
8. South Pacific	73	1,187,339	1,190,235	1,275,625
9. Intra-North America	68	72,579	74,320	82,751
10. Intra-Far East and Pacific	72	4,723,051	4,785,222	5,221,580

To map out the injection of NO_x and other constituents into the atmosphere more accurately, a different set of EIs is used for each of the four conditions. These are stratified by altitude, except for descent, which spans all of the flight altitudes from the top of cruise to ground level. To account for this overlap, the constituent EIs for descent are factored into the takeoff, climb, and cruise indices, based on the ratio of time spent in a particular altitude band while descending. The ratios based on a Mach 3.2 mission are shown in Table 4, but note that such ratios will change with the Mach number. EIs (for NO, NO₂, etc.) provided by engine manufacturers are used with these ratios, resulting in three sets of indices for the stratified altitude bands. The number of molecules of a given constituent at each altitude-by-latitude grid point is calculated from the total fuel burn and the appropriate EI.

FUTURE HSCT SCENARIO REQUIREMENTS

The HSCT scenarios documented here were developed using a simplified approach. Several of the assumptions used by Boeing and McDonnell Douglas in conducting their independent HSCT scenario calculations are being jointly reexamined for future scenario development. The increasing sophistication of global atmospheric chemical-transport models will also require the improvement of both the geographical and altitude resolution of the emission scenarios.

Table 4. Flight Profile Characteristics for a Typical Mach 3.2 Mission, as Used in HSCT Scenarios Developed by McDonnell Douglas

Altitude band	Time spent (%)		
	Takeoff and climb	Cruise	Descent
0-10 km	59.5	—	40.5
10-18 km	49.8	—	50.2
18-30 km	1.1	94	4.9

This section discusses a consolidation of the Boeing and McDonnell Douglas approaches, and it also describes further modifications to the HSCT scenario considered necessary for increasing the accuracy and resolution of the environmental assessments. A common framework must be established that will meet the needs of the NASA HSRP program, of the aircraft industry, and of the atmospheric modeling community. The following methodology, and resultant scenarios, will be fully documented and remain in the public domain; there is no intention in this assessment to develop scenarios as proprietary engineering trade studies for the aircraft manufacturers.

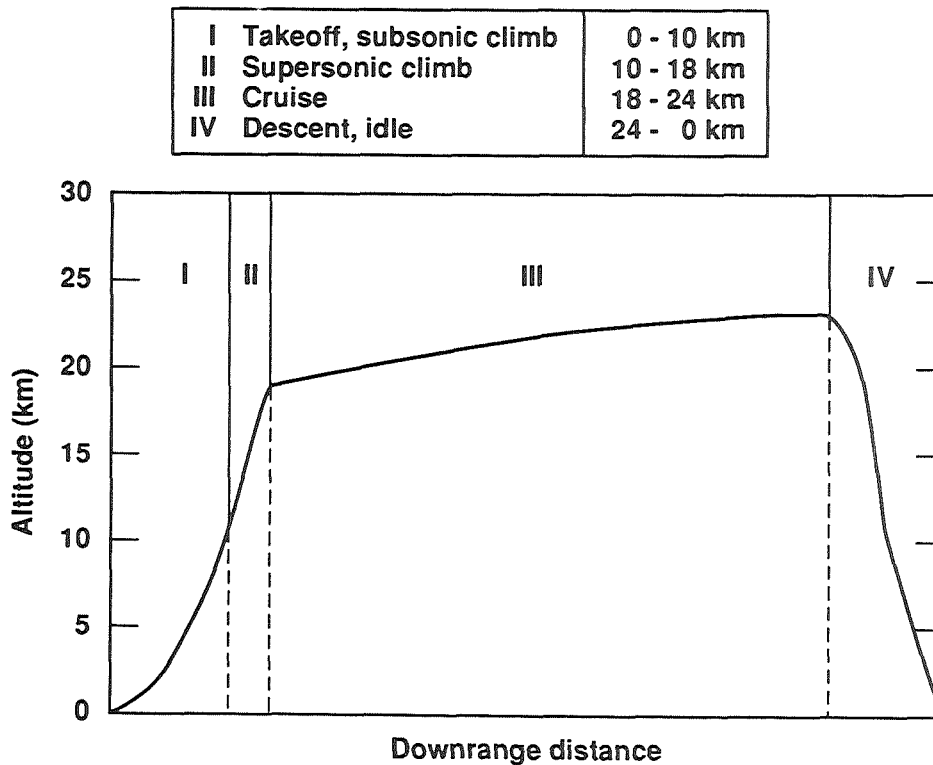


Figure 4. Four stages of Mach 3.2 mission profile considered for engine emissions in HSCT scenarios developed by McDonnell Douglas.

The goal is to generate realistic 3-D scenarios for a relatively mature HSCT fleet and the coexisting subsonic fleet in the year 2015. As a reference, a scenario for a 2015 fleet that has only subsonic aircraft (no HSCTs) will also be determined.

FLEET ASSUMPTIONS

HSCT City-Pair Network

In the earlier work, Boeing and McDonnell Douglas used quite different networks of city-pairs. For future work, a common city-pair network needs to be established. This should include at least 150 city-pairs chosen to adequately represent the global network for air travel demand — including both the subsonic and supersonic routes, and also considering both passenger and cargo flights. Boeing and McDonnell Douglas, in conjunction and coordination with the HSRP, are working to define a network and the associated city-pairs. At this time, the exact roster of city-pairs has not been fully agreed upon.

Fleet Size

Fleet size projections vary according to the performance characteristics of the HSCT and the operating costs, relative to subsonic aircraft. Factors that will influence these projections include aircraft configuration (number of passengers and class mix), speed and productivity of the aircraft, utilization and scheduling, range, and specific fuel consumption. Thus, the technical design of the aircraft and its required performance are strongly coupled to the perceived market and the operating costs of the aircraft. With the preliminary HSCT designs considered to date, many of these details are still unresolved. *The resolution of these marketing assumptions is not necessary for the assessments needed for environmental impact statements.*

The scenarios developed for the HSCT fleet in 2015 will assume that there are approximately 500 aircraft. Although sensitivity studies with atmospheric models should also consider the possibility of additional HSCT aircraft at years beyond 2015, this date provides a good benchmark for evaluating the potential environmental effects. However, if 500 aircraft were found to be environmentally acceptable, while determinations showed that more aircraft were unacceptable, regulatory actions could be used to prevent the global HSCT fleet from growing further, or lower-emissions engines could be required.

One aim for the scenario development will be to establish the minimum size of an economically viable HSCT fleet (i.e., the number of planes that must be sold to at least break even). *The environmental assessment can reasonably be based on this minimum number of HSCTs, since a smaller number (if predicted) would not be built and a larger number, if in demand, could be constrained by environmental regulations.*

Mode of Operation

Supersonic flight may have to operate in a restricted environment because of concerns about atmospheric effects, sonic boom, and community noise. These may include cruise altitude restriction, restrictions over land, and dedicated flight corridors. Possibly, such restrictions will affect range, fuel burn, and fleet size. Future scenarios should examine the potential ramifications of such restrictions.

HSCT emission scenarios should be designed so that the algorithm for flight paths can be adjusted to regulations (e.g., use waypoint routing to avoid supersonic flight over land or fly subsonically unless a means is found to reduce sonic boom) or to other criteria such as meteorology (e.g., search for tailwinds), or a combination of regulations and meteorology (e.g., optimize the flight path with wind fields to minimize stratospheric injections).

Supersonic Operation by the Military and Others

Countries that have supersonic military aircraft may use specific operational supersonic corridors to minimize the impact of the sonic boom over land or else use over water operational areas cleared by air traffic control. An evaluation of the magnitude of current and projected military supersonic operations may be appropriate.

Any potential for supersonic air cargo or charter flights should also be examined.

Polar Routes

Several of the projected supersonic routes are Arctic routes. Because of the unique meteorological conditions of the stratospheric winter polar vortex, the effect of cross-polar routes should be assessed. In the future, there may be a need to reconsider the choice of Arctic routes based on the assessment.

MODELING METHODOLOGY

Data Grids and Traffic Seasonality

Today, two-dimensional models are the workhorses of global stratospheric chemical-transport modeling. These 2-D models represent the longitudinally averaged atmosphere on a latitude-altitude-grid, typically, 5°-10° (or more) by 1-3 km. More comprehensive three-dimensional stratospheric chemical-transport models are at an early stage of development. To support the current 2-D and future 3-D atmospheric models, emissions should be provided on a variable grid with a resolution at least as fine as 5° longitude × 4° latitude × 1 km altitude. However, the assessment scenarios should be developed so that they can be mapped onto any grid appropriate for such models. Since the resolution of these models varies from model to model and is expected to become finer as a function of increasing computing capabilities, the emissions scenarios need to be developed with algorithms that are spatially continuous. The scenarios developed will then be mapped onto the grids appropriate to the assessment models.

As mentioned earlier, expected seasonal variations in emissions may have an important impact and will need to be included in the scenarios.

Future Test Cases

Industry is currently focused on developing basic HSCT technology, with some effort dedicated to considering alternative HSCT designs. The next several years will still be too soon to optimize the design options based on either economic or environmental criteria. The technology risk, cost, and performance are sensitive functions of the aircraft speed. Because of aerodynamic drag, the speed of the aircraft essentially determines the optimum cruise altitude of the aircraft. Thus, high Mach-number aircraft fly at higher altitudes than low Mach-number aircraft. We know from the earlier Climatic Impact Assessment Program (1975) studies (14), as well as more recent modeling studies, that the environmental impact is a sensitive function of the injection altitude. Thus, the flight altitude has the most significant effect on both the airplane design and on the atmospheric evaluation. At this time, we are considering HSCTs with a cruise speed between Mach 1.6 and 2.4. For a given cruise speed and the other specified criteria discussed earlier, the turnaround time and the amount of time the aircraft actually spends in the air is dependent on aircraft cruise speed and will be represented in the scenarios developed.

The question of whether to use a fraction of the total ASM (i.e., seats flown on a great-circle route between city-pairs) or fixed fuel burn as a criterion in the scenario development has

been highly controversial. In general, as the HSCT's speed (and thus cruise altitude) varies, fuel consumption and the economics of the aircraft both change. While an assumption of fixed ASMs for the HSCT might seem attractive, it does not realistically reflect the development of the technology or of the economics of a commercially viable HSCT fleet. Only predictions of ASMs for the total commercial aviation fleet can be meaningfully predicted. On the other hand, given the range of flight operations criteria to be considered (per earlier discussion), it is also not appropriate to fix the amount of fuel burned for the HSCT fleet.

However, having specified the number of aircraft (approximately 500) and given a passenger load of about 300 passengers per aircraft (range, 250 to 350), we can readily develop a definition for fixing passenger demand flow (PDF), defined as the product of seats flown between city-pairs times the direct great-circle distances. The flight speed (Mach number) and average turnaround time will also need to be considered. Therefore, *PDF will be fixed based on this criterion*. An outstanding issue will be the method of allocating between HSCT and subsonic flights among long-range flights.

The process for developing scenarios for this next assessment needs to be open ended. *The primary criterion for developing realistic scenarios for aircraft emissions is to prepare the best scientifically based assessment of the environmental impact of a projected HSCT fleet.* There are too many unknowns currently associated with the HSCTs and their flight operations to impose exacting specifications on the scenario development. The scenario development methodology must also be responsive to the improving understanding of atmospheric processes and to the needs of the HSRP program; the scenarios are to be an active database. As a secondary criterion, a matrix of scenarios like the one developed for this report, but with better-defined flight criteria, would provide meaningful information to HSCT designers. It is also important that a detailed scenario be calculated for at least one HSCT design to accurately account for the geographical and altitude distributions of HSCT emissions.

Summary of HSCT Scenario Methodology

Here is a summary of the methodology determined in this chapter for future HSCT scenarios.

Methodology

The general methodology for calculating realistic emissions scenarios, as previously developed by Boeing and McDonnell Douglas, will continue to be used to determine the emissions from the year 2015 aircraft fleet. Refinement of previous methods will be implemented to meet the needs of the assessment and the atmospheric models, as outlined in the text.

It is important to recognize that the assessment scenarios are an active database that must be publicly documented and available. They will continually be scrutinized, and the approaches used will be reevaluated. The methodology needs to be flexible to the scenario-related needs of the scientific, engineering, and policy-making communities.

The final emissions scenarios should be generated from a set of algorithms, beginning with the demand for air travel between city-pairs, and including a conceptual HSCT, routing algorithms, and EIs, among others.

The scenarios and algorithms developed for the NASA HSRP program are considered to be in the public domain.

Passenger Demand Flow	Total HSCT Passenger Demand Flow will be fixed, as defined in the text. Actual fuel used and ASMs will be determined by the conceptual HSCT chosen. Military, air cargo, and charter flights will be included.
HSCT Cruise Speed	Assume HSCTs will fly between Mach 1.6 and Mach 2.4.
Number of Aircraft	Approximately 500 HSCT aircraft with 250 to 350 passengers per aircraft.
City-Pair Network	At least 150; actual city-pairs to be determined.
Flight Performance	Includes realistic modeling of climb, cruise, and descent.
Operation Restrictions	Allow for use of adaptable algorithms that can account for waypoint routing (to avoid supersonic over land flights), for other environmental considerations, or for meteorological considerations.
Traffic Seasonality	Must be evaluated and included.
Data Grids	Scenarios should be developed from algorithms (e.g., flight performance, routing) that are continuous in spatial resolution and then mapped onto appropriate grids for the atmospheric models.

REFERENCES

1. Boeing Commercial Airplanes, "High-Speed Civil Transport Study Special Factors," NASA Contract Report 1811881, Sept. 1990.
2. Hadaller, O.J., and A.M. Momentyh, "The Characteristics of Future Fuels," Boeing Report D6-54940, 1989.
3. Wuebbles, D.J., and D.E. Kinnison, Sensitivity of Stratospheric Ozone to Present and Possible Future Aircraft Emissions, in *Air Traffic and the Environment - Background Tendencies and Potential Global Atmospheric Effects*, U. Shumann, editor, Springer-Verlog, Berlin, 1990.
4. Johnston, H.S., D.E. Kinnison, and D.J. Wuebbles, Nitrogen oxides from high-altitude aircraft: an update of potential effects on ozone, *J. Geophys. Res.*, 94, 16351-16363, 1989.
5. Ko, M.K.W., D.K. Weinstein, N.D. Sze, J.M Rodriguez, and C. Heisey, "Effects of Engine Emissions from High Speed Civil Transport Aircraft: A Two-Dimensional Modeling Study," Atmospheric and Environmental Research, Inc., Cambridge, MA, 1989.
6. Isaksen, I.S.A., F. Stordal, and T. Berntsen, "Model Studies of Effects of High Flying Supersonic Commercial Transport on Stratospheric and Tropospheric Ozone," Inst. Geophysics, Oslo, Norway, 1989.
7. Wuebbles, D.J., "A Theoretical Analysis of the Past Variations in Global Atmospheric Composition and Temperature Structure," Ph.D. thesis, University of California, Davis, 1983; also Lawrence Livermore National Laboratory Report UCRL-53423, 1983.
8. Liu, S.C., M. McFarland, D. Kley, O. Zafiriou, and B.J. Huebert, Tropospheric NO_x and O₃ budgets in the equatorial Pacific, *J. Geophys. Res.*, 88, 1360-1368, 1983.
9. Athens, P., P. Gott, P. O'Farrell, and B. Huckins, "Stratospheric Emissions Due to Current and Projected Aircraft Operations," Arthur D. Little, Inc., Cambridge, MA, U.S. Department of Transportation Report DOT-FAA-76WAI-603, 1976.
10. Oliver, R.C., "Cruise Aircraft Effects," 1981 status, U.S. Department of Transportation Report FAA-82-6, 1982.
11. "International Energy Annual 1988," Energy Information Admin., U.S. Dept. of Energy Report DOE/EIA-0219, 1988.
12. Nüsser, H.-G., and A. Schmitt, The Global Distribution of Air Traffic at High Altitudes, Related Fuel Consumption and Trends, in *Air Traffic and the Environment - Background Tendencies and Potential Global Atmospheric Effects*, U. Shumann, editor, Springer-Verlog, Berlin, 1990.
13. Sohn, R.A., and J.W. Stroup, "Procedure for Generating Global Atmospheric Engine Emissions Data from Future Supersonic Transport Aircraft," McDonnell Douglas Corporation, NASA Contractor Report 181882, 1990.

14. "Climatic Impact Assessment Program, Report of Findings: The Effects of Stratospheric Pollution By Aircraft," DOT-TSC-75-38, edited by A.J. Grobecker, S.C. Coriniti, and R.H. Cannon, Jr., U.S. Department of Transportation, Washington, D.C., 1975.

55-45

64291

N92-19126

842

Chapter 5

Ozone Response to Aircraft Emissions: Sensitivity Studies with Two-Dimensional Models

Malcolm Ko
Atmospheric and Environmental Research, Inc.
Cambridge, MA

A 6525710

Contributors

D. Weisenstein
Atmospheric and Environmental Research Inc.
Cambridge, MA

A 6525710

C. Jackman, A. Douglass, and K. Brueske
National Aeronautics and Space Administration
Goddard Space Flight Center

NC999967

D. Wuebbles and D. Kinnison
Lawrence Livermore Laboratory
Livermore, CA

LH075075

G. Brasseur
National Center for Atmospheric Research
Boulder, CO

NH 315709

J. Pyle and A. Jones
University of Cambridge
United Kingdom

CE 261061

R. Harwood
University of Edinburgh
United Kingdom

EE 872903

I. Isaksen and F. Stordal
University of Oslo
Norway

O 2736708

R. Seals
National Aeronautics and Space Administration
Langley Research Center
Hampton, VA

ND 210491

114

INTRODUCTION

This chapter presents our first intercomparison/assessment of the effects of a proposed high-speed civil transport (HSCT) fleet on the stratosphere. As an assessment, this report is necessarily interim; it will be followed by a sequence of more detailed assessments and validation studies as part of the High-Speed Research Program (HSRP). These model calculations should be considered more as sensitivity studies, primarily designed to serve the following purposes:

- allow for intercomparison of model predictions;
- focus on the range of fleet operations and engine specifications giving minimal environmental impact; and
- provide the basis for future assessment studies.

The basic scenarios were chosen to be as realistic as possible, using the information available on anticipated developments in technology. They are not to be interpreted as a commitment or goal for environmental acceptability.

The scenarios are minimal, focusing mainly on the emission of NO_x and H_2O , as described under Emissions Scenarios for Supersonic and Subsonic Aircraft. The predicted HSCT fleet could be fully operational by about the year 2015, when the atmospheric concentrations of most trace gases are expected to be different from what they are today. It was decided that the calculations should be performed relative to a background atmosphere for the year 2015. The boundary conditions that define the year 2015 atmosphere are described in the next section. It has been assumed that there will be no reduction in the subsonic fleet with the introduction of the supersonic fleet. Thus, the impact of the supersonic fleet will be compared with the baseline atmosphere, which includes a projected subsonic fleet operating in the year 2015 background atmosphere.

The results from the models are presented in the section, Intercomparison of Model Results. It should be emphasized that the calculations reported in this chapter are performed using gas-phase chemistry only. Heterogeneous chemistry occurring on the global sulfate layer and/or the polar stratospheric clouds (PSCs) could modify the results in a significant way. These effects could be further enhanced if there is an increase in the sulfate layer or an increase in the occurrence of PSCs as a result of the operation of the HSCT. These issues will be discussed under the heading, Concluding Remarks, along with a discussion of how to identify observations that are useful for validating the predicted effects of these reactions in the stratospheric chemistry models.

EMISSION SCENARIOS FOR SUPERSONIC AND SUBSONIC AIRCRAFT

For two-dimensional (2-D) models that simulate the zonal-mean (averaged over longitude) distributions of the trace gases, one must specify the distributions of the emitted materials as functions of latitude, height, and season. The input for the calculations is summarized in Table 1. A brief review of the key parameters is given in this section.

116

Table 1. Parameters for Aircraft Scenarios

		Subsonic Cruise		Supersonic Cruise
		Short Range	Long Range	
FUEL USE 10 ⁹ (kg/yr)				
		20	150	all cases, 70
CRUISE ALTITUDE thousands ft (km)				
		20-30 (6.1-9.1)	30-40 (9.1-12.2)	Mach 1.6 : 47-57 (14.3-17.4) Mach 2.4 : 55-65 (16.8-19.8) Mach 3.2 : 70-80 (21.3-24.4)
LATITUDINAL DISTRIBUTION OF FUEL USE (%)				
80°N-90°N		0		0.6
70°N-80°N		0.4		0.7
60°N-70°N		2.9		0.7
50°N-60°N		15.7		12.3
40°N-50°N		25.2		28.4
30°N-40°N		31.6		18.4
20°N-30°N		11.0		8.4
10°N-20°N		3.7		6.7
Eq-10°N		2.4		6.3
Eq-10°S		1.7		4.9
10°S-20°S		1.6		4.2
20°S-30°S		1.6		4.0
30°S-40°S		2.0		3.1
40°S-40°S		0.2		1.3
50°S-90°S		0		0
EMISSION INDICES (gm/kg fuel)				
Species (gm mol. wt.)	References			
NO _x as NO ₂	(46)	20.7		As specified
H ₂ O	(18)	1230		1230
CO	(28)	1.1		1.5 (1.2-3.0)
HC as CH ₄	(18)	0.2		0.2 (0.02-0.5)
SO ₂	(64)	1.1		1.0
CO ₂	(44)	3160		3160

Total Fuel Use

The calculations will be performed for supersonic fleets with cruise fuel use of 70×10^9 kg/year. This corresponds to a realistic fleet of approximately 500 or more aircraft, which represents an economically feasible size for the HSCT fleet. Fuel use during takeoff, climb, and descent will be ignored in these calculations.

Latitude Distribution of Cruise Fuel Use

The adopted latitudinal distribution of fuel use is given in Figure 1. A detailed distribution for any specific fleet will, of course, depend on flight routes, anticipated demands between city-pairs, and routing to avoid sonic booms over land. The chosen distribution is based on two independent studies that take into account each of these concerns (1,2). Fuel use is distributed according to projected flight paths, and the emitted materials are assumed to be deposited along the flight paths. No adjustment is made to account for the vertical and meridional transport of the plume that may occur in the first few weeks before the emitted material becomes zonally mixed.

Altitude and Mach Number

Aircraft with particular cruise speeds (Mach numbers) operate most efficiently at specific altitudes. The adopted altitude range for each Mach number is specified in Table 1. The assigned spread in altitude is in accord with possible traffic control and the natural climb of cruise altitudes toward the end of a trip, as the fuel is being used up. Here, we ignore the latitudinal variation of the altitude range of injection.

Fuel use and emissions are assumed to be uniform throughout the year.

Emitted Material

The emission index (EI) for oxides of nitrogen, $EI(NO_x)$, is defined as in chapter 1 as equivalent grams of NO_2 emitted per kilogram of fuel use. The NO_x emitted is typically 90% NO and 10% NO_2 , on a molecular basis. This value should be used if a distinction between NO and NO_2 emission is needed. EIs for other species are as specified in Table 1.

Subsonic Fleet

The emissions for the year 2015 subsonic fleet are based on the Boeing B6 references scenario (1). The impact of the subsonic fleet is represented by emissions at two cruise altitudes: 20,000-30,000 ft and 30,000-40,000 ft. The assumed fuel use is 20×10^9 kg/year and 150×10^9 kg/year, respectively. Because of an error, some modeling groups were instructed to distribute fuel use for the lower cruise altitude between 0 and 30,000 ft, but this discrepancy makes little difference, since most results are to be examined in term of changes relative to baseline.

The latitudinal distributions of fuel use for the two cruise altitudes are given in Figure 2. For simplicity, we adopt the distribution for the greater fuel use (30,000-40,000 ft) for both cases. Fuel use is assumed to be constant throughout the year. The EIs for the species included in these sensitivity studies are given in the Table 1.

Background Atmosphere

The change in O₃ will be calculated as a percentage change relative to the baseline atmosphere specified in Table 2 (atmosphere in year 2015, with the subsonic aircraft fleet). Note that, if heterogeneous chemistry is active, the model-predicted ozone content of the 2015 atmosphere is particularly sensitive to the chlorine loading in the atmosphere.

Table 2. Boundary Conditions for Atmospheric Composition

Species	Concentration in		Comment
	1985*	2015+	
CFC-11	220 ppt	260 ppt	The boundary condition for the CFCs is assumed to be half-way between complete phaseout in 2000 (Prather and Watson†, case 1b) and the revised Montreal Protocol.
CFC-12	375 ppt	510 ppt	
CFC-113	30 ppt	70 ppt	
CFC-114	5 ppt	10 ppt	
CFC-115	4 ppt	8 ppt	
CCl ₄	100 ppt	100 ppt	
HCFC-22	80 ppt	200 ppt	The values for HCFC-22 and CH ₃ CCl ₃ reflect use of other substitutes.
CH ₃ CCl ₃	130 ppt	150 ppt	
Halon-1301	1.7 ppt	6 ppt	
Halon-1211	1.5 ppt	2 ppt	
CH ₃ Cl	600 ppt	600 ppt	Assumed natural.
CH ₃ Br	10 ppt	10 ppt	Assumed natural.
N ₂ O	306 ppb	330 ppb	Assumed increase of 0.25% per year.
CH ₄	1600 ppb	2050 ppb	Assumed increase of 15 ppb per year.
CO ₂	345 ppm	390 ppm	Assumed increase of 0.45% per year.

*While it is recognized that other boundary conditions affecting tropospheric chemistry such as CO and NO_x, will change with time, it is recommended that each model keeps its present-day reference troposphere unchanged in the simulations.

+The total chlorine content is about 3.7 ppb in the year 2015 atmosphere.

†M.J. Prather, R.T. Watson, Stratospheric ozone depletion and future levels of atmospheric chlorine and bromine, *Nature*, 344, 729-734, 1990.

Scenarios for Supersonic Fleet

Recent modeling results (3-7) showed that the main impact on ozone depends on the total amount of NO_x emitted and the altitude of injection. For fixed fuel use, the calculated ozone response should be related to the EI(NO_x). The Mach number and the EI for NO_x are

used as the only two independent parameters in this set of sensitivity scenarios. The chosen scenarios are shown in the two-parameter space of EI and Mach number in Figure 3.

The recommended model simulations are:

- one baseline simulation (BSE) : background atmosphere + subsonic fleet;
- seven perturbation runs (A through G) : background atmosphere + subsonic fleet + one of the fleets listed in the figure.

Note that cases F, A, and G represent three cases wherein NO_x EI=15 and cruise speeds are Mach 3.2, 2.4, and 1.6, respectively. Cases B, C, and D represent the same set of cruise speeds, with NO_x EI=5. Case E (EI=45) represents a fleet with present-day technology flying at Mach 2.4.

INTERCOMPARISON OF MODEL RESULTS

The modeling groups that participated in the intercomparison are:

- AER Atmospheric and Environmental Research Inc.: M. Ko and D. Weisenstein
- GSFC NASA Goddard Space Flight Center: C. Jackman, A. Douglass, and K. Brueske
- LLNL Lawrence Livermore Laboratory: D. Wuebbles and D. Kinnison
- NCAR National Center for Atmospheric Research: G. Brasseur
- CAMED-P University of Cambridge and University of Edinburgh: J. Pyle, R. Harwood, and A. Jones
- OSLO University of Oslo: I. Isaksen, F. Stordal

The procedure for this intercomparison assessment made use of the infrastructure set up for previous model intercomparison workshops (8). Dr. Robert Seals, Jr., of the Upper Atmosphere Data Program (UADP) at NASA Langley Research Center is in charge of the database for the model results. Model results in digital format were sent to the database in standard UADP format. Each modeling group was asked to send at least 4 months (March 15, June 15, September 15, and December 15) of latitude-height fields of NO_y , H_2O , Cl_y , O_3 , and noon-time $\text{NO} + \text{NO}_2$ (NO_x), along with latitude-season (12 months) of the column abundance of O_3 for each simulation.

It was agreed that the modelers would use only gas-phase chemistry for the first set of runs. However, as part of the later UNEP/WMO Ozone Assessment, they were encouraged to add heterogeneous chemistry for later studies and the 1992 HSRP/AESA annual meeting will examine these studies with the new heterogeneous, sulfate-layer chemistry. Only the emissions for NO_x and H_2O are to be used in the simulations. The emissions for CO, hydrocarbons (HC), SO_2 , and CO_2 are included in Table 1 for reference, so that sensitivity studies could be made with some models. Preliminary estimates have confirmed that their impacts are minor.

Background Atmosphere

The calculated column abundances of ozone (O_3) for the 2015 atmosphere that include the subsonic fleet from the models are shown in Figure 4. The calculated column abundances of O_3 are quite similar, within 20% of each other. Previous model intercomparison (8) showed that the simulated O_3 abundances for the 1985 atmosphere are within 20%. Model results not shown here indicated that the ozone column for the 2015 atmosphere is within 2% to 5% of the 1985 atmosphere. The consistency among the model results is encouraging. At the same time, one must remember that one is interested in calculated O_3 changes of about a few percent.

The "good" agreement among the models should not be taken at face value as validation of the model results. It has been noted (9) that the ozone decrease over the past decade predicted by models using gas-phase chemistry is smaller than the observed trend. A possible explanation is the omission of the effect associated with enhanced concentrations of the active chlorine species produced by heterogeneous reactions occurring on PSCs and the global aerosol layer.

The concentration of O_3 in the high-latitude lower stratosphere is controlled by a balance between transport and local photochemical removal. The fact that the simulated O_3 concentrations in different models all bear some semblance to the observations does not necessarily imply that the simulated transport rates and chemical removal rates in different models are approximately the same. Similar O_3 distributions may be obtained by combinations of different transport and photochemical removal terms. As a result, the response of the O_3 to changes in the chemical forcing calculated in different models may be very different.

Comparison of the mixing ratios of several species in the high latitude lower stratosphere is shown in the Table 3. Recognizing that the photochemical lifetime of O_3 in the lower stratosphere is on the order of months, we decided to pick a sufficiently large region poleward of $40^\circ N$ and from $z^* = 12$ km to $z^* = 28$ km. The altitude variable z^* is expressed in kilometers and is defined in terms of pressure as $z^* = 16 \log_{10}(1000/p)$, where p is in mb. The values in Table 3 are reported as average mixing ratios, which are defined as the total number of molecule of the species in the region, divided by the total number of air molecules in the same region. In other words, it is the average mixing ratio weighted by the local air-density. In addition, the values reported are averages of the monthly values used to represent annual averages.

Table 3. Average Mixing Ratios for the 2015 Atmosphere*

Model	H_2O (ppmv)	Cl_y (ppbv)	NO_y (ppbv)	$NO+NO_2$ (ppbv)	NO_x/NO_y	O_3 (ppmv)
AER	5.8	1.2	6.5	1.2	0.18	1.8
CAMED-P	9.5	1.1	5.9	1.7	0.16	1.8
GSFC	5.8	0.72	3.6	0.76	0.21	1.7
LLNL	14.6	0.94	5.2	1.2	0.23	1.8
NCAR	3.7	0.97	7.7	2.2	0.29	1.6
OSLO	N/A	0.91	5.1	1.1	0.22	N/A

Values given in the table are annual averages over the region between $40^\circ N$ and $90^\circ N$; $z^ = 12$ km to 28 km.

Note that the H₂O, Cl_y and NO_y concentrations in the lower stratosphere are quite different among models. The degree to which the results from the different models agree with each other may depend on the size of the region chosen for the analysis. For instance, the large value of H₂O in the LLNL model is probably due to the fact that the chosen region includes part of the troposphere in that model. In spite of the great differences in the calculated NO + NO₂ among the models, the calculated O₃ is quite similar. This suggests that there may be significant differences in the functional dependence of O₃ on the calculated photochemical removal rates in the different models.

For further comparison of model results, see reference 8.

Scaling Estimate for Trace Gas Perturbation

With assumed fuel use at 70×10^9 kg/year, a "ball park" estimate of the expected local change in concentration for an inert tracer resulting from the aircraft emissions is about 0.5 ppbv for an EI of 1. In the case of NO_y, where EI is on the order of 10, the expected change in concentration is up to a few ppbv, while for H₂O, an EI of 1000 would cause an increase of about 0.5 ppmv.

Based on the EI values given in Table 1, the biggest changes, when expressed as percentages of the background concentration, are for NO_y and H₂O. We will examine the changes in H₂O and NO_y for each case and compare the residence times for each species in the different models.

Change in NO_y

Table 4 shows the calculated changes in content of NO_y above $z^* = 6$ km in units of kiloton (N). An annual fuel use of 70×10^9 kg/yr would result in an injection rate for NO_y of 107 kiloton (N)/yr for EI of 5; 320 kiloton (N)/yr for an EI of 15; and 959 kiloton (N)/yr for an EI of 45. One can take the change in stratospheric content of NO_y in Table 4 and divide by the corresponding injection rates to obtain stratospheric residence times for the injected NO_y in each of the cases. The results from each model showed that this residence time is independent of EI.

Table 4. Model Calculated Change in Global Content of NO_y above 6 km at Steady State [kiloton (N)]

Mach No./Case	EI = 5			EI = 15			EI = 45
	3.2/B	2.4/C	1.6/D	3.2/F	2.4/A	1.6/G	2.4/E
AER	233	172	63	875	491	184	1472
CAMED-P				834	503	245	
GSFC	184	135	80	528	393	245	1166
LLNL	184	135	59	564	393	172	1166
NCAR	172	113	77	528	344	233	1018
OSLO	233	120	53	675	356	160	1067

The values are given in Table 5 as functions of injection heights or Mach numbers. Note that a large number for residence time implies that the emitted NO_y is retained in the stratosphere for a

longer period of time, so that more NO_y will be added to the stratosphere at steady state for a particular emission rate. As a result, more O₃ will be removed for the same emission.

The results in Table 5 indicate that all models showed different residence times for different injection heights. There is no consistent ranking of the models that applies to all injection heights. The large difference for the Mach 1.6 case is probably due to the difficulty in obtaining an accurate number for the change in NO_y, which is about 10% of the background.

Table 5. Stratospheric Residence Time (Years) of Injected NO_y

Model	Mach 3.2	Mach 2.4	Mach 1.6
AER	2.1	1.5	0.6
CAMED-P	2.6	1.5	0.8
GSFC	1.7	1.2	0.8
LLNL	1.8	1.2	0.5
NCAR	1.7	1.1	0.7
OSLO	2.1	1.1	0.5

The model-calculated changes in NO_y are shown in Figures 5(a)-(g). For case F (Mach 3.2 and EI=15), most models showed an increase of 1 ppbv extending into the way to the southern hemisphere. The CAMED-P model indicated an increase of 2 ppbv. For case A (Mach 2.4 and EI=15), the increase in the southern hemisphere is about 0.5 ppbv, with the maximum local increase in the northern latitude ranging from 2-4 ppbv. In case G (Mach 1.6, EI=15), most models show an increase in the southern hemisphere of about 0.1 to 0.2 ppbv, with the maximum in the northern latitude ranging from 1-1.4 ppbv. The GSFC model is particularly efficient in exporting the material to the southern hemisphere for the Mach 1.6 injection, resulting in an increase of 0.4 ppbv.

The increases in burden of NO_y in the northern lower stratosphere (i.e., 40°N-90°N, 12-28 km, annual average) are given in Table 6. This region is chosen because, based on the photochemical and transport lifetimes of ozone in the lower stratosphere, the changes in ozone in the northern mid-latitudes are expected to be influenced by the changes in photochemical balance in this whole region. If the model can distribute the injected NO_x out of this region, the ozone decrease in the northern hemisphere will be smaller. Table 7 gives the ratio of the increase in regional NO_y abundance (Table 6) to the increase in global burden (Table 4). A smaller value in Table 7 implies that the model is more efficient in exporting the emitted material out of the local region. Values given in Table 7 indicated that the AER model is consistently among those that is least efficient in exporting the NO_y, while the CAMED-P model is the most efficient. Other models show different efficiencies, depending on cruise altitude.

Change in H₂O

Calculated changes in H₂O for case F (Mach 3.2) are shown in Figure 6. Note that, for H₂O, cases B, C, and D are identical to cases F, A, and G, respectively, since there is no change in EI(H₂O) between the two sets. The changes in H₂O are expected to be similar to those for NO_y in the lower stratosphere, where the photochemical removal time for both species is relatively long. They differ in the upper stratosphere, in that the photochemical removal of NO_y is more efficient. The changes in mixing ratio are: 0.2-0.4 ppmv in the NCAR model; 0.4-0.6 ppmv in the AER and LLNL models; and 0.6-0.8 ppmv in the CAMED-P model.

Table 6. Model Calculated Increases in the Burden of NO_y [kiloton (N)] in the Region 40°N-90°N, 12-28 km, Annual Average

Mach No./Model	EI = 5			EI = 15			EI = 45
	3.2/B	2.4/C	1.6/C	3.2/F	2.4/A	1.6/G	2.4/E
AER	94	67	25	281	196	74	580
CAMED-P				290	159	70	
GSFC	70	44	23	215	131	69	402
LLNL	68	42	22	206	122	62	374
NCAR	69	41	27	206	122	81	374
OSLO	80	45	22	243	131	51	402

*Expressed as an average mixing ratio in parts per billion by volume for the region.

Table 7. Rates of Changes in NO_y Regional Abundance Versus Global Abundance

Model	Mach 3.2	Mach 2.4	Mach 1.6
AER	0.41	0.40	0.40
CAMED	0.35	0.32	0.29
GSFC	0.40	0.34	0.29
LLNL	0.37	0.32	0.36
NCAR	0.39	0.37	0.35
OSLO	0.35	0.37	0.42

It is harder to get quantitative results from the H₂O database because it is difficult to define a meaningful region that excludes the troposphere in all the models. Moreover, modeling H₂O in current stratospheric models involves some uncertain assumptions about the microphysical control of H₂O at the tropopause.

Ozone Column Response

Except for the CAMED-P model, the transport circulation and temperatures in the models are fixed so that the effects of dynamic feedbacks are ignored. Thus, changes in O₃ represent responses to modifications in the chemical removal rates resulting from aircraft emissions. Previous modeling results (3-5) showed that the impact from H₂O emission alone is small. Thus, in this discussion, we will concentrate on the sensitivity of the O₃ response to changes in active nitrogen species (NO+NO₂).

The calculated changes in column ozone are shown in Figures 7(a)-(g). The calculated changes in global ozone content are summarized in Table 8. The following observations can be made from the results.

- There is no consistent ordering of the calculated global O₃ decrease among the models. The ordering is different, depending on Mach numbers.
- In the northern hemisphere, the AER, OSLO, and CAMED-P model gave the largest calculated ozone decreases for all cases. The results from the rest of the models were quite similar to the results from GSFC and slightly larger than those from LLNL and NCAR. The spread between the two groups was about a factor of 2.
- In the tropics, the results were similar in all models, except for CAMED-P, which showed a large decrease in the tropics. For case F, all models but CAMED-P showed a decrease of -2%; the CAMED-P model showed -4%. For case A (Mach 2.4 and EI=15), the OSLO model showed a calculated increase in the tropics, while other models calculated a decrease of about -1%. For case G, the AER model and the LLNL model calculated a small increase in the tropics, while the GSFC, NCAR, and CAMED-P model calculated a decrease of -0.4%. The predicted decreases in case E from AER and OSLO were smaller than from the other models.
- In the southern hemisphere, the GSFC and CAMED-P model consistently predicted the largest decrease in ozone. The difference among the models is largest for the Mach 1.6 case.

Table 8. Calculated Decrease in Global Total O₃ (%)

Mach No./Case	EI = 5			EI = 15			EI = 45
	3.2/B	2.4/C	1.6/D	3.2/F	2.4/A	1.6/G	2.4/E
AER	1.2	0.61	0.11	4.3	2.1	0.40	7.5
CAMED-P				5.3	2.5	0.72	
GSFC	1.2	0.50	0.20	4.1	1.7	0.67	5.9
LLNL	0.9	0.50	0.085	3.4	1.7	0.29	6.1
NCAR	0.78	0.31	0.14	3.5	1.4	0.62	4.7
OSLO	1.2	0.15	0.01	4.1	0.72	.002	3.5

Changes in Local O₃ Concentrations

The percent changes in local O₃ for March are shown in Figures 8(a)-(g).

- All models showed large decreases in the region north of 30°N, between 10 and 25 km, where most of the NO_x emissions are deposited.
- Calculations of behavior in the troposphere may depend on the choice of the boundary condition for O₃ in the models. With a fixed mixing boundary condition, the AER model showed slight increases in the troposphere for the southern hemisphere in all cases. In the NCAR model, the increase in tropospheric O₃ is limited to a small area in the tropics. The LLNL and GSFC models predicted an increase only for the Mach 1.6 case.

- The AER, GSFC, LLNL, and CAMED-P models showed increases in the tropical lower stratosphere between 20 and 30 km. The region of increase is most extended for the GSFC model.
- The extent to which the southern lower stratosphere is affected in each model is related to how efficiently NO_y is transported to the southern hemisphere. The CAMED-P model, which has the most efficient global distribution of the emitted NO_y, showed the largest decrease in the south, while the AER model showed the smallest.

Analysis of Ozone Loss

The photochemical removal rate for O₃ caused by the catalytic NO_x cycle is proportional to the concentration of NO_x = (NO + NO₂) calculated in the models. Thus, the increase in the photochemical removal rate is proportional to the increase in NO_x. Table 9 gives the calculated changes in NO_x from the models in the northern lower stratosphere (40°N-90°N, 12-28 km, annual average). Since the NO_x/NO_y ratios are different in different models, it is not surprising

Table 9. Changes in NO_x (= NO + NO₂, ppbv) (40°N-90°N, 12-28 km, Annual Average)

Mach No./Case	EI = 5			EI = 15			EI = 45
	3.2/B	2.4/C	1.6/D	3.2/F	2.4/A	1.6/G	2.4/E
AER	0.16	0.12	0.067	0.67	0.41	0.23	2.1
CAMED-P				1.2	0.68	0.34	
GSFC	0.20	0.13	0.073	0.66	0.42	0.23	1.4
LLNL	0.18	0.13	0.064	0.68	0.41	0.20	1.5
NCAR	0.19	0.14	0.11	0.80	0.54	0.39	1.9
OSLO	0.27	0.14	0.076	0.91	0.48	0.25	0.91

*Expressed as average mixing ratio parts per billion by volume in the region.

that the changes in NO_x do not scale as changes in NO_y. There is actually a repartition of the nitrogen species, in that the ratio changes if the HSCT is operating. The shift in partition is reflected by the increase in the NO_x/NO_y ratio of about 20% for EI = 15 flights and 5% for EI = 5 flights.

The response of O₃ to increases in NO_x depends on how dominant the NO_x cycle is in determining local O₃ concentration and whether changes in NO_x can significantly perturb the other chemical cycles. Preliminary analysis, based on results from gas-phase chemistry, indicates the impact of the other chemical cycles is small and that O₃ is responding to the change in the NO_x cycle. The percent changes of O₃ averaged over northern latitudes are tabulated in Table 10. The corresponding percent change in NO_x is given in Table 11. One can define an O₃ sensitivity index as the percent change in O₃ divided by percent change in NO_x. Again, we found this result to be nearly independent of EI. The values, which are tabulated as functions of Mach numbers, are given in Table 12; they can be interpreted as ratios of the chemical removal

rate from the NO_x cycle to the total removal rate (i.e., the sum of chemical removal rates from all cycles and the removal rate by transport). Note that if O₃ is completely controlled by NO_x chemistry, the index would be 1. However, it should be noted that the converse is certainly not true. A value of 1 would not necessarily imply that ozone is completely controlled by NO_x.

Table 10. Changes in Ozone (%) (40°N-90°N, 12-28 km, Annual Average)

Mach No./Case	EI = 5			EI = 15			EI = 45
	3.2/B	2.4/C	1.6/D	3.2/F	2.4/A	1.6/G	2.4/E
AER	-3.4%	-1.7%	-0.43%	-13%	-6.3%	-1.5%	-21%
CAMED-P				-13%	-6.0%	-2.0%	
GSFC	-3.2%	-1.1%	-0.4%	-11%	-3.8%	-1.4%	-13%
LLNL	-2.0%	-1.1%	-0.25%	-7.9%	-3.7%	-0.85%	-13%
NCAR	-2.1%	-0.82%	-0.38%	-9.6%	-3.6%	-1.6%	-12%
OSLO	NA	NA	NA	NA	NA	NA	NA

Table 11. Changes in NO_x (%) (40°N-90°N, 12-28 km, Annual Average)

Mach No./Case	EI = 5			EI = 15			EI = 45
	3.2/B	2.4/C	1.6/D	3.2/F	2.4/A	1.6/G	2.4/E
AER	14%	10%	6%	57%	42%	19%	82%
CAMED-P				72%	40%	20%	
GSFC	26%	17%	9%	86%	54%	30%	188%
LLNL	5%	10%	5%	56%	34%	16%	124%
NCAR	9%	6%	5%	35%	24%	18%	86%
OSLO	25%	13%	6%	82%	43%	22%	156%

Table 12. Sensitivity Index for Changes in Ozone Relative to NO_x

Model	Mach 3.2	Mach 2.4	Mach 1.6
AER	-0.22	-0.15	-0.08
CAMED	-0.18	-0.15	-0.1
GSFC	-0.13	-0.07	-0.05
LLNL	-0.14	-0.11	-0.05
NCAR	-0.27	-0.15	-0.09
OSLO	NA	NA	NA

Nonetheless, the values defined in Table 12 provide an indication of the sensitivity in each model. The values in the table are on the order of -0.13 to -0.27 for Mach 3.2 injection; -0.07 to -0.15 for Mach 2.4 injection; and -0.05 to -0.1 for Mach 1.6 injection. For Mach 3.2 and Mach 2.4, the AER and NCAR models have the greatest sensitivity. The sensitivity in the GSFC model is particularly small for Mach 2.4.

The differences in the O₃ response can be attributed to the following factors. The CAMED-P results showed the largest increase of both NO_x and NO_y, because the long residence time allows the emitted material to build up over time. The AER results show large O₃ depletion at Mach 2.4 and 3.2 because of the great sensitivity of O₃ to increases in NO_x. The sensitivity index in the NCAR model is just as great (or greater) compared with the AER model, but the O₃ response is tempered by a smaller residence time for the emitted NO_x. Thus, differences in O₃ sensitivity are seen to arise out of differences in the amount of NO_x retained in the stratosphere, as well as the differing degrees to which O₃ is controlled by NO_x chemistry in the lower stratosphere. These differences must be examined and resolved in a way that allows us to select one class of models over another. HSRP is currently sponsoring a major international comparison among models that extends the model-model comparison of 1988 to a suite of model-measurement tests.

CONCLUDING REMARKS

Similarities and Differences Among the Models

It is encouraging that the results within each individual model all show similar dependence on EI for NO_x and cruise altitudes. Thus, all the calculated impacts on O₃ are greater for larger EI and higher cruise altitudes. At the same time, the magnitudes of the calculated O₃ changes differ by as much as a factor of 2. The analysis presented in Analysis of Ozone Loss suggests that the differences can be understood in term of the residence time (Table 5) and O₃ response sensitivity factor (Table 12) peculiar to each model. One must look for observations that can help define these quantities in the current atmosphere.

Validation of Models

There is a sizable database for validating model results. However, the validation of model-predicted response of O₃ to perturbations must go beyond mere comparison of observed and calculated species concentrations. One should try to identify diagnostic quantities from models and observations that are useful for testing the mechanisms that control the O₃ concentrations.

The discussion in the section, Analysis of Ozone Loss, identified the residence time (i.e., tracer dispersion) and the O₃ response sensitivity index to NO_x as two key parameters that characterize the calculated O₃ response. The ¹⁴C data from atmospheric nuclear tests seem ideally suited for deriving residence times for comparison with model results. Other data, such as those on ²³⁸Pu derived from satellite reentry, may also be useful. Analysis of data for H₂O, O₃, and NO_y near the tropopause may provide clues to the actual mechanisms responsible for the troposphere/stratosphere exchange rate. To get a handle on the O₃ sensitivity, one can use measurement programs designed to provide simultaneous observations of many species [e.g., such as Atmospheric Trace Molecule Spectroscopy (ATMOS), balloon measurement campaigns, and aircraft campaigns] to provide directly measured or derived concentrations for the radical species, to define the local chemical removal rates for ozone. Getting a handle on the removal rate by transport is much more difficult. Application of the data assimilation technique

to derive transport wind fields from observations may serve as a starting point for deriving transport fluxes of O₃ on the lower stratosphere.

Other Issues

Recent reviews (6,7) highlighted the various components that should be included in future HSRP modeling efforts. We would like to emphasize two important uncertainties that have not been addressed in the calculations reported in this chapter.

Plume dispersion and plume chemistry

The source function for the emitted materials used in the calculations is assumed to have the same latitude-height distribution as the flight paths, and the chemical composition is assumed to be identical to that of the emission at the tailpipe. Plume subsidence and subsequent dispersion in the first few weeks before the emitted materials become zonally mixed could provide an effective distribution of sources that differs from the flight paths. Chemical transformation, occurring homogeneously and heterogeneously, may alter the composition of the materials.

Heterogeneous chemistry in the atmosphere

The O₃ responses shown here were calculated assuming gas-phase reactions only. Heterogeneous reactions occurring on PSCs or on the global sulfate layer could change these responses in a significant way. In this context, one must also consider the possibility that operation of the HSCT may increase the occurrence of PSCs and the loading and size distribution in the sulfate layer. Future assessments, going beyond this initial intercomparison/assessment, will have to include predictions with models that (1) determine parameters for the effects of heterogeneous chemistry and (2) have been rigorously compared with observations of today's stratosphere.

ACKNOWLEDGMENTS

Many people contributed to the success of this effort. These include various committees that helped to set up the ground work and emission scenarios, all modeling groups that delivered the model results in a timely fashion, the Upper Atmosphere Data Program at NASA Langley, and all those who helped to prepare and review this chapter. Special thanks go to Debra Weisenstein at AER, who helped to develop some of the software for compiling the results; and to Linda Hunt and Karen Sage from NASA Langley, who generated the numbers for the tables and the graphics in this chapter.

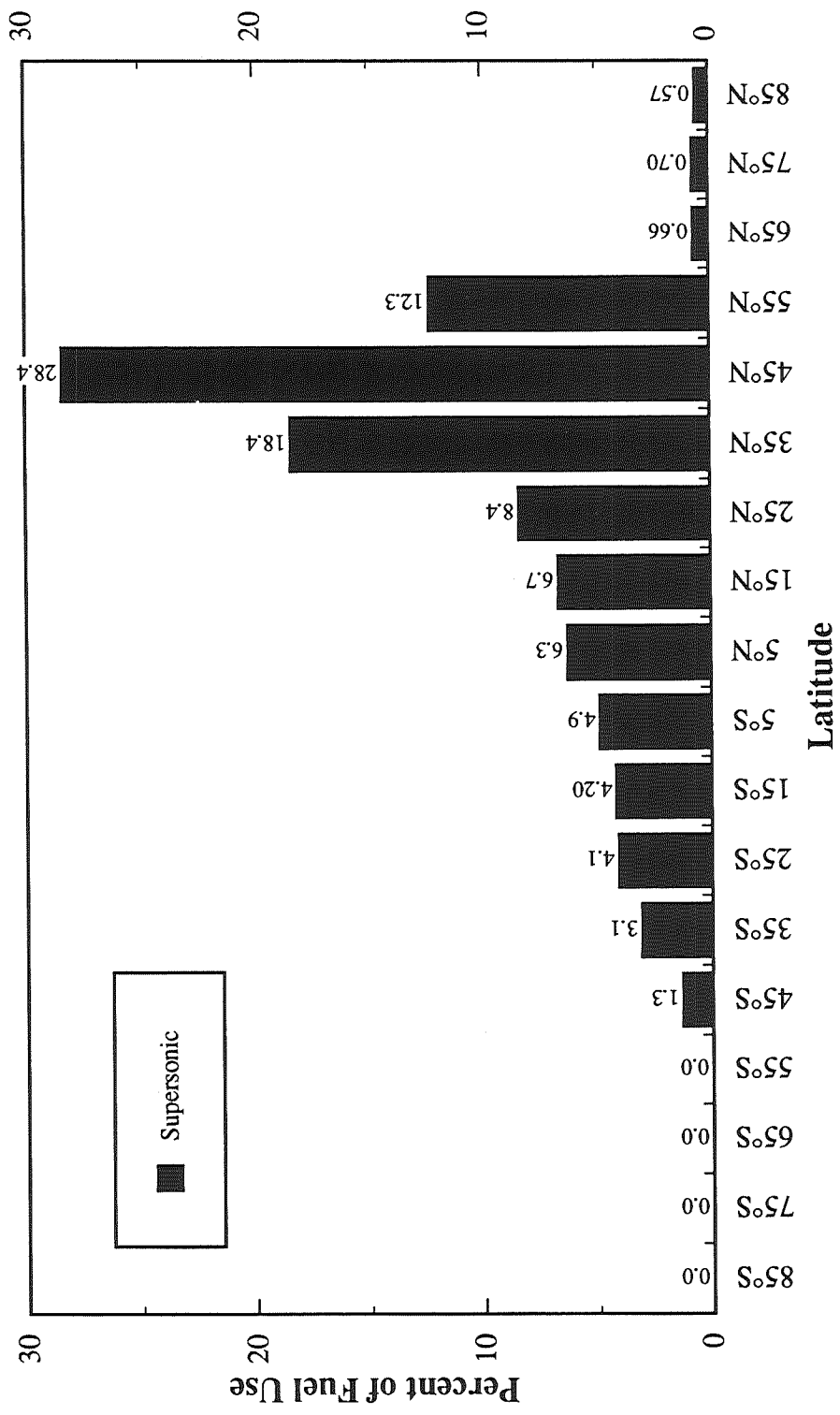


Figure 1. Latitudinal distribution of cruise fuel use for the supersonic fleet, showing the percentage of total fuel use at each latitude.

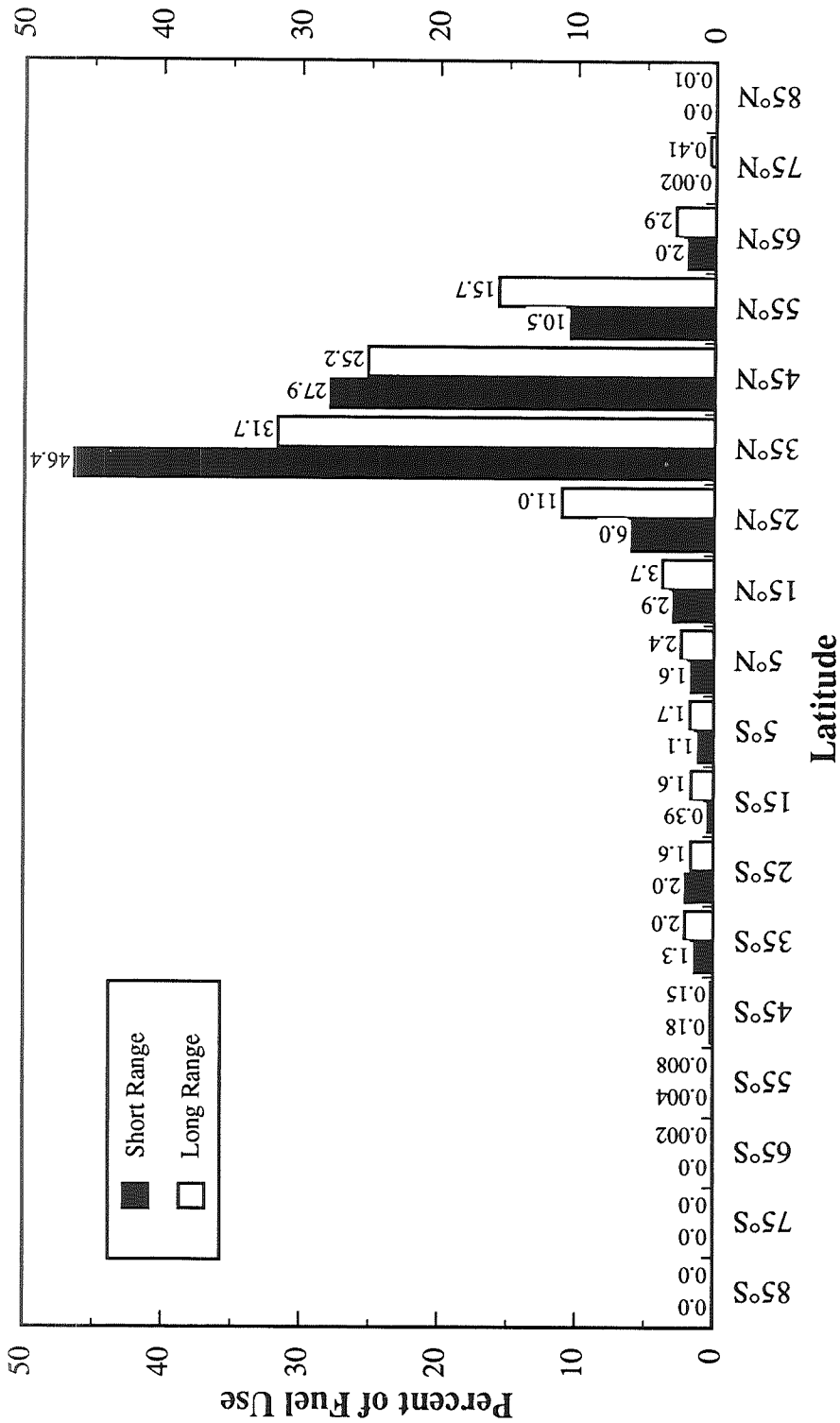


Figure 2. Latitudinal distribution of fuel use for the subsonic fleet at two cruise altitudes, showing the percentage of total fuel use at each latitude.

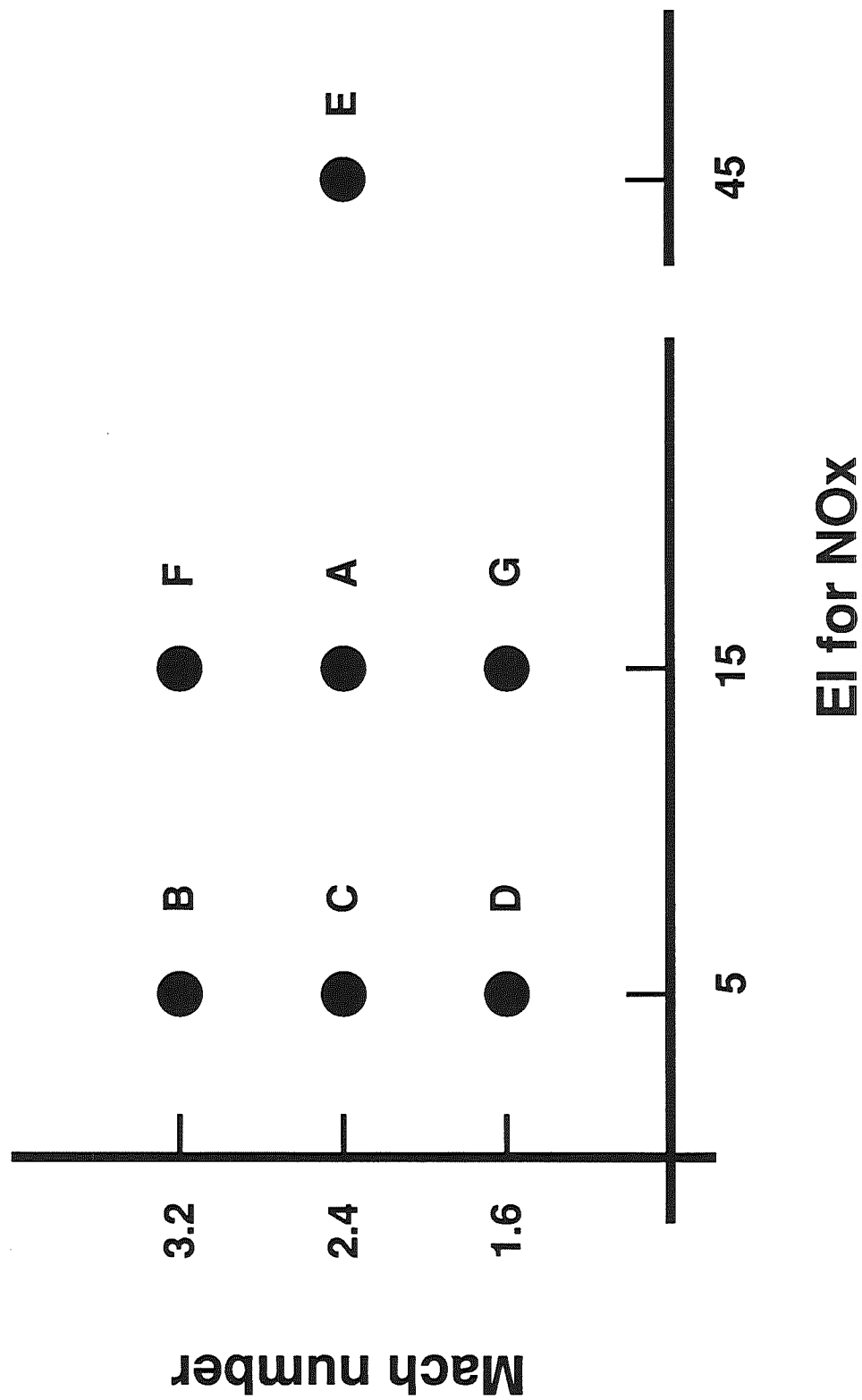


Figure 3. Schematic diagram showing the scenarios in the two-parameter space of EI for NO_x and cruise altitudes.

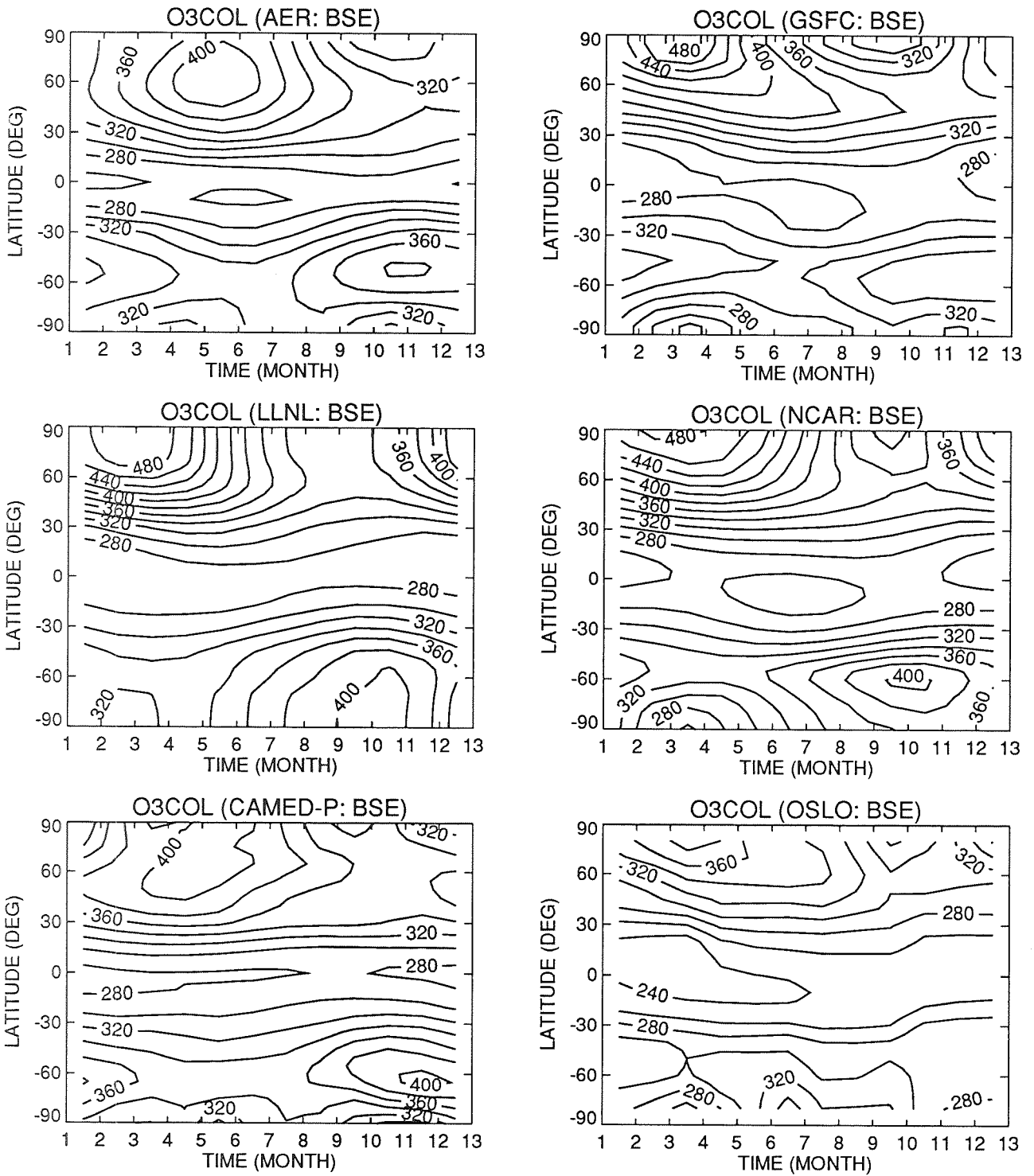


Figure 4. Calculated column abundances of O₃ (Dobson units) for the baseline case (BSE) from the different models.

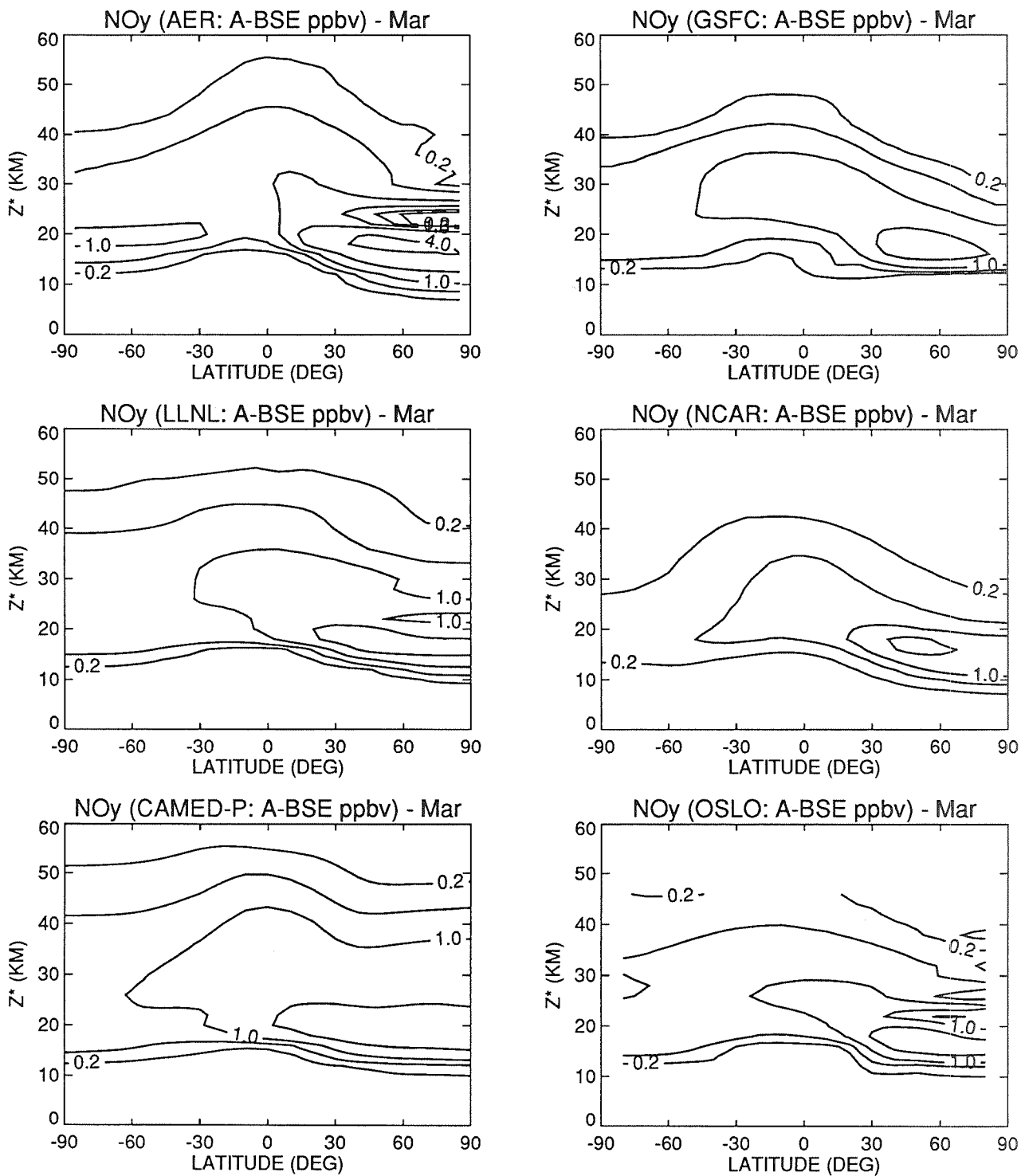


Figure 5(a). Calculated changes in the concentrations of NO_y in parts per billion by volume for March in case A relative to the baseline (BSE). The contours are 0.2, 0.5, 1.0, 2.0, and 4.0 ppbv.

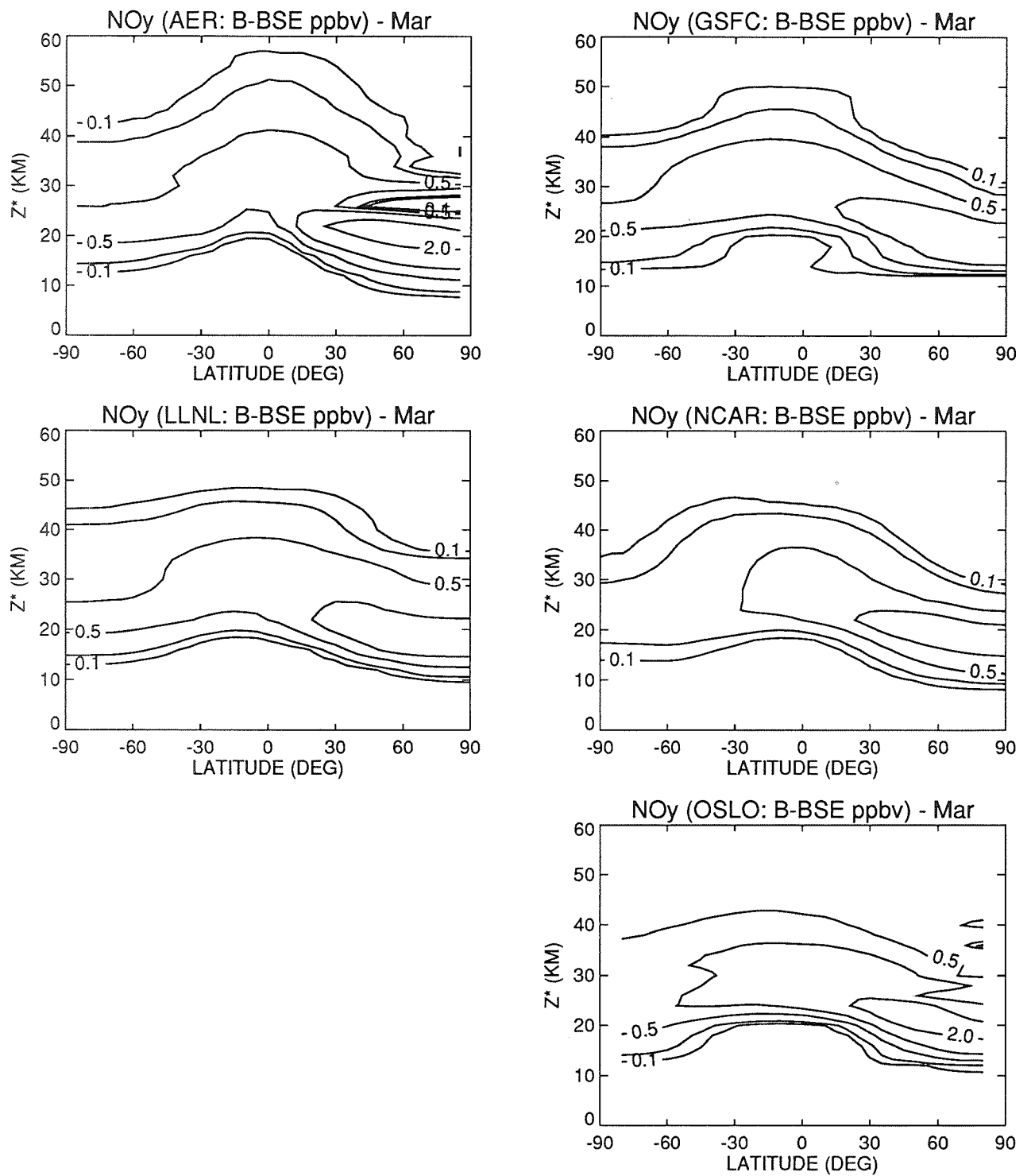


Figure 5(b). Calculated changes in the concentrations of NO_y in parts per billion by volume for March in case B relative to the baseline (BSE). The contours are 0.1, 0.2, 0.5, 1.0, 2.0, and 4.0 ppbv.

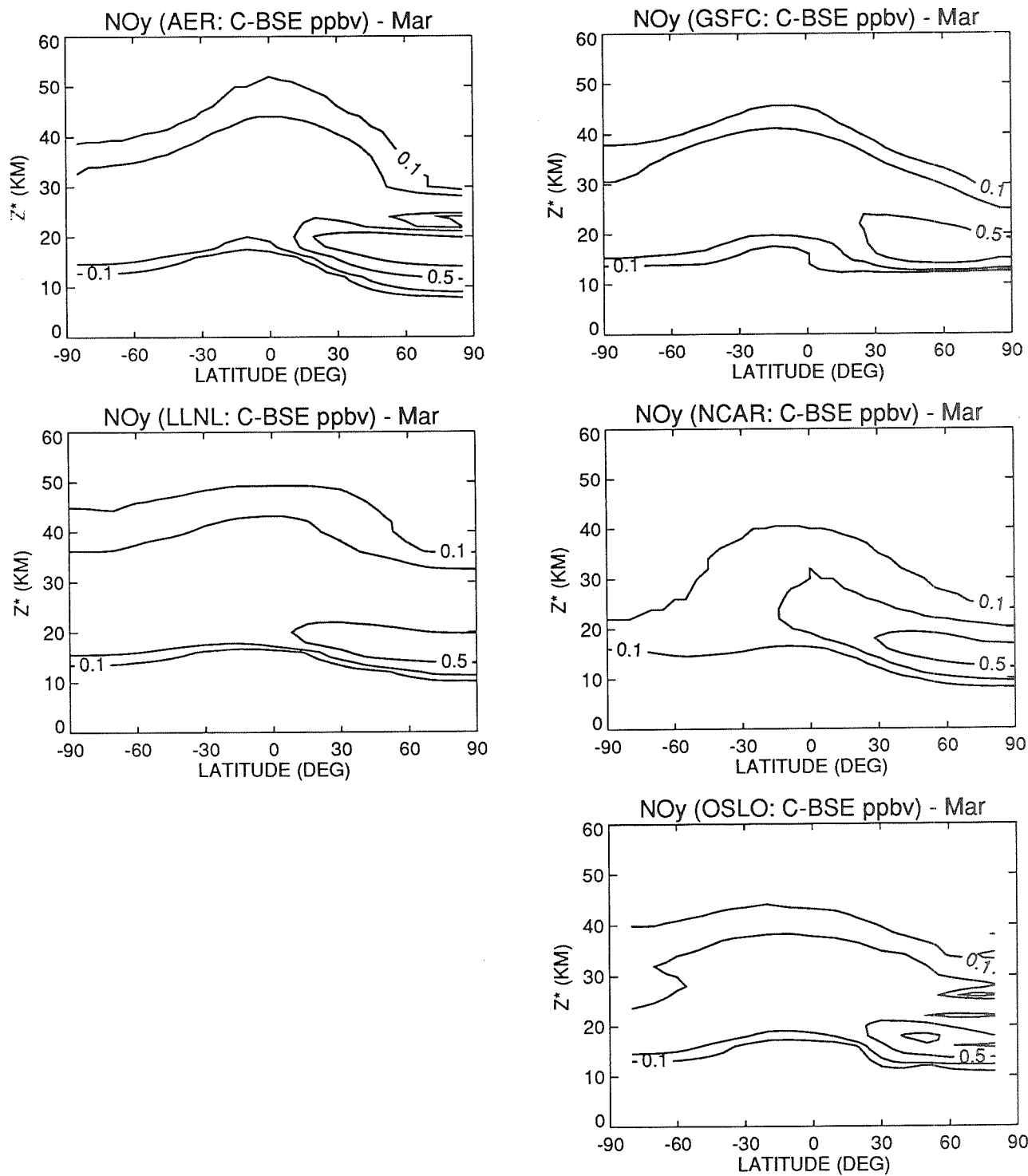


Figure 5(c). Calculated changes in the concentrations of NO_y in parts per billion by volume for March in case C, relative to the baseline (BSE). The contours are 0.1, 0.2, 0.5, 1.0, 2.0, and 4.0 ppbv.

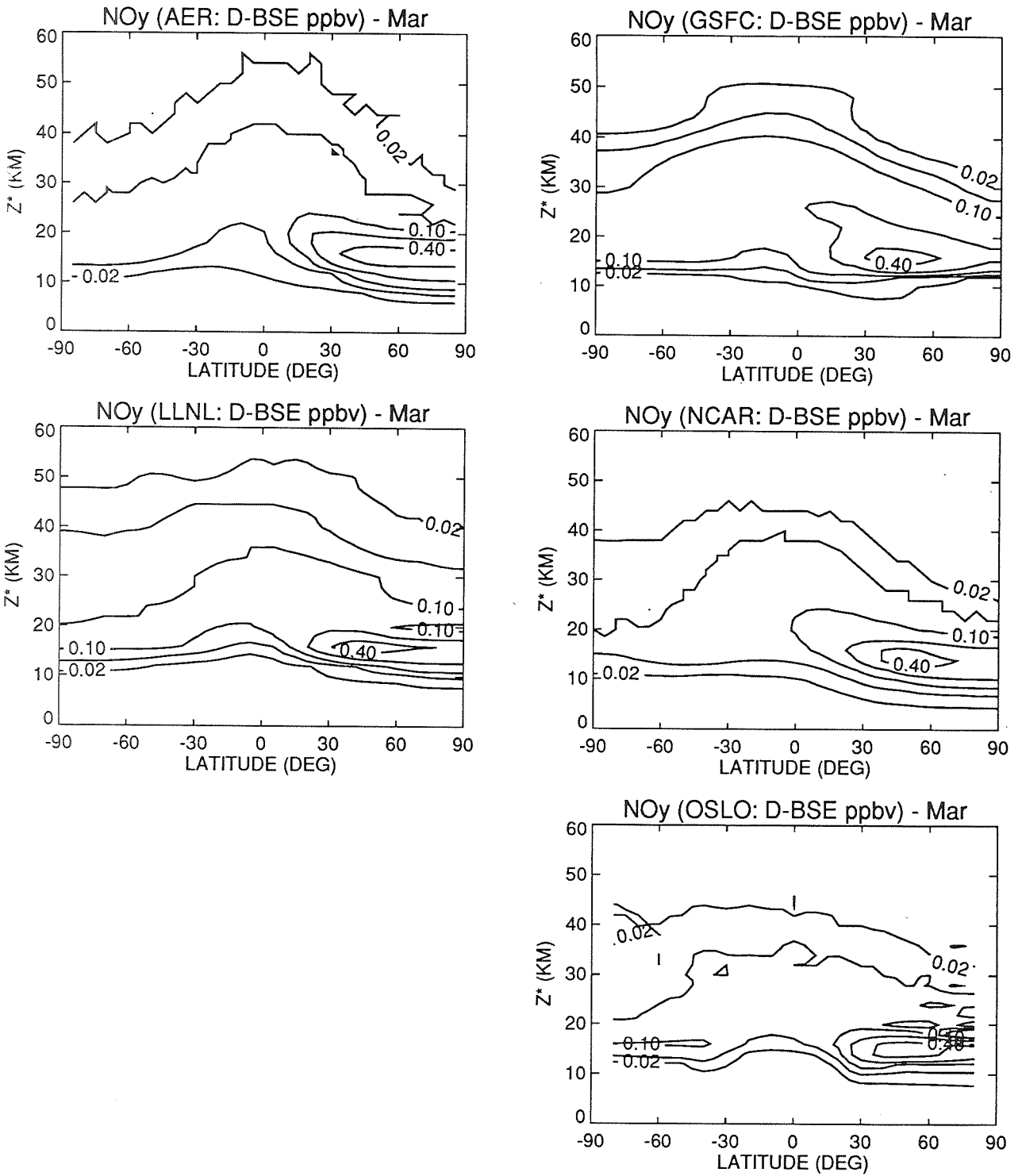


Figure 5(d). Calculated changes in the concentrations of NO_y in parts per billion by volume for March in case D, relative to the baseline (BSE). The contours are 0.02, 0.05, 0.1, 0.2, and 0.4 ppbv.

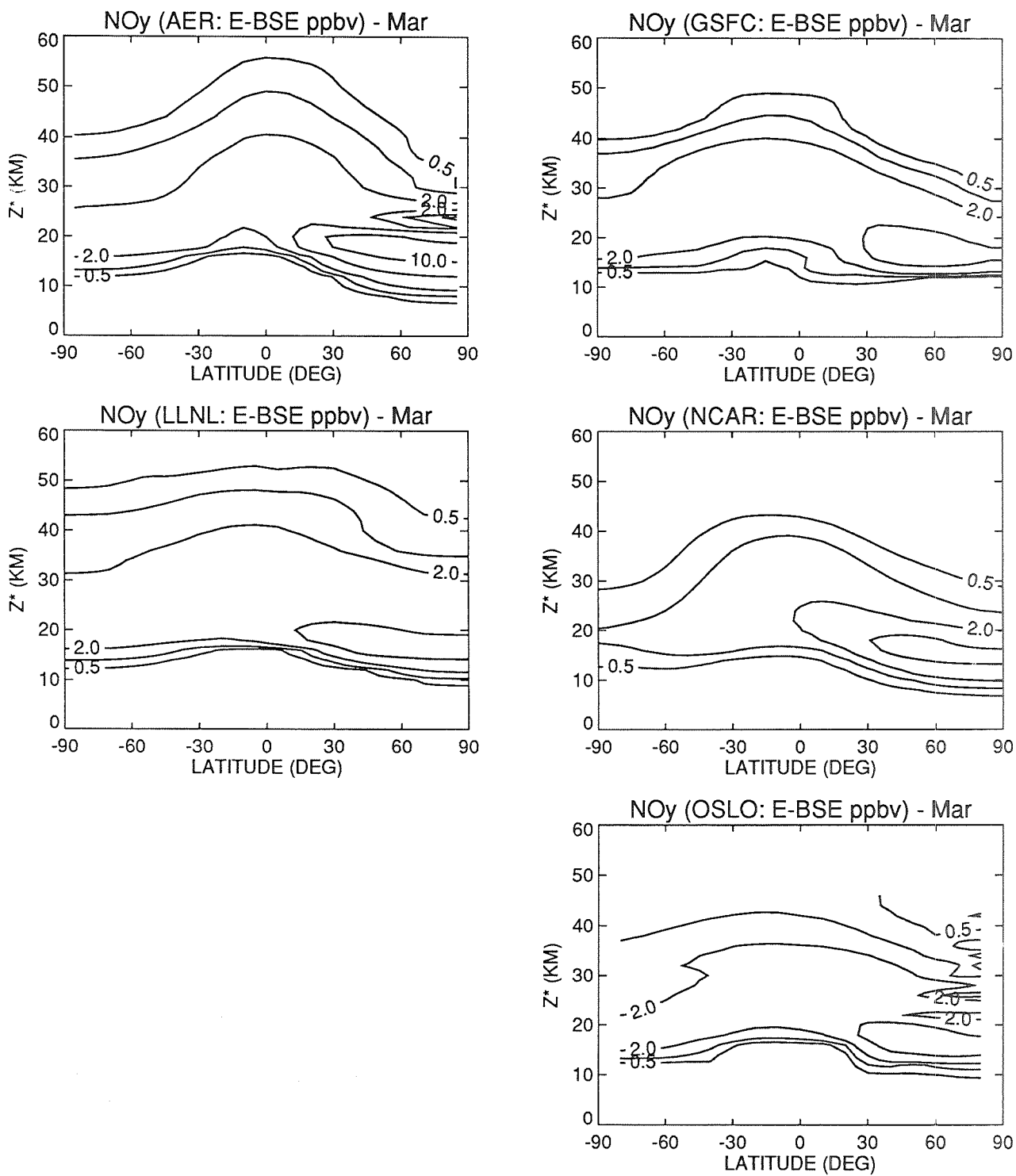


Figure 5(e). Calculated changes in the concentrations of NO_y in parts per billion by volume for March in case E, relative to the baseline (BSE). The contours are 0.5, 1.0, 2.0, 5.0, and 10.0 ppbv.

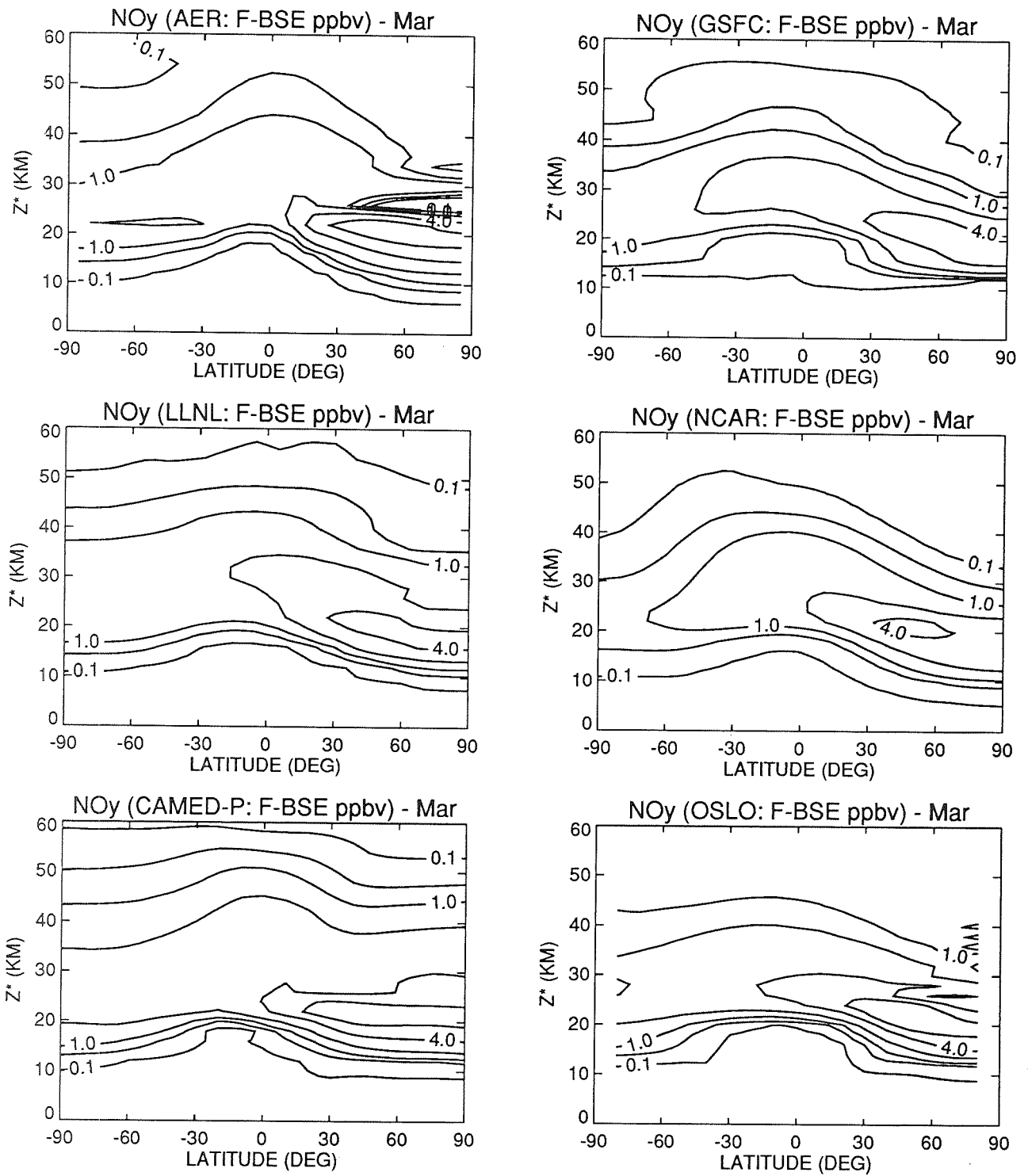


Figure 5(f). Calculated changes in the concentrations of NO_y in parts per billion by volume for March in case F, relative to the baseline (BSE). The contours are 0.1, 0.5, 1.0, 2.0, 4.0, and 6.0 ppbv.

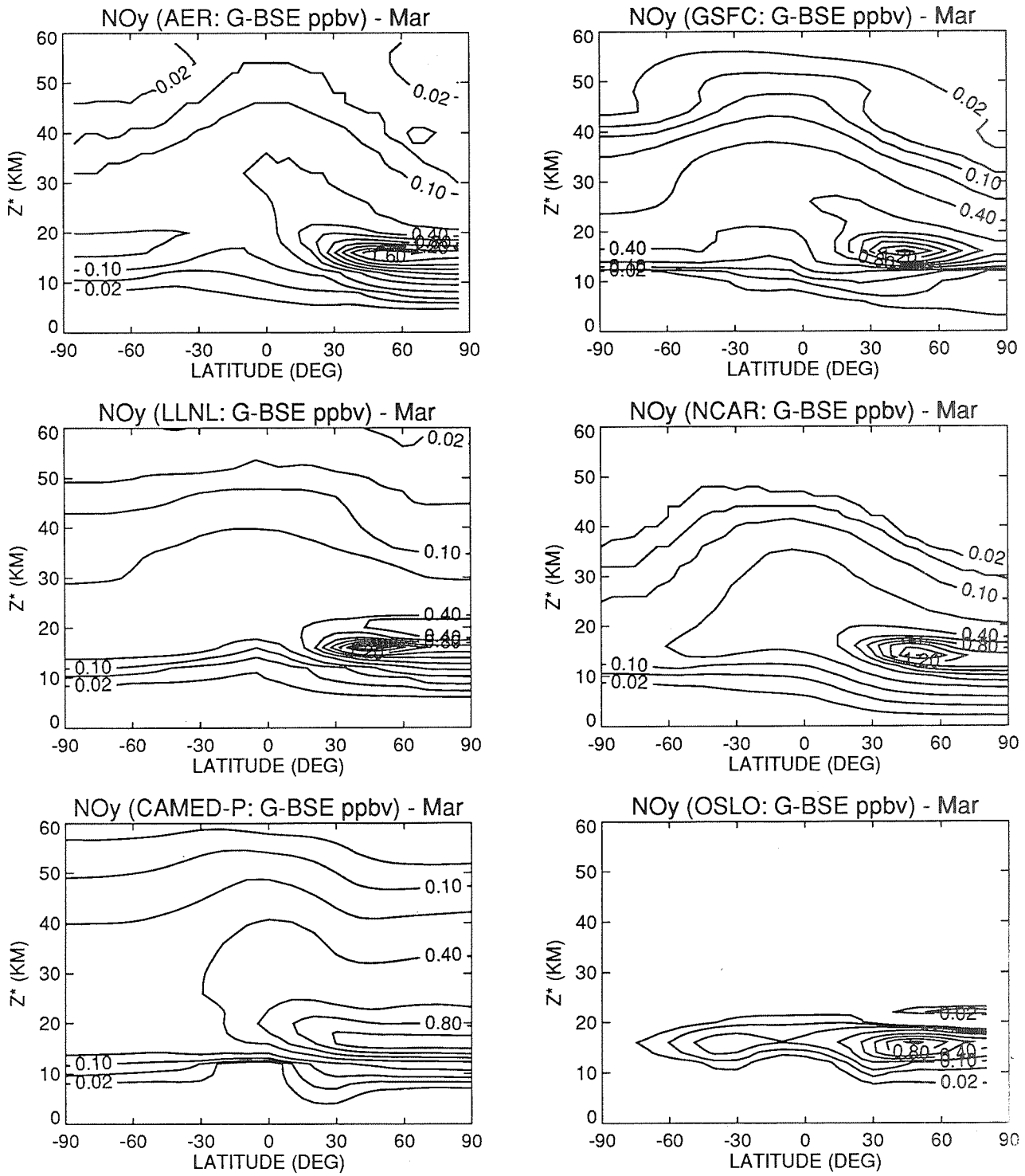


Figure 5(g). Calculated changes in the concentrations of NO_y in parts per billion by volume for March in case G, relative to the baseline (BSE). The contours are 0.02, 0.05, 0.1, and 0.2, in steps of 0.2 ppbv.

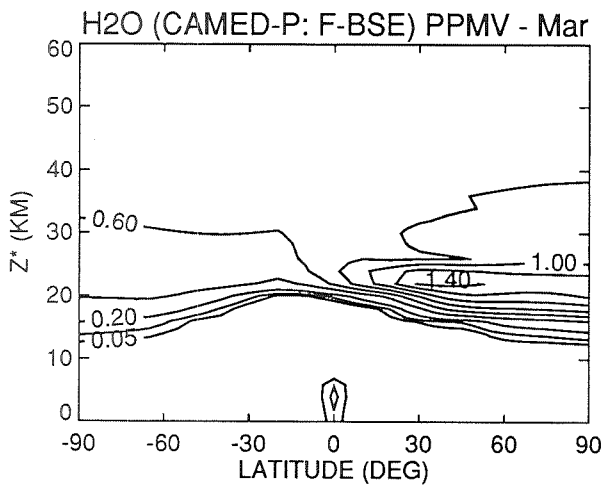
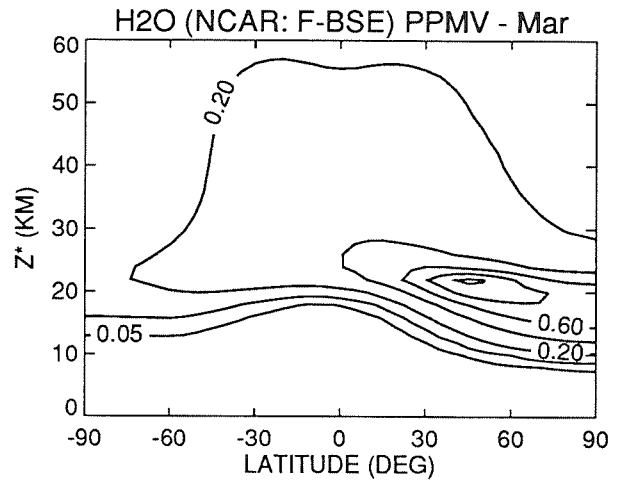
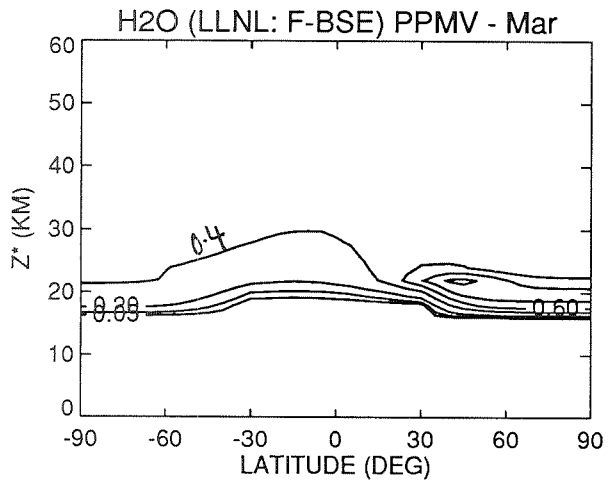
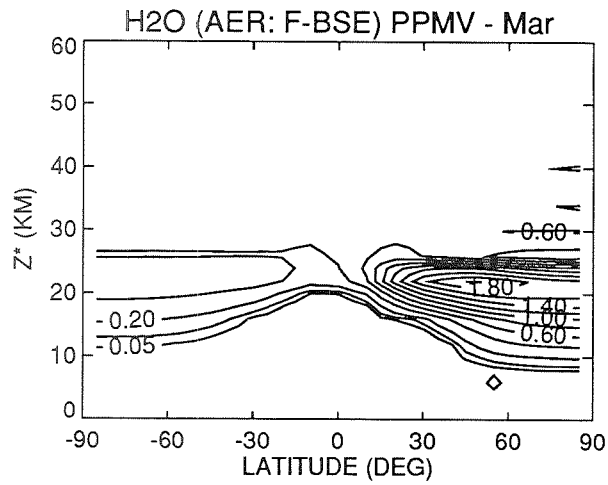


Figure 6. Calculated changes in the concentrations of H₂O in parts per million by volume for March in case F, relative to the baseline (BSE). The contours are 0.05, 0.1, 0.2, and 0.4, in steps of 0.2 ppmv.

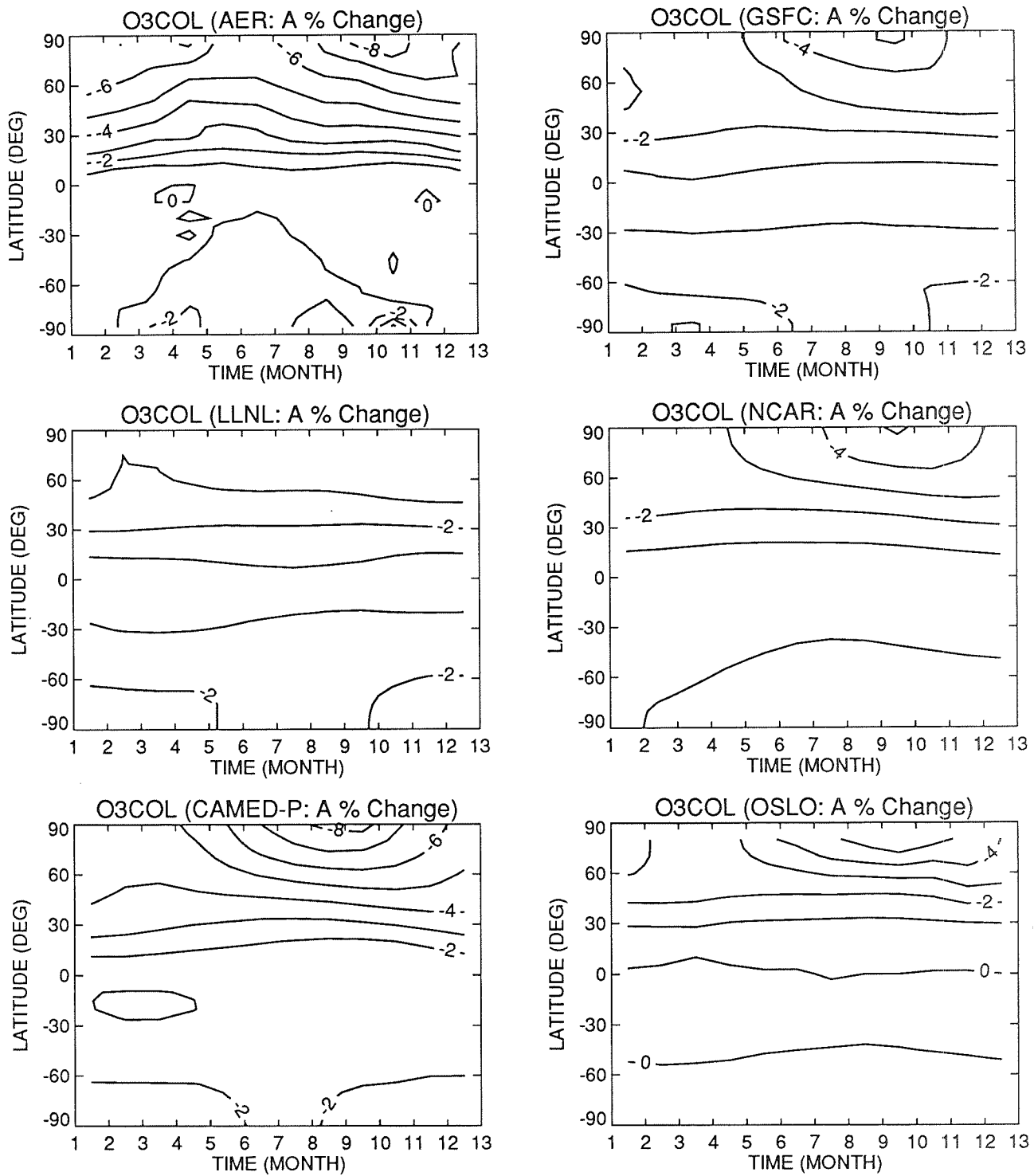


Figure 7(a). Calculated percent changes in the column abundances of O₃ as functions of latitude and season in case A, relative to the baseline (BSE). The contours are 2%, 1%, 0%, -1.0%, to -8.0%, in steps of -1%.

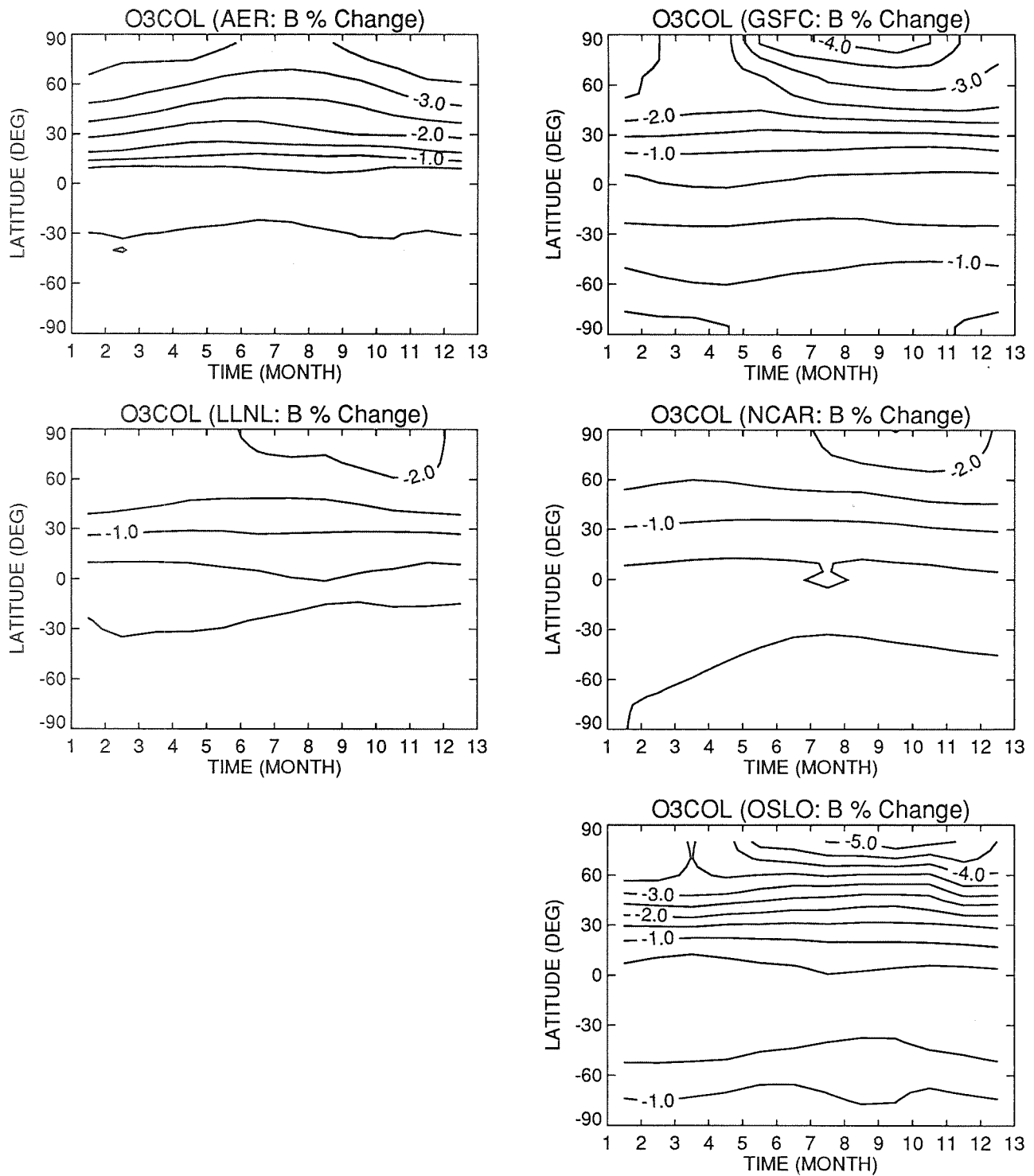


Figure 7(b). Calculated percent changes in the column abundances of O₃ as functions of latitude and season in case B, relative to the baseline (BSE). The contours are -0.5, -1.0, -1.5, -2.0, etc., in steps of 0.5%.

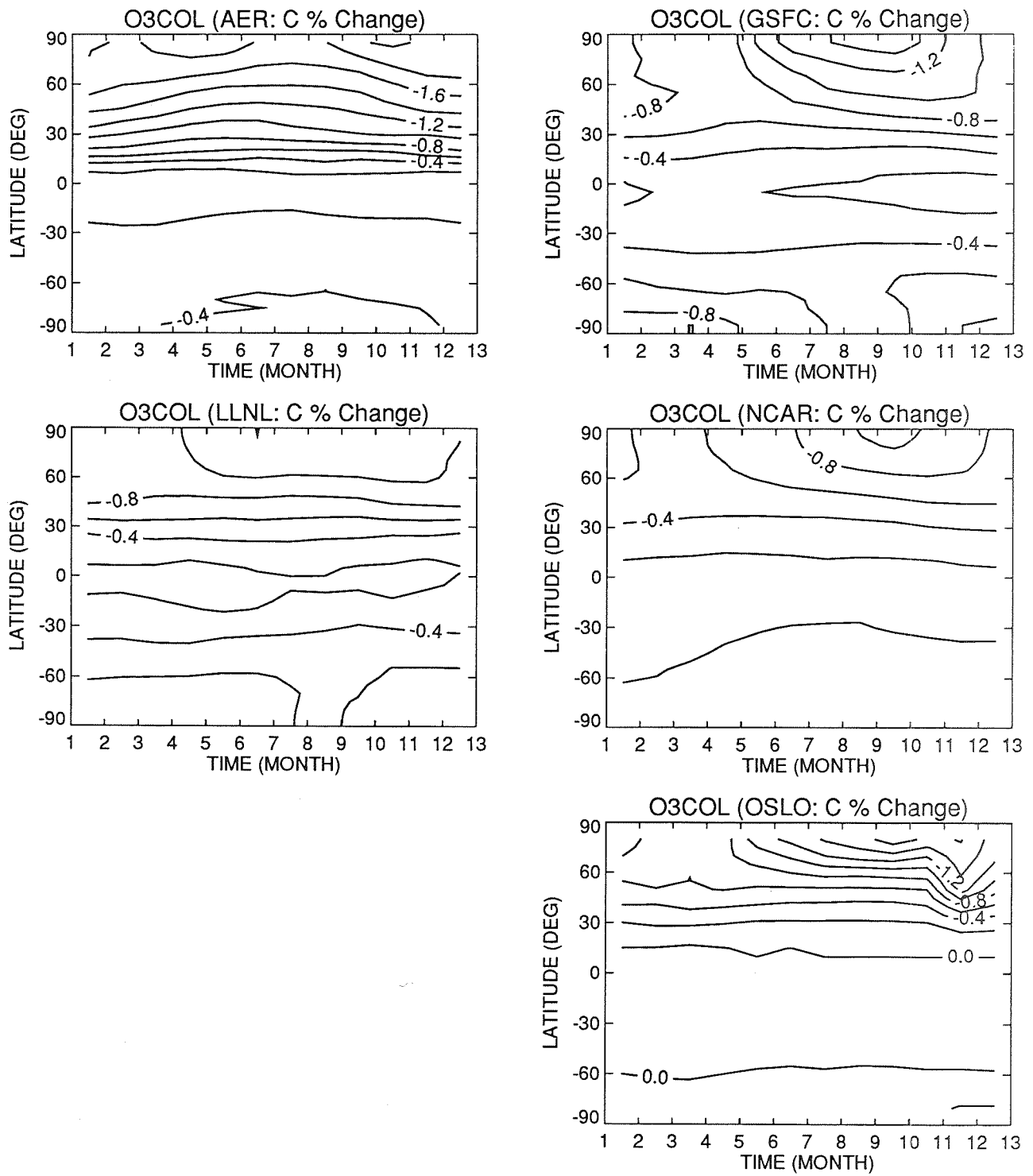


Figure 7(c). Calculated percent changes in the column abundances of O₃ as functions of latitude and season in case C, relative to the baseline (BSE). The contours are 0.0, -0.2, -0.4, etc., in steps of 0.2%.

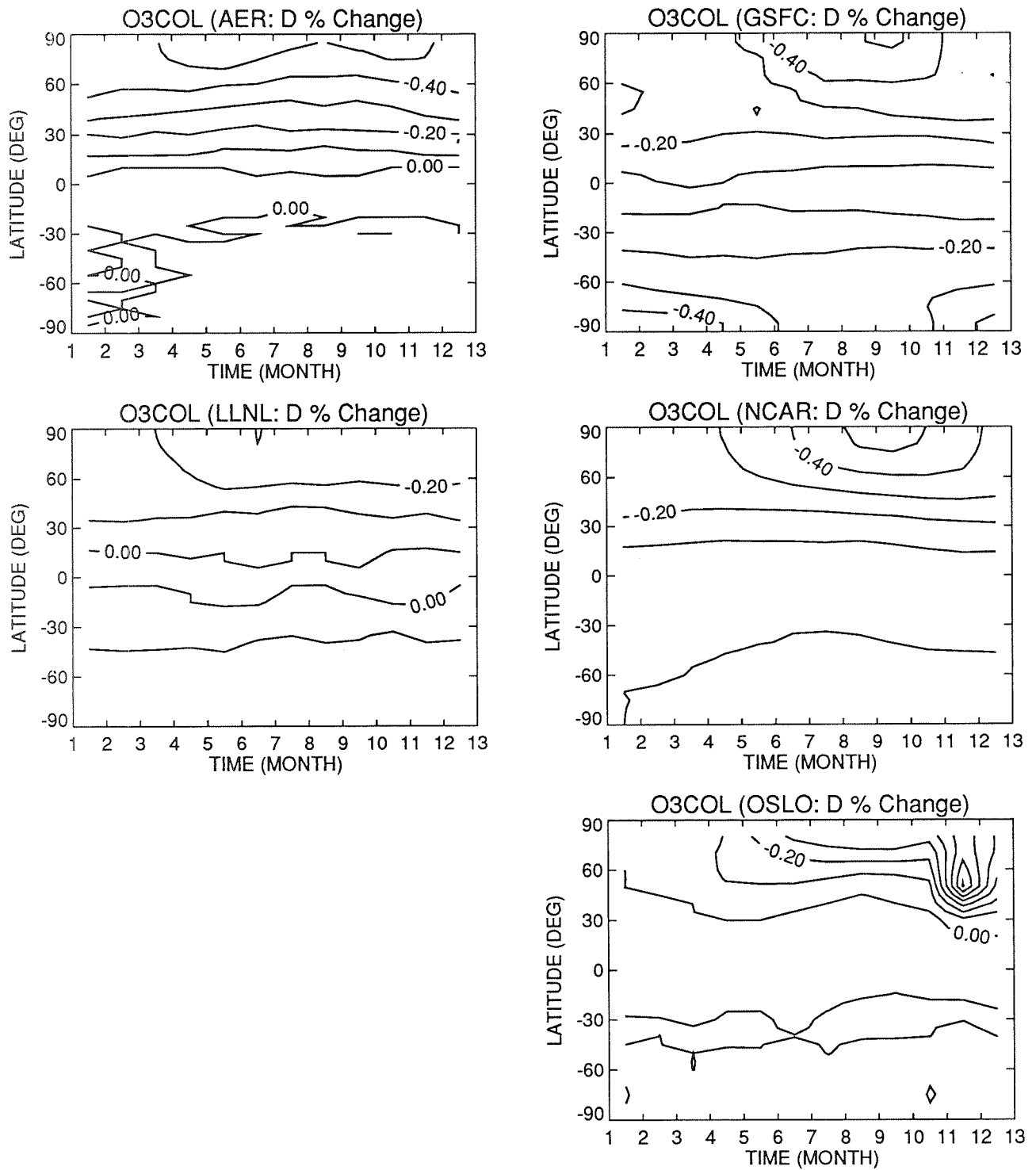


Figure 7(d). Calculated percent changes in the column abundances of O₃ as functions of latitude and season in case D, relative to the baseline (BSE). The contours are 0., -0.1, -0.2, etc., in steps of 0.1%.

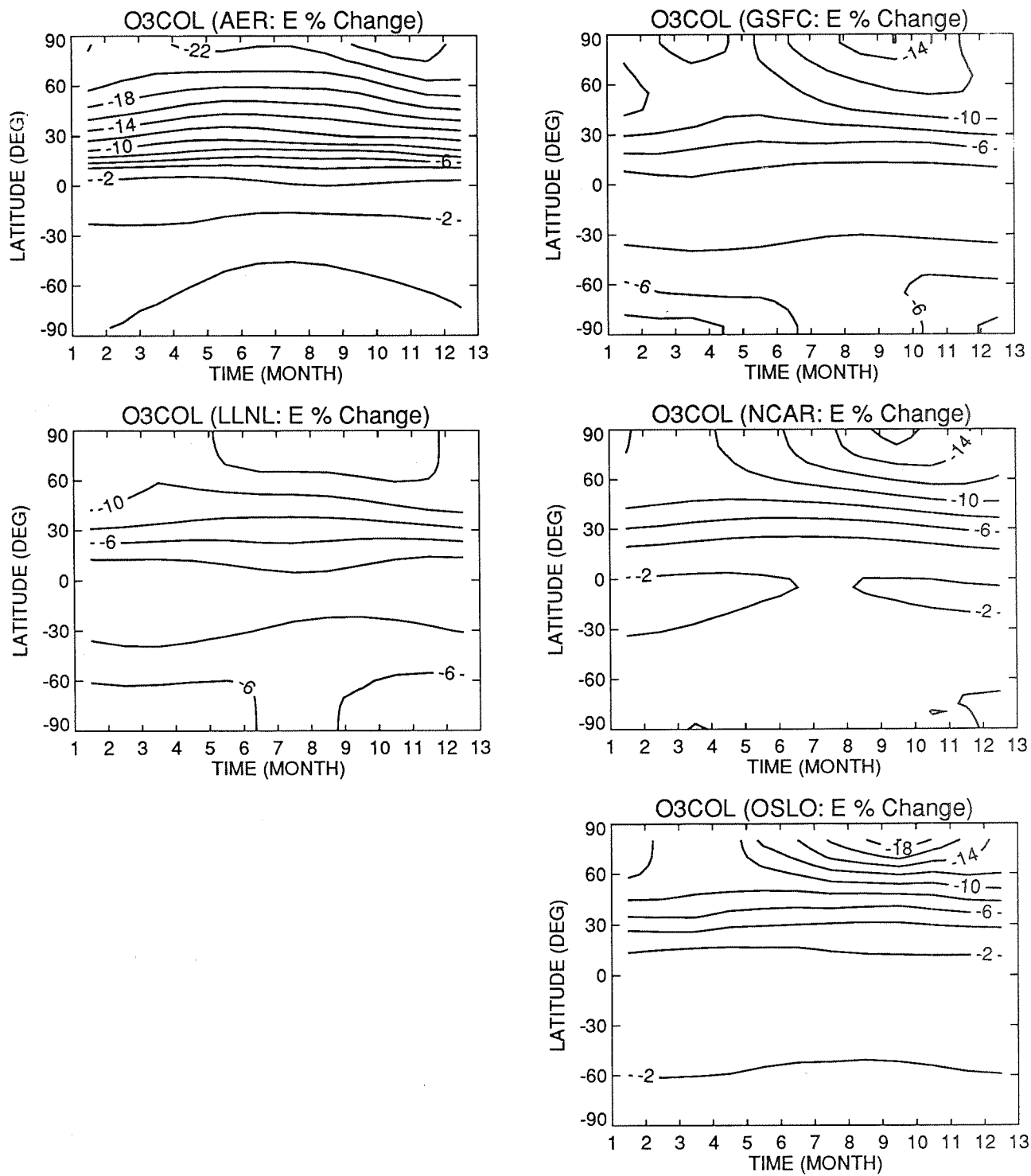


Figure 7(e). Calculated percent changes in the column abundances of O₃ as functions of latitude and season in case E, relative to the baseline (BSE). The contours are -2.0, -4.0, -6.0, etc., in steps of 2.0%.

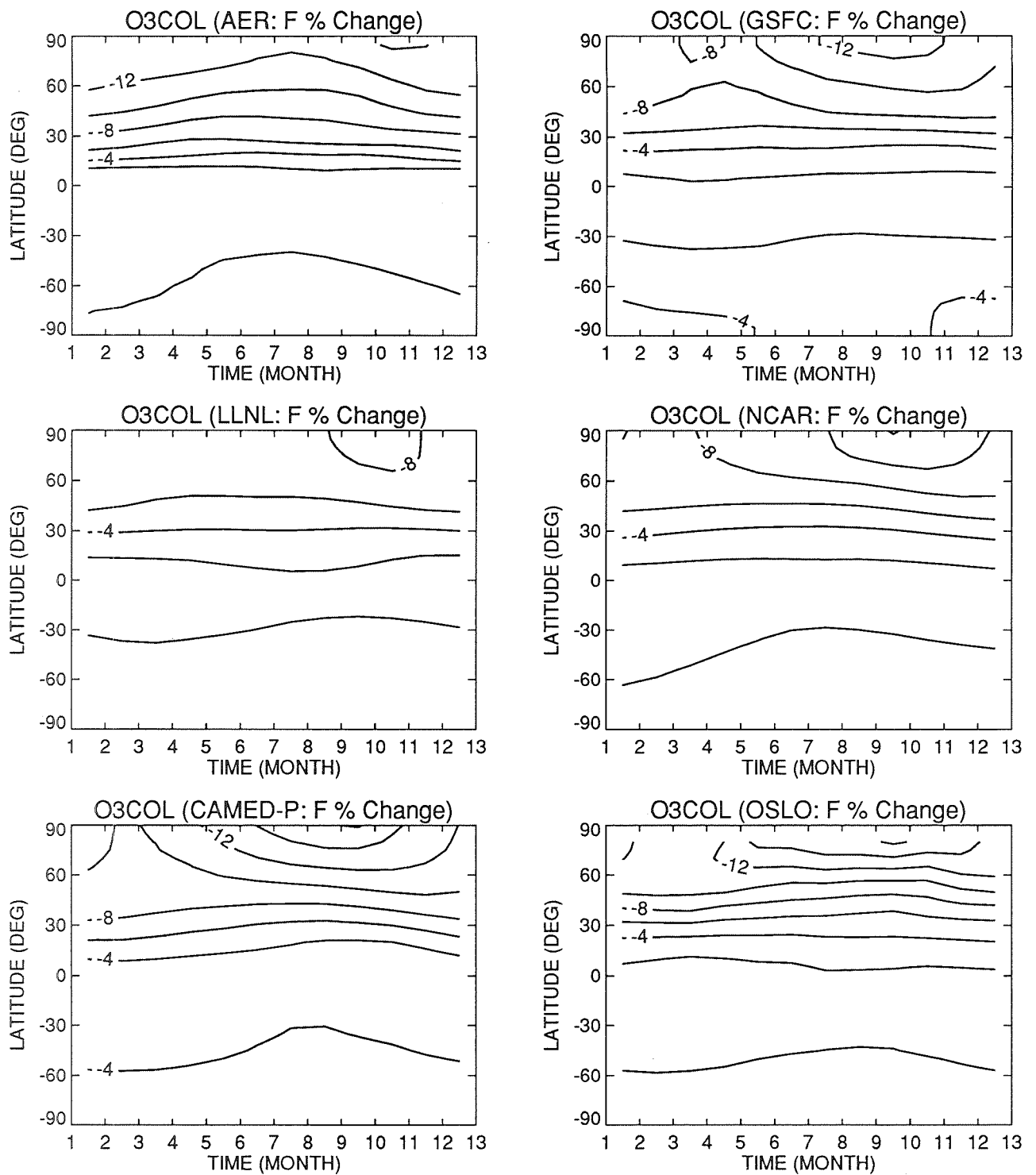


Figure 7(f). Calculated percent changes in the column abundances of O₃ as functions of latitude and season in case F, relative to the baseline (BSE). The contours are +2, 0, -2.0, -4.0, -6.0, etc., in steps of 2.0%.

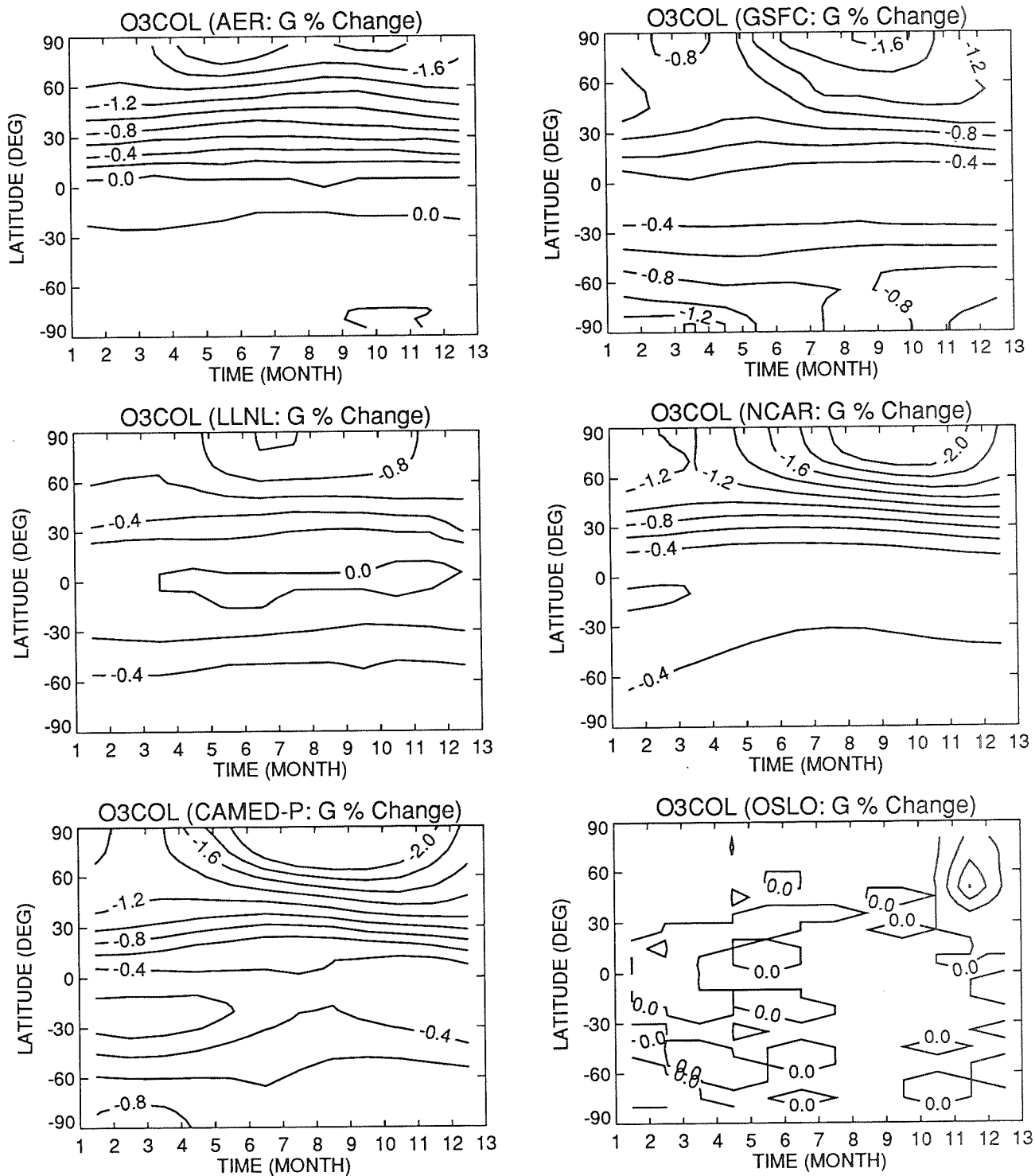


Figure 7(g). Calculated percent changes in the column abundances of O₃ as functions of latitude and season in case G, relative to the baseline (BSE). The contours are 0., -0.2, -0.4, -0.6, etc., in steps of 0.2%.

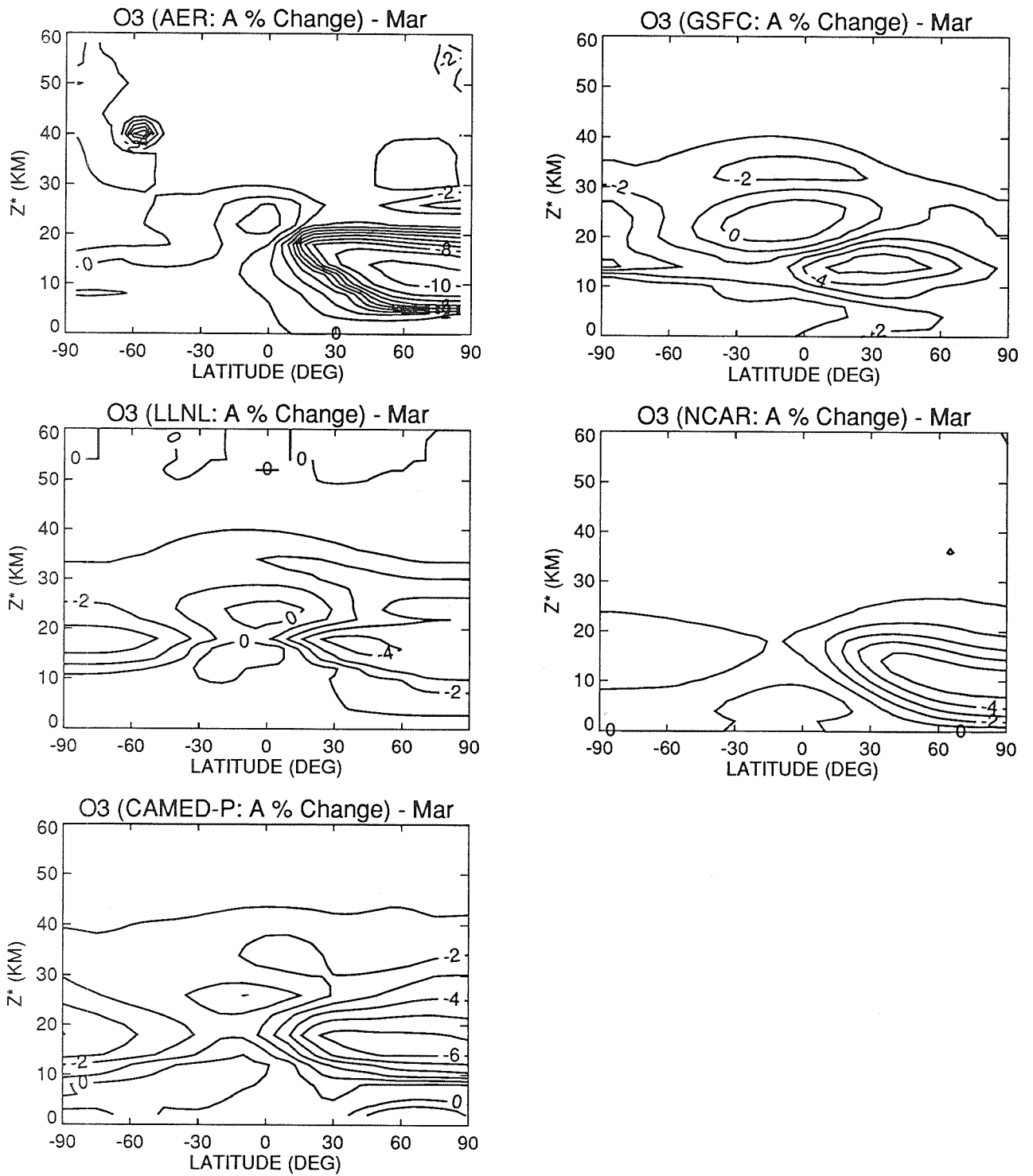


Figure 8(a). Calculated percent changes in the local concentration of O₃ as functions of latitude and height in case A, relative to the baseline (BSE). The contours are +1, 0., -1.0, -2.0, -3.0, etc., in steps of 1.0%.

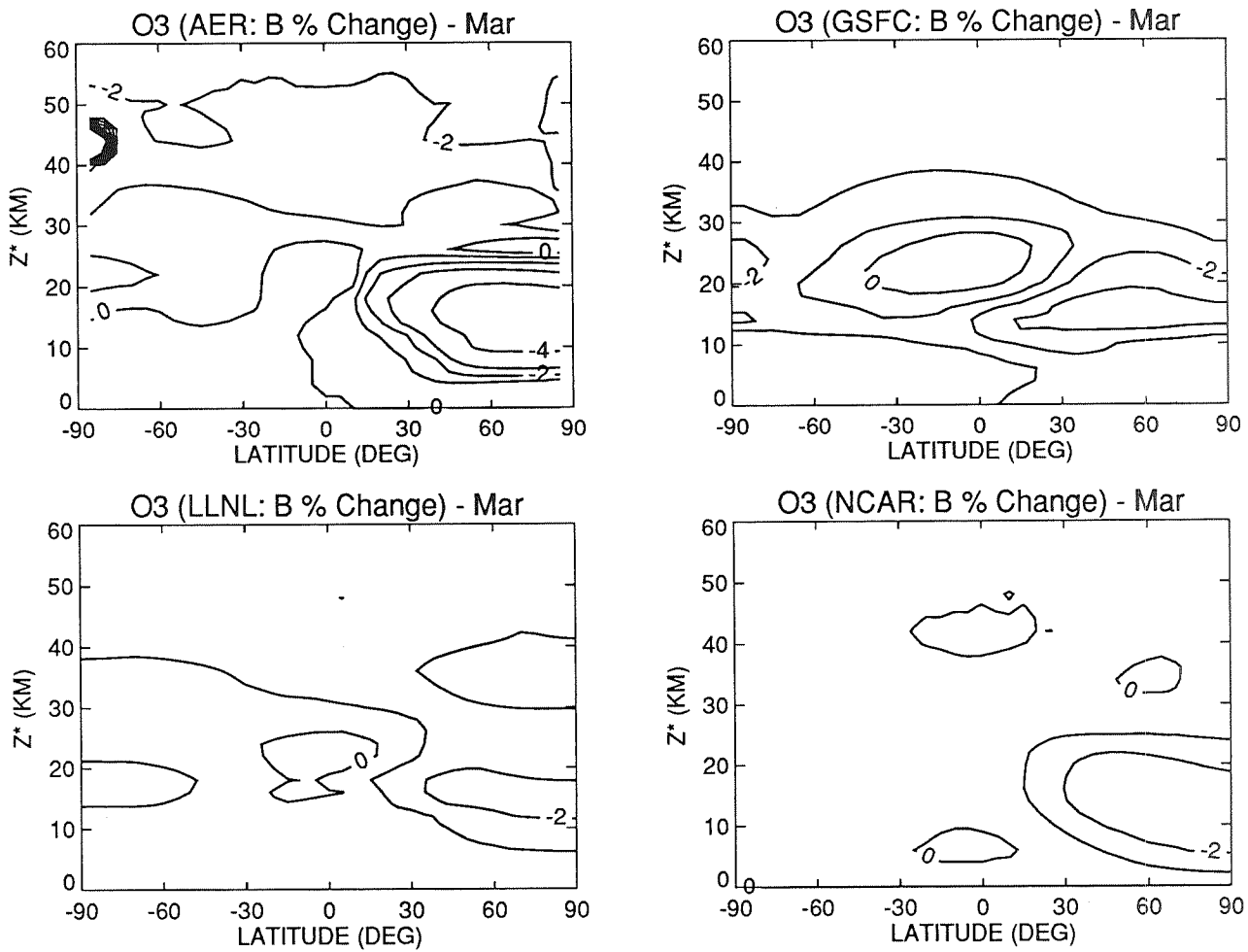


Figure 8(b). Calculated percent changes in the local concentration of O_3 as functions of latitude and height in case B, relative to the baseline (BSE). The contours are +1, 0., -1.0, -2.0, -3.0, etc., in steps of 1.0%.

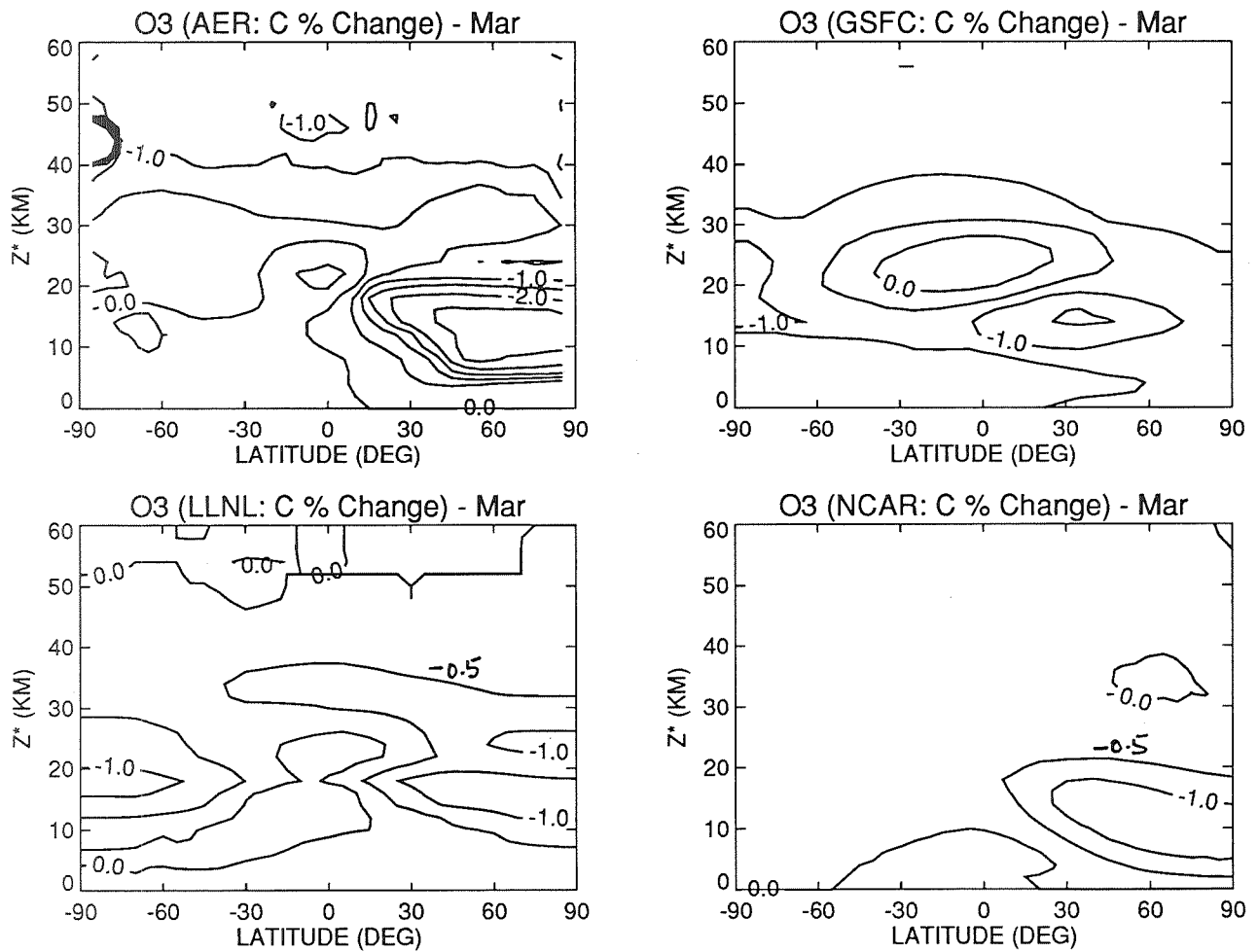


Figure 8(c). Calculated percent changes in the local concentration of O₃ as functions of latitude and height in case C, relative to the baseline (BSE). The contours are 0.5, 0., -0.5, -1.0, -1.5, etc., in steps of 0.5%.

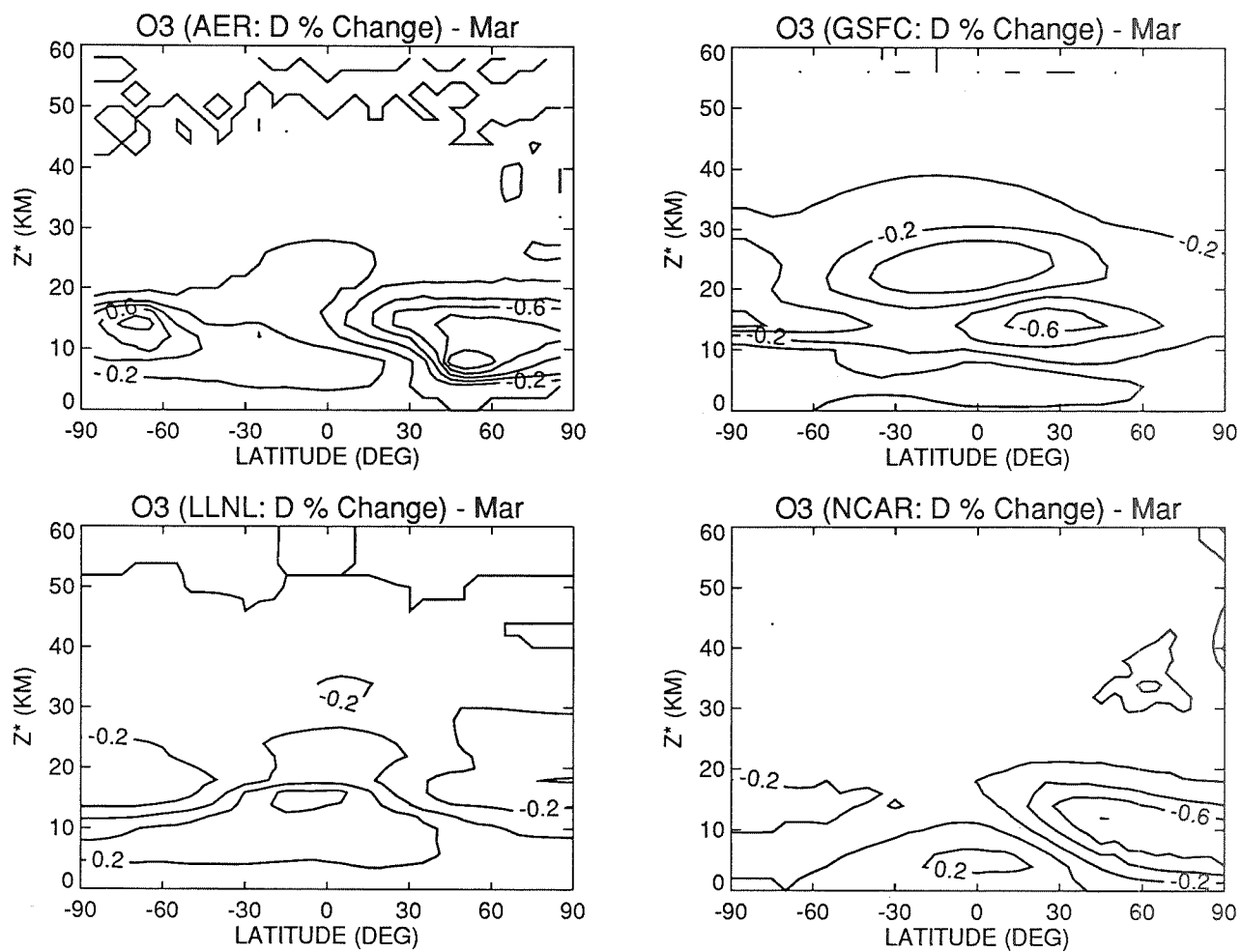


Figure 8(d). Calculated percent changes in the local concentration of O₃ as functions of latitude and height in case D, relative to the baseline (BSE). The contours are +0.8 to -1.0, in steps of 0.2%.

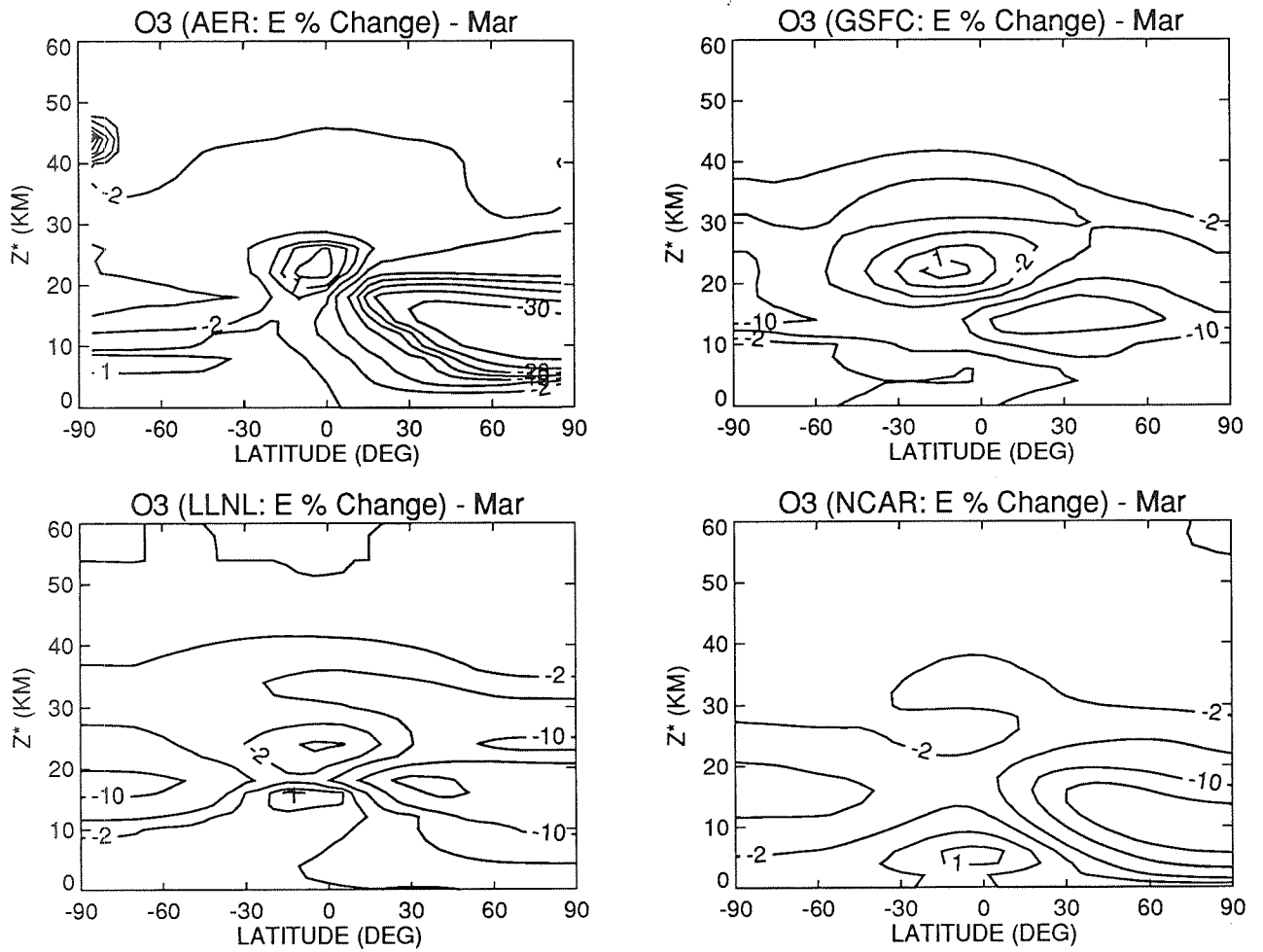


Figure 8(e). Calculated percent changes in the local concentration of O₃ as functions of latitude and height in case E, relative to the baseline (BSE). The contours are +2, +1, 0., -2.0, -5.0, -10, -15, etc., in steps of 5.0%.

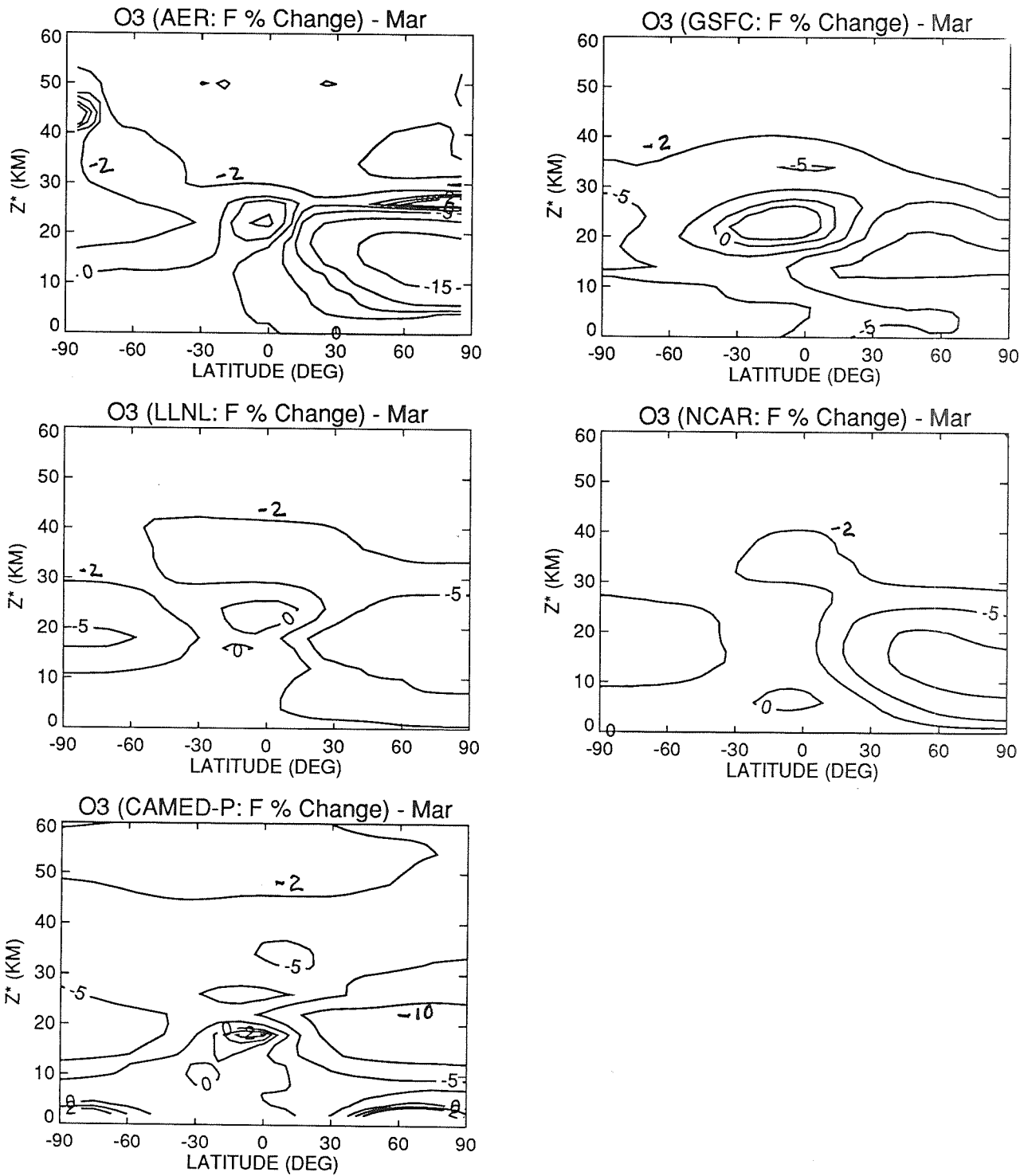


Figure 8(f). Calculated percent changes in the local concentration of O₃ as functions of latitude and height in case F, relative to the baseline (BSE). The contours are +2, +1, 0., -2.0, -5.0, -10, and -15.0%.

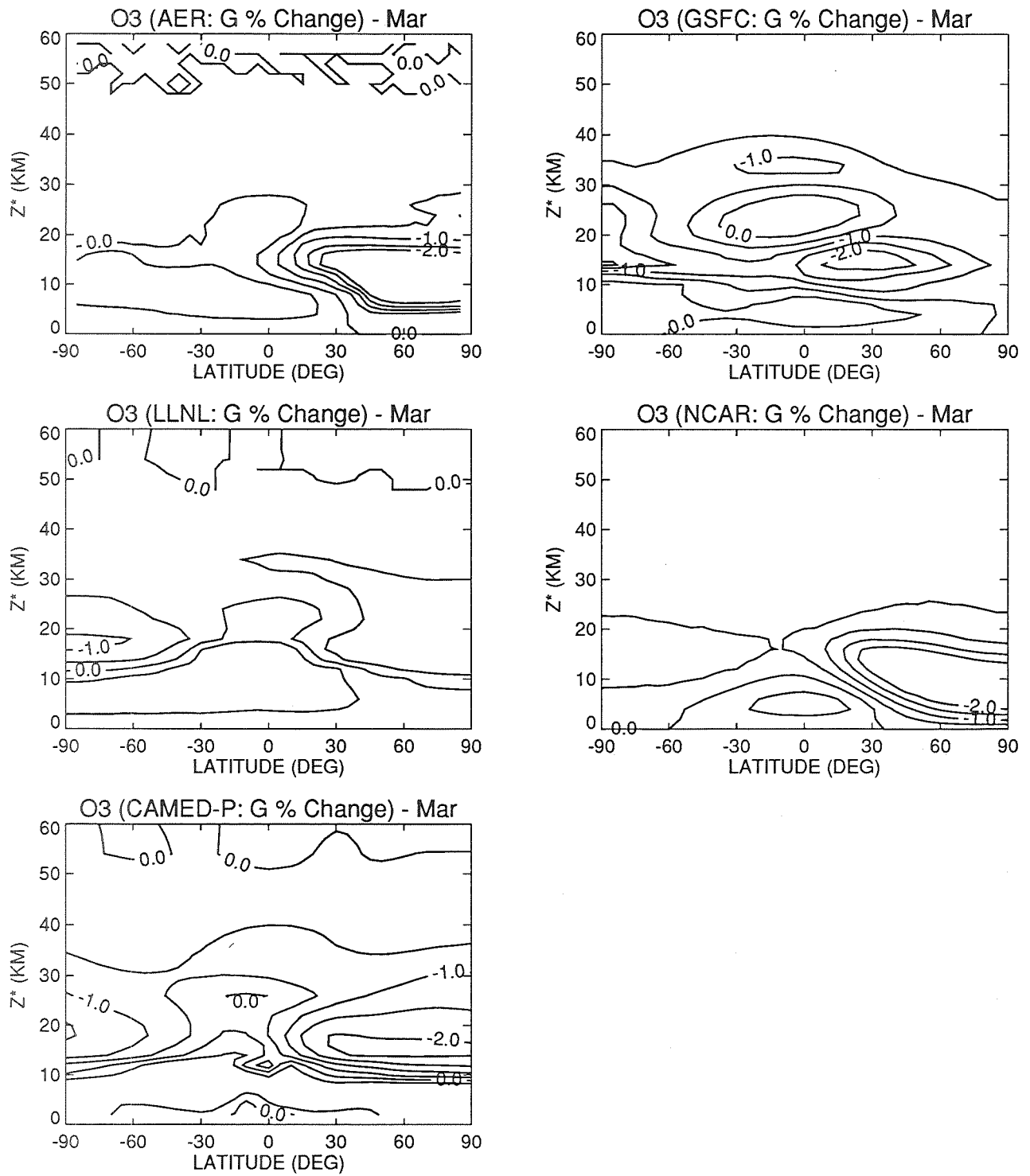


Figure 8(g). Calculated percent changes in the local concentration of O₃ as functions of latitude and height in case G, relative to the baseline (BSE). The contours are +0.5, 0, -1.0, -1.5, and -2.0%.

REFERENCES

1. Boeing Commercial Airplanes, "High-Speed Civil Transport Study, Summary," NASA Contractor Report 4234. Boeing Commercial Airplanes, New Airplane Development, 1989."
2. Douglas Aircraft Company, "Study of High-Speed Civil Transport," NASA Contractor Report 4235. Douglas Aircraft Company, New Commercial Programs, 1989.
3. Johnston, H.S., D.E. Kinnison, and D.J. Wuebbles, Nitrogen oxides from high-altitude aircraft: An update of potential effects on ozone. *J. Geophys. Res.*, 94, 16351-16363, 1989.
4. Ko, M.K., D.K. Weisenstein, N.-D. Sze, R.-L. Shia, J.M. Rodriguez, and C. Heisey, "Effects of Engine Emissions from High Speed-Civil Transport Aircraft: A Two-Dimensional Modeling Study, Part I." Final Report for ST Systems Corporation for period July 1, 1988 through June 30, 1989, 1991.
5. Ko, M.K., D.K. Weisenstein, N.-D. Sze, R.-L. Shia, J.M. Rodriguez, and C. Heisey, "Effects of Engine Emissions from High Speed Civil Transport Aircraft: A Two-Dimensional Modeling Study, Part II." Final Report for ST Systems Corporation for period July 1, 1989 through Dec. 31, 1989, 1991.
6. Johnston, H.S., M.J. Prather, and R.T. Watson, *The Atmospheric Effects of Stratospheric Aircraft: A Topical Review*, NASA Reference Publication 1250, National Aeronautics and Space Administration, Office of Management, Scientific and Technical Information Division, 1991.
7. Douglass, A.R., M.A. Carroll, W.B. DeMore, J.R. Holton, I.S.A. Isaksen, H.S. Johnston, and M.K.W. Ko, *The Atmospheric Effects of Stratospheric Aircraft: A Current Consensus*, NASA Reference Publication 1251 National Aeronautics and Space Administration, Office of Management, Scientific and Technical Information Division, 1991.
8. Jackman, C.H., R.K. Seals, and M.J. Prather, Editors, *Two-Dimensional Intercomparison of Stratospheric Models*, NASA Conference Publication 3042, Proceedings of a workshop sponsored by NASA, Washington, D.C., Upper Atmosphere Theory and Data Analysis Program held in Virginia Beach, VA Sept. 11-16, 1988, 1989.
9. WMO, Scientific Assessment of Stratospheric Ozone: 1989. World Meteorological Organization, Global Ozone Research and Monitoring Project -Report No. 20, 1990.

56-45
64292
821

N92-19127

Chapter 6

Lower Stratospheric Measurement Issues Workshop Report

NJ 920944

Arthur L. Schmeltekopf
National Oceanic and Atmospheric Administration, Retired

INTRODUCTION

The "Lower Stratospheric Measurement Issues" workshop was held at NASA Ames Research Center on 17-19 October 1990. The 3-day workshop was sponsored by the Atmospheric Effects of Stratospheric Aircraft (AESA) component of the High-Speed Research Program (HSRP). Its purpose was to provide a scientific forum for addressing specific issues regarding chemistry and transport in the lower stratosphere, for which measurements are essential to an assessment of the environmental impact of a projected fleet of high-speed civil transports (HSCTs).

The objective of the workshop was to obtain vigorous and critical review of:

- atmospheric measurements needed for the assessment,
- present capability for making those measurements, and
- areas in instrumentation or platform development essential to making the measurements.

This information was obtained from experts in related fields and investigators directly involved in NASA's stratospheric measurement and instrumentation development programs. The final goal of the workshop was to develop recommendations for further study, including measurements, instrumentation, and platforms needed, in support of a focused aircraft campaign to be flown in the 1992-1994 time frame that would address critical elements in the assessment of HSCTs.

WORKSHOP RECOMMENDATIONS

Areas for further study that were stressed most during the workshop include the following:

- *We need critical tests of our understanding of the dynamics of the lower stratosphere.* These tests can best be achieved by obtaining measurements over a climatological range of tracers in the lower stratosphere (minimally: 10 to 25 km, four seasons, and at least five latitudinal locations). For that we can use both the existing data sets and obtain new, more complete data sets particularly for CO₂, CFC11, CFC12, CH₄, and N₂O. Some new instruments will be required.
- *We need critical tests of our understanding of the chemistry of the lower stratosphere.* These tests can best be achieved by obtaining a climatology of as many members of the free radical families (H, N, Cl, and O) as possible. Measurements of chemical species that currently are unmeasured are crucial for these tests. Particularly important are chemical species in the odd hydrogen, reactive nitrogen, and chlorine families.
- *We need critical tests of our understanding of radiation in the lower stratosphere.* These tests are needed to check on photolysis rates as well on the radiation dynamics (scattering). Particular attention must be paid to the possibility that clusters might be playing a role in determining the absorption spectrum (and thus photolysis spectrum) of many molecules under lower stratospheric conditions.
- *We need substantial improvement in our understanding of the character of the aerosols that exist in the lower stratosphere as well as how they might affect the chemistry and radiation there.* It is crucial to know

whether the H₂O from the engine exhaust could increase the production of H₂O-NAT (nitric acid trihydrate) aerosols and thereby dramatically affect the chemistry in the lower stratosphere.

- *We badly need a new aircraft platform that will get us to at least 25 km; and in addition, the new platform must not have the severe safety constraints that are imposed on the ER-2, the current principal aircraft platform.* For the studies indicated above, even if we had the proper measurement instrumentation, we would still lack a platform that can get the instruments to the right place in the lower stratosphere at the right time.
- *We must verify that the measurement techniques used by the engine manufacturers for the emission index (EI) of engines are being made using the same calibration procedures as those used in atmospheric measurements.*
- *We need to do model studies of the aircraft plumes to see whether there are any possible conditions in which plume processing could have a global impact.*

WORKSHOP STRUCTURE

The workshop was organized into seven sessions each of which was keyed to specific issues.

- Known Problems in Lower Stratospheric Chemistry
- Known Problems in Lower Stratospheric Transport
- What Platforms Do We Have or Can We Get
- Present Measurement Capabilities
- New Measurement Techniques
- What Do We Know about Engine Exhaust
- What Is Our Plan of Action

Each session included opening remarks from its chairman, presentations or tutorials given by invited experts, and a panel discussion. Questions were posed to panel members in advance of the workshop to stimulate critical examination of each session's subject matter. The names of contributors and the topics they addressed, as well as the major questions asked of panel members, are given in the workshop agenda in the Appendix at the end of this chapter.

SYNOPSIS OF SESSIONS

Session chairmen provided a written summary of their sessions; each synopsis that follows is drawn from those summations.

SESSION 1. KNOWN PROBLEMS IN LOWER STRATOSPHERIC CHEMISTRY

Chairman

Dr. Carleton J. Howard, Aeronomy Lab, National Oceanic and Atmospheric Administration

Questions/Issues

- What critical laboratory measurements are needed?
- What critical atmospheric measurements are needed?
- Can in situ measurements help us to determine rates directly?

Synopsis

Since it is difficult to discuss in narrative form, the various ways that our understanding of the chemistry of the lower stratosphere needs to be amplified, the following section simply states and lists what is needed. For the reactions listed, the new information required is indicated in the preceding text or in comments given after the reaction. All of these measurements should be done under ambient conditions of the lower stratosphere; that is, with the temperature down to 190 K, pressure between 15 and 300 mb, and ambient mixing ratios of N₂, O₂, H₂O, etc.

Homogeneous Chemistry

Improved laboratory data are required for the following reactions under lower stratospheric conditions:

- O(¹D) + N₂O (NO product yield)
- NO₂ + NO₃ => N₂O₅
- O + NO₂
- HO₂ + NO₂ + M
- OH + HO₂NO₂ (including product yield)
- HO₂ + OH
- HO₂ + O₃
- HO₂ + NO

If HSCT engines introduce significant amounts of hydrocarbon material, then the oxidation reactions of hydrocarbon exhaust products (See item 5, paragraph 2 below) need to be measured.

Improved photolysis rates under lower stratospheric ambient conditions are needed for the following species:

- O₂ In situ measurement, preferred, including O[³P] product
- NO₂
- NO₃ Including products and quantum yields
- N₂O₅ Including products and quantum yields
- HNO₃ Including products and quantum yields
- HO₂NO₂ Including products and quantum yields
- Organic nitrates Including peroxyacetyl nitrate (PAN)
(See item 5, paragraph 2)

Heterogeneous Chemistry

We need more information about the shape, size, and bulk composition of stratospheric particles, as well as the composition and morphology of the surfaces of stratospheric particles. How much and what kind of surfaces are available?

Laboratory measurements of reactions, processes, and surface accommodation efficiencies should be made using surfaces and gaseous concentrations characteristic of the atmosphere. The possibility that reactivity on surfaces is dependent upon the microstructure (the amount of roughness and the presence of cracks and fissures) should be investigated.

Phase diagrams, thermodynamics parameters, and kinetics parameters, such as growth and desorption rates, are needed for the types of particles that exist in the stratosphere.

Studies should be made of the particles emitted by HSCT aircraft, notably soot and metal oxide particles, to determine their potential roles as reaction sites and condensation nuclei in the stratosphere. Studies should be made of the affects on the photolysis rates for molecules (particularly HNO_3) tied up on particulates. What can we say about photolysis of NAT particulates?

Chemical Modeling

Modeling studies should be made to determine the kinetics and photochemical parameters that contribute the greatest uncertainties to the evaluation of HSCT environmental effects.

Model studies should be made to assess possible effects of heterogeneous processes in the stratosphere. Can HSCT emissions cause surface chemistry to play a role at lower latitudes or over longer seasons? The possible effects on halogen chemistry should be included in the evaluation.

Plume Modeling

The role of the aircraft wake vortices in entrainment and transport of exhaust material should be assessed. How much plume material is dispersed into the stratosphere? The possibility of significant chemical processes occurring in the exhaust plume should be assessed. For example, is the NO_x emission conversion to HNO_3 enhanced in the plume?

Miscellaneous Topics

High-quality quantum mechanical studies should be made of selected critical reactions whose rate coefficients, temperature, and pressure behavior are poorly understood, for example, $\text{HO}_2 + \text{OH}$ and $\text{HO}_2 + \text{O}_3$. Similar studies of reactions that occur on or in particles, such as $\text{HCl} + \text{ClONO}_2 \Rightarrow \text{Cl}_2 + \text{HNO}_3$, would be very valuable.

Accurate data are needed on the emissions from proposed HSCT aircraft engines operating at ambient conditions. Nitrogen oxide, hydrocarbon, water vapor, and particle emissions are the most important factors.

Stratospheric perturbations resulting from the current subsonic aircraft fleet should be evaluated. Possible effects from both nitrogen oxide and sulfur oxide emissions should be improved. The amount of NO_x contributed to the stratosphere by lightning should be assessed as well.

SESSION 2. KNOWN PROBLEMS IN LOWER STRATOSPHERIC TRANSPORT

Chairman

Dr. James R. Holton, Department of Atmospheric Science, University of Washington

Questions/Issues

- Will SST exhaust really mix upward?
- Can the high-resolution structure of the transport be important?
- Can exotic tracer experiments be useful?

Synopsis

The discussion of constituent transport can be divided into three categories: (1) the climatology of global transport, particularly as it influences the global distribution of pollutants emitted by aircraft; (2) mechanisms of transport in the lower stratosphere, particularly in regard to stratosphere-troposphere exchange rates at all latitudes and horizontal transport rates in the polar regions; and (3) behavior of aircraft plumes from the wake vortex breakup stage to large-scale dispersion. Issues in each of these categories are discussed next.

Global Transport Issues

The climatology of NO_x is important in evaluating "traditional" aircraft-related ozone depletion concerns (i.e., homogeneous NO_x chemistry). NO_x enhancements above an altitude of ~15 km are expected to deplete ozone, while below that altitude, smog chemistry is expected to produce ozone (neglecting possible complications of heterogeneous reactions; see Figure 1). The major transport issue for this piece of the total problem is to determine the climatology (i.e., the latitude and height distribution and the seasonal variability) of the steady-state perturbation to the "natural" NO_x distribution resulting from emissions from a fleet of HSCTs. There is general agreement that the magnitude of this effect, and its influence on the ozone layer, will be strongly dependent on the altitude at which the HSCTs fly. But, whether there is a "safe" altitude will depend (among other things) on the fate of the emissions introduced into flight corridors. There are important questions concerning the extent to which emissions occurring at a given flight altitude might disperse to higher altitudes, where the ozone depletion potential is greater. If there is rapid quasi-isentropic dispersion from the Atlantic and Pacific flight corridors into the tropics, then emissions would enter the tropical upwelling region and be advected to higher altitudes. A direct observational proof that molecules emitted in the proposed flight corridors will penetrate to any given altitude and latitude would apparently require continuous emission of an exotic tracer into a flight corridor and its concentration measured at a wide range of latitudes and heights for a year or more. The workshop participants, by and large, agreed that there was no practical method to accomplish such a direct test of large-scale plume dispersion. Thus, the only viable way to predict the likely global perturbation of the NO_x distribution by a fleet of HSCTs is by using models that are testing by a wide variety of observations.

Although not all agree, the consensus view is that this type of tracer dispersion study cannot be done in the framework of two-dimensional (2-D) modeling. Eddy mixing by planetary wavebreaking and synoptic scale motions differs considerably from eddy diffusion. There is a strong up-down asymmetry in large-scale mixing processes that cannot be modeled in terms of eddy diffusion. For example, 2-D models seem incapable of simulating the transport into the troposphere that is associated with tropopause fold events.

Studies of global tracer transport must be based on three-dimensional General Circulation Models (GCMs). The basic requirement for such models is that they explicitly resolve the scales that are important for global transport so that parameterization effects are minimized. This implies high vertical resolution (1 km or better, perhaps as low as a few hundred meters) near the tropopause, and sufficient horizontal resolution (a few hundred kilometers at most, and perhaps as few as 10 km) to accurately represent the important scales of eddy variability in the lower stratosphere. Model validation should utilize all available data sources. These include global satellite data (particularly Upper Atmosphere Research Satellite [UARS] trace constituent data), balloons, ground-based remote sensing, and aircraft data. Model validation should also utilize ^{14}C and other radionuclide data from the nuclear weapons testing era. If a model that is calibrated on the basis of one set of tracer data can simulate the global distribution and seasonal variability of all other independent tracers, it may be a credible tool for evaluating the global distribution of pollutants emitted by a fleet of HSCTs. Such a model could then be used to improve the eddy diffusion parameterizations in the 2-D models that will be required for assessment studies.

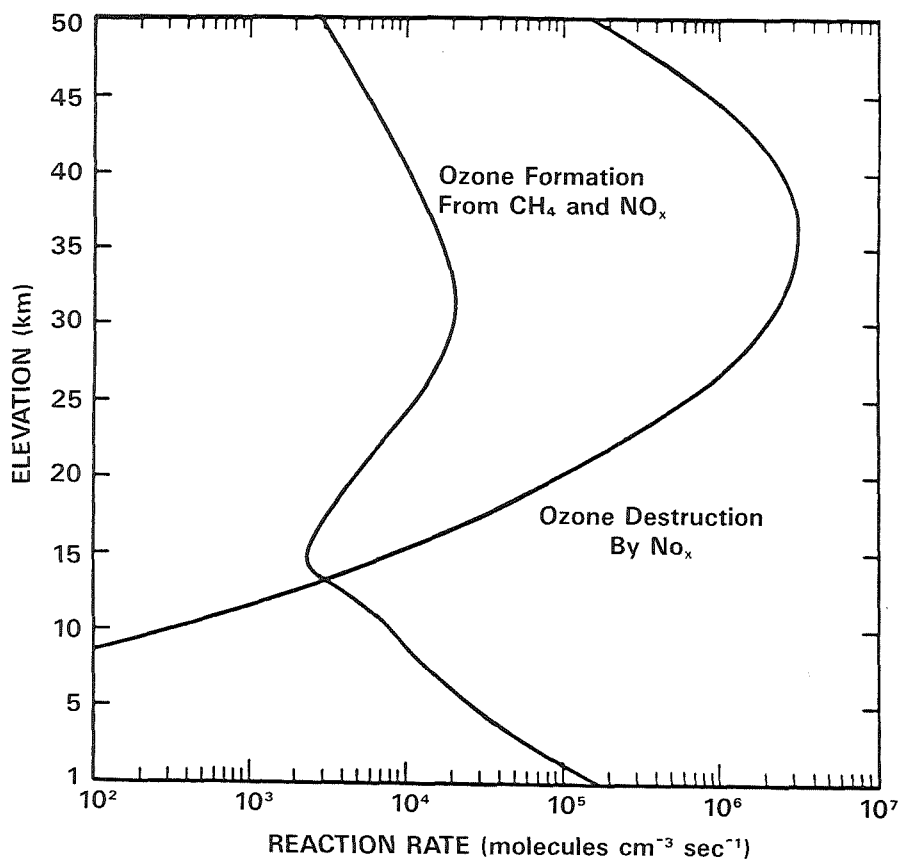


Figure 1. Ozone formation from the smog reactions based on methane and nitrogen oxides (45° latitude, spring).

Transport Problems Related to Heterogeneous Ozone Depletion

Heterogeneous chemical processes are among the most challenging of the problems facing the HSRP. Aircraft engines are not only sources of NO_x but of water vapor, particulates, SO_2 , and perhaps other trace gases as well. Perturbations in these constituents may affect, and be affected by, polar stratospheric clouds (PSCs). Modeling studies at GSFC show, for example, that for the Seattle-London polar flight route an HSCT would fly within the winter polar vortex quite regularly (although this route would be over land, and therefore, might not be allowed at supersonic). If patches of air with elevated levels of water vapor, particulates, and other emissions remain coherent for sufficiently long periods and encounter sufficiently low temperatures, heterogeneous processes leading to ozone depletion might be activated. This possibility must be explored not only for the polar regions, but also near the tropical tropopause, which is also a very cold region that would be affected by any HSCT flights to the southern hemisphere. Investigations of this class of problems cannot be done with UARS or other planned satellite data. UARS trace constituent data will have poor coverage below 20 km, and poleward of 78° latitude. The data also will suffer degradation if there are clouds in the field of view. High vertical and horizontal spatial sampling is needed in the 15-25 km altitude range at a wide number of latitudes to evaluate the potential for heterogeneous processes. Emissions of water vapor by an HSCT fleet may prove to be just as significant as NO_x emissions, and data are needed to define the current water vapor climatology as well as to estimate HSCT impacts. The objective must be more than just process studies of PSCs; changes resulting from emissions of water vapor and aerosols should be assessed as well. Aircraft and balloon observations at a number of latitudes and seasons are required.

Small-Scale Dispersion of Engine Emissions

Dispersion from the wake vortex breakup stage (scale of hundreds of meters) to the large scale (hundreds of kilometers) is not well understood. Deformation by vertical shear of the horizontal winds appears to be the most important process for dispersion on these scales. It is likely that vertical dispersion will be much slower than horizontal dispersion because of the influence of vertical shear. Since the mean winds have a strong seasonal dependence, the rate of dispersion from mean wind shear may also have a strong seasonal dependence. This range of scales is too small to be explicitly resolved in global 3-D models, and so must be parameterized. Thus, more information on dispersion from the small scale to the GCM resolved scales would be highly valuable as an aid to improving tracer simulations based on 3-D models. Direct observations of the plume dispersion in this scale range would clearly be very difficult. Exotic tracers might be useful for this scale, but no specific experimental strategy was agreed on in the workshop.

SESSION 3. WHAT PLATFORMS DO WE HAVE OR CAN WE GET?

Chairman

Dr. Art Schmeltekopf, National Oceanic and Atmospheric Administration, Retired

Questions/Issues

- Do any of these platforms get us far enough?
- High enough?
- Long enough (duration)?

- When can the platforms be ready?

Synopsis

Four types of platforms are available to the HSRP for making the measurements needed to demonstrate our understanding of the atmosphere: 1) satellite, 2) balloon, 3) aircraft, and 4) ground based. The science problems faced by the HSRP are mostly in the 12 to 25 km range and require that measurements be made in many locations around the globe, in all seasons. These measurements are required to be made with high spatial resolution. They need to be made in all types of weather conditions: cloudy, in and out of jet streams, in the polar night, etc. Because the satellite and ground-based platforms are long path and require good visibility, they cannot yield all of the information needed. Balloons are very hard to position accurately, so it would be unlikely that measurement at an exact location in a jet stream could be made, at least on a routine basis. However, the high-resolution vertical soundings that can be made by balloon will provide useful data when available. It is clear that the measurements made by UARS will provide a very important part of the global climatology for many of the species of interest; however, most of the measurements cannot be made low enough, in the dark, or in or below the cloud decks. Ground-based high-resolution lidar and other instruments will provide a very good check on the satellite and aircraft measurements, but they cannot be made in every location and are not possible under cloudy conditions.

It is therefore clear that at least some of the measurements critical to the HSRP mission must be made from an aircraft platform. There are five aircraft platforms available now or proposed for the near future. They are: ER-2, Condor, Perseus, Theseus, and the High-Altitude Aircraft Research Program (HAARP). In addition there are two supersonic platforms that could be used: SR-71 and the Concorde.

The idea of using a supersonic platform was suggested; the obvious problem—Mach heating in the sampling process—was given as the reason that supersonic platforms are not being considered for use by the HSRP. Two ideas were presented to avoid the Mach heating, but both involved cooling the stream through interaction with a cool wall. The effect of the wall on the reactive species that are to be measured was considered prohibitive. In addition, no proposed method would allow the faithful sampling of aerosols from a supersonic platform. The Concorde representatives offered the possibility of using the Concorde as a sampling platform, and that may be feasible for the stable species.

For the reasons stated previously, the most desirable platform for the HSRP is the subsonic aircraft platform, and so the major discussions in the platform session focused on them. The major comparisons to be made about our choices for the subsonic aircraft platform are in Table 1.

ER-2 Platform

The ER-2 needs no discussion since it has been the workhorse used for measurements in the lower stratosphere for many years. For this program has four major limitations: 1) a maximum altitude of ≈ 20 km, at least 5 km below our needs; 2) a range of 5400 km, which will not allow us to get to many important areas from usable airports; 3) since it has a single engine and a pilot, safety requirements place too many restrictions on where and when it can be flown; and 4) it does not operate well below 16 km, and so is not suitable for making many measurements below that altitude (obviously it passes through the altitudes below 16 km on takeoff and landing) and therefore it cannot meet the full requirements of HSRP mission. Although several improvements, are planned for the aircraft, important for its present community of users, they will not substantially affect the limitations stated above.

Table 1. Comparison of Subsonic Aircraft Platforms

	ER-2	Condor	HAARP Gasoline	Perseus Gasoline	Perseus Hydrogen	Theseus
Max Cruise Altitude (km)	21.4	21.4	30.0	28.0	30.0	30.0
Min Cruise Altitude (km)	16.0	0.0	<2.0	0.0	0.0	0.0
Total Mission Duration (hr)	8/15*	71.65	13.0	5.1	4.5	7.9
Total Distance Covered (km)	6036	24,298	9824	1201	1131	3036
Total Time Above 20 km (hr)	6/13*	70	10.83	0.94	0.34	6.28
Payload Weight (kg)	1155	816	1155	50	50	300
Payload Power (kw)						
@ 28VDC	3-4	12	30	0.2	0.2	As needed
@ 115VAC	10	Inverters	Inverters	As needed	As needed	
Min Operating Temp. (K)	<181	<189 <166 Mod	<ER-2	190	150	150
Day-Night OK	Yes Except Polar	Yes	Yes	Yes Unmanned	Yes	Yes
Takeoff-Landing						
Crosswind	<15Kts	<13Kts	<15Kts	<25Kts	<25Kts	<25Kts
Launch Method	Self	Self	Towed	Winched	Winched	Self
Runway Length	No Ice	8000ft	2000ft	Short	Short	4000ft
Runway Surface	Hard	Hard	Any	Any	Any	Hard
Weather	IFR	No ice	Mod turb	VFR	VFR	IFR
When Operating						
After Funds	Now	12-18mo	3+yr	<1yr?	≈1yr?	≈3yr?
Funds Needed to Complete Devel(\$)	<1M	>10M	≈21M	≈2M	>2.5M	≈10M
Cost/copy(\$)	Air Force	>10M	≈10M	≈750K	≈750K	≈2.5M

* Pilot on board/remotely piloted.

NOTES: The ER-2 is powered by a turbojet, while the others are propeller driven. The ER-2 cruise Mach number does not vary with altitude, but for the others it (and airspeed) varies with the cruise altitude. Fuel consumption is a function of altitude so that endurance and range are strong functions of altitude and weaker functions of payload weight. The distance that can be covered is a weaker function of payload weight and altitude. Since the propeller-driven aircraft have a much lower air speed (a very strong function of altitude), the atmospheric winds have a larger influence on the distance traveled than it does on the ER-2. The ER-2 is a manned aircraft, the others are unmanned. The HAARP will be built for either manned or unmanned flight: manned for testing and unmanned for long missions. The Condor is a twin-engine aircraft, the others are single engine. The HAARP is towed off the ground by a Twin Otter or equivalent. "Any" runway surface means paved, grass, dirt, snow, or ice.

Condor Platform

The Condor was designed as a station-keeping, high-altitude platform. Since it is an unmanned, long-duration, twin-engined aircraft, three of the problems associated with the ER-2 are overcome. Its only disadvantage is that its maximum altitude is essentially the same as that of the ER-2. The aircraft has had several successful test flights; however, it is not mission-ready and will need further development before it is useful for HSRP.

Perseus Platform

The Perseus is a highly specialized aircraft. It is expected to be able to take small, light experiments to near 30 km. It now (November 1990) exists as an untested airframe with an as yet untested engine. There seems little doubt that the concept behind it is sound and that the aircraft is likely to perform as expected, but currently it now has several weaknesses. It can remain at altitude for only very short periods and has limited range. On the other hand, it can be launched from almost any solid surface and can thus be taken to most places of interest and launched there. Another weakness is the fact that its payload-carrying capacity of about 50 kg (analogous to a jeep) is so low that it is difficult to get many experiments on board for simultaneous measurements. The proponents of this aircraft expect that the cost per copy of the aircraft is so low that several could be flown at once for simultaneous measurements.

Theseus Platform

The Theseus design concept is expected to overcome several of the problems associated with Perseus. It is expected to carry a heavier payload (analogous to a van) and fly much farther. As now proposed, however, it could not be launched from just any solid surface, but would require a runway.

HAARP Platform

The HAARP is a design concept developed at the request of the NASA Ames Research Center to meet the specifications determined at a workshop held in Truckee, CA, July 15-16, 1989. This aircraft is designed to overcome all of the weaknesses that are evident, in some way, in all of the other aircraft. Thus the aircraft resembles a truck because of its payload capability. It is fairly expensive and it will take several years before it reaches the operational stage (maybe too long to be of interest to the HSRP). It clearly would be a very useful platform to all of the atmospheric science community.

Conclusion

The real difficulty with the platforms described previously is that the atmospheric science community has no way of generating financial support for all of them. The community will thus have to formulate a consensus view and support at most one or two of these platforms. We have the ER-2, so it is clearly a player for the foreseeable future. The Condor does not get high enough to fulfill all of the needs of HSRP. Since the ER-2 can do much of what the Condor does, the Condor cannot be the aircraft of choice. The clear long-term choice is an aircraft that will follow the HAARP's design, but this aircraft cannot be ready for several years and this program needs results before then. It seems clear that the Perseus is the only new platform that has a chance of getting the measurements needed above 20 km in the time frame allotted for the HSRP.

There have been strong advocates for the three new platform designs: Condor, Perseus/Theseus, and HAARP. During the HSRP workshop at ARC those groups got together

to form a loose team and try to help one another as much as possible. Having realized that Perseus is a very viable platform that could solve not only some of our atmospheric measurement issues but also test the models used for calculating the wing, propeller, and engine cooling designs (major areas of concern for the design of Theseus and HAARP), these advocates have now agreed to assist one another in any practical way, sharing information, etc.

SESSION 4. PRESENT MEASUREMENT CAPABILITIES

Chairman

Dr. James G. Anderson, Engineering Sciences Laboratory, Harvard University

Questions/Issues

- Are all of our present capabilities accurate enough?
- Specific enough?
- Fast enough?
- Do we currently have the "Right Stuff?"

Synopsis

Instrumentation available for the HSRP comes from a lineage of balloon and aircraft-borne developments encompassing the past 10 or more years. In Tables 2, 3, and 4 plus the sections that follow, we review the current state of instrument technology with the following constraints:

- The HSRP program needs place maximum emphasis on the dynamics, radiation, and chemistry in the 10 to 30 km region. Thus, any instrumentation for this program must have good spatial and temporal resolution with signal-to-noise ratios of 10 or greater throughout the altitude interval.
- There is an ongoing Upper Atmosphere Research Program (UARP) that supports field efforts (e.g., large-lift, high-altitude balloon soundings) that are too extensive to describe here fully. We will abstract only those instruments that are directly applicable to the needs of HSRP.
- Instruments must be identified with the platforms on which they are deployed; otherwise, an explicit deployment strategy is difficult to articulate.

The challenge for HSRP is to craft a collection of instrument/platform combinations that can push the field forward in the 1992 time frame and stage a new combination of dynamics, chemistry, and radiation observations for 1993-94 which will diagnose for the first time the mix of dynamics and chemistry so central to the scientific objectives of HSRP. For example, the ER-2 instrument array emulates the measurement combination that must be deployed from Equator to pole with intensive uninterrupted coverage in the 10-km to 30-km altitude interval to sort out superposition of transport and chemistry. That platform can contribute to three sub-campaigns:

Table 2. Current Instrument Capabilities Part I: In Situ ER-2 Based

Molecule	Technique	Detection Threshold	Accuracy	PI/Institution
NO/NO _y	Chemiluminescence	50-100 pptv	±20%	Fahey/ NOAA AL
N ₂ O (or CO)	Tunable Diode Laser Loewenstein,Podolske/	1 ppbv	±5%	NASA Ames
ClO/BrO	Atomic Resonance Fluor/Chem Conv.	1 pptv	±25%	Anderson/ Harvard
H ₂ O	Fragment Fluorescence	100 ppbv	±6%	Kelly/ NOAA AL
O ₃	UV Absorption	1.5 x 10 ¹⁰ cm ³	±3%	Proffitt/ NOAA AL
Particle Impactor	Coated Wire Gold Substrate	Indiv. particles	±15% on part. radius	Pueschel/ NASA Ames
HCl, HONO ₂ , CH ₄ , NO ₂	Tunable Diode Laser	~1ppbv, except 100 pptv NO ₂	±10-15%	Webster/ JPL
Condensation Nuclei	Alcohol Saturation	0.02 μ dia. or larger	±20%	Wilson/ U. Denver
Microwave Temp	Microwave Emission	2 km slab above/ below aircraft	0.25 K lapse rate to 10%	Gary/ JPL
Particle Measuring Systems	FSSP ASAS-X	0.3-20 μ 0.1-3 μ	31 bins 31 bins	Dye, Gandrud/NCAR Ferry/NASA Ames
Meteorological Measurements	Pressure, temp. Airflow, Nav. System		Pressure: ±0.3 mb Temp.: ±0.3 K Wind: ±1 m/sec Samp. rate: 5 Hz	Chan/ NASA Ames

- Polar Campaigns - to construct a picture of the stratosphere up to 20 km north of 30° N latitude and south of 30° S latitude.
- Tropical Campaigns - to define the dynamics and photochemistry of the region for 30° S to 30° N latitude. This mission is especially important because we have so little in situ information for this region.
- Tropopause Campaigns - to lay the foundation for understanding stratospheric/tropospheric exchange. We need a new approach here, defining some new ideas about how the process works. The Stratosphere-Troposphere Exchange Project (STEP) campaign was focused on what, apparently, is not the most important process, so we need some new ideas.

Table 3. Current Instrument Capabilities Part II: Balloon-Borne, In Situ and Remote

Molecule	Technique	Altitude	Detection	PI/Institution	Notes
NO, NO ₂ , HNO ₃ , O ₃ , CH ₄ , N ₂ O	TDL/BLISS	23-35 km Balloon restric. limit altitude	150 pptv for NO _x , NO _y 0.1 ppm CH ₄	Webster/ JPL	Heavy lift balloon
OH, HO ₂ , H ₂ O, ClO, BrO, O ₃	LIF, resonance Fluorescence, UV absorption	23-38 km Balloon restric. limit altitude	1 pptv OH/HO ₂ 100 ppb H ₂ O 2 pptv ClO, BrO 5 x 10 ⁹ /cm ³ O ₃	Anderson/ Harvard	Heavy lift balloon
NO, NO _y	Chemilumin.	23-38 km Balloon restric. limit altitude	50 pptv	Ridley/ NCAR	Part of Harvard gondola
HCl, HF, HOCl, NO ₂ , HNO ₃ , HO ₂ , O ₃	Far infrared FIRS-2	25-40 km	Remote sensing S/N good above 30 km	Traub/ CFA	Heavy lift remote sensing
O ₃ , NO, NO ₂ , HNO ₃ , HCl, ClONO ₂	FTIR	25-40 km	Remote sensing	Toon/ JPL	Heavy lift balloon
ClO, O ₃ , HCl, HO ₂ , HNO ₃ , N ₂ O	Microwave, Submillimeter	25-45 km Normal ClO	100 pptv	Stachnik/ JPL	Heavy lift balloon
OH	Far infrared	28-45 km	5 pptv	Pickett/ JPL	Heavy lift balloon

Table 4. Current Instrument Capabilities Part III: Radiation Measurements, UV through IR

MEASUREMENT	INSTRUMENT
• IR radiance, difference, directionality, divergence	IR Interferometer
• IR broadband flux, divergence, difference	Pyrogeometer
• Visible radiance, difference, directionality, divergence	1/4 meter spectrometer with diode array
• Visible flux, divergence, difference	DC pyranometer
• UV radiance, difference, directionality, divergence	DC 1/4 meter spectrometer with diode array
• UV flux, divergence, difference	DC integrating radiometer
• Water vapor, liquid, ice	Lyman-alpha FF
• Ozone	In situ UV absorption
• CO ₂	In situ IR absorption
• CCN aerosols	PMS ASAP-X-M
• Cloud drop and aerosols	PMS FSSP
• 2-D ice crystal images	PMS 2DP
• Temperature, pressure, relative humidity	Aircraft data, MMS

A limited number of heavy-lift balloon launches will provide an occasional glimpse of higher altitude constituent fields. This combination of observations will yield major advances in our understanding.

An attempt should be made to compare the instruments on different platforms, particularly the instruments on balloons, aircraft, and satellites. These intercomparisons, when they are done well (i.e., in the same air mass), give us confidence that the claimed accuracies are real. In the same vein, it is desirable to measure all of the members of a family of molecules that are linked together with fast photochemistry, and then compare the ratios of the members' density to that expected from the theory. From these results one can find errors in either the experiment or the theory; however, in order to close the gap, we need very-high-accuracy experiments.

The goals for HSRP leading to a possible quantification of exhaust emission impacts on global ozone must, however, derive from a careful tailoring of new instrument technology in radiation, dynamics, and chemical observations with new platform development (specifically, high-altitude aircraft), to "sew" the upper troposphere to the middle stratosphere.

Needs for the Future

Recommendations for Radiation Field Measurements in the Lower Stratosphere

Measurement of the direct and diffuse radiation fields at various altitudes in the upper troposphere and lower stratosphere from the S-R bands to the near infrared is needed. Measurements should be made over geographical regions of different, but well-defined, albedo (clouds, ocean, snow, desert, etc.). These measurements would allow detailed comparison with the various multiple scattering theories currently in use in interpreting stratospheric photochemistry. The influence of multiple scattering is large (as much as a factor of 3 in the radiation field [including the direct solar flux]). Absolute level of accuracy required is not high, but it should be at least 20%. Measurement pertinent to $j(\text{O}_2)$ is important in the S-R region. Spectral resolution should be sufficient to verify the models, which is not very high unless detailed modeling of the S-R region is desired.

Measurements of direct and diffuse radiation in and out of clouds (high cirrus and PSCs) would be highly desirable. Ancillary measurements of cloud properties would be desirable (size, density, depolarization ratio, etc.).

Measurement of the IR radiation field is needed for determining the effects on the local energy balance of clouds, albedo, and aerosols. Radiative transfer codes use the line/line spectra from the AFGL tapes and so line/line measurements would be most useful in testing and comparing for these types of models. This would require an FTIR type instrument to adequately resolve the line widths. Specific target species for the lower stratosphere could be H_2O , N_2O , O_3 , ice, CO_2 , and CFCs. In making the measurements for use in model comparison and calculation, it would be necessary to know the temperature profile under the aircraft as well as cloud heights. The effects of clouds and their microphysics (particle size and density) would also be important, particularly for NAT and sulfuric acid aerosols.

Tracer Observations

A glaring practical shortcoming in the measurement arsenal for HSRP is the unavailability of a lightweight instrument for the "real time" detection of tracers, specifically CFC-11, N_2O , and CH_4 . This array, along with CO_2 , would provide invaluable maps of:

- tracers that fall off at dramatically different rates with altitude; and

- a tracer (CO_2) that would quantify the age of a particular air parcel.

For H_2O , we are acquiring a fairly good database, but the precision and accuracy needs some improvement. It is particularly important that we measure H_2O accurately since the equilibrium temperature at which NAT forms is a function of the H_2O concentration, and the chemistry of the lower stratosphere is a sensitive function of the occurrence of NAT. It is thus possible that the aircraft emissions of H_2O could affect the chemistry of the lower stratosphere by affecting the production of NAT aerosols.

Reactive Constituent Observations

The changes that have occurred in the last 15 years regarding the calculated predictions for O_3 depletion have resulted from changes in our understanding of the chemical links between reactive nitrogen and odd hydrogen and of the effects of heterogeneous chemistry. We now have the capability to measure most of the important reactive species (Table 4), but some notable exceptions exist. We have no measurements of the odd hydrogen radicals OH and HO_2 and the species that links chlorine and nitrogen, ClONO_2 . Our capability to measure NO_2 , perhaps the key radical in the lower stratosphere, has not been critically tested for aircraft instruments. We must redouble our efforts to make these measurements. Equally critical is the need to establish the climatology of these reactive constituents. The emerging construction of a climatology for NO_y , for example, has presented us with some interesting scientific questions. Imagine what we will learn when we have acquired simultaneous climatologies for all the important radical species.

There is a clear need for more accurate aerosol measurements. At present, particles that contain sulfuric acid, nitric acid, and water in various abundances in several phases are known to play a role in the chemistry of the stratosphere. Our ability to characterize the composition of these aerosol particles must be improved in order to understand their conditions of formation and their effect on the local chemistry, especially in chemically perturbed air parcels. Expectations are that new light-scattering instruments could significantly improve the accuracy in quantifying particle concentrations and sizes in the range of ~ 0.1 to 20 micron radius. Composition information could be obtained from the particle refractive index as determined from scattering polarization. Success in interpreting new measurements of size, abundance, and composition of aerosol particles is essential to further progress in this area. More detailed information on the full composition of particles that may eventually be needed may be forthcoming near the end of the HSRP program from aerosol mass spectrometer instruments currently under development in the laboratory.

Platforms

The critical variables of altitude and range must be tailored to the scientific objectives, in combination with constraints on payload weight, instrument capability, etc. The desired circumstance, of course, would be to have at least a 300-kg payload capability to 30-km altitude with a range of 3000 to 10,000 km or greater available immediately in an unmanned aircraft platform (with true costs at or below \$1000/hr for operating expenses). While this aircraft may be available in the Theseus by 1994, there is a natural evolution of technology using the ER-2 and Perseus as initial platforms (which can advance the HSRP program in the near term) culminating in a more powerful combination of platforms, including the HAARP, approximately 3 to 4 years from now.

Specifically, we envision an evolution that:

- Uses the ER-2 to stage polar campaigns, tropical campaigns, and tropopause studies up to 20 km. The ER-2 will also serve as a test bed for new instruments along their natural evolutionary path to lightweight status.
- Perseus will be used to deploy subsets of the full instrument array either to high altitude for short duration or for longer duration at lower altitude.

SESSION 5. NEW MEASUREMENT TECHNIQUES

Chairman

Dr. Michael J. Kurylo, National Aeronautics and Space Administration, Headquarters

Questions/Issues

- Which of these new areas looks promising enough to warrant development for use in atmospheric research?
- Can they be ready by 1992?
- By 1994?
- When?

Synopsis

The presentations made during this section of the Workshop clearly demonstrated the vital need for strong synergistic relationship between the HSRP and atmospheric research programs within NASA and other U.S. Government agencies, in order to provide the measurement capabilities for evaluating future atmospheric environmental issues, including those associated with HSCT operations.

The Workshop reports and discussions on new measurement techniques were focused primarily on aircraft-borne instrumentation. This is an area that has seen considerable growth over the last 5 years, largely as a result of developments associated with the Stratosphere Troposphere Exchange Project (STEP), the Airborne Antarctic Ozone Experiment (AAOE), and the Airborne Arctic Stratospheric Expedition (AASE) conducted in the late 1980s by NASA's Upper Atmosphere Research Program (UARP). The current suite of instruments designed for use on the NASA DC-8 and ER-2 aircraft represents a very powerful atmospheric observation capability. These existing measurement opportunities are enhanced further by the more mature balloon-borne and ground-based instrumentation deployed by the UARP for more than a decade to develop atmospheric climatologies in several latitude regions. Nevertheless, there are many recognized limitations in atmospheric sampling that are yet to be overcome. Presentations during this session of the HSRP Workshop demonstrated the wealth of scientific talent now preparing to meet these challenges. Ongoing and planned research activities, while in many cases directed at generic aspects of atmospheric measurement science and trends detection, will provide the capabilities needed for addressing the environmental issues confronting the development of a HSCT.

Presentations on both in situ and remote-sensing instruments were included in the program. While the dominant focus was on existing platforms (i.e., DC-8, ER-2, and large balloons), it was clear from the discussions that there is a growing consensus for directing a

component of instrument development activities towards deployment on small lightweight balloons and/or high-altitude (manned or unmanned) aircraft.

Lidar Instrumentation

Among the remote-sensing instruments, significant improvements have been realized in lidar instrumentation (funded in part by NASA's UAR and Tropospheric Chemistry Programs). Capabilities now exist for investigating background aerosols and all types of stratospheric clouds, including Type II PSCs. Aerosol scattering and depolarization measurements are presently possible (or will be available within the time frame of the HSRP) from the DC-8 in either the zenith or scanning modes and from the ER-2 in nadir, zenith, or scanning modes. Plans are under way to extend the existing DC-8 ozone lidar measurements to an altitude range of 28-30 km. While the current DC-8 water vapor lidar instrument has been limited to measurements in the troposphere, existing and developing technologies could extend such measurements to approximately 8 km above flight altitude within the next few years. An ER-2 tropospheric system currently under development could also be modified for lower stratospheric studies on a similar time scale. Lidar measurements could be used for several other important atmospheric constituents. For example, development of a Raman lidar and its deployment on the DC-8 for simultaneous measurements of stratospheric methane, water vapor, nitrogen, oxygen, and temperature has been proposed and is being evaluated.

Microwave Instrumentation

There have also been improvements in microwave/submillimeter limb-sounding instrumentation. A reasonably lightweight package (developed under NASA's UARP), suitable for balloon or aircraft platforms, can simultaneously measure several species (ClO, O₃, HCl, HO₂, HNO₃, and N₂O) important in atmospheric ozone chemistry and can be extended to other species through the addition of appropriate filter banks. The instrument has the best signal-to-noise ratio and resolution with the platform situated above the atmospheric layer to be measured.

Infrared Instrumentation

Similar advancements in infrared (IR) instrument development have also been achieved. A new tunable diode laser spectrometer has been fabricated for the ER-2 under UARP support and is about to undergo test flights. A four-channel instrument, it is designed to make simultaneous in situ measurements of NO₂, HNO₃, HCl, CH₄, H₂O, and O₃, thereby adding considerably to the existing IR absorption capability on that platform. Some early proof-of-concept investigations have also been conducted for an open path IR absorption cell that should eliminate sampling problems for some of the more reactive gases and may have greater sensitivity than other instruments because the achievable path length is longer. Also under development (with HSRP support) is a laboratory proto-type instrument for in situ CO₂ measurements that use non-dispersed IR analysis. Construction of a flight instrument (scheduled to begin within a year) should greatly enhance dynamic tracer measurement capabilities from the ER-2.

Instrumentation for In Situ Measurement of Radical Species

There has been considerable development of instruments for the in situ measurement of important radical species. Laboratory studies and instrument prototype development has been under way within the UARP for a lightweight OH/HO₂ monitoring instrument. This development (based in large part on the heritage of high altitude balloon instrumentation) will be extended to a package suitable for ER-2 integration under HSRP support. NASA's UARP has also supported the development of a lightweight ClO/BrO instrument (which can be flown on a small balloon or a high-altitude aircraft) and will initiate support for development of a similar

instrument for in situ measurement of ClONO_2 . The measurement of various paramagnetic gases (i.e., radicals such as Cl/ClO , OH/HO_2 , NO/NO_2) may also be possible using a mid-IR magnetic rotation spectrometer. More detailed laboratory study would be required to ascertain the potential of this technique. Finally, the ER-2 chemical measurement suite will soon be further enhanced even with the HSRP-sponsored conversion of the existing NO/NO_y instrument to a three-channel system capable of simultaneous measurements of the species.

Instrumentation for Real-Time Atmospheric Tracer Profile Measurements

One of the more significant gaps in chemical sampling instrumentation lies in the area of real-time atmospheric tracer profile measurements. While the previously mentioned CO_2 instrument will play an important role in this area, there is a need for a lightweight instrument package suitable for deployment on a small balloon or high-altitude aircraft and capable of recording the profiles of CFCl_3 , CF_2Cl_2 , or N_2O to altitudes above the current ER-2 limit. The potential for the development of such an instrument may lie in fast-response gas chromatographic technology or ion mobility spectrometry, and is currently being evaluated.

Instrumentation for Physical and Chemical Characterization of Condensation Nuclei and Aerosols

There have also been (and continues to be) improvements of and developments in instrumentation for the physical and chemical characterization of condensation nuclei (CN) and aerosols. For example, sizing capabilities were greatly improved between the AAOE and AASE. While there are now several new techniques and inlets for sampling the various aerosol size ranges, in general particles over $0.2 \mu\text{m}$ in diameter must be sampled in situ, while smaller sized particles can be brought into the aircraft for analysis. The HSRP is supporting three different instrument studies in the CN/aerosol area. These include improvements in CN counting for the ER-2 instrument, laboratory studies leading to the development of a stratospheric soot-measuring instrument, and development of an aerosol mass spectrometer (laboratory prototype of an aircraft instrument). The latter should yield not only aerosol size and composition information, but also provide identification of trace species in the particles. Finally, there are a number of laboratory research techniques for compositional analysis of particles and clusters that may provide a basis for development of future instruments.

SESSION 6. WHAT DO WE KNOW ABOUT ENGINE EXHAUST AND AIRCRAFT WAKES?

Chairman

Dr. Michael Prather, Goddard Institute for Space Studies, National Aeronautics and Space Administration

Synopsis

A review of the CIAP studies of aircraft exhaust pointed up the difficulties in detecting the exhaust plume unless a visible trail is evident (contrail or fuel "puffs" as in YF-12 experiments). With no in situ measurements, Concorde emission studies have been limited to test-stand studies of the engines. Engine exhaust products for current engines, as well as for the new technologies that may reduce the NO_2 emission index (EI) from 40 to 5 g/kg of fuel, were described. There may be trade-offs in the new technologies between emissions of NO_x and CO (affecting engine efficiency). Information is now available on the detailed mix of organics in engine exhaust. Wake characteristics of aircraft depended on individual aircraft dynamics.

Results were taken from wind tunnel experiments and from computational fluid dynamics work.

A number of key findings emerged from the session:

- It will be extremely difficult to measure chemical products in the exhaust plume of an aircraft without a visible clue (e.g., contrail or colored exhaust) to help find the wake. Our current database on the location of engine exhaust within aircraft wakes (the dynamically created wing-tip vortices may contain part or most of the exhaust products) is based on pictures of the visible plume (i.e., condensed water, possibly environmental) and does not necessarily describe the distribution of engine exhaust.
- It is important to re-analyze the engine test-stand results for exhaust products and to bring in new instruments or experimenters, as necessary, to address the completeness and accuracy for engine EIs of interest to HSRP/AESA.
- It is also important to characterize the size/shape distribution of soot particles from the engine tests and to compare them with the currently collected stratospheric samples. The chemical composition and surface properties of the engine soot should also be measured.

SESSION 7. OKAY, WHAT IS OUR PLAN OF ACTION?

Chairman

Dr. Michael Prather, Goddard Institute for Space Studies, National Aeronautics and Space Administration

Questions/Issues

- Does the chemical climatology tell us where the SST exhaust goes?
- Does it tell us what the exhaust will do to the ozone?
- What instruments do we need?
- What platforms must we use?
- Is there overlap with other programs?
- Where do we need measurements?
 - Tropics?
 - Mid-latitudes?
 - Poles?
- Is the plume worth chasing?
- If so, what is our strategy?
- Do we need to be able to remote sense the plume?

Solve the Following Problems:

- Define 1992 and 1994 missions.
- Coordinate with other aircraft campaigns.
- Set priorities on instrument/platform development.

Synopsis

This final session attempted to draw conclusions from the presentations and discussion of the workshop. In particular, HSRP/AESA needs to put together a plan of action for atmospheric measurements that would be supported or encouraged by the program, i.e., WHERE DO WE GO FROM HERE?

The chair presented a sequence of key scientific questions, identified in Table 5, that were meant to focus the HSRP/AESA measurement program. These questions are listed in sequence, leading from the aircraft emissions up to the global perturbations. They are likely to be asked of the scientific community when its members are assessing the environmental impact of aircraft emissions.

The questions point to the specific measurements that are required to support the development of the assessment models and to corroborate their predictions for the present atmosphere. The discussion that followed worked on identifying the most important measurements or other studies that should be pursued in order to answer these questions.

Table 5. Key Science Questions for HSRP/AESA Assessment

Topic	
Emissions	What really comes out of aircraft?
Wake/Plumes	Can "plume processing" affect NET emissions?
Transport	How do emissions MIX and ACCUMULATE in the atmosphere?
Chemistry	Can we PREDICT the ozone/climate perturbations caused by additions of NO _x , H ₂ O, aerosols, etc?

Emissions and Plume Chemistry

Before we try to measure and calibrate the emission products from engines in flight, it would be best to go back to the engine test stands from which we have derived our current values for aircraft emissions.

- For previous results, we need to check the accuracy of the reported data and the sensitivity of instruments.

- For future work, we should coordinate the atmospheric experimenters with the combustion engineers and possibly make new measurements from engine test facilities with an expanded set of instruments (e.g., NO, NO₂, NO_y, HNO₃, aerosols, CCN, soot, OH, SO₂, SO₃, ions, HC, HCO_x).

In-flight validation of the ground tests may be necessary as part of the political/regulatory process, but is not an immediate priority for the HSRP/AESA studies, since no new ideas have been put forward that need testing or might alter our present understanding of the wake.

It may be important to measure the chemistry and physics (aerosols) within the exhaust plume of an aircraft. Such measurements could examine chemical processing in the unique, highly concentrated environment before the exhaust plume disperses into the background stratosphere. (They also would provide in-flight validation of EIs, a lower priority, as noted previously). Some modeling sensitivity studies have shown that global perturbations are not sensitive to chemical processing within the plume (e.g., conversion of exhaust NO_x to HNO₃ has little impact on ozone depletion), but it is possible that ice crystal growth within the core of the exhaust plume (and subsequent fallout) may lead to transport of combustion products to lower altitudes. Furthermore, plume measurements provide a "laboratory" for testing heterogeneous chemical reactions across a large range of aerosol and trace gas concentrations under stratospheric conditions.

- A clear first step is to pursue the modeling studies (both global and plume) to understand better the conditions in which plume processing has a global impact.

Chemical tracer measurements in aircraft exhaust plumes are not now viewed as a high priority. If they become necessary in the future, then we need to know more about the dynamics of the aircraft wake and the distribution of exhaust products in order to plan a successful field measurement campaign. For example, do the majority of the engine exhaust products roll up into the small (~4 m) wing-tip trailing vortices, or into the larger (~100 m) visible contrail? Some of these uncertainties might be resolved with fluid dynamical modeling or with fluid experiments.

Experimental knowledge about subsonic aircraft wakes might be expanded on a theoretical basis to supersonic wakes.

- Overall, field measurements may not be necessary.

If they were necessary, we would require a remote sensor (e.g., a kind of lidar) to locate the wake in real time and some very high frequency instruments for the exhaust products (CO₂, H₂O, CCN, NO_x) as well as O₃. Perhaps the only way to quantify measurements of this type would be to put some type of chemical tracer into the fuel and then measure all of the other species relative to that tracer.

Global Transport

The critical region for assessing model transport will be in the lower stratosphere, where the projected aircraft would fly, but the exhaust products are expected to mix to some extent throughout the stratosphere. The rate of upward mixing is important, because ozone destruction from added NO_y is more effective at higher altitudes. The rate of downward mixing is equally important, since it controls the steady-state accumulation of exhaust products.

- Measurements that are used to deduce tracer transport within the lower stratosphere must extend from the upper troposphere (about 10 km) to middle stratosphere (about 25 km), from Equator to pole, and in all seasons.

What platforms do we have or anticipate that could make these measurements? The ER-2 (full in situ instrumentation) has an operating range of about 15-20 km. The Concorde (potential for some in situ monitoring) flies regularly over the North Atlantic at 15-18 km. Lower altitudes could be filled by commercial aircraft such as the DC-8 (10 to 12.5 km), but in situ sampling is not as complete as for the ER-2. The gap between 20 and 25 km will technically be filled by UARS and its correlative measurements, but the range of vertical overlap (redundancy) with the extensive ER-2 data will be small, and the need for in situ measurements for some species and for some tests is not met.

- There is a clear need for additional platforms (either balloons or a Perseus/HAARP-type aircraft) to make measurements above ER-2 flight levels. The need to reach greater altitudes is important, but the currently anticipated Perseus/balloons have limited payloads (i.e., only a few species of the ER-2 in situ suite can be measured concurrently).
- The reconstruction and interpretation of aircraft campaign data will require concurrent measurements (or analyzed data) of
 1. dynamical tracers (pressure, temperature, potential temperature, potential vorticity),
 2. ozone and water vapor, as well as
 3. one or more long-lived tracers (N₂O, CFCs, CO₂, CH₄).

The comparison of these observations with model simulations (in order to test the model's predictions for aircraft emissions) will require corresponding predictions of chemical tracer transport variations from 3-D models.

The impact of aircraft flying in the stratosphere today (the Concorde corridor over the North Atlantic at flight levels 500-600; commercial fleets at flight levels 310-390 over the poles in winter) may be detectable. Because of the altitude restrictions on both the ER-2 and the DC-8, some of the interesting altitudes are not presently reachable. The asymmetries in stratospheric NO_y H₂O climatologies between the Arctic and Antarctic may be related to the denitrification/desiccation over Antarctica or may represent aircraft input.

- A full climatology of CO₂-H₂O-NO_y and O₃ in the mid-latitude stratosphere might be able to discern a factor (appropriate enhancements of CO₂-H₂O-NO_y) that matches aircraft exhaust.

It would be extremely useful to develop a unique measure of aircraft perturbation (e.g., Is stratospheric soot a unique product of aircraft, and can it be measured with adequate frequency and accuracy?).

The following examples of trace species or types of measurements were discussed as being important in diagnosing stratospheric transport :

- Soot and CCN spectrum as a measure of current engines
- Is there an isotopic signature (e.g., ¹³C/¹²C, D/H) in Jet-A fuel?

- Transport through tropopause folds, cyclonic events, polar vortex
- Gradients and removal processes in the upper troposphere
- Natural cycles of H₂O and NO_y
- Stratospheric NO_y from tropospheric lightning

Chemical Perturbations

We will need to measure the important chemically active species under as many possible conditions in today's atmosphere in order to test our model predictions of stratospheric photochemistry under highly perturbed conditions predicted for an HSCT fleet (i.e., high NO_x, H₂O, CO, soot, etc.). One important issue would be to verify the crossover region where the addition of NO_x leads to NO_y-catalyzed loss of ozone above about 15 km and to smog-chemistry production of ozone below about 10 km (see Figure 1).

- Along with measurements of the source gases (noted above for determining the global transport and dispersion of aircraft exhaust), we will need to measure the NO-NO₂-HNO₃-NO_y family, the OH-HO₂ concentrations, and the ClO-BrO-ClONO₂ family.

If we achieve the extent of coverage cited above for transport, then we will likely have sampled a sufficiently large range of photochemical environments.

Uncertainty in the kinetics and radiation data for the models could be reduced by atmospheric measurements of specific chemical balances (e.g., the NO₂-NO₃-N₂O₅ equilibrium, the HO_x-NO_x chemistry, of course, along with other key tracers such as O₃, H₂O, CH₄, NO_y, Cl_y). Likewise, certain atmospheric conditions such as mountain lee waves provide an accessible test of heterogeneous chemical processing. It is not clear whether these atmospheric tests would provide clues to missing chemistry. A most difficult question is, how do we determine the role of added aerosols both locally (along aircraft corridors), at the winter poles (in PSCs), and at or near the tropical tropopause?

The following examples of other trace species or types of measurements would be important in diagnosing stratospheric chemistry and its perturbations:

- Look for effects of CCN on PSCs as well as cirrus/radiation
- Determine the natural stratospheric sulfur cycle and particle formation
- Determine molecular clusters that might affect J-values
- Measure UV-visible scattered light to test model photolysis

APPENDIX

LOWER STRATOSPHERIC MEASUREMENT ISSUES: A WORKSHOP

NASA Ames Research Center
October 17-19, 1990

Agenda

MAJOR QUESTIONS:

*What atmospheric measurements are needed for an SST assessment?
Can we make those measurements?*

Wednesday, October 17

Welcome	A. Schmeltekopf/NOAA Retired
Logistics	E. Condon/NASA Ames
Overall High Speed Research Program (HSRP) Perspective	H. Wesoky/NASA HQ
Define Atmospheric Effects of Stratospheric Aircraft Program	M. Prather/NASA GISS

Known Problems in Lower Stratospheric Chemistry

Chairman's Introduction	C. Howard/NOAA AL
Homogeneous Reactions	S. Sander/NASA JPL
Heterogeneous Reactions	M. Tolbert/SRI International
Global Chemical Modeling	S. Wofsy/Harvard
Plume Modeling	C. Kolb/Aerodyne
Panel Discussion	
Additional Panel Member:	W. Brune/Penn State

Questions:

What critical laboratory measurements are needed?
What critical atmospheric measurements are needed?
Can in-situ measurements help us directly determine rates?

Known Problems in Lower Stratospheric Transport

Chairman's Introduction	J. Holton/U. Washington
Large-Scale Dynamics	J. Holton/U. Washington
Stratosphere-Troposphere Exchange	M. Schoeberl/NASA Goddard
Radiative Forcing	D. Crisp/Caltech
Global Transport Modeling	A. Plumb/MIT
Plume Mixing	M. Prather/NASA GISS
Tracer Database: What Can We Learn?	H. Johnston/U. C. Berkeley
Panel Discussion	
Additional Panel Members:	E. Danielsen/NASA Retired A. Tuck/NOAA AL

Questions:

- Will SST exhaust really mix upward?
- Can the high-resolution structure of the transport be important?
- Can exotic tracer experiments be useful?

What Platforms Do We Have or Can We Get?

Chairman's Introduction
ER-2
Condor
Perseus
HAARP
Concorde as a Platform

A. Schmeltekopf/NOAA Retired
J. Barrilleaux/NASA Ames
J. Dale/Boeing Military Airplanes
J. Langford/Aurora Flight
P. Russell/NASA Ames
P. Carlier/Aerospatiale

Panel Discussion (Platforms)

Additional Panel Members:

G. Harris/Leigh Aerosystems
Chairs from first four sessions

Questions:

- Do any of these platforms get us far enough?
- High enough?
- Long enough (duration)?
- When can the platforms be ready?

Thursday, October 18

Present Measurement Capabilities

Chairman's Introduction
Radicals
Source Gases
Aerosols
Dynamic Tracers
Radiation
Panel Discussion

J. Anderson/Harvard
B. Brune/Penn State
M. Loewenstein/NASA Ames
D. Fahey/NOAA AL
M. Schoeberl/NASA Goddard
G. Mount/NOAA AL

Additional Panel Members:

A. Ravishankara/NOAA AL
S. Wofsy/Harvard

Questions:

- Are all of our present capabilities accurate enough?
- Specific enough?
- Fast enough?
- Do we currently have the "Right Stuff?"

New Measurement Techniques

Chairman's Introduction
Lidars
Microwaves
Aerosols
Diode Laser Spectrometer

M. Kurylo/NASA HQ
E. Browell/NASA Langley
R. Stachnik/NASA JPL
C. Wilson/U. Denver
C. Webster/NASA JPL

Aerosols
CO₂
OH/HO₂
Two-Step Laser Mass Spectrometry for
Analysis of Adsorbates and Particulates
Ion Spectroscopy and Dynamics
Spectroscopy and Reactivity of Clusters
Panel Discussion

D. Murphy/NOAA AL
D. Toohey/Harvard
J. Anderson/Harvard

R. Zare/Stanford
C. Lineburger/U. Colorado
V. Vaida/U. Colorado

Questions:

Which of these new areas look promising enough to warrant development for use in atmospheric research?
Can they be ready by 1992?
1994?
When?

Friday, October 19

What Do We Know about Engine Exhaust?

Chairman's Introduction
Wake Studies in CIAP
Concorde

Wake Chemicals
Wake Characteristics

M. Prather/NASA GISS
R. Oliver/IDA
P. Carlier/Aerospatiale
R. Williams/British Aerospace
R. Lohmann/Pratt & Whitney
G. Kidwell/NASA Ames

Okay, What Is Our Plan of Action?

Chairman's Introduction
Panel Discussion

Additional Panel Members:

M. Prather/NASA GISS
All previous panel chairs
C. Lineburger/U. Colorado
D. Zare/Stanford

Questions:

Does the chemical climatology tell us where the SST exhaust goes?
Does it tell us what the exhaust will do to the ozone?
What instruments do we need?
What platforms must we use?
Is there overlap with other programs?
Where do we need measurements?
Tropics?
Mid-latitudes?
Poles?
Is the plume worth chasing?
If so, what is our strategy?
What instruments do we need?
Do we need to be able to remote sense the plume?

Solve the following problems:

Define 1992 and 1994 missions
Coordinate with other aircraft campaigns
Set priorities on instrument/platform development

omit to

END

Chapter 7

HSRP/AESA Research Summaries

This chapter presents individual summaries of research conducted by investigators supported by High Speed Research Program/Atmospheric Effects of Stratospheric Aircraft as of May 1991; see chapter 1 for an overview of the principal investigators and research areas. The summaries follow this format: (A) title, (B) investigators and institutions, (C) abstract of research objectives, (D) summary of progress and results to date, and (E) journal publications. These summaries have been edited where necessary. The principal investigator (denoted by an asterisk) is the contact person responsible to HSRP/AESA for the proposed research.

HSRP/AESA Principal Investigators

James G. Anderson, Harvard University
Guy P. Brasseur, National Center for Atmospheric Research
Anne R. Douglass, NASA Goddard Space Flight Center
David W. Fahey, NOAA Aeronomy Laboratory
Randall R. Friedl, NASA Jet Propulsion Laboratory
R. Stephen Hipskind, NASA Ames Research Center
Ivar S. A. Isaksen, University of Oslo
Vyacheslav U. Khatatov, Central Aerological Observatory
Malcolm K. W. Ko, Atmospheric and Environmental Research, Inc.
Charles E. Kolb, Aerodyne Research, Inc.
Ming-Tuan Leu, NASA Jet Propulsion Laboratory
Richard Miake-Lye, Aerodyne Research, Inc.
Mario J. Molina, Massachusetts Institute of Technology
Daniel M. Murphy, NOAA Aeronomy Laboratory
Rudolph F. Pueschel, NASA Ames Research Center
John A. Pyle, University of Cambridge
Co-Principal Investigator-Robert S. Harwood, University of Edinburgh
Hans R. Schneider, Atmospheric and Environmental Research, Inc.
Robert K. Seals, Jr., NASA Langley Research Center
Margaret A. Tolbert, SRI International
Richard P. Turco, University of California, Los Angeles
James C. Wilson, University of Denver
Stephen C. Wofsy, Harvard University
Douglas R. Worsnop, Aerodyne Research, Inc.
Donald J. Wuebbles, Lawrence Livermore National Laboratory
Glenn K. Yue, NASA Langley Research Center



A. Title of Research Task

Development of Techniques for the In Situ Observations of OH, HO₂, ClO, BrO, ClONO₂, O₃, P, and T, Between 10 and 30 km for Studies of the Impact of High-Latitude Supersonic Aircraft on the Stratosphere

B. Investigators

*James G. Anderson
Atmospheric Research Project
Engineering Sciences Laboratory
Harvard University
40 Oxford Street
Cambridge, MA 02138

C. Research Objectives

The atmosphere is particularly complex between 10 and 30 km, where chemical and dynamical time constants are roughly equivalent. Our objective is to develop in situ instrumentation for the detection of several key radicals-most notably, OH, HO₂, ClO, and BrO, as well as related reservoir molecules and ozone, which will fly first on the NASA ER-2 and then evolve to the new generation of Perseus unmanned aircraft for flights to and above 25-km altitude. The first step in this evolution is the development of a solid-state laser system for laser induced fluorescence detection of OH and HO₂ for the ER-2.

D. Summary of Progress and Results:

(Support received November 1990) The first-order question in designing the ER-2 flight system was to select the pump laser. Development of the copper vapor laser for balloon-borne systems led to superb performance in stratospheric tests for both OH and HO₂. Results are summarized in the Figures 1 and 2.

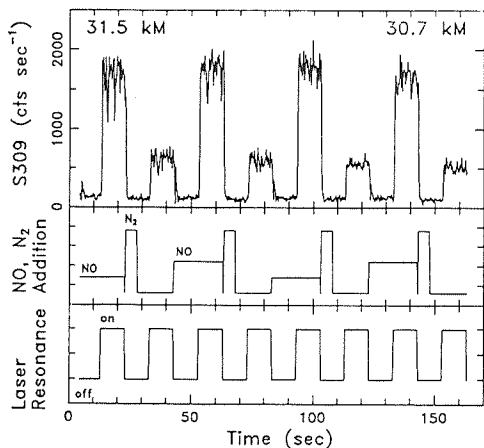


Fig. 1. Unaveraged 309 nm detector count rate data (top). NO and N₂ gas addition sequence (middle), and laser tuning cycle (lower) vs. time, during balloon descent through the 31.5–30.7 km interval.

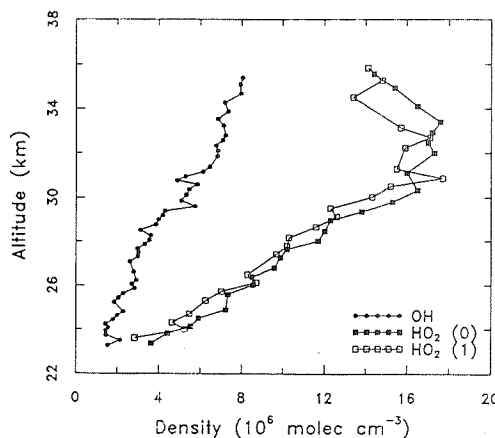


Fig. 2. [OH] and [HO₂] vs. altitude observed Aug. 25, 1989, over a solar zenith angle variation of 51°–61°. HO₂ (0) and (1) refer to high and low NO flow rate results, respectively.

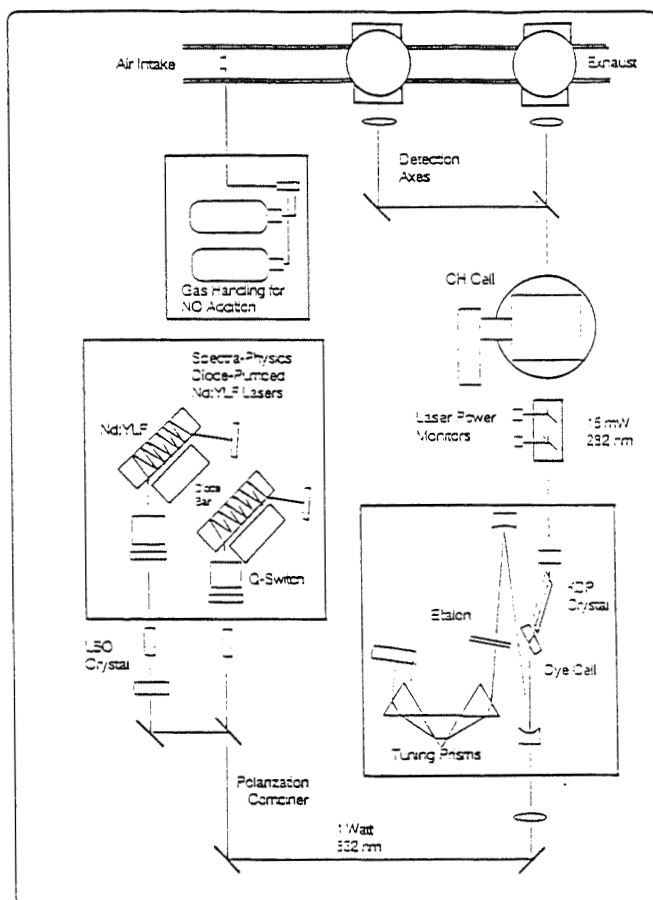
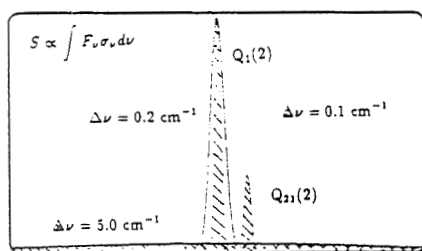
These data clearly revealed the level of sensitivity that could be achieved with the copper vapor laser system. In mid-1990, however, the research branch of Spectra Physics announced a breakthrough in the development of diode-pumped neodymium (Nd) systems--specifically, the achievement of ≈ 1 W of output at 530 nm at a repetitive rate of 5 kHz. The diode-pumped Nd system was dramatically simpler and lighter. We therefore focused on determining which system would provide the best balance among performance, weight, and reliability. These results are summarized in the panels below.

ER-2 OH and HO₂ Measurements

System Performance: A comparison with the Harvard balloon-borne laser OH system

	ER-2 solid state laser system	Balloon-borne copper laser system
Output power (mW) at 282 nm	15	15
Laser frequency width (cm ⁻¹)	0.2	5.0
Power Consumption (Watts)	400	2000
Weight (kg)	< 200	1000
Signal /ppt (counts/sec)	600	35

• The dramatic increase in the responsivity is due to the use of an intra-cavity etalon in the dye laser. The 0.2 cm⁻¹ frequency width is a much better match to the OH doppler width (1.1 cm⁻¹).



E. Journal Publications

None.

A. Title of Research Task

Modeling the Atmospheric Effects of Stratospheric Aircraft

B. Investigators

*Guy P. Brasseur
Philip J. Rasch
National Center for Atmospheric Research
P. O. Box 3000
1850 Table Mesa Drive
Boulder, CO 80307-3000

Richard P. Turco
Department of Atmospheric Sciences
University of California, Los Angeles
Los Angeles, CA 90024-1565

C. Research Objectives

The purpose of the project is to understand and predict the atmospheric effects of a projected fleet of stratospheric aircraft. A three-dimensional, chemical-transport model will be used to assess, on time scales of weeks or less, the dispersion and chemical transformation of aircraft effluents. A two-dimensional (2-D) chemical-radiative-transport model will be used to predict, on time scales of months to years, the effects on stratospheric ozone of the enhanced levels of NO_x and H_2O resulting from perturbations by aircraft.

D. Summary of Progress and Results

Our (2-D) model has been used to evaluate the potential response of ozone to the emissions of supersonic aircraft in the stratosphere. Different scenarios reviewed by the Emissions Scenarios Subcommittee of the NASA HSRP have been considered. Model calculations show that the ozone response to enhanced levels of NO_x is greatest at high latitude in late summer. The changes in the concentration of other gases (CO_2 , CO, etc.) are generally minor except for that of water vapor. The 2-D model has been modified to include the effect of polar stratospheric clouds (PSCs) and sulfate aerosols. When these processes are taken into account, the ozone perturbation to NO_x emission is reduced.

A semi-Lagrangian transport (SLT) model has been used in an exploratory mode to simulate the dispersion, during 90 days, of a passive tracer (e.g., NO_y) continuously released in flight corridors. Three different corridor geometries have been considered. The SLT scheme used for these simulations was coupled to the NCAR Community Climate Model (CCM) (version 2). The NCAR CCM and the associated SLT model have been significantly modified to include more realistic physics and to make them computationally more efficient. An "off-line" version of the SLT model has been developed and will be used for further studies.

E. Journal Publications

Brasseur, G. P., C. Grainer, and S. Walters, Future changes in stratospheric ozone and the role of heterogeneous chemistry, *Nature*, 348, 626-628, 1990.

Rausch, P. J., and D. L. Williams, The sensitivity of a general circulation model climate to the moisture transport formulation, accepted *J. Geophys. Res.*, 1991.

Rausch, P. J., and D. L. Williams, Computational aspects of moisture transport in global models of the atmosphere, *Q. J. R. Meteorol. Soc.*, 116, 1071-1090, 1990.

A. Title of Research Task

Two-Dimensional and Three-Dimensional Model Studies of Stratospheric Aircraft Emissions

B. Investigators

*Anne R. Douglass
Charles H. Jackman
Richard B. Rood
Richard S. Stolarski
Code 916
Atmospheric Chemistry and Dynamics Branch
Goddard Space Flight Center
National Aeronautics and Space Administration
Greenbelt, MD 20771

C. Research Objectives

This research involves the coordinated, parallel use of the NASA/GSFC 2-D model and the 3-D chemistry and transport model (3-D CTM). Chemical assessments of the impact of aircraft exhaust on stratospheric ozone employ the 2-D model. In addition to examining a wide range of scenarios, the 2-D model is being used for sensitivity studies to chemical and transport inputs and assumptions. (These calculations are known to be sensitive to lower stratospheric transport, and particularly to stratosphere/troposphere exchange.) The 3-D dispersion of tracers is being examined using the 3-D CTM. This model uses winds from a data assimilation procedure and provides a realistic simulation of tracer dispersion. Following a critical analysis of stratosphere-troposphere exchange in the 3-D CTM, tracer experiments will examine the sensitivity of horizontal and vertical tracer transport to altitude, latitude, and season of injection. Further experiments will allow a direct comparison of 2-D and seasonally average 3-D transports. This should result in better quantification of the uncertainty in the 2-D representation of stratosphere/troposphere exchange.

D. Summary of Progress and Results

All scenarios provided by the program have been completed using the 2-D model. The results from these calculations have been submitted to the Upper Atmosphere Data Base. Additional 2-D model studies have included the sensitivity of ozone response for a given scenario to the lower stratospheric circulation. The calculated excess ^{14}C , N_2O , and total ozone for different circulations have been compared with measurements. Generally, the calculation with the best simulation of ^{14}C also has the greatest sensitivity of ozone to aircraft emissions.

Calculated ozone provides an important measure of model validity, because it is sensitive to the circulation and can be compared with measurements. Modeling studies of the tropospheric ozone column revealed a strong sensitivity to the vertical advection scheme. To improve the resolution near the tropopause, the Prather transport scheme has been adopted for the vertical advection in the 3-D CTM. In our previous results, using the Van Leer scheme, the buildup of ozone in the troposphere was more rapid than when the Prather scheme was used; however, this was an indication of poor resolution of the sharp vertical gradient of ozone near the tropopause. Such a sharp gradient at the tropopause is anticipated for aircraft exhaust, and this analysis will be continued by considering, for example, the

transport to the troposphere inferred from the residual circulation that is calculated from the 3-D wind field, and by examining the importance of vertical resolution.

The dispersion of aircraft exhaust in a North Atlantic corridor was examined using the 3-D CTM for the winter of 1989. The concentration of pollutant within the corridor exceeded the zonal mean by a factor of 3 or 4 during most of the winter. However, there were occasions of low transport, during which the concentration in the corridor grew and exceeded the zonal mean by a factor of 10 or more.

The pollutant was injected into the 3-D CTM at one pressure surface in a latitude band centered at 45°N for comparison with a similar calculation using the 2-D model. Both horizontal and vertical transport were faster in the 3-D CTM than in the 2-D model. Several factors make this comparison inconclusive. The 3-D CTM uses meteorological data from a specified year, as opposed to the climatological circulation and diffusion coefficients of the 2-D model. Over the winter season, pollutant in the 3-D CTM is injected into a range of potential temperature values of 470-540 K; in the 2-D model, the range is only 504-510 K. There are substantive differences in both horizontal and vertical transport, and current analysis will attempt to interpret the differences.

E. Journal Publications

None.

A. Title of Research Task

A Dual Channel NO/O₃ Chemiluminescence Detector for Measurements of NO and NO_y on Board the NASA ER-2 Aircraft

B. Investigators

*David W. Fahey
R/E/AL6
Aeronomy Laboratory
National Oceanic and Atmospheric Administration
325 Broadway
Boulder, CO 80303-3328

C. Research Objectives

A new multi-channel instrument will be designed and built for the measurement of NO and NO_y on board the NASA ER-2 aircraft. The measurements will be simultaneous and will have high spatial resolution. The technique uses catalytic conversion of NO_y species to NO and NO/O₃ chemiluminescence. A third chemiluminescence channel will be incorporated to accommodate the development of NO₂ detection capability. The speciation and abundance of the NO_y reservoir in future aircraft missions will be used to understand the atmospheric impact of a proposed fleet of supersonic aircraft on stratospheric ozone. Specific goals are to (1) define a reference state for model simulations and (2) characterize exhaust plume chemistry in the wake of comparable aircraft.

D. Summary of Progress and Results

The design and construction of the multi-channel chemiluminescence detector is well under way. Approval has been obtained from Lockheed for the integration of the new instrument in the Q-bay of the ER-2 aircraft. Procurement of long-lead-time components is complete. Laboratory and prototype tests of ozone addition and water addition subsystems are nearing completion. Test flights of the two-channel system occurred in late August 1991, in anticipation of science flights to begin with the 1991 NASA Arctic Ozone Mission in October.

E. Journal Publications

None.

A. Title of Research Task

Chemical Kinetics Studies of Hydrocarbons from Stratospheric Aircraft

B. Investigators

*Randall R. Friedl
Stanley P. Sander
William B. DeMore
Mail Stop 183-901
Jet Propulsion Laboratory
National Aeronautics and Space Administration
4800 Oak Grove Drive
Pasadena, CA 91109

C. Research Objectives

Non-methane hydrocarbons are significant constituents of aircraft engine exhaust. The primary objective of this task is to study the rates and mechanisms of key elementary gas-phase and gas-surface reactions that relate to the processing of non-methane hydrocarbons in the lower stratosphere. Initially, the focus of this task is directed towards an elucidation of the dominant chemical production and loss processes of peroxyacetyl nitrate (PAN), an important reservoir of odd nitrogen in the atmosphere and a common intermediate in the atmospheric oxidation of small non-methane hydrocarbons.

D. Summary of Progress and Results

A discharge flow-mass spectrometer system has been significantly modified to include (1) a laser induced fluorescence detection system for studies of the gas phase reaction of OH with PAN and (2) a special reactor for studies of heterogeneous processes involving PAN and water ice surfaces.

Results have been obtained for the interaction of PAN with solid water ice and with HCl-doped water ice. These results were obtained by flowing PAN (approximately 0.01 mtorr) through an ice-coated, temperature-controlled (200 K), tubular reactor. Detention of PAN was accomplished by electron-impact mass spectrometry. Detection limits of 1×10^8 and 1×10^9 molecules cm^{-3} were obtained at ion masses (m/e) 43 and 46, respectively.

Uptake of PAN was observed on all ice surfaces studied. The rate of uptake was found to decrease with increasing observation time. We attribute these observations to saturation of the ice surface by PAN. Support for this interpretation was obtained from observations of PAN desorption from the surfaces upon interruption of the external PAN flow into the reactor. The amount of PAN adsorbed on/in the ice was estimated to be less than 1 mg per gram of ice.

In addition to the adsorption process, a slow decay of PAN was observed. A reaction probability of less than 10^{-4} was derived from the experimental data. The addition of HCl into the ice had little effect on the measured reaction probability.

During the year, substantial advances were also made in the construction of an experimental apparatus for studies of PAN photolysis products. A new excimer laser was installed, and a gas handling manifold was designed and constructed. In addition, a gated-pulse counting detection strategy for the PAN photolysis products was devised, and the required hardware components were successfully obtained.

E. Journal Publications

Publications on the results of the interactions of PAN with water ice will be prepared in the coming year.

A. Title of Research Task

Data Management and Meteorological Support for HSRP Aircraft Field Campaigns

B. Investigators

*R. Stephen Hipskind
Patricia Hathaway
Steven E. Gaines
Mail Stop 245-5
Ames Research Center
National Aeronautics and Space Administration
Moffett Field, CA 94035-1000

C. Research Objectives

The focus of this research is to provide mission support for aircraft field campaigns, including both data management and meteorological support. Data management entails providing format standards for data exchange, obtaining and archiving field data, and reproducing the data for distribution. Meteorological support entails obtaining conventional analysis and forecast data for mission planning, as well as obtaining real-time meteorological satellite imagery using the Ames Meteorological Satellite Downlink and Display System.

D. Summary of Progress and Results:

A revised format standards document has been written in the past year in connection with the polar ozone campaigns; these standards will be applied to HSRP campaigns. An agreement with Goddard Space Flight Center and National Meteorological Center has been implemented and tested, whereby NMC data products can be obtained via existing NASA network connections. A new SUN workstation has been purchased to handle the duties of ingesting and archiving the aircraft data during field campaigns.

E. Journal Publications

None.

A. Title of Research Task

The Impact of High Flying Aircraft: Model Studies and Analysis

B. Investigators

*Ivar S. A. Isaksen
Institute of Geophysics
University of Oslo
P. O. Box 1022 Blindern
0315 Oslo 3
Norway

C. Research Objectives

We will use a 2-D global model to study the impact on ozone from a future fleet of high-speed aircraft flying in the stratosphere, and subsonic aircraft flying in the troposphere. Heterogeneous chemistry occurring at high latitudes during periods of PSCs and on a global scale in connection with stratospheric aerosol particles, will be incorporated in the study. Analysis of model results will be performed in order to improve the predictive capability for mid- and high-latitudinal changes in the lower stratosphere.

D. Summary of Progress and Results

The 2-D model used extensively in the past to study the impact of man-made releases of pollutants on ozone is used to study the impact of NO_x emission from high flying aircraft.

Several future scenarios for NO_x emissions, in which the source strength and emission height vary, have been performed. These studies consider gas phase chemistry only. The results show considerable dependence on emission heights. Emissions at 23 km and above show a substantially greater reduction in total ozone than emission at lower heights (below 19 km). Ozone reductions are greatest at northern latitudes, and pronounced throughout the year. This is in contrast to the impact of CFC, for which maximum ozone reductions are found during winter and spring months.

The model has been further developed to include stratospheric heterogeneous reactions. Such reactions are assumed to take place during PSC events at high latitudes, and on aerosols in the stratospheric Junge layer. Reactions included are those between N_2O_5 and HCl, N_2O_5 and water vapor, ClONO_2 and HCl. The ClONO_2 and HCl reaction is important on PSC particles, while the N_2O_5 and H_2O reaction is of particular importance in connection with the Junge layer.

A few test runs of long-term, time-dependent calculations, up to year 2015, in which both heterogeneous chemistry and releases of NO_x from supersonic aircraft released at different altitudes, have been performed. The results indicate that the NO_x impact on the ozone layer could be substantially different when heterogeneous chemistry is included in the calculations compared with instances when it is not. Furthermore, background aerosols affect the ozone reduction from NO_x more than do PSCs, as a result of the different heterogeneous reactions involved. Results indicate that the calculated ozone reductions from high flying aircraft emission could be highly sensitive to the way that heterogeneous processes are included in the models. At present, the calculation of future ozone depletion in which heterogeneous chemistry is included is connected with major uncertainties. The studies will be continued in 1991.

E. Journal Publications

None.

A. Title of Research Task

Modeling of the Stratospheric Effects of Stratospheric Aircraft

B. Investigators

*Vyacheslav U. Khattatov
Evgeny A. Jadin
V. I. Khvorostyanov
M. F. Khaytoudinov
Central Aerological Observatory
3, Pervomayskaya Street
Dolgoprudny, Moscow Region, USSR

S. P. Smyshljaev
V. A. Yudin
Institute for Hydrometeorology
Leningrad, USSR

Michael N. Kogan
Department of Fundamental Research
Central Aerohydrodynamics Institute (TsAGI)
Zhukovsky
Moscow Region
140160, USSR

C. Research Objectives

A global 2-D model with gas-phase chemistry and diabatic circulation is used to study the impact of increased NO_x emission from a possible fleet of supersonic aircraft on the stratospheric ozone layer for NASA scenarios (a) to (f). The influence of the chemical eddies on the simulation is examined. The chemical eddy coefficients, $K_{yy}(\text{O}_x)$, $K_{yy}(\text{NO}_x)$, $K_{yy}(\text{Cl}_x)$, are calculated by using a planetary wave model.

D. Summary of Progress and Results

The renewed interest by the aircraft industry in the development of high-speed aircraft has also brought about a renewed interest in the environmental effects from such aircraft. The numerical assessments of the impact of stratospheric aircraft on ozone layer reduction can be made by using a 2-D model of atmospheric chemistry and circulation. The simulation was conducted for different scenarios taking into account the EI for nitrogen oxides and cruise at Mach speed. The basic results, which were obtained in the Soviet 2-D model, are as follows:

- ozone reduction depends strongly on the fuel composition and the height of emission;
- maximum ozone losses occur at the middle and high latitudes of the northern hemisphere at about a 20-to 25-km level;
- seasonal ozone losses are maximum in the northern hemisphere in springtime.

These assessments were made by using fixed eddy transport coefficients similar to Luther's coefficients. But the influence of chemical eddies on the transport of different species (O_x ,

NO_x , Cl_x) by planetary waves in the stratosphere can cause changes in these assessments. The lifetimes of these families change with height and latitude, while wave disturbances depend on season, so the chemical eddy transport can lead to the redistribution of different species, especially in wintertime. Using the planetary wave model, the chemical eddy coefficients $K_{yy}(\text{O}_x)$, $K_{yy}(\text{NO}_x)$, and $K_{yy}(\text{Cl}_x)$ were calculated. These coefficients have a complex structure. The maxima of K_{yy} 's ($\sim 10^{11} \text{cm}^2/\text{s}$) occur at the middle and high latitudes of the winter stratosphere. The positions of K_{yy} 's maxima are different for different species. The preliminary results of the simulation have shown that the effects of chemical eddies can result in increased NO_2 and ClO concentrations at the high stratospheric latitudes of the northern hemisphere during winter.

For the calculation of heterogeneous reactions in the aircraft wake, it is important to know the characteristics and evolution of ice crystals formed from water vapour emitted by aircraft engines. A 2-D time-dependent model of the turbulent transport of ice crystals has been developed. The model comprises equations for potential temperature and humidity transport and a kinetic equation for a crystal size distribution function. The calculated sizes of crystals are 5-10 micrometers, concentrations $\sim 10 \text{m}^{-3}$, surface areas of about $10^{-4} \text{cm}^2/\text{m}^3$. There is a strong dependence of the temporal evolution of vapor trail on wind shifts.

E. Journal Publications

None.

A. Title of Research Task

Impact of Engine Emissions of a Proposed High-Speed Stratospheric Aircraft Fleet on the State of the Atmosphere

B. Investigators

*Malcolm K. W. Ko
Debra K. Weisenstein
Nien-Dak Sze
Jose M. Rodriguez
Larry W. Knowlton
Atmospheric and Environmental Research, Inc.
840 Memorial Drive
Cambridge, MA 02139

C. Research Objectives

We will examine the impact of the engine emissions of a proposed high-speed stratospheric aircraft (HSSA) fleet on the state of the atmosphere using a suite of 2-D numerical models. Emissions from HSSA will be highly localized and deposited near the tropopause, where they will react chemically with the surrounding ambient air. Proposed model improvements specific to evaluating the impact on ozone of HSSA emissions consist of (1) inclusion of ethane and PAN chemistry, (2) modification the treatment of the NO_y family such that HNO_3 can be transported separately, and (3) increasing the vertical resolution to resolve better the tropopause height and stratosphere-troposphere exchange. The AER 2-D chemistry transport model will be used to investigate the sensitivity of ozone to emissions from HSSA aircraft, including nitrogen oxides, water vapor, carbon monoxide, and hydrocarbons. Calculations will examine the sensitivity of ozone to emissions at different altitudes, to different background atmospheres, and to emissions which vary by season. The AER interactive 2-D model will be used to investigate the response of the radiative balance of the atmosphere to ozone perturbations and to increases in CO_2 , SO_2 , and H_2O resulting from HSCT emissions.

D. Summary of Progress and Results

The AER 2-D chemistry transport model was modified for improved treatment of hydrocarbon chemistry by adding ethane (C_2H_6) and its degradation products, including PAN. The model was also modified to explicitly transport HNO_3 to allow for improved simulation of the behavior of odd nitrogen species important to the HSSA emissions problem. The impact of this model change on the HSCT ozone impact was evaluated and was found to enhance the calculated ozone decrease by a factor of 1.15. These changes were incorporated into the model used for HSCT scenario evaluations.

We performed model calculations to determine the impact on ozone of HSCT emissions from the seven scenarios designated for intercomparison at the January 1991 workshop. These scenarios were designed to evaluate the impact of an HSCT fleet operating at three different altitudes, corresponding to Mach numbers of 1.6, 2.4, and 3.2, and at three different NO_x emission indices (EIs; 5, 15, and 45). These scenarios were run within a year 2015 atmosphere, including subsonic emissions, and compared with the 2015 atmosphere, including subsonic emissions. We also compared them with the 2015 atmosphere, without subsonic emissions, and the year 1985 atmosphere, with and without subsonic emissions (1985 subsonic emissions were assumed to be half of those for 2015).

The stratospheric residence time of injected NO_x was found to be a function of emission altitude. For Mach 1.6, the stratospheric residence time of emitted NO_x was 0.3 years; for Mach 2.4, it was 1.4 years; and for Mach 3.2, it was 1.9 years.

We repeated the baseline runs for 2015 and 1985 and also HSCT case A (Mach 2.4, EI = 15) using heterogeneous chemistry with the reaction $\text{N}_2\text{O}_5 + \text{H}_2\text{O} = \text{HNO}_3 + \text{HNO}_3$ acting on the global aerosol layer with a sticking coefficient of 0.1. With heterogeneous chemistry, the chlorine cycle became the dominant loss mechanism for ozone even at 20 km. The addition of nitrogen oxides from HSCT emissions produced more chlorine nitrate and reduced the chlorine loss cycle, resulting in increased ozone up to 20 km with the case A emissions. (For detailed evaluation of these results, see chapter 5.)

E. Journal Publications

None.

A. Title of Research Task

Plume Chemistry and Dispersion Modeling to Evaluate the Atmospheric Effects of Stratospheric Aircraft

B. Investigators

*Charles E. Kolb
Robert C. Brown
Richard C. Miake-Lye
Manuel Martinez-Sanchez
Aerodyne Research, Inc.
45 Manning Road
Billerica, MA 01821

Martinez-Sanchez is also associated with the Department of Aeronautics and Astronautics, Massachusetts Institute of Technology, Cambridge, MA 02139

Jose M. Rodriguez
Curtis Heisey
Malcolm K. W. Ko
Atmospheric and Environmental Research, Inc.
840 Memorial Drive
Cambridge, MA 02139

C. Research Objectives

The exhaust gases for prospective, advanced high altitude supersonic aircraft will be rich in nitrogen oxides (NO_x), water vapor, sulfur oxides (SO_x), carbon monoxide, condensation nuclei, and other trace species, when compared with ambient stratospheric air. As these exhaust gases mix with the ambient air, a complex series of fluid dynamic and radiative processes will spread the exhaust trail both laterally and vertically and may raise or lower the exhaust plume/ambient mix in altitude. Exhaust plume chemistry will tend to oxidize NO_x to NO_3 , N_2O_5 , and HNO_3 and SO_x to SO_3 ; these oxidative species may, in turn, activate exhaust soot particles to cloud (contrail) condensation nuclei. Wingtip vortices will entrain and confine the exhaust plumes, cooling them by centripetally driven pressure drops. The exhaust water vapor may condense into ice contrails providing active surfaces for environmentally important trace species include HNO_3 , ClNO_3 , N_2O_5 , HCl , H_2SO_4 , etc., changing the chemical speciation in the exhaust perturbed air. Furthermore, contrail particles may grow to sufficient size to settle gravitationally, displacing water and possible other trace species such as HNO_3 to lower altitudes. Since the chemistry and dynamics of the exhaust plume may significantly impact the inputs to large scale 2-D and 3-D assessment models, it is necessary to assess systematically the chemical and physical processes driving the plume and its dispersion. The goal of this project is to model the major physical and chemical processes occurring in the aircraft exhaust plumes, wake vortices, and entrained ambient atmosphere to connect intelligently what will issue from aircraft engine nozzles to large-scale photochemical models of the stratosphere.

D. Summary of Progress and Results

The chemical, radiative, and fluid dynamic processes important to this project divide naturally into three regimes: the exhaust plume region, the vortex wake regime, and the wake dispersion process. During the first year, we have initiated modeling and/or analysis activities in all three areas. The highlights are summarized below.

Exhaust Plumes: The exhaust plume region is modeled with a modified version of the Department of Defense's Standard Plume Flowfield (SPF). This model accepts estimates of the exhaust composition and gas properties at the engine exit plane and calculates the turbulent mixing of the exhaust with the atmospheric freestream using an eddy diffusion mixing model. We modified the normal SPF model by adding an equilibrium condensation model for water vapor (to predict contrail formation) and modifying and upgrading the chemical kinetics data set with finite rate models for NO_x and SO_x oxidation. The water condensation model within SPF successfully reproduces contrail condensation under conditions consistent with the Appleman algorithm developed by the U.S. Air Force. Oxidation of NO_x and SO_x within the plume is jointly driven by non-equilibrium levels of OH radicals exiting the engine (estimated at about 10 ppmv) and O_3 entrained from the atmosphere. Our model for a Mach 2.4 aircraft at 18.4-km altitude predicts that 5% of the NO_x is oxidized to HNO_3 , and 10% of the SO_2 is oxidized to SO_3 (sulfuric acid anhydride) by normal gas phase kinetic processes. While these chemical changes probably do not change subsequent photochemistry significantly, they may lead to significant oxidation/activation of exhaust soot particles, affecting the level of active condensation nuclei available for contrail and stratospheric cloud condensation.

Wake Vortices: An initial analysis of the wake vortex entrainment of the exhaust plumes for HSCT-type aircraft indicates that the wingtip vortex/exhaust plume interaction takes place about 40 wingspans (~1.7 km) behind the aircraft and is probably much stronger than similar phenomena in subsonic aircraft. Centripetal forces in the vortex drive exhaust gases toward a lower pressure regime at the vortex center. The temperature near the vortex center appears to be 5-7°C cooler than equivalent equilibrium mixtures of ambient air and exhaust gases. This temperature differential may lead to contrail formation within the vortices at altitudes and ambient H_2O vapor levels that would not normally permit equilibrium contrail formation. The wake vortex structure can be predicted to last about 0.5 minutes, persisting for 15 to 20 km. The size of the contrail ice particles formed will depend critically on conditions within the wake vortices, including the degree of exhaust concentration, the temperature, and the number of active condensation nuclei. A great deal of effort will be needed to model these parameters accurately.

Wake Dispersion Regime: After the breakup of the wake vortices, the exhaust-rich remnants disperse into the background atmosphere. The time scale for this mixing will be roughly 30 to 3000 seconds after emission. The mixing is affected by small-scale turbulence, wind shear, and buoyancy effects. We have created a far wake Lagrangian box model to simulate this regime. An exponential entrainment model for background air is included, with an initial entrainment time of 780 seconds which dilutes the wake remnants by a factor of 100 in an hour. The Lagrangian box model has a full complement of homogeneous gas phase photochemical processes as well as parameterized polar ozone heterogeneous processes for reservoir C1 and NO_x species. Initial model runs indicate that no surprising chemical transformations occur without the presence of persistent contrails. If persistent contrail particles are present, a large amount of HNO_3 is created over a one hour time scale, via N_2O_5 reaction with condensed ice particles. When this HNO_3 is released to the gas phase via particle evaporation, its photodissociation can lead to OH levels significantly higher than that found in unperturbed background air.

E. Journal Publications

R.C. Miake-Lye, R.C. Brown, M. Martinez-Sanchez, and C.E. Kolb, Plume and wake dynamics, mixing, and chemistry behind an HSCT aircraft, to be submitted to *J. Aircraft*.

A. Title of Research Task

Laboratory Studies of Heterogeneous Processes Important in Stratospheric Aircraft Emissions

B. Investigators

*Ming-Taun Leu
Leon F. Keyser
Liang Chu
Mail Stop 183-901
Jet Propulsion Laboratory
National Aeronautics and Space Administration
4800 Oak Grove Drive
Pasadena, CA 91109

C. Research Objectives

This task focuses on heterogeneous processes that are potentially important in assessing the environmental impacts of high-altitude aircraft emissions. The work aims to investigate the effects of water ice, nitric acid trihydrate, sulfuric acid aerosol, and soot on atmospheric species important in the ClO_x , NO_x , and HO_x cycles that include: HCl , ClO , ClONO_2 , NO , NO_2 , O_3 , N_2O_5 , HNO_3 , OH , HO_2 , H_2O_2 , and SO_2 . Flow reactor mass spectrometry and discharge flow resonance fluorescence are used to measure sticking or reaction probabilities on these aerosols. Several analytical techniques, which include mass spectrometry, chloride ion electrode, infrared absorption, electron microscopy, X-ray diffraction and BET surface area analysis, are employed to identify products and characterize the condensed phase.

D. Summary of Progress and Results

The heterogeneous reactions, $\text{ClONO}_2 + \text{HCl} \rightarrow \text{Cl}_2 + \text{HNO}_3$ (1) and $\text{ClONO}_2 + \text{H}_2\text{O} \rightarrow \text{HOCl} + \text{HNO}_3$ (2), on vapor-deposited $\text{HNO}_3\text{-H}_2\text{O}$ ice substrates have been investigated at 196 K by using a fast flow reactor coupled with a quadrupole mass spectrometer. The reaction probability for (1) is 0.10 ± 0.02 and independent of both the HNO_3 and HCl concentrations in the substrate compositions studies. For (2), the reaction probability is approximately 1×10^{-5} near 53.8 wt% HNO_3 , the composition of pure nitric acid trihydrate, and is about 1×10^{-3} at 45 wt% HNO_3 . The sticking coefficient of HCl on these substrates was also found to be a strong function of the substrate composition, ranging from less than 1×10^{-5} (>55 wt% HNO_3) to 5×10^{-3} at 45 wt% HNO_3 .

In addition, infrared spectra of nitric acid trihydrate and nitric acid monohydrate using Fourier transform infrared spectroscopy, were also investigated.

E. Journal Publications:

Moore S. B., L. F. Keyser, M-T Leu, R. P. Turco, and R. H. Smith, Heterogeneous reactions on nitric acid trihydrate, *Nature*, 345, 333, 1990.

Keyser, L. F., S. B. Moore, and M-T. Leu, Surface reaction and pore diffusion in flow-tube reactors, in press.

Smith, R. H., M-T. Leu, S. B. Moore, and L. F. Keyser, Infrared spectra of solid films formed from vapors containing water and nitric acid, in press.

Leu, M-T., S. B. Moore, and L. F. Keyser, Heterogeneous reactions of chlorine nitrate and hydrogen chloride on nitric acid-ices, in press.

A. Title of Research Task

Determination and Assessment of Emission Scenarios for the Program on Atmospheric Effects of Stratospheric Aircraft

B. Investigators

*Richard C. Miake-Lye
Alan H. Epstein
Charles E. Kolb
Aerodyne Research, Inc.
45 Manning Road
Billerica, MA 01821-3976

A. Epstein is also associated with the
Department of Aeronautics and Astronautics
Massachusetts Institute of Technology
Cambridge, MA 02139

C. Research Objectives

Predictive modeling of the dispersal and reaction of stratospheric pollutants must be based on reliable projections of combustion emissions. An independent review and assessment of current efforts at NASA and industry combustor research centers will be directed toward supplying relevant projected emission data to the plume modeling effort. Current progress and future trends will be assessed for the control of critical exhaust species, as required by the concurrent modeling activity. A supplementary analysis stage will facilitate the integration of the emission data into the modeling by identifying pollution chemical mechanisms to which the models may be particularly sensitive. Such integrations will tie the required emission scenario data to the needs of the plume modeling efforts and global stratospheric models.

D. Summary of Progress and Results

Contact was established with propulsion research laboratories, HSRP workshops were attended to collect data on emissions from proposed HSCT engines. Emissions estimates were obtained for NO, NO₂, CO, CO₂, H₂O, and SO₂ as well as particulates and unburned hydrocarbons from both GE Aircraft Engines and Pratt & Whitney. These estimates are based on correlations developed using measurements of existing engines and their components, which are extended to HSCT engine operating conditions. MTU Motoren-und Turbinen Union of Germany provided estimates of NO_x, CO, and unburned hydrocarbons emissions based on their ongoing studies of HSCT engines.

These estimates were described in a report to be included as a chapter of the HSRP annual report. This chapter summarizes relevant earlier work dating back to the Climatic Impact Assessment Program (CIAP) studies of the early 1970s, and as well as the current propulsion research efforts. The recent work provides estimates of the chemical composition of an HSCT's exhaust, and these estimates are reported as EIs. Other aircraft emissions that are not due to combustion processes are also summarized; these emissions are much smaller than the exhaust emissions. Future advances in propulsion technology, in experimental measurement techniques, and in understanding of upper atmospheric chemistry may affect these estimates of the amounts of trace exhaust species, or their relative importance, and revisions may well become necessary in the future.

E. Journal Publications:

Miake-Lye, R.C., R.C. Brown, M. Martinez-Sanchez, and C.E. Kolb, Plume and wake dynamics, mixing, and chemistry behind an HSCT aircraft, to be submitted to *J. Aircraft* (1991).

A. Title of Research Task

Laboratory Studies of Stratospheric Aerosol Chemistry

B. Investigators

*Mario J. Molina
Atmospheric Chemistry, 54-1320
Department of Earth, Atmospheric, and Planetary Sciences
Massachusetts Institute of Technology
Cambridge, MA 021139

C. Research Objectives

Aerosols with sizes and compositions similar to those of stratospheric particles will be generated by the "diffusive trapping" technique: the gaseous aerosol precursors will be injected into a chamber containing an inert gas at moderate pressures and low temperatures. The physical characteristics of the aerosols will be determined by monitoring the absorption and Mie scattering of laser radiation. The chemical composition of the system will be studied using Fourier transform infrared spectroscopy and mass spectrometry. The uptake of HCl vapor and the chemical reactivity toward ClONO_2 and N_2O_5 will be investigated for water-ice crystals and for various hydrates of nitric and sulfuric acid.

D. Summary of Progress and Results

The aerosol chamber used in conjunction with the "diffusive trapping" technique has been designed and constructed. It is now being tested, together with the FTIR spectrometer to which it is attached. Ice particles in the 5 micron size range are being generated; their infrared spectra are successfully being recorded.

Initial survey experiments were carried out to characterize the aerosol particles using a He-Ne laser large-angle scattering technique. To better establish the concentration and size distribution of the particles, a commercial particle size distribution analyzer was acquired (Malvern MS1000), which incorporates the appropriate computer and software analysis package; it also operates using Mie scattering of laser radiation, but at small scattering angles. The aerosol chamber has been modified and coupled to the particle analyzer.

Experiments with injectors of various designs are being carried out to generate aerosol particle populations with the desired sizes and narrow size distribution.

E. Journal Publications

None.

A. Title of Research Task

Real Time Measurement of the Composition of Individual Aerosol Particles with a Mass Spectrometer

B. Investigators

*Daniel M. Murphy
Adrian Tuck
Aeronomy Laboratory
National Oceanic Atmospheric Administration
325 Broadway
Boulder, CO 80303

C. Research Objectives

Aerosol particles are important to both the chemistry and radiative processes in the lower stratosphere. High-speed aircraft would emit SO₂, water, soot, trace metals, and other effluents that could influence aerosol processes. We are constructing a laboratory instrument for particle analysis by laser mass spectrometer (PALMS). It will measure the trace and bulk composition of individual, sized aerosol particles. This will allow better understanding of the origins, chemistry, and radiative properties of aerosol particles. The instrument uses light scattering to identify and size aerosol particles. A pulsed laser is then triggered for single-shot desorption and ionization of the aerosol particle. A time-of-flight mass spectrometer is used to record the entire ion mass spectrum. Recent improvements in the design of time of flight mass spectrometers, the technology of compact, powerful lasers, and high-speed electronics make it practical to build a laser ionization mass spectrometer that can be taken into the field. The laboratory instrument is being constructed using technology that can be easily adapted to an aircraft instrument.

D. Summary of Progress and Results

The year 1990 was one of design and construction. The scientific design of the mass spectrometer was completed. A custom time-of-flight mass spectrometer with pulse focusing in

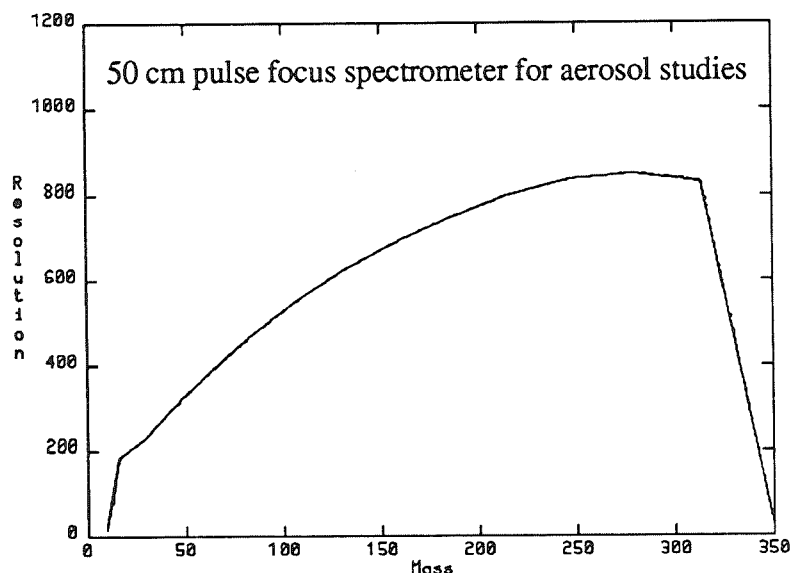


Figure 1. Resolution of mass spectrometer as a function of mass.

the drift region, was selected. It uses a 50-cm path for ease of future aircraft installation. Computer simulations predict a resolution of over 300, even for very hot ions and a 150-ns-long ionization pulse.

The optical system for imaging the lasers on the ion source region, the vacuum system, and much of the data acquisition system have been constructed and tested.

We also completed feasibility experiments, funded by NOAA, in conjunction with the University of Colorado. These experiments were designed to demonstrate the concept of single-particle analysis and to provide data to aid in the design of the PALMS instrument. While the laser and mass spectrometer used in these experiments were not optimal, they still showed an excellent signal-to-noise ratio for individual-particle analysis. We were also able to verify significant portions of the computer code used to design the new instrument. Sample data from the feasibility experiments are shown below.

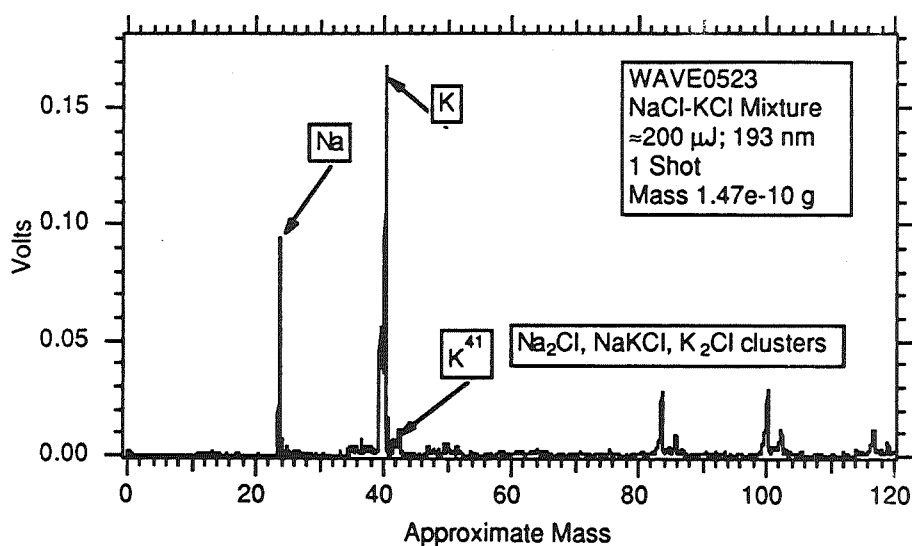


Figure 2. Mass spectrum of a single salt aerosol approximately 6 μm diameter.

E. Journal Publications

None.

A. Title of Research Task

Optically Absorbing Aerosols in the Lower Stratosphere

B. Investigators

*Rudolf F. Pueschel
Kenneth G. Snetsinger
Mail Stop 245-4
Ames Research Center
National Aeronautics and Space Administration
Moffett Field, CA 94035-1000

Anthony D. A. Hansen
Mail Stop 70A-3363
Lawrence Berkeley Laboratory
University of California, Berkeley
1 Cyclotron Road
Berkeley, CA 94720

C. Research Objectives

The objectives are (1) to establish a "baseline" value of current stratospheric burden of light-absorbing aerosol, (2) to compare this measurement with observations of light extinction and absorption of the past, and (3) to use this value to assess future perturbations by, e.g., supersonic commercial air transport. The approach is to apply aerosol light-absorption techniques to stratospheric aerosol samples collected aboard the NASA ER-2 high-altitude aircraft.

D. Summary of Progress and Results

During 1990 we collected aerosol samples by Lambertian impactors mounted on the left wingtip of the ER-2 aircraft. Analyses of these samples yielded a mean loading of light absorbing aerosols of 2.0 ± 0.8 ng per standard cubic meter, corresponding to an absorption coefficient of $2.0 \pm 0.8 \times 10^{-8}$ per meter. These results are similar to those obtained by Clarke et al. (*Geophys.Res.Lett.*, 10, 1017, 1983). In connection with total extinction measurements by the SAGE II sun photometer, and/or computed from total aerosol size distributions sampled aboard the ER-2 (Oberbeck et al., *J. Geophys. Res.*, 94, p.8367, 1989), the single scattering albedo of the lower stratospheric aerosol is larger than 0.99. These measurements constitute a beginning for setting a "baseline" for concentration and effects of light absorbing in the stratosphere.

E. Journal Publications

None.

A. Title of Research Task

The Environmental Impact of High-Flying Aircraft Studied Using Two-Dimensional Models

B. Investigators

*John A. Pyle
Anna E. Jones
Department of Chemistry
University of Cambridge
Lensfield Road
Cambridge, CB2 1EP
United Kingdom

*Robert S. Harwood
J. Kinnersley
Department of Meteorology
University of Edinburgh
King's Buildings
Edinburgh, EH9 3JZ
United Kingdom

C. Research Objectives

The likely impact of proposed fleets of high-speed civil aircraft on stratospheric composition will be assessed using enhanced versions of a 2-D model derived from the early Harwood-Pyle model. The chemical aspects of this model will be further developed by the Cambridge group, including parameterization of the effects of heterogeneous chemistry, while the Edinburgh group will improve the dynamical formulation, principally by recasting the model to have specific entropy as a quasi-Lagrangian vertical coordinate. Chemical perturbation studies will be carried out using the same chemistry in both dynamical formulations, so as to test the sensitivity of the predicted effects of pollution to the dynamical formulation.

D. Summary of Progress and Results

The Cambridge group has carried out experiments to assess the effects of High-Speed Civil Transports (HSCT's) assuming homogeneous chemistry, using the Eulerian model. This has dynamics as in the original Harwood and Pyle model (see *Quart. J. R. Met. Soc.* 106, p.395, 1980, and references therein). The chemical and radiation schemes have been considerably advanced since the early formulation (see, e.g., *Nature*, 329, p.616 1987, and references therein).

Three experimental cases were considered corresponding to HSRP scenarios (a), (g), and (f). These consisted of a latitudinally varying subsonic and supersonic fleet, the supersonic transports (SST_s) emitting NO_x (emissions index=15), and water vapor. The effect of flying at different altitudes was examined. The altitude ranges specified in the experiments corresponded to 14-17.5 km (scenario g), 17.5-21 km (scenario f). Instantaneous mixing in each model box was assumed. A baseline scenario, equivalent in every respect apart from the fact that it contained a subsonic fleet only, was run in parallel to the experiments; all were run out to steady state. The background atmosphere corresponded to the year 2015, in terms of trace gas concentrations specified by suitable boundary conditions.

Results from the three experiments, when compared to the baseline run, show a marked decrease in ozone concentration in the stratosphere, especially at high latitudes of the northern hemisphere. (For more detailed results and evaluation see chapter 5.) The results also predicted that NO_x from SST engines could be transported down into the troposphere, with consequent production of ozone through methane oxidation reactions.

Some preliminary results have been obtained for runs containing a simplified treatment of heterogeneous chemistry.

The revision of the model dynamics has been completed by the Edinburgh workers to the stage where a dynamics-only versions of the entropy coordinate model has been run for several years. In these runs, essential dynamical fluxes (such as the poleward flux of potential vorticity) have been specified based on observations or parameterized in a very much simplified way. Early indications are that realistic simulation of the zonal mean distributions of wind and temperature can be obtained in the new formulation and that some undesirable features of the previous Eulerian model, namely excessive troposphere-stratosphere exchange, are less severe in the new version.

In the coming year, this work will be consolidated by introducing the chemical routines to the new dynamical model and by further developing the parameterized treatment of eddy transports.

E. Journal Publications

None.

A. Title of Research Task

Three-Dimensional Transport of Emission Products from High Speed Stratospheric Aircraft by Large Scale Winds: Construction of Appropriate Source Functions for 2-D Assessment Models

B. Investigators

*Hans R. Schneider
Malcolm K. W. Ko
Run-Lie Shia
Atmospheric and Environmental Research, Inc.
840 Memorial Drive
Cambridge, MA 02139

C. Research Objectives

Emissions from high speed stratospheric aircraft are localized sources of tracer material for the stratosphere. Within 10 to 20 days after emission, the material is redistributed zonally, as well as latitudinally, by the large-scale wind field. For the assessment of the long-term impact of high-altitude flights, source functions for 2-D assessment models are needed that take the initial redistribution into account. We study the large-scale redistribution, using an isentropic transport model, assuming that for time periods of the order of 20 days, the material stays on the isentropic surface on which it was deposited. The isentropes and the winds on the isentropic surfaces are determined from 8 years of National Meteorological Center daily temperature and geopotential height analyses extending from 1000 to 0.4 mb. Balanced winds are used. By calculating the initial transient adjustment of the tracer field for a large number of episodes and different flight paths, appropriate average source functions for 2-D models for different times of the year will be constructed. Sensitivity studies for small-scale diffusion and motion through the isentropes will be done; we will also examine the resolution needed to describe adequately tracer transport in the lower stratosphere. For these sensitivity studies, we plan to utilize model winds from a high resolution General Circulation Model.

D. Summary of Progress and Results

We have adapted our 3-D transport model, which utilizes the square root scheme to calculate transport on isentropic surfaces. So far, we have selected and studied three episodes: the winter of 1979 (late December 1978 and the first half of January 1979) and two summer cases, June of 1982 and June of 1985. The winter case was selected, because it has been used in many modeling studies before and is characterized by a large wave number, one that did not lead to a warming during the time under consideration. The summer cases were used because the data record was complete for those periods, and the winds for the two summer periods are different from each other. Transport studies were done on the 500 K isentropic surface (average height, 20.5 km) and the 380 K surface (average height, 16.5 km). Two different source distributions were used, a zonally symmetric source, centered at 50° N and a strip-source extending from 20° N across the pole to 20° N.

Our preliminary results indicate that the latitudinal transport by large-scale winds is important not only in the winter, but in the summer cases as well. If zonal averages of the tracer mixing ratio are calculated, the latitudinal gradient north of 40° N vanishes after about 10 days in the winter and after 20 days in the summer cases considered. In all cases, the tracer distribution becomes zonally homogeneous, to a great extent after 10 to 15 days. Variations along longitude circles are typically of the order of 30%. The latitudinal redistribution of the

tracer material occurs faster than is achieved by the typical latitudinal diffusion specified in 2-D models. This is because the 2-D diffusion coefficients are determined for tracer distributions that are already large scale and equilibrated with the flow field. The initial, transient redistribution of localized injections acts on a faster time scale.

These first calculations were done with a relatively coarse resolution in the transport ($3 \times 5^\circ$), and the 380 K surface may not be that relevant for the HSRP problem. Experiments with higher resolution and narrower sources are in progress.

E. Journal Publications

None.

A. Title of Research Task

Model and Measurements Data Base for Stratospheric Aircraft Assessments

B. Investigators

Robert K. Seals, Jr.
Mail Stop 401A
Atmospheric Sciences Division
Langley Research Center
National Aeronautics and Space Administration
Hampton, VA 23665-5225

C. Research Objectives

A fundamental requirement of the Atmospheric Effects of Stratospheric Aircraft (AESA) program is the capability to assimilate model predictions and measurement data to understand the response of the atmosphere to potential aircraft emission scenarios. This task is focused on compiling, distributing, intercomparing, and archiving these data sets, in support of AESA studies and of associated workshops and intercomparison activities. Emphasis is on assembling model prediction results and pertinent measurement data sets; making them available in a coherent electronic format; and supporting the intercomparison, manipulation, and display of key parameters. The approach is to augment activities of the existing Upper Atmosphere Data Program (UADP), funded through the NASA Upper Atmosphere Theory Program.

D. Summary of Progress and Results

Primary emphasis in 1990 was on assembling a workstation system capable of (1) providing required data storage, manipulation, and display capacity and (2) transported to meeting sites to provide real-time data support for workshops. A SUN-based high-resolution color display system with 1.4 GByte magnetic disk, rewritable optical disk storage, and both laser printer and high-resolution color plot output was implemented. It is electronically networked via both Decnet and TCP/IP protocols to the existing UADP computer and to other sites.

In the latter part of 1990, preparations were begun to support the initial phase of model emission scenario calculations. The standard data grid and data file format developed as part of previous 2-D model intercomparison activities were adopted to facilitate data comparison. Work was also initiated on transporting existing data sets to the workstation system. Zonal mean data sets from the Limb Infrared Monitor of the Stratosphere, Stratospheric and Mesospheric Sounder, and Solar Backscatter Ultraviolet Radiometer experiments have been completed thus far.

E. Journal Publications

None.

A. Title of Research Task

Heterogeneous Chemistry Related to Stratospheric Aircraft

B. Investigators

*Margaret A. Tolbert
Mail Stop PSO39
Chemistry Laboratory
SRI International
333 Ravenswood Avenue
Menlo Park, CA 94025

David M. Golden
Mail Stop PSO31
Chemistry Laboratory
SRI International
333 Ravenswood Avenue
Menlo Park, CA 94025

C. Research Objectives

We are performing laboratory experiments aimed at characterizing nitric acid/ice films representative of PSCs. Specifically, we are developing experiments to measure the composition, formation rates, and evaporation rates of model PSC surfaces. Our goal is to determine the conditions under which PSCs form so that we can accurately predict the effects of HSCTs on PSC abundances.

D. Summary of Progress and Results

Model PSC films are grown by dosing calibrated mixtures of nitric acid and water onto a support surface held at low temperature. The films are probed in real time during growth using in situ Fourier transform infrared (FTIR) absorption. Depending on experimental conditions, we are able to make either amorphous solid solutions of nitric acid in ice, or crystalline nitric acid hydrates. Film thicknesses, d , are determined from the optical interference of the infrared radiation using $d = m\lambda/2\eta$, where m is a positive integer, λ is the wavelength of light, and η is the refractive index of the material. Thicknesses determined in this way are used to obtain absolute calibrations of the infrared absorption intensities for the various peaks of the nitric acid/ice films.

Film stoichiometries are obtained using temperature-programmed desorption (TPD), in which the film is rapidly heated and gaseous HNO_3 and H_2O are observed mass spectrometrically. After calibrations of the mass spectrometer sensitivity for HNO_3 and H_2O , ratios of $\text{H}_2\text{O}/\text{HNO}_3$ in the film are obtained from the relative mass spectrometer signals during film evaporation. Using this technique, we have identified three stable hydrates of nitric acid: NAT, nitric acid dihydrate (NAD), and nitric acid monohydrate (NAM).

In addition to measuring the evolved gases during a TPD experiment, we are able to probe the condensed phase in real time during evaporation using FTIR spectroscopy. This results in a so-called temperature-programmed infrared (TPIR) curve for each evaporation experiment. The infrared spectra are used to probe for any changes in the crystal structure that occur during annealing and subsequent desorption.

The combination of TPD and TPIR techniques has allowed us to distinguish between amorphous and crystalline forms of nitric acid/ice. Vapor condensation at lower temperatures ($\leq -110^{\circ}\text{C}$) results in the formation of amorphous films. Upon annealing, these amorphous films crystallize into nitric acid hydrates, which have different infrared spectra. The TPD measurements indicate that no evaporation occurs during this annealing to crystalline hydrates. Condensation of nitric acid and water at temperatures between -105 and -90 C results in crystalline NAM, NAD, and NAT films whose spectra are identical to those obtained from annealing low temperature films. TPIR spectra indicate that upon further annealing of crystalline NAT, a second phase change occurs prior to film evaporation. Crystalline NAD and NAM show no such second phase change upon annealing.

We are currently performing experiments to determine which type (or types) of nitric acid/ice are likely to form under a range of stratospheric conditions.

E. Journal Publications:

Koehler, B.G., A.M. Middlebrook, and M.A. Tolbert, Characterization of model polar stratospheric cloud films using Fourier transform infrared spectroscopy and temperature programmed desorption, submitted to *J. Geophys. Res.*

A. Title of Research Task

Investigation of High-Altitude Aircraft Plumes and Contrail: Physical and Chemical Processes and Global Implications

B. Investigators

*Richard P. Turco
Department of Atmospheric Sciences
University of California, Los Angeles
Los Angeles, CA 90024-1565

Owen B. Toon
Mail Stop 245-3
Earth System Sciences Division
Ames Research Center
National Aeronautics and Space Administration
Moffett Field, CA 94035-4000

C. Research Objectives

A physical/chemical model describing the evolution and chemical effects of contrails formed behind HSSA will be developed. The model treats the formation and growth of ice particles in an aircraft plume, and the chemical processing that occurs on the ice and other aerosols. An existing microphysics model for noctilucent (mesospheric) and PSCs provides the basis for the simulation. Processes that are treated in detail include water vapor nucleation to ice, condensational growth and evaporation of ice crystals, the behavior of the soot aerosol in the presence of ambient sulfate particles, and the heterogeneous chemical processing of trace gases on ice and on other aerosols, including soot and sulfates. Sensitivity tests will be used to investigate uncertainties in the predictions and identify parameters that require greater accuracy. Computational results will be used to quantify important effects including: the perturbation of the chemical composition of the lower stratosphere caused by aircraft activity, including effects of injected water vapor, soot particulates, and chemical transformations in the contrails (e.g., chlorine activation and de-NO_x-ification); the impact of contrails and exhaust products on the radiation budgets of the stratosphere and troposphere; and possible climatic implications. Distinct chemical and physical signatures of the aircraft plume will be sought to aid in the design of field experiments to study the impacts of high-altitude flight.

D. Summary of Progress and Results

A microphysics/physical-chemistry model has been developed to simulate the formation, evolution, and composition of high-altitude aircraft contrails. The model can simulate stratospheric contrails that might be formed with various engine designs and operational conditions, as well as investigate the sensitivity of contrail formation and effects to key physical and chemical parameters. The model will be used to (1) estimate the degree of chemical processing that occurs in expanding aircraft plumes through ice-catalyzed reactions and chemical reactions on other aerosols that could be present in the plumes and (2) analyze contrail simulations, in light of field and laboratory data to identify the key potential environmental impacts, useful observational diagnostic parameters, and major sources of uncertainty. During the first six months of the project (covered by this report), we have focused on three specific research areas: nucleation phenomena in aircraft exhaust plumes, ice microphysics in contrails, and heterogeneous reactions on aerosols perturbed by aircraft effluents.

Nucleation Phenomena: We have developed new, highly efficient algorithms for calculating the nucleation rates of ice crystals and sulfuric aerosols in aircraft contrails. Ice crystals are the principal particulate in aircraft wakes because of the high-water-vapor content of the exhaust. We have constructed a fast algorithm for calculating the ice nucleation rate on soot particles emitted by the aircraft engines. Both homogeneous ice nucleation and heterogeneous nucleation on existing particles are considered, since these processes are competitive. A numerically accurate and fast method of calculating the sulfuric acid particle nucleation rate under conditions expected in an aircraft exhaust stream has been formulated. In particular, the nucleation rate is calculated for assumed concentrations of H_2SO_4 in the exhaust stream, on the assumption that a small fraction of the fuel sulfur is oxidized by radicals into sulfuric acid. Similar algorithms have been employed to compute the rates of competitive nucleation processes in the far-wake environment, including homogeneous heteromolecular and heterogeneous heteromolecular nucleation of sulfuric acid; preliminary results were presented at the HSRP January meeting. We plan to utilize the nucleation models to compute the acid nucleation rates on soot particles for a range of reasonable values for the soot properties (size distribution--from test data and surface morphology--from independent laboratory investigations). We will compare predictions of nucleation rates with observed contrail particulate concentrations, sizes and compositions, particularly regarding the relative number of ice crystals and volatile and nonvolatile condensation nuclei.

Ice Microphysics: A physical/chemical model for the evolution and chemical effects of contrails formed behind HSSA will soon be operational. We are currently developing data on specific engine effluents and an empirical model for the temperature and mixing history of the plume to drive the microphysics model. The contrail model will include water vapor nucleation processes, condensational growth and evaporation of ice crystals, soot aerosol and ambient sulfate particle effects, and heterogeneous chemical processing of trace gases on ice and on other aerosols. It is important to specify the microphysical processes in detail in order to place realistic limits on the surface areas available for chemical processing and the duration of the processing. To date, no comparable detailed microphysical simulations of aircraft contrails have been made available.

We are currently adding heterogeneous chemical processes to the ice contrail model. The formation of contrails and possible heterogeneous chemical processing on the ice particles represent important uncertainties in the impacts of high-altitude aircraft on the stratosphere. Planned investigations include: simulations of coupled contrail physics and chemistry, to identify the critical processes leading to chlorine activation on ice particles that might lead to ozone depletion; sensitivity tests to investigate uncertainties in the predictions and identify physical and chemical parameters that require experimental refinement; analyses to quantify important effects such as the impact of contrails and exhaust products on the radiation budgets of the stratosphere and troposphere and associated climatic implications, and on perturbations of the chemical composition of the lower stratosphere; assessment of the chemical and physical signatures of high-altitude aircraft plumes, to aid in the design of field experiments to study the impacts of high-altitude flight.

Heterogeneous Chemistry: The heterogeneous chemistry of ice particles in aircraft contrails is being developed along two lines. For macroscopic calculations, we are treating ice processing in terms of mass transfer rates between the gas and particulate phases using laboratory measurements of reaction efficiencies on ice. We are also developing basic microscopic models of heterogeneous physical and chemical processes on ice surfaces and in bulk ice based on surface physics and the interpretation of laboratory observations. The latter models will provide a critical interface between laboratory investigators on the one hand and atmospheric photochemical modelers on the other.

Project Personnel at UCLA (including part-time appointments)

Prof. Richard Turco (UCLA, Principal Investigator)

Prof. Patrick Hamill (San Jose State University, Consultant on nucleation and micro-physics)

Dr. Scott Elliott (UCLA, Postdoctoral Researcher)

Katja Drdla (UCLA, Graduate Student)

Azadeh Tabazadeh (UCLA, Graduate Student)

Jingxia Zhao (UCLA, Graduate Student)

E. Journal Publications

Drdla, K., High-Speed Stratospheric Aircraft: New Factors Affecting their Climatic Effect, draft paper (1991).

Zhao, J., Homogeneous Nucleation Algorithms for Aircraft Plume Modeling, draft report (1991).

Drdla, K., and R. P. Turco, Denitrification through PSC formation: A 1-D model incorporating temperature oscillations, *J. Atmos. Chem.*, in press (1990).

Elliot, S., R. P. Turco, O. B. Toon, and P. Hamill, Application of physical absorption thermodynamics to heterogeneous chemistry on polar stratospheric clouds, in preparation (1990).

Turco, R., P. Hamill, and O. Toon, Chlorine activation on sulfate in the pre-winter stratosphere, draft manuscript (1991).

Turco, R. P. , S. Elliott, O. B. Toon, and P. Hamill, On the nucleation of polar stratospheric clouds and their relationship to the polar, *Geophys. Res. Lett.*, 17, 425-428 (1990).

A. Title of Research Task

Counting Particles Emitted by Stratospheric Aircraft and Measuring Size of Particles Emitted by Stratospheric Aircraft: Instrument and Development

B. Investigators

*James C. Wilson
Charles Brock
Department of Engineering
University of Denver
Denver, CO 80208-0177

C. Research Objectives

Most of the particles emitted by aircraft engines are smaller in diameter than $0.1 \mu\text{m}$. Currently there are no instruments on the ER-2 capable of continuously measuring the size distribution of particles smaller than $0.1 \mu\text{m}$. The primary purpose of this research is to evaluate techniques for measuring size distributions in this size range. A program to develop the best technique into an ER-2 instrument is to be proposed. The resulting instrument will be used to determine the impact of particles emitted by jet engines on the stratospheric aerosol. A second objective, undertaken after an HSRP workshop, is to develop a device that would serve as a soot detector.

D. Summary of Progress and Results

The evaluation of candidate measurement techniques has focused on physical size segregation methods to be used upstream of the ER-2 condensation nucleus counter (CNC). These techniques include diffusion batteries, differential mobility analyzers, and low-pressure impactors. Each technique has a size-dependent particle removal mechanism that allows certain particles to pass and removes others. The size dependence of the removal mechanisms can be altered by changing some parameter of the system. The concentration of particles reaching the ER-2 CNC for differing removal characteristics is measured. This instrument response contains information about the aerosol size distribution and must be inverted to determine the size distribution. Thus, each technique consists of a physical particle removal mechanism and a data inversion technique: they are being examined together to find the most appropriate technique.

Although the differential mobility analyzer has very good resolution, uncertainties about charging at low pressures makes that technique risky at present. Low pressure impactors that have good resolution for small particles have recently been developed. However, their performance is not well enough understood at this time to permit them to be extended over the desired size and pressure range. The diffusion battery is well understood and is easy to implement, but often has poor resolution. Inverting diffusion battery data by the Maximum Entropy Technique shows some promise, and numerical experiments suggest that careful design of the diffusion battery and careful data inversion permit this technique to achieve the desired accuracy and resolution for the expected size distributions.

A candidate optical detection technique is being developed by PMS in Boulder, CO. This system will be compared with the ER-2 CNC-based techniques before a sizing instrument is proposed.

A soot detection scheme was presented at an HSRP workshop and will be proposed.

E. Journal Publications

None.

A. Title of Research Task

Development of a High-Sensitivity Fast Response Instrument for In Situ Determination of CO₂

B. Investigators

*Steven C. Wofsy
Room 100A, Pierce Hall
Department of Earth and Planetary Science
Harvard University
29 Oxford Street
Cambridge, MA 02138

Darin W. Toohey
Atmospheric Research Project
Engineering Science Laboratory
Harvard University
40 Oxford Street
Cambridge, MA 02138

Ralph Keeling
Atmospheric Chemistry Division
National Center for Atmospheric Research
P. O. Box 3000
Boulder, CO 80307

C. Research Objectives

This grant was provided to test and build a CO₂ sensor for the ER-2 aircraft.

D. Summary of Progress and Results

Selection and primary testing of components for this instrument is nearly complete. It was found that a commercially available instrument from LICOR Corporation could, with suitable modification, be used as the CO₂ detector. The modifications of the first unit are in progress. A constant-pressure system for atmospheric sampling is in the design verification phase, with testing scheduled for April 1991. A data acquisition system is in the design phase.

Delivery of a flight-testable prototype was originally proposed for December 1991. Since the last chance to flight test on the ER-2 for the Arctic mission is August 20, 1991, we are attempting to speed up the process, but the likelihood that we will meet this deadline is still less than 25%.

E. Journal Publications

None.

A. Title of Research Task

Heterogeneous Chemistry Related to Stratospheric Aircraft

B. Investigators

*Douglas R. Worsnop
Mark S. Zahniser
Aerodyne Research, Inc.
45 Manning Road
Billerica, MA 01821

Steven C. Wofsy
Room 100A, Pierce Hall
Department of Earth and Planetary Science
Harvard University
29 Oxford Street
Cambridge, MA 02138

P. Davidovits
Boston College
Chestnut Hill, MA 02167

C. Research Objectives

Assessment of the potential impact of HSCT aircraft on stratospheric photochemistry requires detailed understanding of heterogeneous chemistry on aerosols, on ambient (background) particles as well as on potential aircraft induced (contrail) particles. This project involves a laboratory program that focuses on experimental measurements of two aspects of heterogeneous chemistry: (1) aerosol formation/composition and (2) kinetics of gas/surface interactions. In particular, thermodynamic properties of the H₂O/HNO₃/HCl gas/solid phase diagram will be determined via vapor pressure measurements at stratospheric temperatures and densities. This involves infrared absorption measurements in a temperature-controlled cell. In separate laboratory experiment, studying gas/liquid droplet interactions, the kinetics of gas uptake and reactivity of HNO₃, HCl, N₂O₅, and ClONO₂ will be measured on cold sulfuric acid droplets, which are representative of the background stratospheric aerosol.

D. Summary of Progress and Results

H₂O/HNO₃ Vapor Pressures over Nitric Acid Trihydrate: The vapor phase diagram of H₂O/HNO₃ mixtures has been determined using a new apparatus based on gas density measurement via molecular infrared optical absorption. A temperature-regulated cell containing a multiple-pass absorption cell is coupled with a tunable infrared diode laser. Vapor pressure measurements in the temperature range 194-217 K agree well with previous results of Hanson and Mauersberger (1988). At stratospheric gas density and pressure, these vapor pressure curves correspond to gas equilibration with solid NAT, as indicated by the vapor pressure relationship, $P_{\text{H}_2\text{O}} P_{\text{HNO}_3} = K_T$.

Gas/surface equilibration is easily perturbed by small additions of H₂O or HNO₃ vapor. This indicates that equilibration of the surface and interior within the solid sample is limited by solid diffusion, which is much slower than gas/surface equilibration. This equilibration of the solid composition takes 10⁴-10⁵ seconds for samples of several micrometer thickness. This corresponds to a solid phase diffusion coefficient on the order of $D \sim 10^{-13} \text{ cm}^2 \text{ s}^{-1}$.

These results explain previous observations of "water rich" NAT samples and show that, in the laboratory, surface composition is very sensitive to ambient gas composition. In the atmosphere, for small particles and long time scales ($>10^3$ sec), particle composition should be well described by NAT/ice vapor pressure curves.

We also observe significant supersaturation of HNO_3 vapor pressure, with respect to NAT, after HNO_3 gas was added to the gas chamber. At low $\text{H}_2\text{O}/\text{HNO}_3$ ratios, this supersaturation is consistent with formation of metastable monohydrate and dihydrate phases (indicated by the vapor pressure relations $P_{\text{H}_2\text{O}} P_{\text{HNO}_3} = K_m$ and $P_{\text{H}_2\text{O}}^2 P_{\text{HNO}_3} = K_D$, respectively). Over pure ice, supersaturations in P_{HNO_3} of a factor of 5 to 10 are required for nucleation of NAT on the solid sample surface. These supersaturations are transient with laboratory lifetimes from minutes to days, depending inversely on temperature and the degree of supersaturation. These observations may explain stratospheric observations of appearance thresholds of Type I NAT aerosols at temperatures 1 to 3 K lower than predicted by the Hanson and Mauersberger vapor pressure relations.

Gas Uptake on Sulfuric Acid Droplets: Heterogeneous chemistry on background sulfuric acid aerosol may have a significant impact on stratospheric photochemistry. This is particularly true for $\text{N}_2\text{O}_5(\text{g})$ to $\text{HNO}_3(\text{g})$ conversion, which previous results for HNO_3 and N_2O_5 uptake have shown is efficient on sulfuric acid surfaces (e.g., $\gamma = 0.06$ for N_2O_5 at 238K). In contrast, uptake of gaseous HCl into aqueous sulfuric acid is constrained by its liquid solubility in $\text{H}_2\text{O}/\text{H}_2\text{SO}_4$ solution. This indicates that chlorine chemistry on sulfuric acid aerosol may not be important. Progress in the HSRP project has involved modification of experimental apparatus to extend gas uptake measurements to cold (down to 230-240 K) sulfuric acid droplets.

E. Journal Publications:

Fox, L. E., S. C. Wofsy, D. R. Worsnop, and M. S. Zahniser, Vapor pressures and gas/solid equilibration of nitric acid trihydrate, to be submitted to *J. Geophys. Res.* (1991).

A. Title of Research Task

2-D MAGI: Two-Dimensional Modeling of Aircraft Global Impacts

B. Investigators

*Donald J. Wuebbles
Douglas E. Kinnison
Keith E. Grant
Atmospheric and Geophysical Sciences Division, L-262
Lawrence Livermore National Laboratory
7000 East Avenue
Livermore, CA 94550

C. Research Objectives

This research project emphasizes the application of the LLNL 2-D chemical radiative transport model to determining the impact of present and potential future aircraft emissions on the global atmosphere. The intention is to reduce uncertainties and better define the range of possible effects of aircraft emissions on the atmosphere. Realistic scenarios for aircraft emissions are examined to evaluate past as well as future effects on the atmosphere. Further development and improvement of the model will be done to meet the special needs of the HSRP program. Tracer studies will contribute to the evaluation of the model's ability to treat lower stratospheric transport and tropospheric-stratospheric exchange processes. Radiative forcing effects on climate will be determined for aircraft scenarios.

D. Summary of Progress and Results

The research studies during this first year of the project were designed to build upon the sensitivity studies relating to aircraft emissions we published in late 1989 (Johnson et al., 1989). These studies included a more realistic representation of expected fleet emissions as a function of latitude and altitude than included in the prior work. We also examined the possible effects of the current fleet of commercial aircraft on tropospheric and stratospheric ozone. Several sensitivity studies examined some of the uncertainties associated with aircraft emission effects on ozone. These various research studies have been published in a book (Wuebbles and Kinnison, 1990), in a journal article (Wuebbles and Connell, 1990), and in a conference proceedings (Kinnison and Wuebbles, 1991).

Some of the major findings from these studies included the following. (1) Current aircraft emissions may be having an impact on upper tropospheric ozone, leading to increasing concentrations of ozone in the upper troposphere. However, the analysis was very preliminary. (2) A matrix of HSCT scenarios evaluated over a wide range of mean flight altitudes and magnitudes of NO_x emissions confirmed previous analyses showing that ozone destruction becomes larger as the emissions of NO_x increase and as the altitude of injection increases. (3) Model calculations indicate that a major reduction in emissions would allow the stratosphere to recover to unperturbed conditions in about a decade. (4) Sensitivity studies indicate that water vapor emissions have a moderate effect on the change in total ozone, while carbon monoxide emissions had a negligible effect. (5) Injection of NO_x as HNO_3 has only a moderate (less than 10%) effect on the calculated change in total ozone. (6) The calculated change in ozone for the HSCT scenarios was very sensitive to the background atmosphere. This suggests that assessment analyses of future HSCT fleets should carefully consider the appropriate background atmosphere for the time period in which the aircraft will fly.

As part of the *HSRP Program Report*, Don Wuebbles put together a working group to write chapter 4 of this report on a methodology for the next generation of scenarios for future air travel. This working group brings together members of the aircraft industry for determining a mutually agreed upon approach for future scenario development.

E. Journal Publications

Kinnison, D. E., and D. J. Wuebbles, Influence of present and possible future aircraft emissions on the global ozone distribution, Lawrence Livermore Nat. Lab., Report UCRL-JC-194677, 1990; also *Proceedings of AMS Symposium on Global Change Studies*, American Met. Soc., Boston, MA, 1991.

Wuebbles, D. J., and Connell, P. S., Protecting the ozone layer, *Energy and Technology Review*, May-June, 1990.

Wuebbles, D. J. and D. E. Kinnison, Sensitivity of stratospheric ozone to present and possible future aircraft emissions, in *Air Traffic and the Environment -Background Tendencies and Potential Global Atmospheric Effects*, U. Schumann, editor, Springer-Verlag, Berlin, 1990.

Wuebbles, D. J., et al., Methodology for next generation of scenarios for future Air travel, chapter 4 , *NASA High Speed Research Program Special Report*, 1991.

A. Title of Research Task

Modeling of Microphysical Effects on Aerosol Properties Due to Stratospheric Aircraft Emissions

B. Investigators

*Glenn K. Yue
Lamont R. Poole
Mail Stop 475
Langley Research Center
National Aeronautics and Space Administration
Hampton, VA 23665-5225

C. Research Objectives

The objectives of this research are: (1) to better understand aerosol formation and growth mechanisms after expected increases in particles, H_2O , HNO_3 , HCl , and H_2SO_4 caused by emissions from stratospheric aircraft; and (2) to assess the impact on optical properties of aerosol particles in the lower stratosphere and upper troposphere. Homogeneous nucleation models will be developed to study the possibility of forming new particles under different aircraft emission scenarios. The change of optical properties of aerosol particles and PSCs resulting from emissions from stratospheric aircraft flying at different geographical locations will be studied and the impact will be compared with those caused by volcanic eruptions observed by satellite experiments (SAM II, SAGE II) and other measurements.

D. Summary of Progress and Results

Aerosol Formation Mechanisms: Models were developed to study the formation of new particles through homogeneous, heterogeneous, and ion-induced mechanisms in the binary sulfuric acid-water vapor system. In general, aerosol particles in the lower stratosphere and around the tropopause are generated by heteromolecular condensation, but doubling the ambient water vapor concentration and/or sulfuric acid concentration will make it possible to form ultrafine particles directly through gas-to-particle conversion. The rate of ion-induced nucleation under different ambient concentrations of trace gases and temperature is investigated. Since ions are an important constituent of aircraft emission plumes and their presence dramatically increases the nucleation rate, ion clusters may play an important role in the formation of aircraft contrails.

Composition of Background Aerosol Particles: Based on the global water vapor data set obtained by the SAGE II experiment, the composition of aerosol particles for different seasons, latitude bands and heights were estimated. It was found that droplets are about 54% H_2SO_4 by weight at an altitude of 13 km in the tropics, but about 74% H_2SO_4 by weight in high-latitude regions at the same height. Since laboratory experiments have shown that the uptake of HCl and HNO_3 molecules by aqueous sulfuric acid droplets is a function of acid concentration, this information on aerosol composition will be used to estimate the influence of aerosol particles on the gaseous species in the aircraft exhaust.

Identifying Clouds from Satellite Occultation Data: High-level (upper tropospheric) clouds appear to cover about 35% of the globe on average, and their interaction with gaseous species and condensation nuclei emitted by the aircraft should be studied. In situ measurements of these clouds are sporadic, but solar occultation data obtained by the SAGE II experiment contain potentially valuable climatological information. Based on the results of a parametric study, a method to distinguish extinction resulting from cloud particles from that

caused by background aerosol particles was developed. The proposed method will be used to obtain the global distribution of high-level clouds.

Optical Properties of Aerosol Particles after the Eruptions of Volcanos Ruiz and Kelut: To compare the impact of natural aerosol sources with that predicted from the HSCT, the change of optical properties after the eruptions of Volcanos Ruiz (November 1985) and Kelut (February 1990) was studied. Preliminary results show that new particles in the nucleation mode were formed around the tropopause and in the lower stratosphere after the eruption of Ruiz. Kelut was a much weaker eruption and apparently affected aerosol particles only in the tropical region where the volcano is located.

E. Journal Publications:

Yue, G. K., and G. S. Kent, Deducing Aerosol and Cloud Particles Size from Satellite Occultation Data (to be submitted to *Geophys Res Lett.*).

Yue, G. K., and L. R. Poole, Temperature Dependence of the Formation of Sulfate Particles in the Presence of an Ionization Source (in preparation).

Yue, G. K., and L. R. Poole, The Observation of a Nucleation Mode in the Stratospheric Aerosols After the Eruption of Ruiz (in preparation).

Appendix A

HSRP/AESA Program Report Chapter Reviewers

Appendix A
HSRP/AESA Program Report Chapter Reviewers

Dr. Martin Albers
MTU Munich GbmH
Postfach 50 06 40
D-8000 Munchen 50
FEDERAL REPUBLIC OF GERMANY

Dr. William H. Brune
Department of Meteorology
520 Walker Building
Pennsylvania State University
University Park, PA 16802

Mr. Willard J. Dodds
Mail Drop A-309
GE Aircraft Engines
1 Neumann Way
P. O. Box 156301
Cincinnati, OH 45215-6301

Dr. Anne R. Douglass
Code 916
Goddard Space Flight Center
National Aeronautics and Space Administration
Greenbelt, MD 20771

Professor Frederick L. Dryer
D316 Engineering Quadrangle
Princeton University
Princeton, NJ 08544-5263

Dr. David W. Fahey
R/E/AL6
Aeronomy Laboratory
National Oceanic and Atmospheric Administration
325 Broadway
Boulder, CO 80303-3328

Dr. Rolando R. Garcia
National Center for Atmospheric Research
P. O. Box 3000
1850 Table Mesa Drive
Boulder, CO 80307

Dr. Patrick Hamill
Department of Physics
San Jose State University
San Jose, CA 95192-0106

Dr. Anthony D. A. Hansen
Mail Stop 70A-3363
Lawrence Berkeley Laboratory
University of California, Berkeley
1 Cyclotron Road
Berkeley, CA 94720

Dr. Robert S. Harwood
Department of Meteorology
University of Edinburgh
King's Buildings
Mayfield Road
Edinburgh, EH9 3JZ
UNITED KINGDOM

Dr. James D. Holdeman
Mail Stop 5-11
Lewis Research Center
National Aeronautics and Space Administration
21000 Brookpark Road
Cleveland, OH 44135

Dr. Chris J. Hume
No 8 Design Office
Airbus Division, Future Projects
British Aerospace Commercial Aircraft Ltd.
Bristol BS99 7AR
UNITED KINGDOM

Dr. Charles H. Jackman
Code 916
Goddard Space Flight Center
National Aeronautics and Space Administration
Greenbelt, MD 20771

Professor Harold S. Johnston
Department of Chemistry
College of Chemistry
University of California, Berkeley
Berkeley, CA 94720

Miss Anna Jones
Department of Chemistry
University of Cambridge
Lensfield Road
Cambridge, CB2 1EW
UNITED KINGDOM

Dr. Jack A. Kaye
Code SED05
Headquarters
National Aeronautics and Space Administration
Washington, DC 20546

Dr. George H. Kidwell, Jr.
Mail Stop 237-11
Ames Research Center
National Aeronautics and Space Administration
Moffett Field, CA 94035-1000

Dr. Robert P. Lohmann
Mail Stop 165-03
Pratt and Whitney
400 Main Street
East Hartford, CT 06108

Dr. Nicole Louisnard
Physics Department
Office National d'Etudes et Recherches
Aerospaciales
29 Avenue Division Leclerc
BP 72 92322 Chatillon Cedex
FRANCE

Dr. Robert C. Oliver
Science and Technology Division
Institute for Defense Analyses
1801 North Beauregard Street
Alexandria, VA 22311-1772

Dr. Michael Oppenheimer
Environmental Defense Fund
257 Park Avenue South, 16th Floor
New York, NY 10010

Dr. Lamont R. Poole
Mail Stop 475
Langley Research Center
National Aeronautics and Space Administration
Hampton, VA 23665-5225

Dr. Rudolf F. Pueschel
Mail Stop 245-4
Ames Research Center
National Aeronautics and Space Administration
Moffett Field, CA 94035-1000

Dr. A. R. Ravishankara
R/E/AL2
Environmental Research Laboratories
National Oceanic and Atmospheric Administration
325 Broadway
Boulder, CO 80303

Dr. Ellis E. Remsberg
Mail Stop 401B
Langley Research Center
National Aeronautics and Space Administration
Hampton, VA 23665-5225

Dr. Jose M. Rodriguez
Atmospheric and Environmental Research, Inc.
840 Memorial Drive
Cambridge, MA 02139

Dr. Margaret A. Tolbert
Cooperative Institute for Research in
Environmental Sciences
Campus Box 216
University of Colorado
Boulder, CO 80309-0216

Dr. Adrian Tuck
R/E/AL6
Aeronomy Laboratory
National Oceanic and Atmospheric Administration
325 Broadway
Boulder, CO 80303-3328

Mr. Albert Veninger
Hot Section Technology
Rolls-Royce Inc.
Suite 450
2849 Paces Ferry Road
Atlanta, GA 30339-3769

Ms. Debra Weisenstein
Atmospheric and Environmental Research, Inc.
840 Memorial Drive
Cambridge, MA 02139



Report Documentation Page

1. Report No. NASA RP-1272	2. Government Accession No.	3. Recipient's Catalog No.	
4. Title and Subtitle The Atmospheric Effects of Stratospheric Aircraft: A First Program Report		5. Report Date January 1992	6. Performing Organization Code
		8. Performing Organization Report No.	10. Work Unit No.
7. Author(s) M. J. Prather, H. L. Wesoky, R. C. Miake-Lye, A. R. Douglass, R. P. Turco, D. J. Wuebbles, M. K. W. Ko, A. L. Schmeltekopf		11. Contract or Grant No.	13. Type of Report and Period Covered Reference Publication
		14. Sponsoring Agency Code	
9. Performing Organization Name and Address NASA Office of Space Science and Applications Earth Science and Applications Division			
12. Sponsoring Agency Name and Address National Aeronautics and Space Administration Washington, DC 20546			
15. Supplementary Notes			
16. Abstract <p>This document presents a first report from the Atmospheric Effects of Stratospheric Aircraft (AESA) component of NASA's High-Speed Research Program (HSRP). Studies have indicated that, with sufficient technology development, future high-speed civil transport aircraft could be economically competitive with long-haul subsonic aircraft. However, uncertainty about atmospheric pollution, along with community noise and sonic boom, continues to be a major concern; and this is addressed in the planned 6-year HSRP begun in 1990. Building on NASA's research in atmospheric science and emissions reduction, the AESA studies are guided by a panel of international scientists, with particular emphasis on stratospheric ozone effects. Because it will not be possible to directly measure the impact of an HSCT aircraft fleet on the atmosphere, the only means of assessment will be prediction. The process of establishing credibility for the predicted effects will likely be complex and involve continued model development and testing against climatological patterns. In particular, laboratory simulation of heterogeneous chemistry and other effects, and direct measurements of well-understood tracers in the troposphere and stratosphere, will continue to be used to improve the current models.</p>			
17. Key Words (Suggested by Author(s)) stratospheric chemistry, ozone, aircraft emissions, upper atmosphere aerosols, stratospheric aircraft, high-speed civil transport		18. Distribution Statement Unclassified - Unlimited Subject Category 45	
19. Security Classif. (of this report) Unclassified	20. Security Classif. (of this page) Unclassified	21. No. of pages 244	22. Price All

National Aeronautics and
Space Administration
Code NTT

Washington, D.C.
20546-0001

Official Business
Penalty for Private Use, \$300

NASA

National Aeronautics and
Space Administration

Washington, D.C.
20546

**SPECIAL FOURTH CLASS MAIL
BOOK**

Postage and Fees Paid
National Aeronautics and
Space Administration
NASA-451

Official Business
Penalty for Private Use \$300



L1 001 RP-1272 911223S090569A
NASA
CENTER FOR AEROSPACE INFORMATION
ACCESSIONING DEPT
P O BOX 8757 BWI ARPRT
BALTIMORE MD 21240

NASA

POSTMASTER: If Undeliverable (Section 158
Postal Manual) Do Not Return
